UNIVERSITY OF TRENTO - Italy

International Doctoral School in Biomolecular Sciences
XXV Cycle

Molecular and cellular effects of supercritical carbon dioxide on some important food-borne pathogens

Tutor

Olivier Jousson

Centre for Integrative Biology (CIBIO)

Ph.D. Thesis of

Sabrina Tamburini

Centre for Integrative Biology (CIBIO)

Academic Year 2012-2013

This Ph.D research work was mainly performed at Centre for Integrative Biology (CIBIO) in the Laboratory of Microbial Genomics (Professor Olivier Jousson) of the University of Trento, Italy. The Supercritical Carbone Dioxide treatments were carried out in collaboration with Dr. Sara Spilimbergo and Dr. Giovanna Ferrentino at the Department of Materials Engineering and Industrial Technologies of the University of Trento.

This work was supported by the European Community's Seventh Framework Program (FP7/2007–2013) under grant agreement nr. 245280, acronym PRESERF "Processing Raw Materials into Excellent and Sustainable End products while Remaining Fresh.

Abbreviations

Δ	Chemical shift scales
λ_{em}	Emission Wavelength
λ_{ex}	Excitation Wavelength
ANZFA	Australia New Zealand Food Authority
BCECF	2′,7′-bis-(2-carboxyethyl)-5-(and-6)-carboxyfluorescein)
AM	Acetoxymethyl
BHI	Brain Heart Infusion medium
cDNA	complementary DNA
CD_3OD	Deuterated methanol
CDP	Cytidine diphosphate
CdsA	CDP-diglyceride synthase
CFSAN	Center for Food Safety and Applied Nutrition
CFU	Colony Forming Units
Ct	Cycle threshold
$DiBAC_4(3)$	Bis-(1,3-Dibutylbarbituric Acid)Trimethine Oxonol
$DiOC_6$	3,3′-dihexyloxacarbocyanine iodide
DMSO	Dimethylsulfoxide
DVC	Direct Viable Count
EB	Ethidium Bromide
ESI	Electrospray Ion Source
FALS	Forward Angle Light Scatter
FCM	Flow Cytometry
FISH	Fluorescent in situ hybridization
FL1	Green fluorescence
FL3	Red fluorescence
FRET	Fluorescence Resonance Energy Transfer
FSIS	Food Safety and Inspection Service
gDNA	genomic DNA
GRAS	Generally Recognized As Safe
gyrA	DNA gyrase (type II topoisomerase), subunit A
hlyA	hemolysin A

HACCP	Hazard Analysis and Critical Control Points
HHP	High Hydrostatic Pressures
HPLC	High Performance Liquid Chromatography
invA	Invasion protein
IT	Ion Trap
LALS	Large Angle Light Scatter
LB	Luria-Bertani medium
LC	Liquid Chromatograph
mdoG	periplasmic glucan (OPG) biosynthesis periplasmic protein
MAP	Modified Atmosphere Packaging
mRNA	messenger RNA
MS	Mass Spectrometer
NMR	Nuclear Magnetic Resonance
OD_{600}	Optical Density at 600 nm
PBS	Phosphate Buffered Saline
PC	Phosphatidylcholine
PCR	Polymerase Chain Reaction
PE	Phosphatidylethanolamine
PEF	Pulsed Electric Field
PG	Phosphatidylglycerol
PgpA	phosphatidylglycerophosphatase A
PgpB	phosphatidylglycerophosphate phosphatase B
PgpC	phosphatidylglycerophosphate phosphatase C
PgsA	phosphatidylglycerophosphate synthetase
Psd	phosphatidylserine decarboxylase
PI	Propidium Iodide
PL	Phospholipids
PlsB	glycerol-3-phosphate O-acyltransferase
PMA	Propidium Monoazide
Ppm	parts per million
PssA	phosphatidylserine synthase
qPCR	quantitative PCR
rRNA	ribosomal RNA

RTE	Ready-to-Eat
RT-qPCR	Reverse Transcription quantitative PCR
SC-CO_2	Supercritical Carbone Dioxide
SEM	Scanning Electron Microscopy
SYBR-I	SYBR Green I
TEM	Transmission Electron Microscopy
Tm	melting Temperature
UI	Unsaturation Index
uidA	beta-glucuronidase
UV	Ultraviolet
VBNC	Viable But Not Culturable
WHO	World Health Organization

Contents

Abstract

In the 2007 report of World Health Organization (WHO) it was reported that in 2005 a great proportion of 1.8 million people died because of food and drinking water contamination (Velusamy *et al*., 2010). Fresh food product such as, fruits and vegetables carry a natural non-pathogenic epiphytic micro-flora, but during the food chain: harvest, transportation and further processing and handling the produce can be contaminated with pathogens from human or animal sources (Anon, 2002).

While conventional methods used to evaluate pasteurization efficiency are based on cultivation in vitro, it has been ascertained that, under environmental stress conditions (e.g. nutrient limitation, pressure, temperature), a number of pathogens enter in a so-called Viable But Not Cultivable (VBNC) state, becoming eventually more resistant to stress and thus escaping to detection by cultivation methods. Improving health risk assessment associated with the increasing consumption of minimally processed fresh food products is a crucial need. To reach this objective, in the first part of my PhD project I set up and validated cultivation-independent bacterial viability assays, propidium monoazide quantitative PCR (PMA-qPCR) and flow cytometry (FCM), to monitor bacterial populations in food after Supercritical Carbon Dioxide (SC-CO_2) treatment, that is one of the most promising non-thermal pasteurization technology in the age of the increasing demand for "ready-to-eat" and minimally-processed food products. The efficiency of SC-CO_2 treatment was evaluated on bacterial liquid cultures, on bacteria spiked both on a synthetic solid substrate (LB agar) and on some fresh food products, including carrots, coconut and dry cured ham. The results indicated that the treatment is more efficient on bacteria spiked on LB agar, and that bacterial inactivation is accompanied by a reduction of their biovolume. Total bacterial inactivation on food products was reached for both *Escherichia coli* and *Listeria monocytogenes*, satisfying both the US and European requirements (CFSAN/FSIS, 2003; European Commission, 2005). *Salmonella enterica* was instead more resistant to treatment, suggesting future experiments consisting in the application of a combination between SC-CO_2 and other techniques alternative to heat pasteurization, such as ultrasounds or Pulsed Electrical Field.

FCM and PMA-qPCR data showed that a fraction of bacterial cells not detectable by plate counts maintained the integrity of their membrane (at least 10^2 cells/g for each bacterial species) suggested that the cells entered in a VBNC state.

Comprehensively, the FCM assay showed the best performance as a bacterial viability test method, permitting to evaluate with high sensitivity the efficiency of treatment, to discriminate subpopulations of cells with different level of membrane permeabilization, and to identify variations in biovolume and alterations of the cellular surface. The method could be applied, with some adjustments, to any field where determining microbial viability status is of importance, including food, environment or in the clinic.

Permeabilization of the cell membrane has been proposed to be the first event leading to cell inactivation or death after SC-CO_2 treatment (Garcia-Gonzalez *et al.*, 2007; Spilimbergo *et al*., 2009).The Permeabilization of membrane induced by SC-CO_2 was also observed in *Salmonella enterica* (Kim *et al*., 2009a; Tamburini *et al*., 2013) and in *Saccharomyces cerevisiae* (Spilimbergo *et al*., 2010). Whether SC-CO_2 has a direct effect on the bacterial membrane or permeabilization is a consequence of cell death remains an open question. In the second part of the Thesis to increase knowledge on the mechanism of bacterial inactivation mediated by SC-CO_2 lipidomic profiles (HPLC-IT-ESI-MS), bacterial depolarization/permeabilization analysis (FCM) and gene expression studies of enzymes involved in phospholipids biosynthesis were performed on *E. coli* K12 MG1665. The data indicated that after 15 min of SC-CO_2 treatment most of bacterial cells lost their membrane potential (95%) and membrane integrity (81% of permeabilized and 18% of partially-permeabilized cells). Bacterial permeabilization was associated to a 20% decrease of cellular biovolume and to a strong reduction (more than 50%) of all Phosphatidylglycerol (PG) membrane species, but without altering their average unsaturation index (1.30 ±0.02) and the average acyl chain on the glycerol backbone (33.30 ±0.03). The process acts more efficiently on PG than on PE (Phosphatidylethanolamine) head group phospholipids. Bacteria responded to treatment up-regulating the expression level of *PssA* gene, involved in PEs synthesis, since PssA activity is regulated by mole fraction of PGs and Cardiolin in the membrane. However still remains to understand why only PG species have been found to strongly decrease during the treatments. Further studies would be necessary, including phospholipid biosynthesis mutant analysis.

Chapter 1: **Introduction**

1.1 Food Microbiology

Food microbiology is a discipline concerned with the study of the microorganisms, not only bacteria, but also fungi and viruses, that inhabit, create or contaminate food.

In the 2007 report of World Health Organization (WHO) it was reported that in 2005 a great proportion of 1.8 million people died because of food and drinking water contamination (Velusamy *et al*., 2010). Fresh food product such as fruits and vegetables carry a natural non-pathogenic epiphytic microflora, but during the food chain, which include harvesting, transportation and further processing and handling the product can be contaminated with pathogens from human or animal sources (Anon, 2002). In addition, most of the food products contain high levels of nutrients or a high water activity; therefore they are particularly susceptible of microbial spoilage which results in a deterioration of their organoleptic characteristics, and may even risk the health of immune-compromised individuals (Tournas *et al*., 2006).

Escherichia coli, *Salmonella* spp. and *Listeria* spp. are the most common food-borne bacterial pathogens in industrialized countries. These bacteria are typically transmitted to humans from raw meat, vegetables, cheese, eggs and milk (Czajka and Batt, 1994, Thévenot *et al*., 2006). Agricultural irrigation with polluted surface water can be one of the sources of enteropathogenic contamination of vegetables and fruits, such as the Gram-negative *E. coli* and *Salmonella* (Velusamy *et al*., 2006). *Escherichia coli* is a member of the coliform group that is commonly used as indicator microbe of fecal contamination in water samples and in food products (Edberg *et al*., 2000; Raj and Liston, 1960; Montville and Matthews, 2008). *Salmonella* constitutes a major public health burden and its control measures lead to high costs in many countries (WHO 2005). In 2005 in the United States, approximately 40% of the food-borne infections were caused by *Salmonella* (Vugia *et al*., 2006). *Listeria monocytogenes* is a Gram-positive pathogen that has a large ability to adapt to different environmental stresses (Gandhi *et al*., 2007). This pathogen causes human listeriosis and other serious diseases

in immune-compromised adults (Mead *et al.,* 1999). Every year in the United States, this microbe produces 2500 serious illnesses and 500 deaths (CDC, 2003).

In an attempt to reduce disease burden, the monitoring of food-borne diseases and pathogens in the food chain has been implemented and a farm-to-fork approach has been adopted encouraging all sectors of the food production chain to improve hygiene and actively incorporate structured approaches to food safety, such as HACCP principles (Newell *et al*., 2010).

1.2 Food pasteurization

During the last two decades, consumers demand for fresh but also ready-to-eat (RTE) fruits and vegetables has increased considerably, providing a constant and diverse supply of fresh products, which is not always possible, especially when off-season products have to be dealt. Preservation and safety of RTE products has become one of the main issue for the food industry since fresh vegetables and fruits are vehicle for international outbreak of foodborne diseases (EFSA, 2013), considering that traditional techniques -as thermal pasteurization, addition of preservatives or ionizing radiations, etc.- present some drawbacks in their exploitations in food applications. Thermal pasteurization (up to 80◦C) and sterilization (up to 120◦C) generate great scepticism because the high temperature degrades nutrients and vitamins in food products. Ionizing radiation and chemical treatments such as chlorine, ethylene oxide or hypochlorite (Winthrop *et al*., 2003; Beuchat *et al*., 2001) negatively affect the sensorial properties of products, decreasing their overall quality (Spilimbergo *et al*., 2012). As a consequence, the interest in innovative “minimal processing” techniques has increased considerably in the last years. A number of non-thermal pasteurization methods have been developed, which inactivate microbes while not adversely compromising food integrity and nutritional quality, including high hydrostatic pressure (HHP) and pulsed electrical fields (PEF) (Devlieghere *et al*., 2004), dense CO_2 (DCO_2), or supercritical CO_2 (SC-CO_2) (Spilimbergo and Bertucco, 2003). Among these methods, one of the most promising is the use of SC-CO_2, since it is considered to be a GRAS (Generally Recognized as Safe) solvent, implying that it can be used in food products. This method presents some fundamental advantages related to the mild operating conditions employed, particularly because it allows processing at low temperature and low

pressure (Garcia-Gonzalez *et al*., 2007). Indeed it avoids retention of flavor, denaturation of nutrients, production of side toxic reactions and changes in physical and optical properties of the treated materials, thus preserving the fresh-like qualities of food (Spilimbergo and Bertucco, 2003). The SC-CO_2 treatment reduces microbial load improving the safety of the food. However a great challenge is the control of process parameters (pressure, temperature and treatment time) considering that they can affect molecular interactions and protein conformation causing color and structural changes in food products. The SC-CO_2 treatment does not seem suitable for all solid foodstuffs due to the physical consistency of the products and their ability to positively react to the process in terms of microbial inactivation and retention of quality attributes. It seems to be more suitable for foods that retain their structure or maintain an appeal for the consumers although in soft form (Ferrentino and Spilimbergo, 2011).

1.3 Supercritical Carbone Dioxide

"The critical phenomena were discovered by Cagniard de la Tour in 1822, who died 150 years ago…In 1822, in the context of his interests in acoustics, he placed a flint ball in a digester partially filled with liquid. Upon rolling the device, a splashing sound was generated as the solid ball penetrated the liquid-vapour interface. Cagniard de la Tour noticed that upon heating the system far beyond the boiling point of the liquid, the splashing sound ceased above a certain temperature. This marks the discovery of the supercritical fluid phase. In this phase there is no surface tension as there is no liquid-gas phase boundary. The supercritical fluid can dissolve matter like a liquid and can diffuse through solids like a gas."

Berche et al., 2009

1.3.1 Supercritical CO_2 characteristics

Every substance has a critical point, having a critical pressure (Pc), critical temperature (Tc) and critical density (ρ_c) above which it can neither be in the liquid state nor in the gaseous state, but in the supercritical state (the vapor-liquid equilibrium). The critical point of a pure fluid represents a state of mechanical instability, where the density and all thermodynamic properties of the gas and liquid

become indistinguishable and the liquid-vapor meniscus disappears (Figure 1.1). In this state the fluid has both properties of a liquid, with a similar density, and a gas, with a similar viscosity. It has the unique ability to diffuse through solids like a gas and dissolve materials like a liquid. In addition, it has no superficial tension, because there is no liquid/gas phase boundary, which promotes penetration into micro-porous materials (Lucien and Foster, 1999).

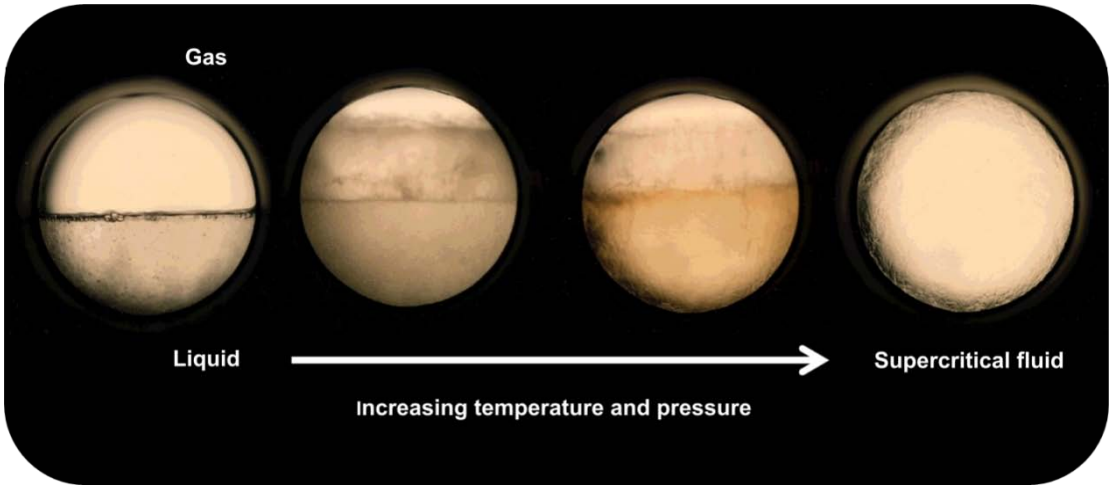

Figure 1.1. Disappearance of phase boundary (meniscus) on heating between gas and liquid state of CO_2. The meniscus between gas and liquid under critical point is easily observed. With an increase in temperature the meniscus begins to diminish. Above the critical point the meniscus can no longer be seen. One homogenous phase called the "supercritical fluid" phase occurs which shows properties of both liquids and gases. http://www.nasa.gov/vision/earth/technologies/harvestingmars_prt.htm

Supercritcal Carbone Dioxide (SC-CO_2) is particularly attractive for food preservation, since temperature and pressure values at its critical point are relatively mild and readily attained (Tc = 31.5°C; Pc=75.8 bar) and it can readily change in density upon minor changes in temperature or pressure (Figure 1.2). CO_2 is non-toxic, non-flammable, odourless, colourless, inert, cheap and environmentally and physiologically safe (Hong *et al*., 1999; Brunner, 2005; Gonzalez *et al*., 2007). Additionally, CO_2 is a non-polar solvent able to dissolve into lipids; insoluble compounds in water, like oils, butter, fats, are soluble in CO_2, while polar compounds, like sugar, proteins and salts are insoluble in CO_2 (Sahena *et al*., 2009).

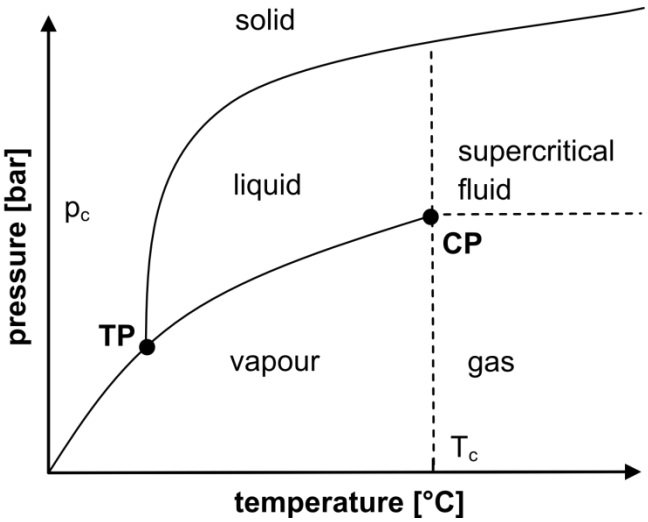

Figure 1.2. Carbon dioxide pressure-temperature phase diagram. The regions of the different substance state are indicated. The supercritical point is at 31.5°C and 75.8 bar (Spilimbergo *et al*., 2009).

1.3.2 Antimicrobial activity of CO_2

The antibacterial action of CO_2 on bacterial growth is known from more than 100 years. Gonzalez et al. (2007) reviewed the antibacterial effect of different states of CO_2. The gas is able to inactivate microorganisms both in its subcritical and supercritical state, but is more efficient in the latter state. The enhanced antimicrobial action could be attributed to its physico-chemical properties, but its mechanism of action remains unknown. The antibacterial action of SC-CO_2 has been extensively studied in the past years, on different microorganisms, in different culture conditions, and by using different SC-CO_2 systems. CO_2 is also commonly used in the Modified Atmosphere Packaging (MAP) technique to increase the shelf life of food products by removing O_2 and replacing it by N_2 or CO_2.

1.3.3 Parameters influencing SC-CO_2 treatment

There are a number of factors that may affect the inactivation rate induced by CO_2 treatment, including pressure, temperature, agitation of the system, water content, depressurization rate, bacterial species and initial bacterial load (Garcia-Gonzalez *et al*, 2007).

Pressure and Temperature. It is known that microbial inactivation increases by raising the CO_2 pressure, thus even a short exposure time is needed for a given amount of cells (Hong *et al*., 1999; Hong and Pyun, 1999). In addition, pressure affects the

solubilization rate, that at higher pressure facilitates both the acidification of the external medium (Spilimbergo, 2002) and the contact of CO_2 itself with the cells due to higher solvating power at high pressure. At specific combination of temperature and pressure, CO_2 acquires solvent properties to extract lipids from sample matrix (Sahena *et al*., 2009). On the other hand, the inactivation rate increases with increasing temperatures due to the higher diffusivity of CO_2 and higher fluidity of membranes (Hong *et al*., 1999).

Agitation and depressurization rate. The agitation of liquid samples during treatment enhance the antibacterial effect probably because the solubilization of CO_2 and its contact with bacterial cells increase in these conditions (Tsuji *et al*., 2005; Spilimbergo *et al*., 2010a). Another important parameter is the depressurization rate, since flash depressurization could mechanically disrupt the bacterial cells. Since 1951 many experiments have been carried out to demonstrate the bursting action of CO_2 on cells. Although mechanical disruption of bacterial cells induced by depressurization may be the cause of bacterial death, Enomoto *et al*. (1997) demonstrated that faster decompression is not always associated with maximal bacterial inactivation.

Water activity and suspending medium. SC-CO_2-mediated microbial inactivation seems to depend on the water content of the medium and the bacterial cells. Reducing water cellular content could increase the bacterial resistance to the treatment. The effect of water is probably the result of an increase of CO_2 solubility, given that the water in contact with pressurized CO_2 becomes acidic due to the formation of H_2CO_3, and dissociation in HCO_3^- and H^+, consequently reducing the pH of solution (Spilimbergo, 2002). The pH of pure water is strongly affected by adding CO_2 respect to acidic matrices such as orange juice (Hong and Pyung, 1999; Spilimbergo 2002). Indeed, Lin *et al.* (1994) reported that bacteria re-suspended in a complex media respect to a saline solution were more resistant to SC-CO_2. These results could be due to buffering action of the solutes in the medium that prevent pH decrease.

Microbiological aspects. Another remarkable factor is the different susceptibility to the treatment of different bacterial species, which could be related to variations of the cellular envelope and its permeability (Spilimbergo and Bertucco, 2003). In general, Gram-positive bacteria seem to be more resistant than Gram-negative to the treatment, presumably due to their thick cell wall (Garcia-Gonzalez *et al*., 2007). However, scanning electron microscopy studies Dillow *et al*. (1999) did not reveal

alterations of the cellular surface in Gram-negative bacteria such as *E. coli*. Because most treated cells appear to have intact cell walls, it can be hypothesized that the CO_2 antibacterial mechanism is independent of cellular disruption. The initial bacterial load also affects the effectiveness of the treatment: the highest level of bacterial inactivation is obtained with the lowest bacterial concentration. It seems that high bacterial concentration results in mutual protection (Garcia-Gonzalez *et al.*, 2007) and low concentration appear to more readily expose cells to the action of CO_2 (Tahiri *et al*., 2006). A other important aspect of bacterial inactivation is the growth phase. Bacterial cells in the stationary phase are much more resistant to treatment than those in the exponential phase. The entrance of Gram-negative bacteria in the stationary phase is indeed a highly regulated process governed by the alternative sigma factor RpoS, that induce many changes in gene expression pattern, aiming to produce a more resistant cell, promoting changes in all structures of the cell envelope (outer membrane, periplasm, peptidoglycan and cytoplasmic membrane) and in the cytoplasm, while the nucleoid condenses to protect the DNA (Navarro Llorens *et al*., 2010).

1.3.4 Hypotheses of antibacterial SC-CO_2 action

SC-CO_2 was first proposed as an alternative to heat-based pasteurization in the 1980's. Many articles have described the efficiency of the treatment on different microorganisms in liquid and on solid samples by using different techniques. In 1985 Daniels *at al*. proposed possible bacteriostatic mechanisms of CO_2. Three recent reviews summarize current knowledge about the effects of SC-CO_2 treatment on bacterial cells, but the inactivation mechanism has not been deciphered yet (Spilmbergo and Bertucco, 2003; Damar and Balaban, 2006; Garcia-Gonzalez *et al*., 2007). Potential incativation mechanisms can be summarized as following: (i) physical-mechanical disruption of cells; (ii) alteration of the cell membrane and extraction of cellular components; (iii) decrease of extracellular pH or cytoplasmic pH; (iv) metabolic inhibition and perturbation of the intracellular electrolyte balance. Most of these steps may not occur consecutively, but rather take place simultaneously in a complex and interrelated manner (Figure 1.5).

Physical-mechanical disruption of cells. In 1951, Fraser demonstrated cell disruption in *E. coli* after rapid release of gas pressure in less than 5 min by using Petroff-Hauser direct microscopic cell count method but without bacterial staining.

Other groups also investigated the cellular disruption of microorganisms after SC-CO_2 treatment by using transmission or scanning electron microscopy (TEM or SEM) (Ballestra *et al*., 1996; Dillow et al., 1999; Liao *et al*., 2010). SEM analysis on *Saccharomyces cerevisiae* cells showed some burst cells and other with wrinkles or holes on their surface (Folkes, 2004) (Figure 1.3 A,B). Similar results were obtained by Liao *et al*. (2010) and Yuk *et al*. (2010) on *E. coli* cells (Figure 1.3 C,D). TEM analysis after rapid decompression highlighted a decrease of the outer layer thickness of *Absidia coerula* spores (Liu *et al*., 2005). Furthermore, Lin *et al*. (1991) used an indirect method to verify cellular disruption by measuring protein concentration released in the supernatant. Conversely, Hong and Pyun (1999) and Kim *et al*. (2007) demonstrated the inactivation of *Lactobacillus plantarum* and *Salmonella enterica*, even if TEM and SEM analyses did not reveal bacterial disruption but only the occurrence of more "veins" and smalls vesicles on the cell surface (Figure 1.3 E,F).

Modification of cellular membrane. CO_2 may diffuse into the cell membrane and accumulate in the phospholipid bilayer (Isenchmid *et al*., 1995). Spilimbergo (2002) measured the theoretical affinity between CO_2 and the plasma membrane, revealing the capability of CO_2 to dissolve into the membrane with very high affinity, using the common membrane model mostly made up of phosphotidiletanol amines and phosphatidilglycerol. The accumulation of CO_2 into the plasma membrane is known to increase the fluidity and disorder of the membrane due to an order loss of the lipid chains also called "anaesthesia effect". The diffusion of molecular CO_2 into the plasma membrane compromises the construction of membrane domains and increases its permeability (Jones and Greenfield, 1982; Isenschmid *et al*., 1995). GC-MS analysis of *Salmonella enterica* revealed that the fatty acid profiling in control and treated samples were almost identical (Kim *et al*. 2009b). However, the minor component of fatty acids tended to increase after SC-CO_2 treatment probably duo to an alteration of bacterial cells, that made the extraction of the minor fatty acids more easily from membrane.

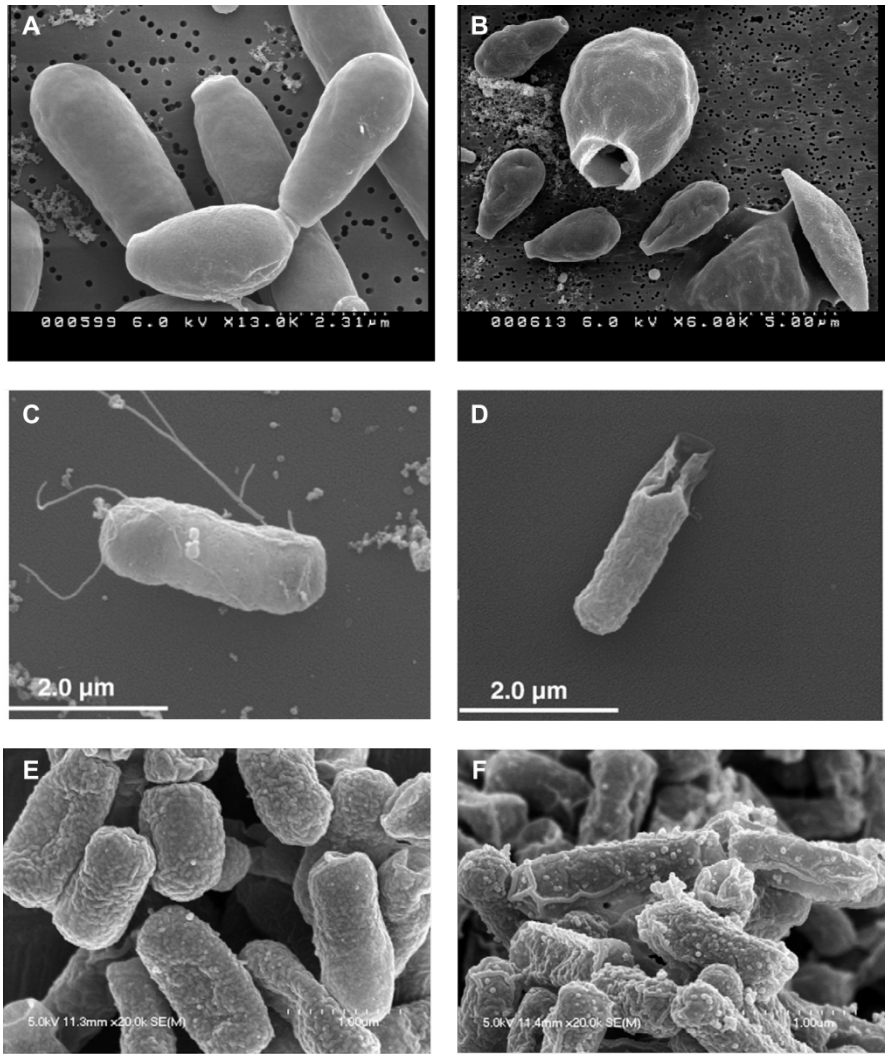

Figure 1.3. Representative scanning electron microscope (SEM) micrographs of micro-organisms treated with SC-CO_2. (A,B) *Saccharomyces cerevisiae* in fresh beer untreated and treated at 27.6 MPa, 10% CO_2, at 21°C for 5 min (Folkes, 2004); (C,D) *Escherichia coli* in K12 in apple cider untreated and treated at 8% CO_2 at 34 °C (Yuk *et al*., 2010); (E,F) *Salmonella typhimurium* in phosphate-buffered saline (PBS) untreated and treated at 35 °C and 100 bar for 30 min (Kim *et al*., 2007).

The effect of the treatment on the structure of the cell membrane has been proposed to be the first event leading to a progressive cell membrane permeabilization and consequently cell inactivation or death (Garcia-Gonzalez *et al.*, 2007; Spilimbergo *et al*., 2009). Membrane permeabilization in *E. coli* and in *L. monocytogenes* cells induced by SC-CO_2 treatment was investigated by Garcia- *et al*. (2010a) on the basis of the uptake of propidium iodide (PI) in the permeabilized bacterial cells analyzed by spectrofluorometry together with morphological observations by TEM. The authors demonstrated the relationship between irreversible membrane permeabilization (identified by PI uptake) and the loss of bacterial ability to grow on rich media

following SC-CO_2 treatment. Kim *et al.* (2009a) reported the ability of SC-CO_2 to permeabilize *Salmonella enterica* serotype Typhimurium cells by using flow cytometry coupling wit SYTO 9 and PI. Membrane permeabilization was also observed in *Saccharomyces cerevisiae* cells exposed to SC-CO_2 treatment (Spilimbergo *et al*., 2010a). In addition, treated *Salmonella* cells have been shown to lost their efflux pump activity (Kim *et al*., 2009a).

Extraction of cellular components. Hong and Pyun (1999) observed by SEM that *Lactobacillus plantarum* cells remained intact after SC-CO_2 treatment, but TEM images showed cell membrane modifications with possible cytoplasm leakage **(**Figure 1.4 A-C); a large periplasmic space and empty spaces in the cytoplasm appeared. In *E. coli* the cytoplasm lost its organization and seem to concentrate at the cell periphery (Figure 1.4 D-F) whilst in *L. monocytogenes* SC-CO_2 induced protrusion of cytoplasmic content through pores in the cell wall (Figure 1.4 G-I). In *S. cerevisiae* cells the cytoplasm was less dense in treated cells respect untreated cells (Figure 1.4 L-N) (Garcia-Gongalez *et al*., 2010). The total fatty acid quantity of *S. enterica* cells decreased significantly after SC-CO_2 treatment and revealed also qualitative differences in the protein profile, as well as quantitative differences that consisted in a decrease in intensity of 33 spots; eleven down regulated protein spots were identified by using MALDI-TOF MS, which were identified as enzymes involved in cell metabolism (Kim *et al*., 2009b). White *et al*. (2006) did not note any appreciable degradation of *Salmonella typhimurium* proteins and did not identify any differentially expressed protein in 2D gels. In *E. coli*, the amount of total protein decreased after treatment and accumulated in the supernatant with increasing treatment time (Liao *et al*., 2011). Increasing the temperature in the range of 40-50°C rendered triglycerides soluble whilst with temperatures of 80-100°C, all lipids species become extracted (Sahena *et al*., 2009). In addition, Hong and Pyun (2001) the release of intracellular ions, including Mg^{2+} and K^{+} was reported in *Lactobacillus plantarum.*

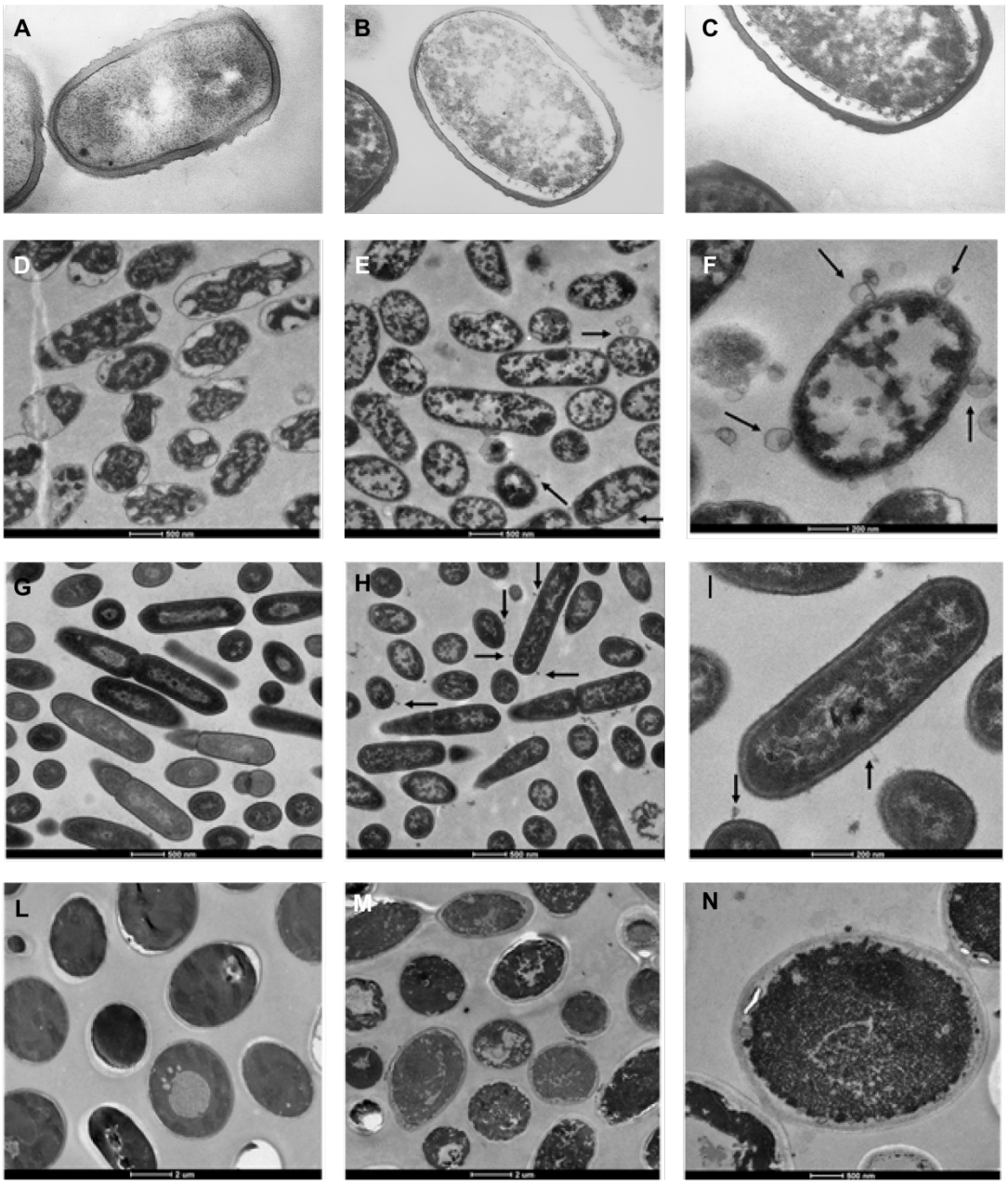

Figure 1.4. Representative transmission electron microscope (TEM) micrographs by ultra-thin sectioning of micro-organisms untreated and SC-CO_2-treated. *Lactobacillus plantarum* untreated (A) and treated (B,C) at 70MPa, at 30°C for 1 h (Hong and Pyun, 1999*). Escherichia coli* untreated (D) and treated at 21 MPa and 45°C up to 60 min (E,F); *Listeria monocytogenes* untreated (G) and treated at 21 MPa and 45°C up to 60 min (H,I); *Saccharomyces cerevisae* untreated (L) and treated at 21 MPa and 45°C up to 60 min (M,N) (Gonzalez *et al*., 2010a). The arrows show the cytoplasm bulging through smallpores in the cell wall.

pH lowering effect. CO_2 is able to decrease the pH of solution when it dissolves in the water. CO_2 reacts with water forming the carbonic acid, which further dissociates in bicarbonate and H^+ ions lowering the pH solution (Spilimbergo *et al.*, 2005):

$$CO_2+H_2O \leftrightarrow H_2CO_3$$

$$H_2CO_3 \leftrightarrow H^+ + HCO_3^- \qquad pKa=6.57$$

$$HCO_3^- \leftrightarrow H^+ + CO_3^{-2} \qquad pKa=10.62$$

Such lowered extracellular pH may inhibit microbial growth and force bacteria to consume more energy to maintain pH homeostasis. However, a reduction of external pH alone cannot efficiently inactivate microorganisms, since other acids used to lower medium acidity have been shown to have a less inhibitory effect than CO_2 (Haas *et al*., 1989; Wei *et al*., 1991; Lin *et al*., 1993). Lin *et al*. (1994) suggested that lowered external pH increases cellular permeability, thus facilitating the entry of CO_2 into the cells.

Acidification of cytoplasm. The increase of CO_2 in the medium likely leads to greater membrane fluidity, increasing the passage of CO_2 across the membrane. Aqueous CO_2 reacts with cytoplasmic water and increase the concentration of intracellular H^+ ions. Spilimbergo *et al.* (2010b) measured the decrease of intracellular pH in *Listeria monocytogenes* after SC-CO_2 treatment by using fluorescent pH-sensitive dyes, and reported that the intracellular pH decreased from 7.9 in control samples respect to <5 in SC-CO_2 treated samples. Furthermore, phosphoric and hydrochloric acids generally used for acidification of medium did not have a strong inhibitory effect like SC-CO_2 (Haas *et al*., 1989). An hypothesis is that CO_2 penetrates the cells at a much faster rate than other molecules that do not produce acidification of the medium and other acid molecules. It is known that viable cells need to maintain a transmembrane pH gradient with their internal pH (pH_i) above the acidic external pH (pH_{ex}). A failure in maintaining pH_i homeostasis indicates that the bacterial cell is severely stressed which ultimately leads to a loss of cell viability (Kastbjerg *et al*., 2009). The concentration of aqueous CO_2 and HCO_3^- are controlled by pH buffering to maintain a rather constant intracellular pH. Some microorganisms, such as lactic acid bacteria, possess systems to regulate intracellular pH by using cytoplasmic buffering, proton symport systems, production of bases and proton pumps (Hutkins and Nannen, 1993; Slonczewski *et al*., 2009). Acidification of cytoplasm likely inactivates key cellular enzymes, specifically those with an acidic isoelectric point (Ballestra *et al*., 1996).

Disordering of the intracellular electrolyte balance. Intracellular CO_2 may be converted into HCO_3^- and then CO_3^{2-}, and may precipitate with intracellular inorganic electrolytes (such as Ca^{2+} and Mg^{2+}) (Lin *et al*., 1993). In addition the collapse of the proton-motive force across the membrane due to the external pH lowering may produce a Ca^{2+} cytosolic disorder since Ca^{2+} extrusion is catalyzed by the Ca^{2+}/H^+ antiporter system in bacteria (Gangola and Rosen, 1987).

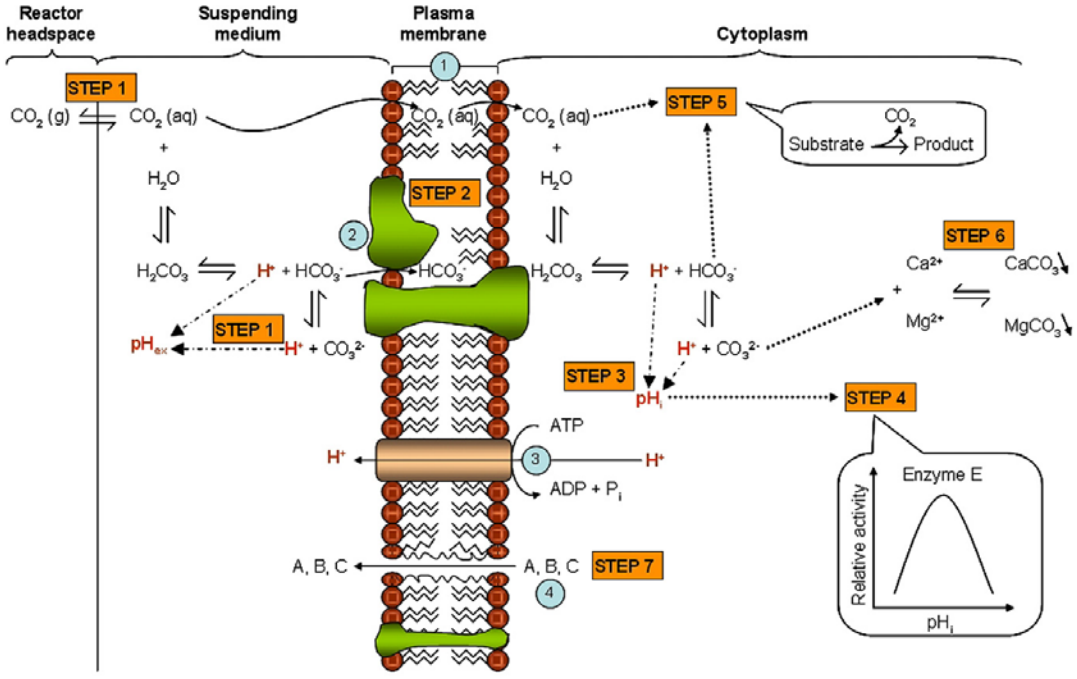

Figure 1.5. A schematic diagram of how SC-CO_2 may affect the bacterial cells. The different steps of the inactivation mechanism are shown (Garcia-Gonzalez *et al*., 2007).

1.4 What is life?

It is difficult answering to the common question "What is life?" and to the inverse question "What is dead?" The answer for the second question may be "the absence of life", making the definition of life and dead inseparable (Davey, 2011). The Oxford dictionary defines "life" as "the condition that distinguishes animals and plants from inorganic matter, including the capacity for growth, reproduction, functional activity, and continual change preceding death".

Susan Watanable, Editor of the NASA homepage (2007), tried to provide the Life's Working Definition. "*Living creatures respond, and their stimulation fosters a reaction-like motion, recoil, and in advanced forms, learning. Life is reproductive, as some kind of copying is needed for evolution to take hold through a population's mutation and* natural selection*. To grow and develop, living creatures need foremost to be consumers, since growth includes changing* biomass*, creating new individuals, and the shedding of waste. To qualify as a living thing, a creature must meet some variation for all these criteria. For example, a crystal can grow, reach equilibrium, and even move in response to stimuli, but lacks what commonly would be thought of as a biological nervous system*".

Applying these definitions to microbes is difficult. Whether bacterial cells are viable or dead is a fascinating and not trivial question. The answer is often part of the basis of decisions related to such matters as the safety of food and drinking water, the sterility of pharmaceuticals and medical devices, and so on. Microscopic observation of a bacterial cell does not tell the microbiologist whether the cell is viable or dead, only that it exists. The common definition of bacterial life is the cellular capability to divide and generate a population, typically a visible colony on the surface of a nutrient agar plate (Bogosian and Bourneuf, 2001).

1.4.1 Viable But Non Cultivable (VBNC) cells

Since the original study by Xu *et al*. (1982) many articles have been published about the occurrence of a VBNC state in bacterial cells. Many bacteria, including a variety of important human pathogens, are known to respond to various environmental stress by entering in a VBNC state, in which bacteria fail to grow on standard media, but remain alive (Olivier, 2010). It has been proposed that some readily cultivable species of bacteria, when subjected to various stresses, including nutrient starvation, incubation outside the normal temperature range of growth, elevated or lowered osmotic concentrations, heavy metals and food preservatives (Oliver, 2010), may enter a long-term survival state in which they are not detectable by culture-based methods. Cells in the VBNC state demonstrate very low levels of metabolic activity but on resuscitation are again cultivable (Bogosian and Bourneuf, 2001). Some pathogens entering in the VBNC state result more resistant to antibiotics and are able to re-grow and reinitiate

infections. For instance, uropathogenic *E. coli* cells are not completely eliminated by antibiotic treatment, but a part of cells not detectable by plate counts resist (Mulvey, 2001). It has been demonstrated that a number of VBNC pathogens are not able to initiate disease. VBNC cells of *Vibrio harveyi* are not able to kill zebra fish (Sun *et al*., 2008), but resuscitated cells are lethal.

1.4.2 Viability concept

To overcome the limit of plate counts, by which only bacteria able to grow can be detected, new viability definitions were proposed and new viability assays to quantify total and viable cells were developed.

Nucleic acids detection. The presence of intact DNA sequences was initially used as an indicator of cell viability assuming that DNA would become degraded more rapidly in a dead cell than other cellular components (Jamil *et al*., 1993). Given its highly labile nature and very short half-life, mRNA has been used as a marker of viability, and should provide more closely correlated indication of viability status than DNA-based methods (Keer and Kirch 2003). Ribosomal RNA (rRNA) has also been investigated as a viability indicator. For *Chlamydia pneumoniae* the detection of 16S rRNA was demonstrated to provide a better infection indicator than immunocytochemical detection of specific antigens, but because of longer half-life of rRNA species and their variable retention following a variety of bacterial stress treatments makes rRNA a less accurate viability indicator than mRNA targets (Keer and Birch, 2003). mRNA, on the other hand, degrades rapidly after cells have lost viability (Belasco, 1993), but the same intrinsic instability results in technical problems if used as a molecular target.

Cellular integrity. Other viability definitions are based on physiological state of the cell. Membrane integrity demonstrates the protection of constituents in intact cells and the capability of metabolic/enzymatic activity and, potentially, reproductive growth. Cells without an intact membrane are considered permeabilized and can be classified as dead cells (Ziglio *et al*., 2002). As their structures are freely exposed to the environment they will eventually decompose (Nebe-von-Caron *et al.,* 2000). Several papers have

reported the use of molecular dyes, such as Propidium Iodide (PI), to detect dead bacterial cells. (Müller and Nebe-von-Caron, 2010). PI often is combined with other DNA fluorescent dyes, such as Syto-9 (Barney *et al*., 2006) or Sybr-Green-I (Barbesti *et al*., 2000) or metabolic fluorescent dyes, such as calcein-AM (Hiraoka and Kimbara, 2002).

Pump activity and membrane potential. Metabolic activity is a more restrictive condition, because it requires that cells are able to demonstrate one of the following functions: biosynthesis, pump activity, membrane potential. Among these properties, the loss of pump activity can be measured by Ethidium Bromide (EB) uptake, whilst the loss of membrane potential by using molecular dyes, such as $DiBAC_4(3)$ for Gram-negative bacteria and $DiOC_6$ for Gram-positive bacteria, allow to quantify depolarized cells (Berney *et al*., 2006; Müller and Nebe-von-Caron, 2010).

Enzymatic activity. Fluorogenic probes are often used to detect metabolically active bacteria (Ziglio *et al*., 2002). The general principle is that cells become fluorescent through the action of intracellular enzymes. An example is BCECF-AM, a not fluorescent compound, hydrolyzed by intracellular esterases into fluorescent molecules. Its retention in intact cells is an indication of cellular membrane integrity, thanks to its hydrophobic tail which anchors the molecule on the lipids of the cell membrane. Variations of fluorescence intensity has been be used to measure changes of intracellular pH (Meyer-Rosberg *et al*., 1996).

According to the viability concept proposed by Nebe-von-Caron *et al*. (2000) (Figure 1.7) microbial cells can be classified based on their physiological status: (i) cultivable cells detected by plate counts; (ii) viable-but-non-cultivable cells (VBNC) and (iii) dead cells. Each cell category can be detected and quantified by using many fluorescent viability indicators (Breeuwer and Abee, 2000). Viable cells are considered as the sum of cultivable and VBNC cells, on the basis of their metabolic activity or membrane integrity (Nebe-von-Caron *et al*., 2000; Nocker *et al*., 2012).

1.4.3 Methods to assess bacterial viability

In response to environmental conditions, bacteria may become no more cultivable, making microbial risk evaluation difficult. Moreover, cultivation is time-consuming with positive results often lagging behind the required timeline for preventive measures. Figure 1.6 summarizes the range of approaches used to assess bacterial viability. Alternatives to colony counting include the application of: (i) flow cytometry (FCM) coupled with fluorescent staining to assess cellular integrity; (ii) DVC test and detection of respiration to verify the metabolic activity, and (iii) PCR, RT-PCR, qPCR and other molecular techniques to detect and quantify mRNA, rRNA and DNA. However, due to the persistence of DNA after cell death (Josephson *et al*., 1993; Masters *et al*., 1994), DNA-based quantification can lead to a substantial overestimation of the pathogenic risk or to false-positive results.

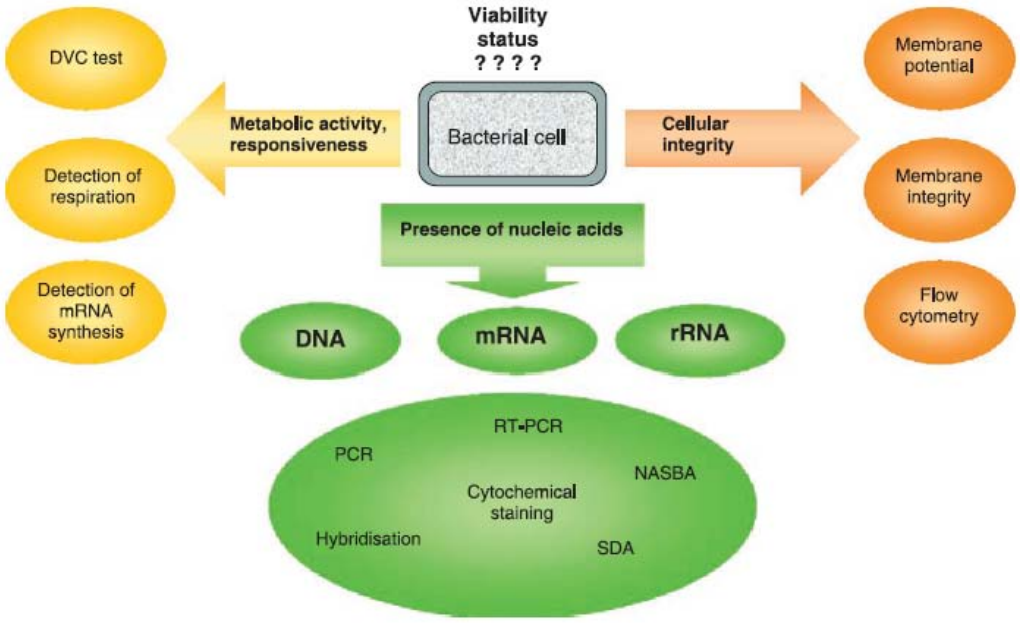

Figure 1.6. Schematic diagram illustrating the range of approaches used in the assessment of bacterial viability (Keer and Birch 2003).

PMA-qPCR analysis. Nocker *et al*. (2006) developed a viability assay, by coupling an analogous of propidium with quantitative PCR (qPCR), in order to quantify only the DNA from viable cells. Propidium monoazide quantitative PCR (PMA-qPCR) is a qPCR amplification performed after PMA staining. PMA is an analogue of Propidium Iodide (PI) with a covalently-linked azide group, used as a marker of bacterial cells with permeabilized membrane. After photoactivation, PMA binds

irreversibly to double strand DNA, thus inhibiting DNA amplification during qPCR or causing DNA loss together with cellular debris during DNA extraction. PMA was used to discriminate intact and permeabilized cells in an environmental matrix (Nocker *et al*., 2007a, Figure 1.7) and was applied to monitor the effect of disinfection treatments altering membrane integrity (Nocker *et al*., 2007b).

Flow cytometry. FCM is a multi-parametric and single-cell analysis technique for high-throughput and real time quantification of multiple cellular parameters, such as cell size, surface granularity and physiological state. In FCM, two light scattering signals can be collected simultaneously from each bacterial cell: the Forward Angle Light Scatter (FALS), which is related to bacterial size (Foladori *et al*., 2008), and the Large Angle Light Scatter (LALS), measuring cell density or granularity (Müller and Nebe-von-Caron, 2010). In FCM studies, SYBR Green I fluorophore (SYBR-I) is often used as total cell marker, given its ability to cross the cell membrane and to bind DNA (Barbesti *et al*., 2000), whilst propidium iodide (PI) is used as dead cell marker, since it penetrates only cells with permeabilized membrane (Ziglio *et al*., 2002). In permeabilized cells the simultaneous presence of SYBR-I and PI activates Fluorescence Resonance Energy Transfer (FRET), due to the total absorption of the fluorescent emission spectrum of SYBR-I by PI. In these conditions, it is possible to distinguish intact cells emitting green fluorescence from permeabilized ones emitting red fluorescence. FCM coupled with fluorescent dyes (SYBR-I and PI or Syto9 and PI) was used to discriminate intact and permeabilized cells in wastewater treatment plant (Foladori *et al*., 2010) and to monitor the effect of various antibacterial treatments (Wouters *et al*., 2001; Kim *et al*., 2009a).

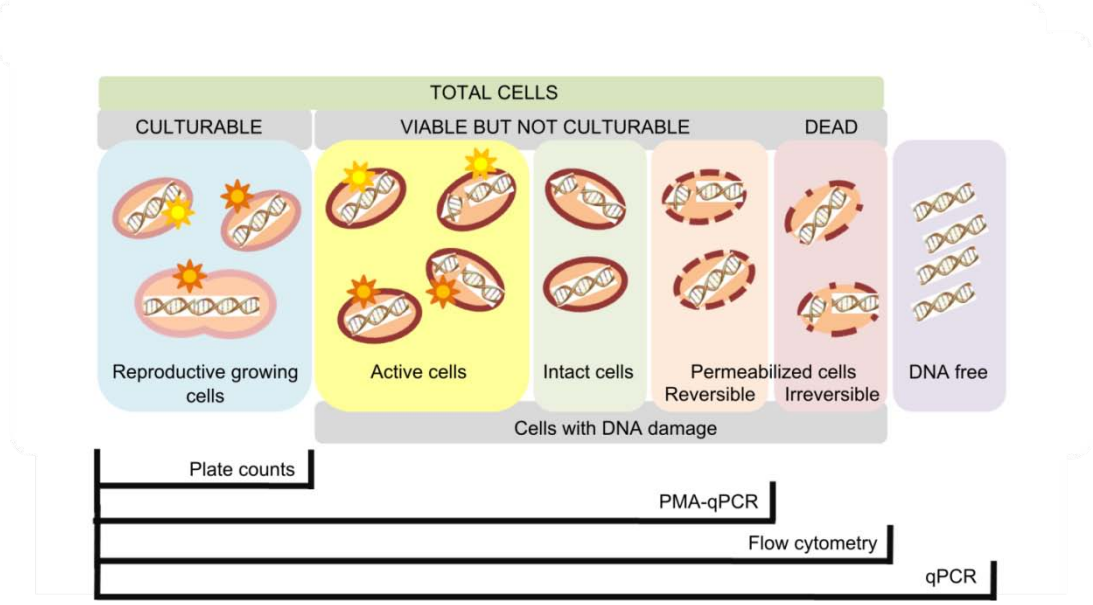

Figure 1.7. Cellular viability concept according to Nebe-von Caron (2000). The viable cells are represented by the sum of culturable and VBNC cells. Total DNA can be detected by PCR or qPCR, but without distinguishing DNA from viable and dead cells. PMA-qPCR and FCM coupled with fluorescent dyes discriminate viable and dead cells on the bases of membrane integrity, which is the less restrictive viability parameter. PMA-qPCR only quantifies viable cells, whilst FCM quantifies all cells including viable and dead cells.

Chapter 2: **Aim of the PhD project**

SC-CO_2 treatment is one of the most promising non-thermal pasteurization technology in the age of an increasing demand for "ready-to-eat" (RTE) and minimally processed food products. Many studies evaluated the inactivation efficiency of the treatment on different bacterial species, either in pure culture or spiked on food products. Inactivation efficiency was deduced from c.f.u plate counts, therefore measuring the bacterial ability to form colonies upon standard growth conditions. Since under environmental stress conditions (e.g. nutrient limitation, pressure, temperature), a number of pathogens enter in a so-called viable but not cultivable (VBNC) state, becoming eventually more resistant to stress and escaping to detection by cultivation methods, the use of alternative viability assays is needed to correctly evaluate biohazard issues associated with minimally processed food products.

The aim of the first part of my PhD project was to define the optimal parameters of SC-CO_2 treatment, including temperature, pressure and time, to inactivate three important food-borne pathogens in liquid cultures or spiked both on solid synthetic substrate and on food products. To overcome the limits of plate count methods, cultivation-independent bacterial viability assays including propidium monoazide PCR and flow cytometry were set up to discriminate and quantify viable bacterial cells on the basis of membrane integrity.

Although microbiological hazards in the food processing and application of food preservation technologies have yet been evaluated, microorganisms adapt very quickly to stress developing new resistant mechanisms increasing the potential biosafety hazard associated to RTE food products. It is therefore crucial to increase knowledge on the mechanism of action of SC-CO_2 on the bacterial cells to prevent the rise of bacterial resistance. Given that bacterial permeabilization induced by SC-CO_2 is believed to be the first event leading to bacterial inactivation or death, lipidomic analysis of bacterial membranes and gene expression analysis of membrane phospholipid biosynthesis pathways were performed.

Chapter 3: **Materials and Methods**

3.1 Bacterial strains and sample preparation.

Three common food-borne pathogens used in this study were purchased at the American Type Culture Collection (ATCC, Manassas, VA, USA). *Salmonella enterica* ATCC 14028 and *Escherichia coli* ATCC 29522 were grown on solid Luria-Bertani (LB) agar medium (Sigma-Aldrich Co., Milan, Italy) at 37°C for 16 h. *Listeria monocytogenes* ATCC 19111 was grown on solid Brain Heart Infusion (BHI) medium (Becton Dickson, NJ, USA) at 37°C for 16 h. One colony was picked and inoculated into 200 ml of corresponding broth medium. Bacterial cultures were incubated at 37°C with constant shaking (200 rpm) to stationary phase (16 hours). Cells were collected by centrifugation at 6000 rpm for 10 min and were re-suspended in an equal volume of phosphate buffered saline (Sigma-Aldrich Co., Milan, Italy).

Escherichia coli K12 strain MG1665 was used to study lipidomic profiles and gene expression. It was grown on solid Luria-Bertani (LB) agar medium (Sigma-Aldrich Co., Milan, Italy) at 37°C for 16 h. One colony was picked, inoculated into 10 ml of LB medium and incubated at 37°C with constant shaking (200 rpm) to stationary phase (16 hours). The cells were re-inoculated into 200 ml of LB medium and incubated at 37°C with constant shaking (200 rpm) to reach the exponential phase, with OD=0.6.

3.2 Synthetic substrate and solid food contamination

$5x10^6$ cells of *E. coli* ATCC 25922, 10^7 cells of *S. enterica* ATCC 14028 and $3x10^7$ cells of *L. monocytogenes* ATCC 19111 were spiked on a synthetic solid substrate made of LB agar with a surface of about 380 mm^2 (Sigma-Aldrich Co., Milan, Italy).

Carrots (*Daucus carota*), Coconut fruit **(***Cocos nucifera*) and slices of dry cured ham surface were purchased from a local market. Carrots were washed with water, cut into 2-gram pieces and spiked with 50 µL of *E. coli* ATCC 25922 at a concentration of 10^8 CFU/mL. The edible part of the coconut was cleaned, washed with water and cut in

2-gram pieces with a surface of about 100 mm^2. The coconut pieces were spiked with 50 µl of *S. enterica* suspension at an initial concentration of 10^7 CFU/mL). Slices of dry cured ham were cut in 2-gram pieces of rectangular shape (surface area of about 200 mm^2) and spiked with 50 µL of *L. monocytogenes* at a concentration of 10^9 CFU/mL.

All spiked samples were left 1 h in a sterile chamber at room temperature to let the microbial suspension absorb on synthetic substrate and solid food products were loaded in a SC-CO_2 multi-batch apparatus.

3.3 SC-CO_2 treatment

The SC-CO_2 treatment was performed in a multi-batch apparatus as described by Mantoan and Spilimbergo (2011). Briefly, the system consisted of 10 identical 15 ml-capacity reactors operating in parallel. All reactors were submerged in the same temperature-controlled water bath to maintain the desired temperature constant throughout the process. Each reactor was connected to an on-off valve for independent depressurization and had an internal magnetic stirrer device, to guarantee homogeneous dissolution in the cell suspension (Figure 2.1) Aliquots of 10 ml of each bacterial suspension, prepared as described in sample preparation section, or 50 µl spiked on solid substrates, as described in synthetic substrate and fresh solid food contamination section, were transferred into the reactors. The SC-CO_2 treatment was carried out with the conditions reported in Table 1. Each treatment was interrupted by slowly depressurizing the reactor over approximately 1 min.

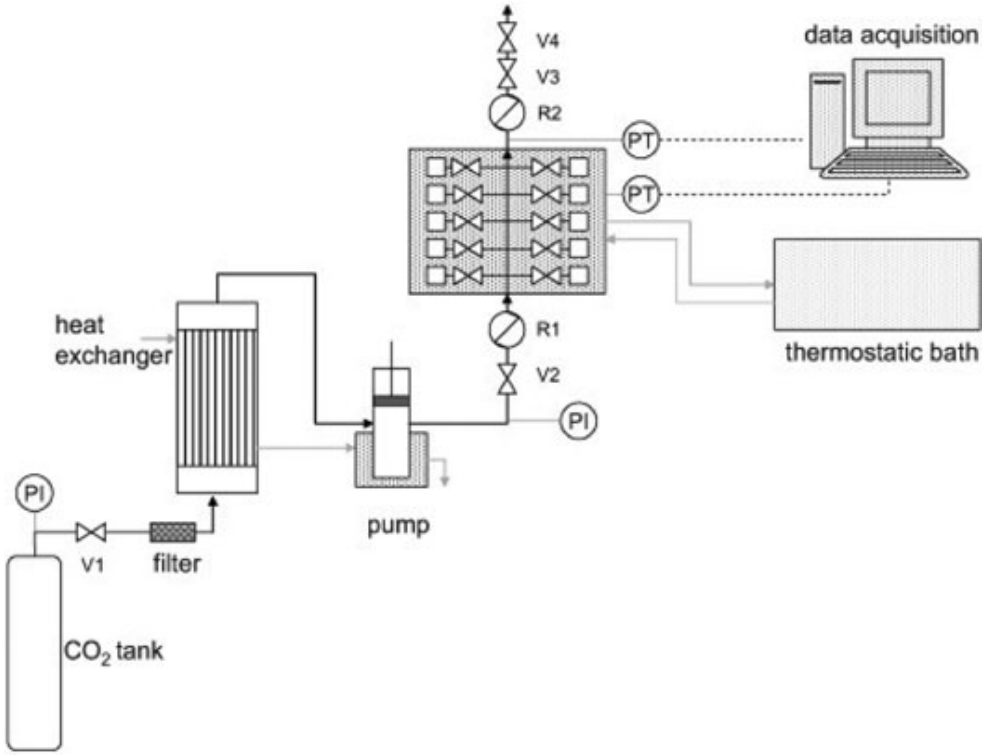

Figure 2.1 Schema of the SC-CO_2 multi-batch apparatus. V-1 to V-4 = valves; R1, R2 = electrical resistance; PT = pressure transducer; PI = pressure manometer

Table 1. Microorganisms, matrices and SC-CO_2 conditions

Target microorganism	**Medium**	**Process conditions**
S. enterica ATCC 14028	PBS	120 bar; 35°C; up to 60 min
	LB agar	120 bar; 35°C; up to 60 min
	Coconut	120 bar: 40,50°C up to 60 min
E. coli ATCC 25922	PBS	120 bar; 35°C; up to 60 min
	LB agar	120 bar; 35°C; up to 60 min
	Carrot	80-120 bar; 22,35°C; up to 30 min
*L. monocytoge*nes ATCC 19111	PBS	120 bar; 35°C; up to 60 min
	LB agar	120 bar; 35°C; up to 60 min
	Dry cured ham	80,120 bar; 45,50°C up to 30 min
E. coli K12 MG1665	LB Broth	120 bar; 35°C; up to 45 min

3.4 Sample homogenization

Untreated and treated solid samples were collected and re-suspended in 4 mL of PBS in a sterile plastic bag (Reinforced Round Bag- 400, International P.B.I., Milan, Italy) and homogenized in a Stomacher 400 (International P.B.I., Milan, Italy) at 230 rpm for 2 min. The resulting homogenate was taken from the sterile bag and used for plate counts, FCM and PMA-qPCR analyses.

3.5 Plate counts.

Untreated and SC-CO_2 treated cells were serially diluted with 1x PBS (900 µl of PBS and 100 µl of sample) and were spread-plated on chromogenic coli/coliform agar (Liofilchem, Teramo, Italy) for *E. coli*, on chromatic Salmonella agar (Liofilchem, Teramo, Italy) for *S. enterica*, and on O.A. Listeria agar (Liofilchem, Teramo, Italy) for *L. monocytogenes*. The plates were incubated at 37°C for 24h. Three independent experiments were performed for each species.

3.6 Genomic DNA extraction and PMA staining.

107-108 control or treated cells were stained with PMA (Biotium Inc., Hayward, CA, USA), at a final concentration of 50 µM, and incubated at room temperature in the dark for 5 min. Stained samples were then exposed to UV light for 5 min and centrifuged for 10 min at 12000 rpm. Cell pellets were stored at -20°C. Genomic DNA (gDNA) was extracted from unstained and PMA-stained samples using QIAGEN DNeasy Blood and Tissue Kit (Qiagen, Milan, Italy), according to the manufacturer's instructions. A modified protocol was used for L. monocytogenes: cells were incubated at 37°C for 1 hour with the enzymatic lysis buffer provided by the supplier. Cells were then incubated at 56°C for 30 min and were treated with RNAse A. After column purification, DNA was eluted with 100 µl of 10 mM Tris-HCl pH 8.0. DNA quality was assessed by 0.7% agarose gel electrophoresis, run at 70 V for 30 minutes and followed by ethidium bromide staining. DNA concentration and purity was assessed by measuring the absorbance at 260nm (A260) and the ratio of the absorbance at 260 and 280nm (A260/A280) with a NanoDrop ND-1000 spectrophotometer (Thermo Scientific, Wilmington, DE, USA).

3.7 Real-time quantitative PCR (qPCR)

Primer and Taqman probe set sequences targeting the *hlyA* and the *invA* gene were used for *L. monocytogenes* and *S. enterica* quantification, respectively (Suo *et al*.,

2010). The best candidate primers and probe sets for *E .coli* detection and quantification were designed in-house on the *uidA* marker gene with AlleleID7.0 software (PREMIER Biosoft International, Palo Alto, CA, USA). Primer sequences and their features are shown in Table 2. The reaction mixture contained 1x iQ^{TM} Multiplex Powermix (Bio-Rad Laboratories, Milan, Italy), 200 nM each primer, 200nM probe and 2 µl template gDNA (or 2 µl distilled H_2O for the no-template control) in a total volume of 25 µl. Each TaqMan PCR assay was performed in triplicate using a CFX96 Real Time PCR Detection System (Bio-Rad Laboratories, Milan, Italy), with the following cycling program: 3 minutes at 95°C, 15 seconds at 95°C and 1 minute at 60°C for 40 cycles. PCR results were analyzed using CFX Manager 1.1 software (Bio-Rad Laboratories, Milan, Italy). The correlation between PCR Ct values and gene copy numbers was obtained by means of a standard curve. The cell number equivalents were then extrapolated by taking in account the average bacterial genome size for each target bacterium available at NCBI (http://www.ncbi.nlm.nih.gov/genomes/MICROBES/microbial_taxtree.html"), assuming each gene is present in a single copy per genome. The number of gDNA copies for experimental samples was determined by using the inverse formula of linear equation of each species (DNA copies=$10^{[(Ct-q)/m]}$). The amplification efficiency for each primer/probe set was calculated as E=$10^{(-1/slope)}$-1 (Klein, 2002). Assays were performed in parallel on cell suspensions before and after PMA staining, in order to quantify total and intact cell number equivalents, respectively.

Table 2. Gene targets, primers and probes used for qPCR.

Oligo Name	Gene Target	Sequence (5'-3')	T_m (°C)	Dye (5'-3')	Reference
EC-uidAF	uidA	CTCTGCCGTTTCCAAATC			This work
EC-uidAR		GAAGCAACGCGTAAACTC			
EC-uidAP		AATGTAATGTTCTGCGACGCTCAC	70.1	HEX/BHQ1	
SE-invAF	invA	GTTGAGGATGTTATTCGCAAAGG			Suo *et al*., 2010
SE-invAR		GGAGGCTTCCGGGTCAAG			
SE-invAP		CCGTCAGACCTCTGGCAGTACCTTCCTC	69.0	FAM/BHQ1	
LM-hlyAF	hlyA	ACTGAAGCAAAGGATGCATCTG			Suo *et al*., 2010
LM-hlyAR		TTTTCGATTGGCGTCTTAGGA			
LM-HlyAP		CACCACCAGCATCTCCGCCTGC	70.0	TR/BHQ2	

Tm, melting temperature. Dyes refer to the reporter and quenching fluorophores linked to the TaqMan probe sequences

3.8 Flow cytometry (FCM)

Untreated and SC-CO_2 treated samples were diluted to 10^7-10^8 cells/ml and divided in two subsamples. 1 ml of each sample was stained with 10 µl SYBR-I (Merck, Darmstadt, Germany), at 1:30000 final concentration in DSMO, and 10 µl PI at 1 mg/ml (Invitrogen, Carlsbad, CA, USA) to quantify intact and permeabilized cells. The depolarized cells were measured adding10 µl of 1mM $DiBAC_4(3)$ (Invitrogen, Carlsbad, CA, USA), only *E. coli* depolarized cells emit green fluorescence and the percentage of depolarized cells was calculated using the total count measurements. Excitation and emission wavelengths were at λ_{ex}=495 nm, λ_{em}=525 nm for SYBR-I;λ_{ex}=536 nm, λ_{em}=617 nm for PI and λ_{ex}=490 nm, λ_{em}=516 nm for $DiBAC_4(3)$. Samples were incubated at room temperature, in the dark for 15 minutes. FCM analyses were performed with an Apogee-A40 flow cytometer (Apogee Flow Systems, Hertfordshire, UK) equipped with an Argon laser emitting at 488 nm. For each cell crossing the focus point of the laser, two light scattering signals and two fluorescence signals (green, FL1 and red, FL3) were collected. The Large Angle Light Scatter (LALS), measuring cell density or granularity (Müller and Nebe-von-Caron, 2010) and the Forward Angle Light Scatter (FALS), which is related to bacterial size (Foladori *et al*., 2008). LALS and FALS were collected on a 256-channel linear scale while fluorescence signals were collected with logarithmic amplifier gain. The conversion of FALS intensities into biovolumes was performed as proposed by Foladori *et al.* (2008). Non-fluorescent silica microspheres (MicroParticles GmbH, Germany) of different diameters were used to assess the calibration curve of FALS intensity used in bacteria sizing. Six sizes of silica microsphere with diameters ranging from 0.5 mm to1 mm were selected.

3.9 Phospholipid extraction

10^9 *E. coli* cells K12 MG1665 (control and treated) were collected by centrifugation at 6000 rpm for 10 min. The pellets were suspended into 500 µl of sterile water. 75 µl of internal standardphosphatidylcholin**(**PC, 12:0/12:0) solution (10 ng/µl)were add to each sample to normalized the amount of extracted phopholipids, then3ml of $CHCl_3$/CH_3OH (2:1) solution (Sigma-Aldrich Co., Milan, Italy; Carlo Erba, Milan, Italy) were added to each sample.Bacterial cells were disrupted by using an

Ultrasound processor S-4000sonicator (Misonix. Inc, Farmingdale, NY,USA) operating at 20 kHz. Each sample was subjected to two cycles of sonication with the following program: treatment time of 150 s; amplitude of 40; pulse time 3 s and pause time 2 s.The main parameters (transferred power, P;time, t; treated volume, V) were used to calculate the transferred specific energy as reference parameter, indicated afterward as Es and expressed in kJL^{-1} (Es=Pxt/V). Transferred power instead of applied power was used for Es calculation, in order to obtain results comparable with those obtained from different instruments. After sonication the samples were centrifuged for 10 min at 10000 rpm and at 4°C. The lower organic phase of each sample was recovered, brought to dryness and re-suspended in 650 µL of CD_3OD (99.90% purity) for ^{31}P-NMR and liquid chromatography-mass spectrometry (LC-MS) analyses.

3.10 NMR measurements

^{1}H-NMR (400.13 MHz) and ^{31}P-NMR (161.98 MHz) were recorded at 300 K on a Bruker-Avance 400 MHz NMR spectrometer in CD_3OD (99%, Aldrich) by using a 5 mm BBI probe. The ^{1}H and ^{31}P chemical shift scales (δ) were calibrated on the residual proton signal of CD_3OD (δ_H = 3.310 ppm) and on the signal of PC 18:1/18:1 (δ_P -0.55 ppm), respectively. Composite pulse decoupling was used to remove any proton coupling in ^{31}P-NMR spectra. Generally, 4000 free induction decays were processed using an exponential line broadening of 0.3 Hz prior to Fourier transformation. Probe temperature was maintained to ±0.1 °C by a Bruker B-VT 1000 variable temperature unit. Resulting 1D NMR spectra were analyzed by MestreNova 8.1 software (Mestrelab research S.L.2012, Escondido, CA).

3.11 RPLC-IT-ESI-MS analysis

The raw methanol extract was analyzed by LC-MS using a Hewlett-Packard Model 1100 series liquid chromatograph coupled to a Bruker Esquire-LC^{TM} quadrupole ion-trap mass spectrometer (Bruker-Franzenm, Bremen, Germany) equipped with electrospray ion source (ESI). The ESI was operated in positive mode for phosphatidylcholine (PC) analysis and in negative mode for phosphatidylglycerol (PG) and phosphatidylethanolamine (PE) analysis. The chromatographic separation of

phospholipids was carried out at room temperature on a Kinetek^{TM} C18 column (length: 100 mm; particle size: 2.6 µm; internal diameter: 2.1 mm; pore size: 100 Å) purchased by Phenomenex (Torrence, Ca, USA). The solvent system consisted of A, CH_3OH/H_2O 7:3 containing 12 mM ammonium acetate and B, CH_3OH also containing 12 mM ammonium acetate. The linear gradient, at a constant flow rate of 1.0 mL/min, started from 30% B to reach 100% B in 40 min, followed by column wash using 100%B for 15 min and column re-equilibration at starting conditions. Nebulizer gas was high purity nitrogen at a pressure of 20-30 psi, at a flow of 6 L/min and 300°C. The mass spectrometer scan range was 13,000 units per second in the range 50-1500 *m/z*. Relative proportions of fatty acids ranging from C16:0 to C34:0 were calculated from peak areas.

3.12 Gene expression analyses

Three replicates of control and treated samples were harvested during exponential phase at $O.D_{600}$ of 0.6 and were pelleted by centrifugation (6,000 g for 5 min at 4°C). Total RNA was isolated from bacterial pellets by using the RNeasy Mini Kit (Qiagen, Milan, Italy) as described by the manufacturer. RNA concentration and purity were determined by UV absorption (260:280 nm) using a NanoDrop ND-1000 spectrophotometer (Thermo Scientific, Wilmington, DE, USA) and 0.8% agarose gels stained with ethidium bromide.1 µg of RNA was reverse-transcribed into cDNA using First Strand cDNA Synthesis Kit (Fermentas, Milan, Italy). cDNAs were amplified by real-time PCR using Kapa Sybr Fast qPCR Mastermix (KapaBiosystems, Resnova, Rome, Italy) using a CFX96 Real Time PCR Detection System (Bio-Rad Laboratories, Milan, Italy). PCR conditions were as follows: 95°C for 3 min, 40 cycles of 15 sec at 95°C, 30 sec at 60°C and 5 sec at 75°C, with a final melting curve analysis from 75°C to 95°C, with increments of 1°C every 5 sec. Real-time PCR amplifications were performed with three experimental replicates for each sample. Primers were designed by using AlleleID7.0 software (PREMIER Biosoft International, Palo Alto, CA, USA). Primers sequences are reported in Table 3. Each primer pair was controlled for dimer formation by melting curve analysis and PCR efficiency was calculated over a five-fold dilution series. The *gyrA* and *mdoG* genes were used as housekeeping genes (Heng *et al*., 2011). Amplification profiles were analyzed using BioRad Manager Software (Bio-Rad Laboratories, Milan, Italy) and cycle threshold (Ct) values for each target gene

were normalized to the geometric mean of the Ct of *gyrA* and *mdoG* amplified from the corresponding sample. The fold-change of target genes for each strain respect to untreated samples was calculated using the delta-delta Ct method.

Table 3. Primer sequence for gene expression analysis

Target gene	**Forward (5'-3')**	**Reverse (5'-3')**
Plsb	CCTACCTTAACCAGCATG	CGGCAGCAATATTATTGAC
CdsA	ACAGCTTAGCGGTTTTAC	GCAACAGAAAAAGCATCAG
PssA	GAGCAGAAACTAACCATC	CGCAGATTGATCTCATAG
PgsA	GTGGCAGATAAAGTTCTC	TAGCGCAGAAATAATAATTTC
Psd	CCGAATGTACTGGTCATG	GAGGTAAGTGGTCACAAAC
PgpA	TTCGGAAGTGGATTAAGC	CCGTTTGATGACAAAGATAG
PgpB	GGCGTTAAATCCTGGATC	TCAGCCAACTGTTCTTTC
PgpC	ACCGATTATAGCCATTGC	GTCTGTAAACGTGCTTCG
Housekeeping gene		
gyrA	TCTGGATTATGCGATGTC	TTGCCTAGTACGTTCATG
mdoG	CCGGGTAAAGAGATGAAC	CCACAAAGGCGATAGTAC

Chapter 4: **Development of bacterial viability assays and their application to evaluate SC-CO_2 treatment efficiency**

4.1 Comparison of viability assays on pure liquid culture

The SC-CO_2 treatments using the multi-batch apparatus described by Mantoan and Spilimbergo (2011) were performed on pure liquid culture of three important food-borne pathogens: *Listeria monocytogenes*, *Escherichia coli* and *Salmonella enterica*.

Flow cytometry experiments coupled with SYBR Green I (SYBR-I) and Propidium Iodide (PI) (Ziglio *et al*., 2002) and Propidium monoazide qPCR (PMA-qPCR) assay (Nocker and Camper, 2006) were set up for the three bacterial species. Both viability assays are based on membrane integrity and were applied to evaluate the efficiency of SC-CO_2 treatment, overcoming the limits of plate counts. Data from FCM and PMA-qPCR were compared with plate counts and fluorescent microscopy to evaluate which method is the most appropriate to correctly discriminate viable from dead cells after treatment. The obtained results were published in the following article: Tamburini, S., Ballarini, A., Ferrentino, G., Moro, A., Foladori, P., Spilimbergo, S., Jousson, O: "**Comparison of quantitative PCR and flow cytometry as cellular viability methods to study bacterial membrane permeabilization following supercritical CO_2 treatment"** (*Microbiology* 159, 1056–1066, 2013) (Appendix: Publication A).

Plate counts revealed >5 log of bacterial inactivation after 60 min of treatment, but this method probably overestimate the level of bacterial inactivation, since VNBC cells escape detection by cultural methods. PMA-qPCR and FCM produced strongly correlated results for two out of three bacterial species tested, which was expected as both methods quantify cellular subpopulations on the basis of membrane permeability. FCM analyses highlighted a diverse effect of the treatment on the level of membrane permeabilization of *L. monocytogenes* compared with *E. coli* and *S. enterica*. The FCM assay showed the best performance as a bacterial viability test method as it allowed not only to quantify the efficiency of treatment rapidly and with high sensitivity, but also to discriminate the subpopulations of partially-permeabilized cells from totally-

permeabilized cells and identify variations in biovolume and alterations of the cellular surface.

4.2 Evaluation of SC-CO_2 treatment on synthetic solid substrate

PMA-qPCR and FCM coupled with SYBR-Green I and Propidium Iodide analyses were also performed on *L. monocytogenes*, *E. coli* and *S. enterica* spiked on synthetic solid substrates before and after SC-CO_2 treatment at 120 bar, 35°C and up to 60 min to simulate the action of treatment on solid food products.

4.2.1 Bacterial membrane permeabilization evaluated by PMA-qPCR

TaqMan qPCR analyses were performed on gDNA samples extracted from cell homogenized suspensions before and after PMA staining, to quantify both total and intact cell unit equivalents before and after SC-CO_2 treatment (Table 4). qPCR is a highly sensitive method able to detect fewer than 10 genome equivalents per reaction and is therefore the technique of choice for quantification of microorganisms at low concentrations. qPCR data revealed that a large fraction (97%) of *L. monocytogenes* cells were permeabilized by the treatment after 15 min, whilst 94% of *E. coli* cells were permeabilized after only 5 min. The percentage of *E. coli* cell permeabilization increased up to 98.6% after 45 min of treatment. Also a large fraction of *S. enterica* (more than 80%) cells were permeabilized after only 5 min, but the fraction of permeabilized cells did not exceed 90% at successive time points.

Table 4. Target gene copy numbers determined by qPCR following SC-CO_2 treatment.

Species and fluorophores	Treatment time (min)	Target gene copy numbers		
		-PMA (Total cell equivalents)	+PMA (Intact cell equivalents)	% Intact cells reduction
L. monocytogenes hlyA (Texas Red)	0	$3.42x10^8$±0.06	$3.47x10^8$±0.85	NA
	5	$3.50x10^8$±1.04	$3.66x10^8$±1.83	NA
	15	$9.36x10^7$±0.55	$6.99x10^6$±0.01	97.94±0.51
	30	$2.56x10^7$±0.27	$3.67x10^6$±0.54	98.93±0.11
	45	$1.17x10^7$±0.20	$3.70x10^6$±0.82	98.93±0.02

Continue

	60	$4.48x10^7$±0.47	$1.34x10^7$±0.12	96.07±0.61
E. coli uidA (HEX)	0	$2.18x10^8$±0.52	$3.63x10^8$±0.46	NA
	5	$7.36x10^7$±1.11	$1.89x10^7$±0.31	94.79±0.20
	15	$9.69x10^7$±1.37	$9.93x10^6$±3.02	97.29±0.49
	30	$5.46x10^7$±0.72	$7.00x10^6$±1.84	98.09±0.27
	45	$4.74x10^7$±0.53	$4.77x10^6$±1.56	98.70±0.27
	60	$2.53x10^7$±0.02	$5.08x10^6$±1.71	98.62±0.30
S. enterica invA (FAM)	0	$8.07x10^7$±0.51	$1.03x10^8$±0.23	NA
	5	$3.07x10^7$±0.82	$1.98x10^7$±0.07	80.44±3.72
	15	$2.01x10^7$±0.35	$1.07x10^7$±0.04	89.39±1.95
	30	$1.68x10^7$±0.29	$9.99x10^6$±0.70	90.16±1.54
	45	$2.91x10^7$±0.65	$2.75x10^7$±0.43	73.22±1.83
	60	$2.85x10^8$±0.15	$9,01x10^6$±2.28	91.30±0.24

The average target-gene copy number were repeated in triplicates for each species and each treatment time. The percentages of intact cells reduction were calculated as the ratio of treated PMA-stained cells relative to untreated

4.2.2 Detection of intact and permeabilized cells by FCM

Homogenized suspensions of untreated and SC-CO_2 treated bacteria, spiked on synthetic solid substrates, were stained with SYBR-I and PI and analyzed with FCM counting viable (intact) and dead (permeabilized) cells. The detection limit of the flow cytometer used in this study is approximately 1 cell per µl. Fluorescent signals acquired for each bacterial cell were plotted in a two-dimensional dot plot, where the horizontal axis shows the green fluorescence intensity (FL1) emitted by SYBR-I, and the vertical axis shows the red fluorescence intensity (FL3) emitted by PI (Figure 3.1). Upon staining four regions could be distinguished in the two-dimensional dot plot. The two regions on the right included a region of intact cells, emitting only high FL1 intensity due to the absence of intracellular PI, and a region of partially-permeabilized cells emitting high fluorescent intensity both in FL1 and FL3 channels, due to incomplete FRET between SYBR-I and intracellular PI. The two regions on the left included one with totally-permeabilized cells emitting only high FL3 intensity, due to the simultaneous presence of SYBR-I and PI in the cells and complete FRET, and one due to noise caused by non-biotic particles emitting FL1 and FL3 signals lower than the instrument background threshold. The kinetics of cell membrane permeabilization was specific for each bacterial species (Figure 3.1) and the percentage reported in each quadrant of each cytogram represent the proportion in percentage of each subpopulation. With regards to *L. monocytogenes*, the percentage of intact cells was 98.4% in the untreated suspension and after only 5 min of treatment most of *Listeria*

cells (97.8%) moved from the region of intact cells to the one of permeabilized cells. After 15 min of treatment the percentage of permeabilized cells reached the maximun value (99.3%). Surprisingly, a small fraction of cells (8-9%) was intact after 30 and 60 min of treatment as if in the range of 30 min same cells were replicated during the treatment.

After only 5 min of treatment the most of *E. coli* cells moved from region of intact cells to one of partially-permeabilized (93.3%) and a small fraction of cells moved to the region of permeabilized cells (6%). After 15 min a fraction of partially-permeabilized cells became permeabilized (26.6%). As for *E. coli* cells also for *Salmonella* cells most of them were partially-permeabilized (68.6%) and permeabilized (29.6%) after 5 min of SC-CO_2 treatment, and by increasing the treatment time, the permeabilized cells increased up to 64.9%.

For all three bacterial species 15 min of the treatment at 120 bar and 35°C seemed to be the best condition to permeabilize all most of the bacterial cells (>99%).

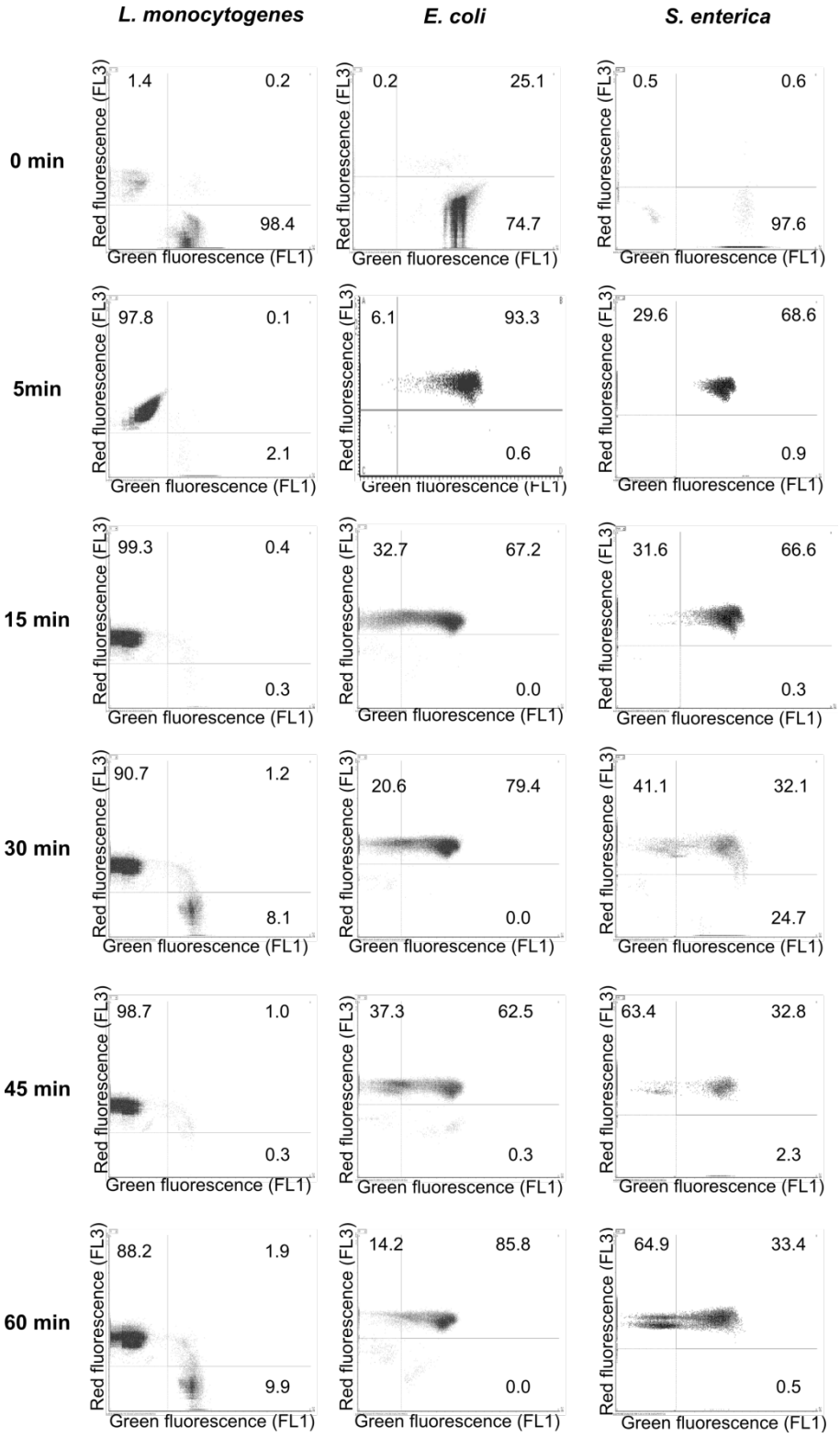

Figure 3.1. Membrane permeabilization observed by FCM assay upon SC-CO_2 treatment. The percentages of intact, partially-permeabilized and permeabilized cells are shown within each cytogram quadrant.

4.2.3 SC-CO_2 treatment induces disruption of a fraction of bacterial cells

The concentration of bacterial cells in untreated samples was compared with the bacterial concentration in SC-CO_2 treated samples. After 5 min of treatment the concentration of bacterial cells decreased in all three species, by 62% for *L. monocytogenes*, by 34.3% for *E. coli* and by 16% for *S. enterica*. The fraction of disrupted cells was compared to the intact, partially-permeabilized and permeabilized cell subpopulations for each treatment time, the percentage of each subpopulation was re-calculated and plotted in Figure 3.2. After 15 min of treatment 84% of *L. monocytogenes* cells were disrupted and about 15% were permeabilized. The same data was obtained after 45 min, whilst at 30 min and 60 min a small part of cells, 1.7% and 2.4%, respectively, remained intact (Figure 3.2a). The treatment seemed to be less efficient *E. coli* respect to *L. monocytogenes*; on average 40% of cells were permeabilized during the treatment and the remained cells were partially-permeabilzed and permeabilized (Figure 3.2b). Only 15% of *S. enterica* cells were disrupted after 15 min of treatment, 58% were partially-permeabilized and 27% were permeabilized. After 30 min it seemed that a fraction of cells grew in the reactor, but after 45 min also these cells were permeabilized (Figure 3.2c).

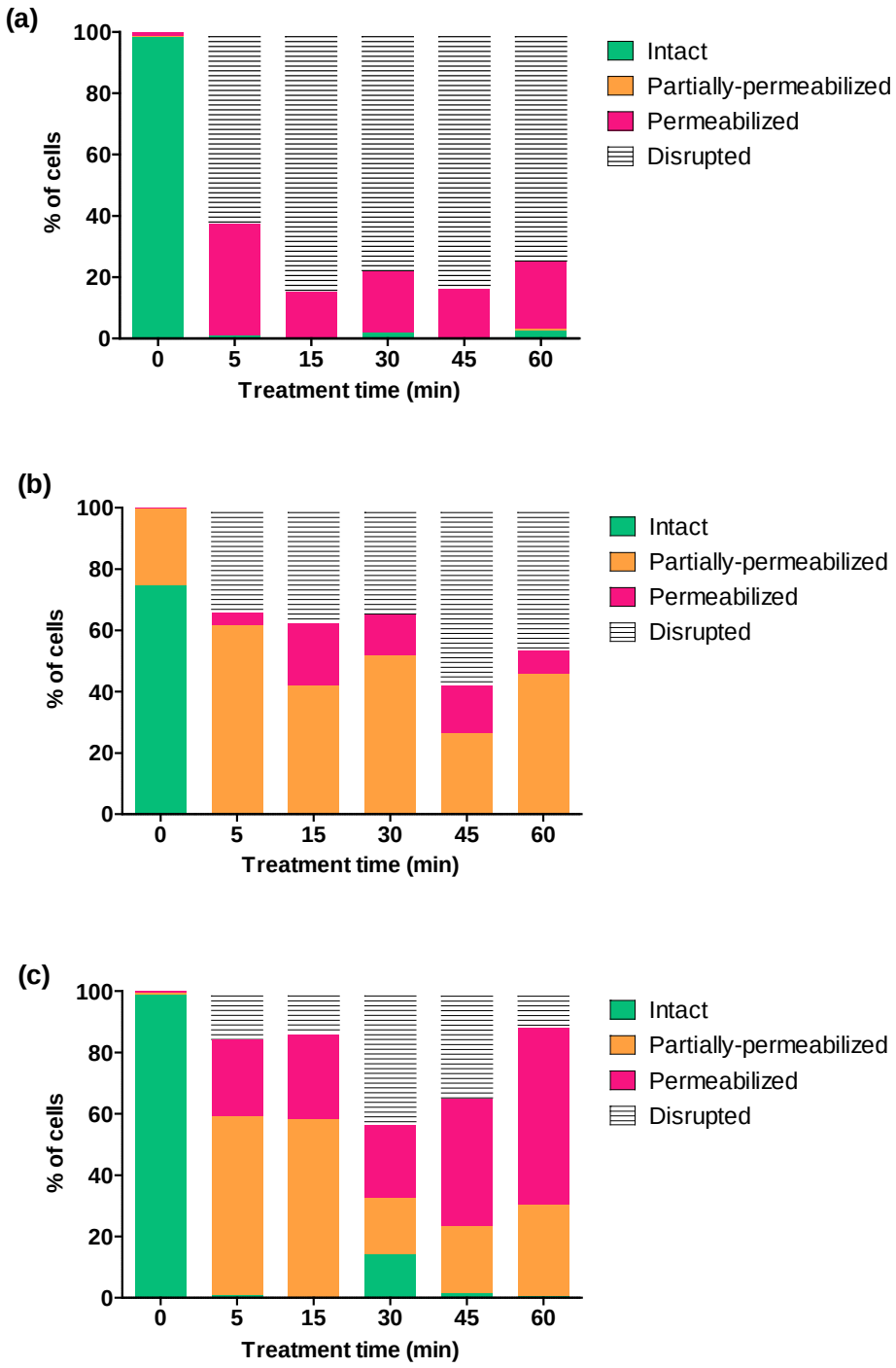

Figure 3.2. Percentages of bacterial cells subpopulations before and after SC-CO_2 treatment at 120 bar, 35°C up to 60 min. (a) *L. monocytogenes*; (b) *E. coli* and (c) *S. enterica*.

4.2.4 Morphological changes evaluated by FALS and LALS signals

FCM analysis collected two light scattering signals simultaneously from each bacterial cell: the forward-angle light scatter (FALS), which is related to bacterial size (Foladori *et al.*, 2008), and the large-angle light scatter (LALS), measuring cell density or granularity (Müller and Nebe-von-Caron, 2010).

The scattering signals of untreated and SC-CO_2 treated samples were overlapped for each bacterial species (Figure 3.3). The signal from untreated and treated cells is shown in green and in purple, respectively. The FALS and LALS signals were referred to an arbitrary scale divided in 256 channels. All tree bacterial species showed a shift of the peak signals after SC-CO_2 treatment. The FALS mean channel of untreated *L. monocytogenes* cells was 31, whilst the channel of treated cells 13. The peak of untreated and treated *E. coli* cells shifted from 137 to 94, whilst the peak of *S. enterica* cells shifted from 118 to 35. SC-CO_2 treatment induced a reduction of biovolume in all three species, *L. monocytogenes* by 58%, *E. coli* by 32%, and *S. enterica* by 70%.

A significant shift of the LALS medium channels was observed for *L. monocytogenes* and *S. enterica* cells; the complexity of cells decreased of 38% and 42%, respectively. *E. coli* cells did not show a significant shift of LALS media channel.

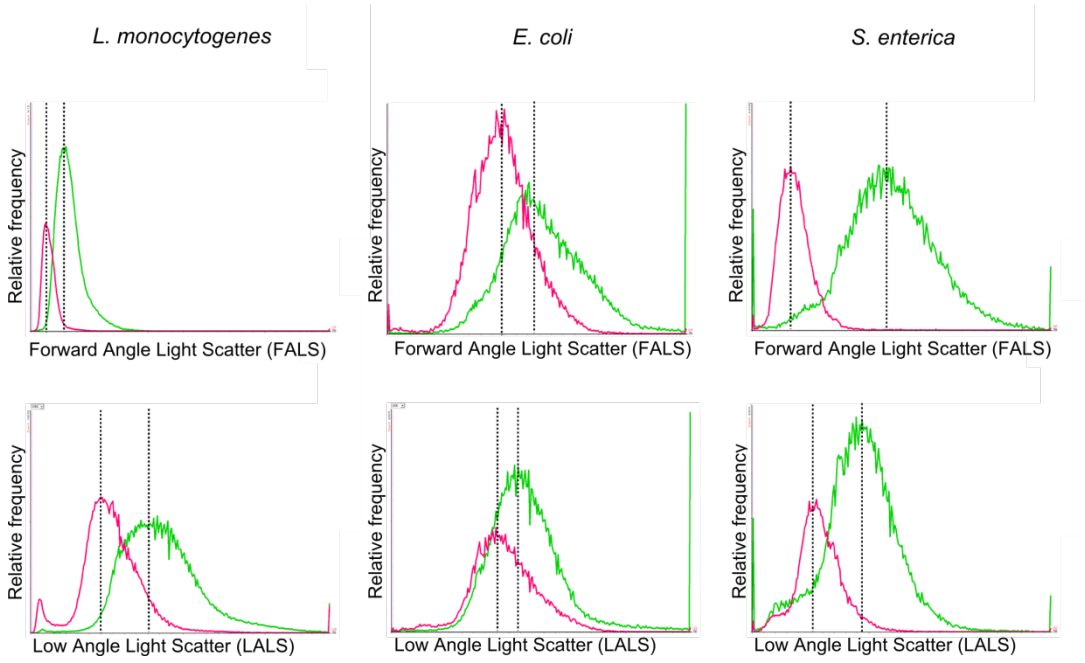

Figure 3.3. Scattering signals FALS and LALS obtained by FCM analysis of *L. monocytogenes*, *E. coli* and *S. enterica* before and after 5 min of SC-CO_2 treatment at 120 bar and 35°C. The signals from untreated cells are in green; signals from SC-CO_2 treated cells in purple.

4.2.5 Comparison between PMA-qPCR and FCM methods to evaluate cell viability

The results obtained by qPCR and by PMA-qPCR were expressed as number of total and intact equivalent cells per ml, respectively, whilst the results obtained by FCM were expressed as total and intact cells per ml. These results were compared in Figure 3.4. The same general trend was obtained with both viability assays, with the exception of *L. monocytogenes* after 5 min of treatment. Pearson correlation coefficients (r) were calculated to determine if the two viability assays are correlated. High and good correlations were obtained for *E. coli* and *S. enterica* cells (r=0.99 and 0.96, respectively). The correlation for *L. monocytogenes* was poor (r=0.60), but excluding the inconsistent data point (5 min of treatment) the correlation coefficient became high (r=0.99).

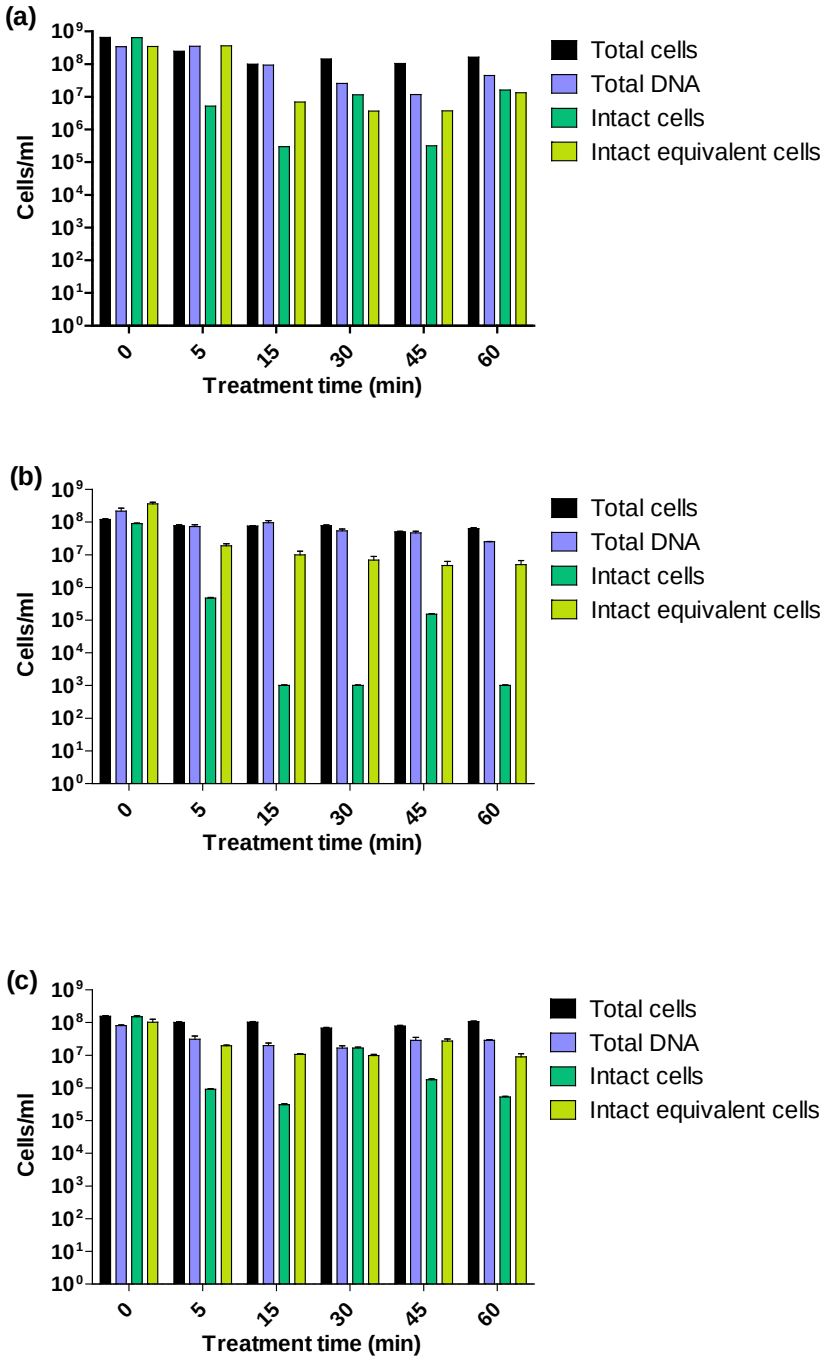

Figure 3.4. Number of total and viable or intact cells monitored during SC-CO_2 treatment and inferred from qPCR and FCM for *L. monocytogenes* (a), *E. coli* (b) and *S. enterica* (c). Error bars represent standard deviations from three replicates.

4.3 Comparison of SC-CO_2 treatment efficiency between liquid cultures and synthetic solid substrate

The FCM analysis of bacterial cells treated in liquid cultures showed that the ability of the fluorescent dyes to enter the cells depends on the level of outer membrane permeabilization for SYBR-I and on the level of both outer and cytoplasmic membrane permeabilization for PI. Upon staining with SYBR-I, untreated *E. coli* and *S. enterica* cells spiked on synthetic solid substrate showed a green fluorescent signal brighter than the signal of untreated cells in liquid broth (Figure 3.5), whereas *L. monocytogenes* cells did show any significant difference. In addition, treated bacterial cells spiked on synthetic substrate showed a significant shift of both FALS and LALS signals, indicating biovolume reduction and surface alteration after 5 min of treatment.

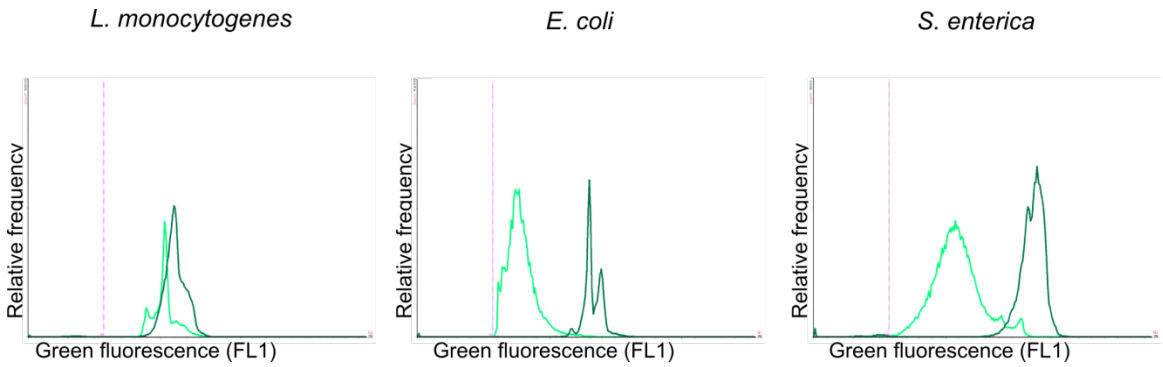

Figure 3.5. The FL1 green fluorescent signals of untreated bacterial cells in liquid broth (light green line) and spiked on synthetic solid substrate (dark green line) after SYBR-I staining were overlapped.

The data obtained by FCM and PMA-qPCR before and after SC-CO_2 treatment for the three bacterial species treated in liquid cultures and spiked on synthetic solid substrate were compared and expressed as percentages of bacterial inactivation (Figure 3.6). The SC-CO_2 treatment was more efficient when applied on bacterial cells spiked on synthetic solid substrate rather than on cell suspensions. Most of the cells of the three species spiked on synthetic solid substrate were inactivated after only 5 min, whilst the inactivation in liquid broth required at least 30 min of treatment.

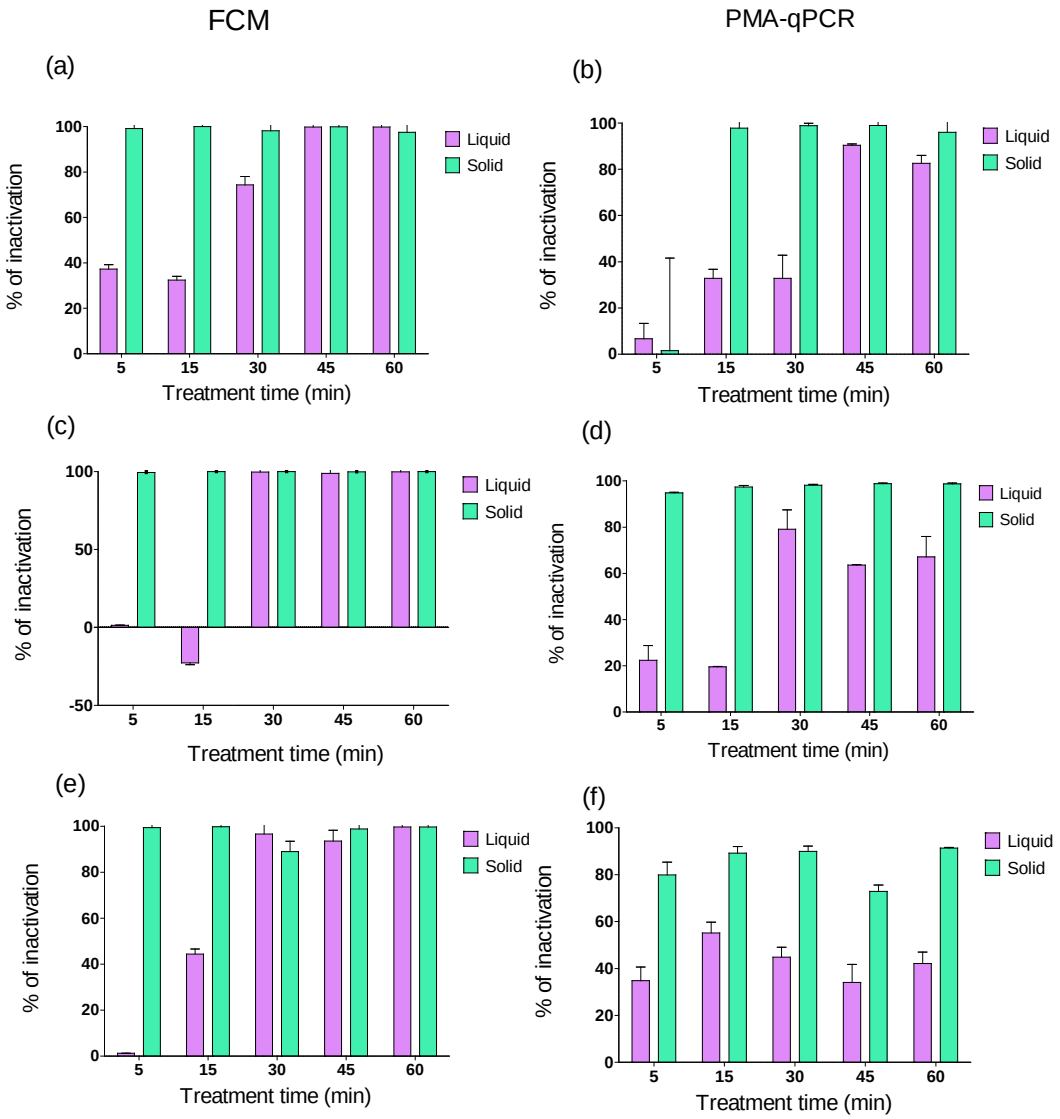

Figure 3.6. The efficiencies of SC-CO_2 treatment on bacterial cells in liquid culture and spiked on synthetic solid substrate were compared; percentage of bacterial inactivation of *L. monocytogenes* (a,b), of *E. coli* (c,d) and of *S. enterica* (e,f).

Spilimbergo *et al*. (2010a) reported that the utilization of a stirring system during SC-CO_2 treatment of liquid culture is important to homogenize the sample and increase the surface of contact between cells and dense CO_2. Stirring likely increase the rate of dense CO_2 dissolution inside the liquid phase. The action of SC-CO_2 on solid substrate was more efficient, presumably because the supercritical fluid acted directly on bacterial cells without the need to dissolve in the liquid phase. Batch tests showed that the bacterial inactivation in liquid proceeds in two phases: the early one is characterized by a slow rate of reduction of microbes number, which then sharply decrease at a later stage, confirming previously published results (Dillow *et al*., 1999). Conversely, on

solid substrate the first stage of inactivation proceeds at a fast rate of bacterial inactivation and the second one at a slow rate.

Chapter 5: **Bacterial inactivation on solid food products**

The SC-CO_2 process is less applied to solid foods than to liquid products, due to the complexity of the matrix, which can make the CO_2 bactericidal action less efficient, and to the lack of document edevidence about the inactivation mechanism (Ferrentino and Spilimbergo, 2011). The process has been applied to different kind of solid foods including meats (Erkmen *et al*., 2000; Meurehg g*et al*., 2006), vegetables (Kuhne and Knorr, 1990;Zhong *et al.*, 2008), alfalfa seeds (Mazzoni *et al*, 2001; Jung *et al*., 2009), fruits (Haas *et al*., 1989; Valverde *et al*., 2010), and fish (Meujo *et al*., 2010), but the bacterial inactivation has been mainly evaluated by using only standard cultivation-based methods (Jung *et al*., 2009; Bae *et al*., 2011). Although cultivation methods are applied routinely, they may lead to strong underestimations of the real concentration of microorganisms in the analyzed samples (Keer and Birch, 2003; Oliver, 2005). Some bacterial species, when exposed to environmental stress (e.g. nutrient limitation, pressure, temperature), may become no more cultivable although remaining alive, becoming even more resistant to stress (Bogosian and Bourneuf, 2001; Oliver, 2010).

In this thesis, FCM and PMA-qPCR analysis were applied to evaluate the efficiency of SC-CO_2 treatment on viable and viable but not cultivable (VBNC) cells of three important common food-borne pathogens spiked on solid fresh food products. The exact function of the VBNC state in bacteria and the mechanisms to reach it are currently unknown and could differ from bacterium to bacterium. In the VBNC state, pathogens could survive in environmental matrices over one year and maintain the capability to develop diseases in their host (Oliver 2010). Improving health risk assessment associated with the increasing consumption of minimally processed fresh food products is a crucial need. To reach this objective, the development and standardization of fast and accurate cultivation-independent assays (FCM and PMA-qPCR) providing cellular and molecular information on microorganisms associated with food products are required.

5.1 SC-CO_2 inactivation of *Escherichia coli* spiked on fresh cut carrots

Carrot (*Daucuscarota L.*) is among the top-ten most economically important vegetable crops in the world, since it is a good source of natural antioxidants such as carotenoids and phenolic compounds and is consumed all year around (Simon *et al*., 2008) as fresh but also as ready-to-eat (RTE) product. Carrot cut or grated carrot is widely used in ready-to-eat salads, and preservation and safety of RTE products has become one of the main issue for the food industry. Maximum level of *E. coli* inactivation on fruits and vegetables required by EU normative is < 20 CFUs/g (Regulation (EC) No. 2073/2005). *E. coli* cells with high load were spiked on fresh cut carrots to evaluate the maximum efficiency of treatment. The best SC-CO_2 conditions to treat this fresh vegetable have been tested on their natural flora by Splimbergo *et al*. (2012). The manuscript submitted to *International Journal of Food Microbiology* with the title: "**Flow cytometry as an accurate tool to monitor *E. coli* subpopulations on solid food products after SC-CO_2 treatment" (**Tamburini, S., Foladori, P., Ferrentino G., Spilimbergo S., Jousson O.) is included at the end of this document (Appendix: Publication B) The article reports the development of protocols to identify the FCM profiling of *E. coli* cells spiked on carrots and the inactivation kinetics obtained by plate counts and FCM analysis to quantify the viable and VBNC *E. coli* cells during the treatment.

5.2 SC-CO_2 inactivation of *Salmonella enterica* spiked on coconut

Coconut (*Cocos nucifera L.*) is one of the 10 most exploited tree species worldwide as primary source of food, drink, and shelter. The white meat (flesh) of the nut can be eaten either raw or shredded and dried as an ingredient in a wide variety of foods from cakes to beverages. Similar to other fruits that are consumed raw, coconut can be a source of pathogenic or spoilage bacteria (Strawn *et al*., 2011). EU normative (2005) states that in 25 grams samples of fruits or vegetables *Salmonella* must not be detected. SC-CO_2 conditions to inactivate natural flora of coconut have been evaluated by plate count methods (Ferrentino *et al*., 2012a) and sensorial analyses have showed that were not detected significant differences in terms of texture, taste, appearance, and

aroma; however, color instrumental analyses reported significant differences in lightness between control and treated samples (Ferrentino *et al*., 2013).

5.2.1 Inhibition of S. enterica cells to grow

The inactivation kinetics of *Salmonella enterica* spiked on fresh cut coconut at 120 bar, 40 and 50°C as a function of the treatment time ranging from 5 to 60 min measured with plate counts are reported in Figure 4.1.The inactivation rate increased with the treatment time: at 120 bar, 50°C, 60 min, 99.9% (5 Log) of microbial inactivation was achieved. The results also indicated that changing the temperature from 40 to 50°C did not significantly increase the inactivation rate.

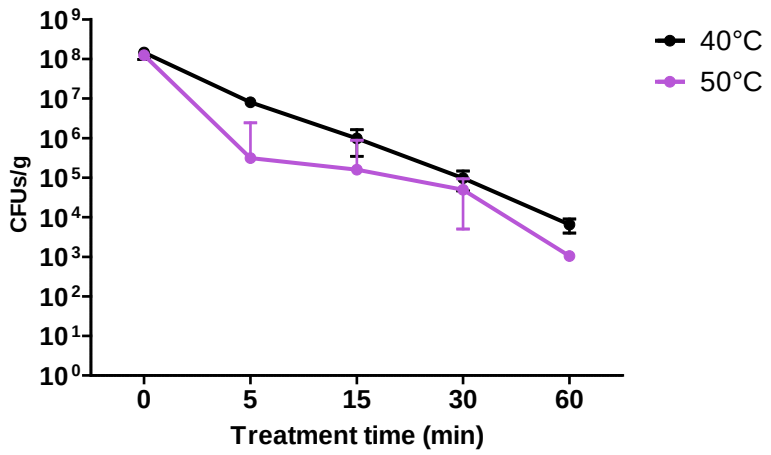

Figure 4.1. Inactivation kinetics of *Salmonella enterica* spiked on fresh cut coconut expressed as CFUs per gram.

5.2.2 Salmonella profiling by FCM and SC-CO_2-induced inactivation

Homogenized suspensions of *S. enterica* spiked on fresh coconut surface were stained with SYBR-I and PI and analyzed with FCM to detect both the profiles of natural microbial flora of coconut and *Salmonella* cells. The FCM scattering profiling was used to distinguish *Salmonella* cells from coconut debris. Referring to an arbitrary scale divided in 256 channels, the FALS histogram of *Salmonella* cells was used to discriminate the bacterial cells from other particles that emit green and red fluorescence. Green (FL1) and red (FL3) fluorescent signals acquired for each bacterial cell were plotted in a two-dimensional dot plot (cytogram). The populations of coconut debris

with auto-fluorescence or unspecific staining are indicated in gray whilst the population of *Salmonella* cells particles with bacteria size is in red (Figure 4.2). Most of *Salmonella* cells were intact (99.8%) at t=0, and after 15 min 94.3% of cells were partially-permeabilized. No further permeabilization was observed by increasing treatment time.

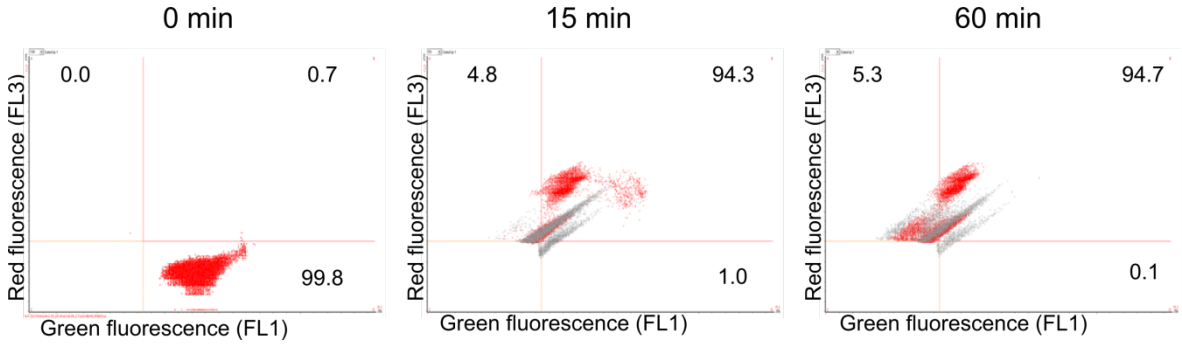

Figure 4.2 Cytograms of *Salmonella* cells spiked on fresh coconut untreated and SC-CO_2 treated at 120 bar and 50°C up to 60 min. The *Salmonella* population e particles with bacteria size are in red, and the debris in gray.

After 5 min of SC-CO_2 treatment, the total cell concentration strongly decreased of more than 50%. The fraction of disrupted cells was compared to the intact, partially-permeabilized and permeabilized cell populations for each treatment time. The respective percentages are plotted in Figure 4.3. A large disruption of bacterial cells occurred even in the first 5 min of treatment and within 15 min the second one. The increase of the exposure to the treatment did not carry out a further reduction of the percentage of intact cells.

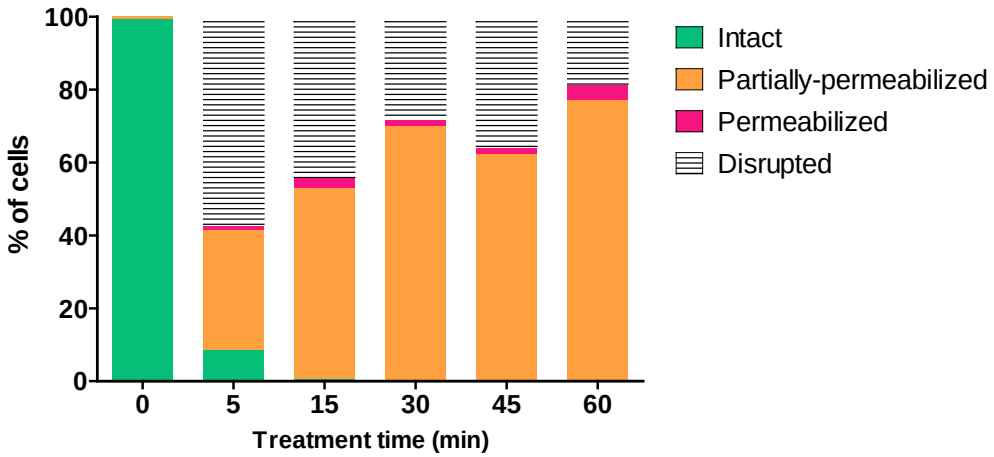

Figure 4.3. Fraction of intact, partially-permeabilized, permeabilized and disrupted cells of *Salmonella* spiked on fresh cut coconut. The samples were treated with SC-CO_2 at 120 bar and 50°C up to 60 min.

5.2.3 PMA-qPCRquantification of intact equivalent Salmonella cells and degraded DNA

InvA gene was selected as target gene to detect and to quantify *S. enterica* by qPCR. Fresh cut coconut pieces spiked with *Salmonella* were treated with SC-CO_2 at 40°C and50°C up to 60 min. The TaqManq PCR analyses were performed on gDNA samples extracted from homogenized suspensions before and after PMA staining, to quantify both total *invA* gene copies and *invA* gene copies from intact *Salmonella* cells. Both values decreased after SC-CO_2 treatment suggesting that, besides cellular permeabilization, SC-CO_2 also induces, directly or indirectly, the degradation of genomic DNA. The treatment at 40°C affected significantly *Salmonella* cells after 60 min (Figure 4.4a). Inversely, the treatment at 50°C showed a reduction of the 75% of intact equivalent cells after only 5 min and gDNA copies reduction of more than 50% (Figure 4.4b).

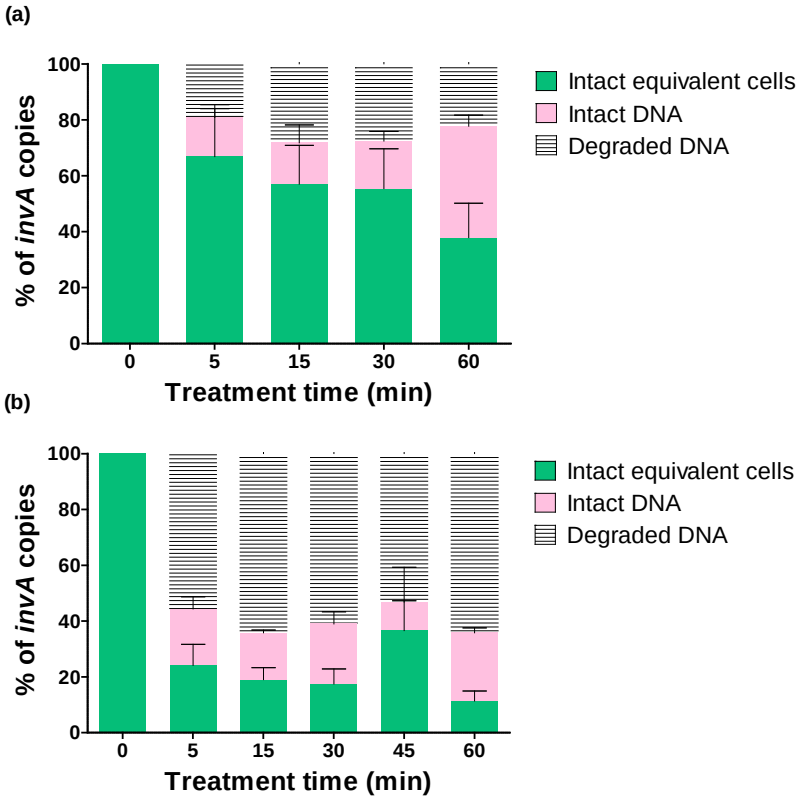

Figure 4.4. Fraction of intact equivalent cells, intact DNA and degraded DNA of *Salmonella* cells spiked on fresh cut coconut treated at 120 bar and (a) at 40°C and (b) 50°C up to 60 min.

5.2.4 Comparison of cultivable, intact and equivalent intact Salmonella cells

The cultivable *Salmonella* cells spiked on fresh cut coconut were compared with intact cells (considered as viable) obtained by FCM and intact equivalent cells obtained by PMA-qPCR (Figure 4.5). Cultivable cells obtained by plate counts were expressed as CFUs per gram, the intact cells obtained by FCM were expressed as intact cells per gram whilst the intact cells obtained by PMA-qPCR were expressed as intact equivalent cells per gram. After 60 min at 50°C the maximal *Salmonella* reduction (5 Log) was obtained by plate count, but 10^3 *Salmonella* cells remained cultivable. FCM data reported 10^5 intact *Salmonella* cells per gram (3 log reduction), indicating that about 10^2 *Salmonella* cells entered in the VBNC state. PMA-qPCR data showed only 2 Log of cell inactivation.

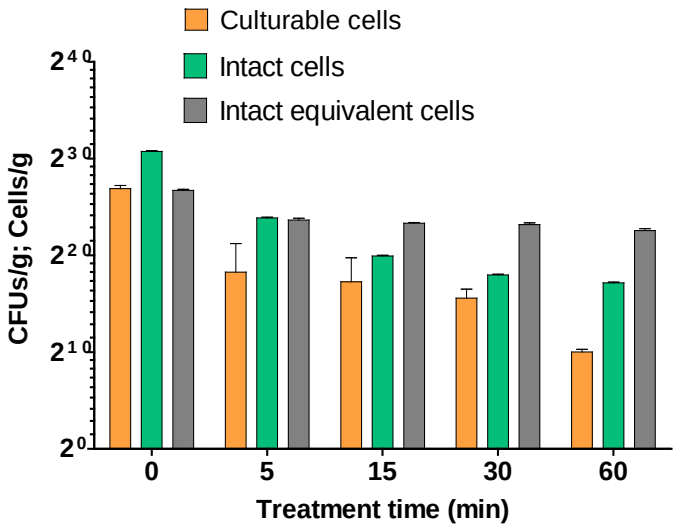

Figure 4.5. Viable cells per gram of *Salmonella enterica* afterSC-CO_2 treatment at 120 bar and 50°C evaluated with plate count, PMA-qPCR and FCM.

5.3 SC-CO_2 inactivation of *Listeria monocytogenes* spiked on dry cured ham

Dry cured ham prepared in small portions, slices or pieces, and obtained from the processed raw product is one of the most diffused RTE product provided by the meat industry (Toldra, 2004). During the post-processing procedures of cutting, slicing and repackaging dry cured ham can be easily contaminated by pathogenic *Listeria monocytogenes*, since once established on food processing equipment, it is very difficult to eliminate it (Møretrø and Langsrud, 2004). Elimination or reduction of *L. monocytogenes* is a compulsory step before marketing the product. Some countries such as USA (CFSAN/FSIS 2003), Australia and New Zealand (ANZFA 2001) accept only *L. monocytogenes*-free RTE meat products. In the European Union the criterion "not detected in 25 g" is applied before the product leaves the production plant (European Commission, 2005).The SC-CO_2 parameters for total *Listeria* inactivation have been tested preserving the overall acceptability and sensory quality of the dry cured ham (Ferrentino *et al*., 2012b), but re-growth phenomena could be not excluded.

5.3.1 Inhibition of L. monocytogenes growth

The inactivation by SC-CO_2 treatment of cultivable *L. monocytogenes* cells spiked on cubes of dry cured ham was evaluated quantifying bacterial cells able to replicate by plate counts. A set of experiments at 45°C or 50°C, and 80 or 100 bar were performed to evaluate the best conditions for bacterial inactivation, expressed as $Log_{10}(N/N_0)$ as a function of treatment time (Figure 4.6).

At 120 bar, either at 45°C or 50°C, the total inactivation to undetectable levels (about 8 Log reduction) was obtained in 30 min and 15 min, respectively.

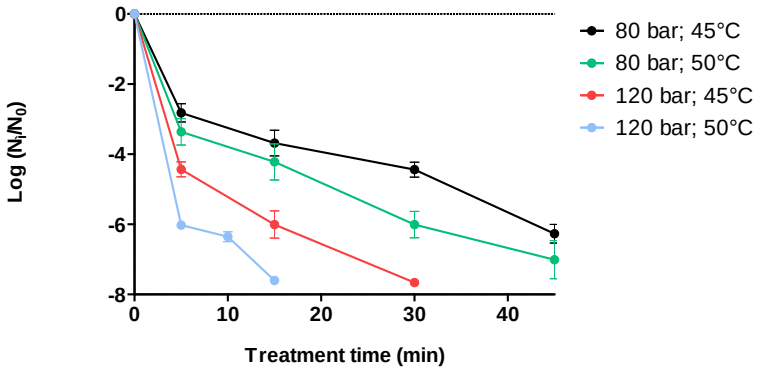

Figure 4.6. Inactivation of cultivable *L. monocytogenes* cells spiked on dry cured ham surface expressed as $Log_{10}(N_i/N_0)$ as a function of treatment time. SC-CO_2 treatment was performed at (a) 45°C and (b) 50°C.

5.3.2 FCM analysis of L. monocytogenes and natural microflora of dry cured ham surface

An high concentration of *Listeria monocytogenes* ($5x10^7$ CFUs) was inoculated on dry cured ham surface. Homogenized suspension of *L. monocytogenes*-spiked on dry cured ham surface were stained with SYBR-I and PI and analyzed with FCM to detect both profiling of natural microbial flora of dry cured ham and *L. monocytogenes* cells (Figure 4.7a). The FCM scattering profiling was used to distinguish *L. monocytogenes* cells from food debris. Referring to an arbitrary scale divided in 256 channels, the FALS histogram of *L. monocytogenes* cells was used to discriminate the bacterial cells from other particles emitting green and red fluorescence.

Green (FL1) and red (FL3) fluorescent signals acquired for each bacterial cell were plotted in a two-dimensional dot plot (cytogram) (Figure 4.7). Food debris with auto-fluorescence or unspecific staining are indicated in gray whilst the population of *L. monocytogenes* cells and bacterial natural flora with FALS signals similar to *Listeria* are in red. The bacteria identified and quantified on the untreated dry cured ham surface (composed by *L. monocytogenes* spiked on ham and natural microflora) can be divided in three different subpopulations: 10^8 cells/g were permeabilized, 10^7 cells/g were partially-permeabilized and $4.2 \cdot 10^7$ cells/g were intact.

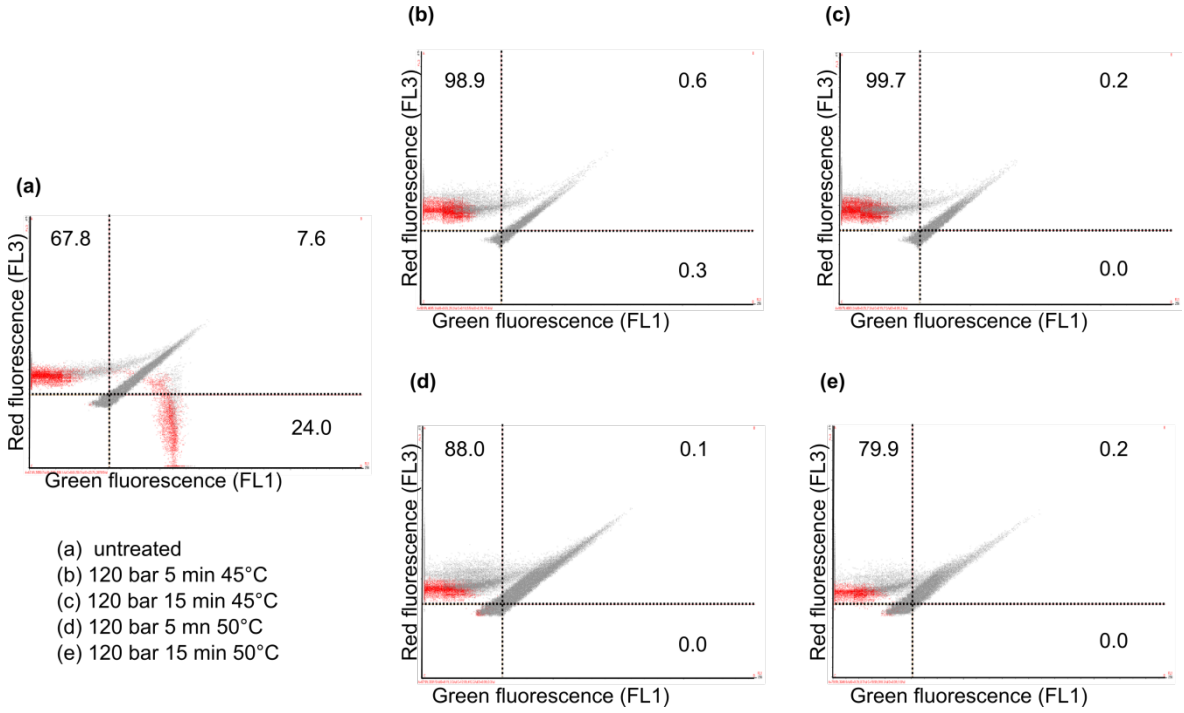

Figure 4.7. FCM cytograms of untreated and treated *L. monocytogenes* cells spiked on dry cured ham surface. The percentages of intact, partially- and totally-permeabilized cells are shown within each cytogram quadrant. The bacterial populations are in red and the food debris in gray.

5.3.3 FCM analysis to evaluate the efficiency of SC-CO_2

In Figure 4.7 the cytograms obtained by FCM coupled with SYBR-I and PI before and after SC-CO_2 treatment at 120 bar both 45°C and 50°C are shown. *Listeria* cells inoculated on dry cured ham surface were viable on the basis of membrane integrity, and assumed to be intact cells. After only 5 min at 120 bar and 45°C only 0.3% of bacterial cells remained in the region of intact cells, and after 15 min all cells

moved to the region of permeabilized cells (Figure 4.7b,c). Eventual intact cells were under the detection limit of the instrument. At 50°C, the number of intact *Listeria* cells were undetectable even after 5 min and all cells were partially-permeabilized or permeabilized (Figure 4.7d).The disruptive action of SC-CO_2, measured as the reduction of the number of total cells, and cellular permeabilization were observed within 5 min of treatment at both 45°C and 50°C (Figure 4.8).The number of total cells decreased by 46% after 5 min at 45°C and by 60% at 50°C. The fraction of disrupted cells was compared to the intact, partially-permeabilized and permeabilized cell populations for each treatment time. The respective percentages are plotted in Figure 4.8. After 30 min of SC-CO_2 at 45°C a similar level of cellular disruption was observed as after 5 min at 50°C. After 15 min at 50°C 90% of bacterial cells were disrupted and 10% of them were permeabilized.

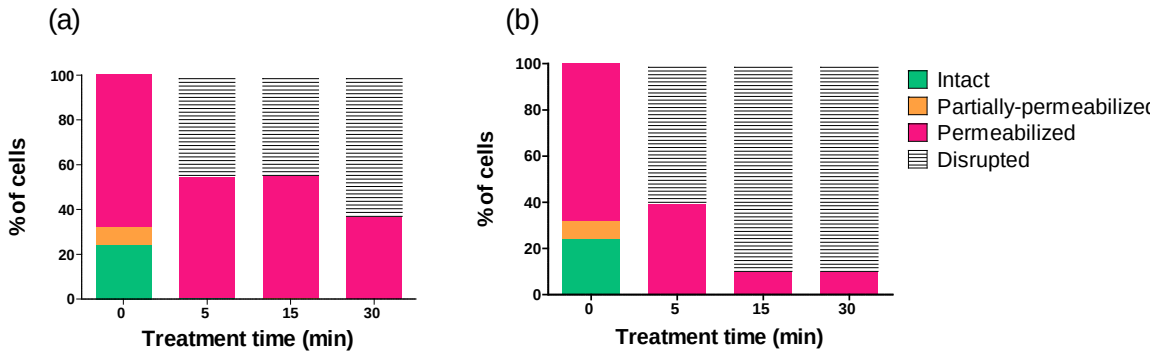

Figure 4.8. Percentages of *L. monocytogenes* cells subpopulations before and after SC-CO_2 treatment at (a) 45°C and (b) 50°C.

5.3.4 PMA-qPCR quantification of intact equivalent Listeria cells

The target gene selected for *Listeria monocytogenes* detection was *hlyA* encoding hemolysin A. $5x10^7$ CFUs of *L. monocytogenes* cells were inoculated on dry cured ham surface. The samples were treated with SC-CO_2 at 45°C and 50°C up to 30 min. The TaqManq PCR analyses were performed on gDNA samples extracted from homogenized suspensions before and after PMA staining, to quantify both total *hlyA* gene copies and *hlyA* gene copies from intact *Listeria* cells. Both values decreased after treatment. The reduction of total gene copies indicated that genomic DNA is exposed to

degradation, whilst the difference between total gene copies and gene copies from intact cells indicated that a part of the cells were permeabilized or disrupted. The maximum level of gDNA degradation (>60%) was obtained at 50°C after 30 min of treatment. Comparing the number of intact equivalent cells between control and treated samples revealed that 70% of intact equivalent cells decreased after 5 min of treatment both at 45°C and 50°C (Figure 4.9).

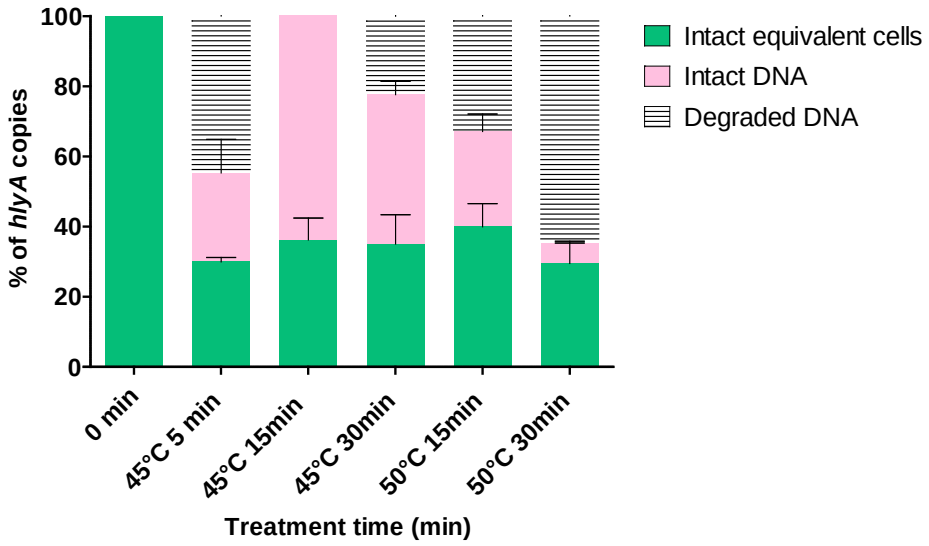

Figure 4.9. Percentages of *hlyA* gene copies of (i) intact equivalent cells, (ii) intact DNA and (iii) degraded DNA before and after treatment.

5.3.5 Comparison of cultivable, intact and equivalent intact Listeria cells

The cultivable *L. monocytogenes* cells spiked on dry cured ham surface were compared with intact cells (considered as viable) obtained by FCM and intact equivalent cells obtained by PMA-qPCR (Figure 4.10). Cultivable cells obtained by plate counts were expressed as CFUs per gram, intact cells obtained by FCM were expressed as intact cells per gram, and intact cells quantified by PMA-qPCR were expressed as intact equivalent cells per gram. All *Listeria* cells spiked on dry cured ham surface were cultivable and intact. After 5 min of the treatment both at 45°C and 50°C more than 10^4 and 10^6 CFUs per gram were no more cultivable and 10^2 and 10^4 were no more intact. These results indicate that part of *Listeria* cells (10^2 cells per gram) were viable but not cultivable. Conversely, the PMA-qPCR data showed only 1 Log of *Listeria* cell inactivation after 5 min of treatment. Increasing the treatment time the

number of cultivable and intact cells per gram decreased, but the difference between intact and cultivable cells remained in the range of 10^2 cells per gram.

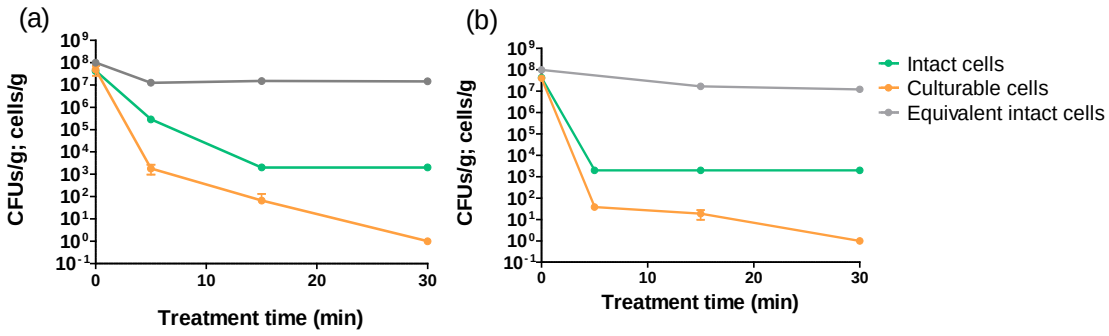

Figure 4.10. Comparison of cultivable, intact and intact equivalent *L. monocytogenes* cells per gram before and after SC-CO_2 treatment at 120 bar and at (a) 45°C and (b) 50°C.

5.4 Conclusions

Total inactivation was reached for both *Escherichia coli* and *Listeria monocytogenes*, therefore satisfying both US and European food safety requirements. Longer treatment times were required to inactivate *Salmonella enterica* respect to *E. coli*. To reach total inactivation of *Salmonella* SC-CO_2 could be combined with others methods alternative to heat pasteurization techniques, including ultrasounds or PEF.

The comparison of results obtained by plate counts, FCM and PMA-qPCR showed that a fraction of intact bacterial cells escaped detection by plate counts. This would suggest that these cells entered in a VBNC state, confirming that plate counts do not detect a significant proportion of cells that may re-grow after treatment.

Real-time quantitative PCR (qPCR) is a highly sensitive method able to detect fewer than 10 genome equivalents per reaction and permit to quantify bacteria at low concentration. The use of primers and fluorescent Taqman probes allows to identify with high specificity and accuracy the microorganisms within a mixed community such as in food products. A main disadvantage of PMA-qPCR applied to viable bacterial quantification is that genomic DNA extraction and PMA staining may cause biases in the bacterial quantification. In addition, qPCR is an indirect method to quantify cells and it does not discriminate between cells that have achieved the division process and cells in division with double content of genomic DNA. Conversely, FCM is a multi-parametric, single-cell analysis method. When coupled with SYBR-I and PI, this

technique permits to discriminate directly viable from dead cells. FCM provides information about cell viability, volume and structure of cell surface, but it shows some limitations when applied to complex environmental matrixes such as food products, because it is not species-specific. The use of FCM in combination with complementary techniques, including both fluorescent species-specific antibodies and probes for Fluorescent In situ Hybridization (FISH) could be applied to evaluate bacterial viability in a species-specific manner. Furthermore, the combination between FCM and single cell sorting could allow to evaluate whether the cells that remained intact after treatment are able to re-grow and to study their physiology (Wang *et al*., 2010).

FCM and PMA-qPCR are innovative and fast approaches for cell viability assessment and bacterial monitoring, though not yet fully standardized, and offer the possibility to critically evaluate culture-based methods. They could be applied routinely, overcoming the limitations of cultivation methods, and defining new parameters of microbiological risk assessment.

Chapter 6: **Effects of SC-CO_2 on *E. coli* cells**

6.1 Supercritical CO_2 induces marked changes in membrane phospholipids in *Escherichia coli* K12

Permeabilization of the cell membrane has been proposed to be the first event leading to cell inactivation or death (Garcia-Gonzalez *et al.*, 2007; Spilimbergo *et al.*, 2009). Membrane permeabilization in *E. coli* and in *L. monocytogenes* cells induced by SC-CO_2 was investigated by Garcia-Gonzalez *et al.* (2010a) using spectrofluorometry and transmission electron microscopy. These authors demonstrated the relationship between irreversible membrane permeabilization and the inability of bacteria to grow on rich media. SC-CO_2-induced membrane permeabilization was also observed in *Salmonella enterica* (Kim *et al.*, 2009a; Tamburini *et al.*, 2013) and in *Saccharomyces cerevisiae* (Spilimbergo *et al.*, 2010a) by using flow cytometry coupled with viable dyes. Whether SC-CO_2 has a direct effect on the bacterial membrane or permeabilization is a consequence of cell death remains an open question. Kim *et al.* (2009b) applied GC-MS to analyze fatty acid profiling of *Salmonella enterica* serotype *Typhimurium*. Their results suggested that the inactivation of *Salmonella* could be related to an increase of minor compounds of the fatty acid profile, though SC-CO_2 could also alter the membrane so that minor fatty acids become more efficiently extracted. SC-CO_2 is indeed used as a solvent to extract non-polar compounds such as triglycerides and fat (Sahena *et al.*, 2009). Flow cytometry analysis, LC-ESI-MS, and ^{31}P-NMR analyses were applied to examine the membrane lipidomic profile per cell of *Escherichia coli K12* (in exponential growth phase) before and after SC-CO_2 treatment. In addition, phospholipid biosynthesis gene expression experiments were performed to study the bacterial response to the treatment (Figure 5.1).

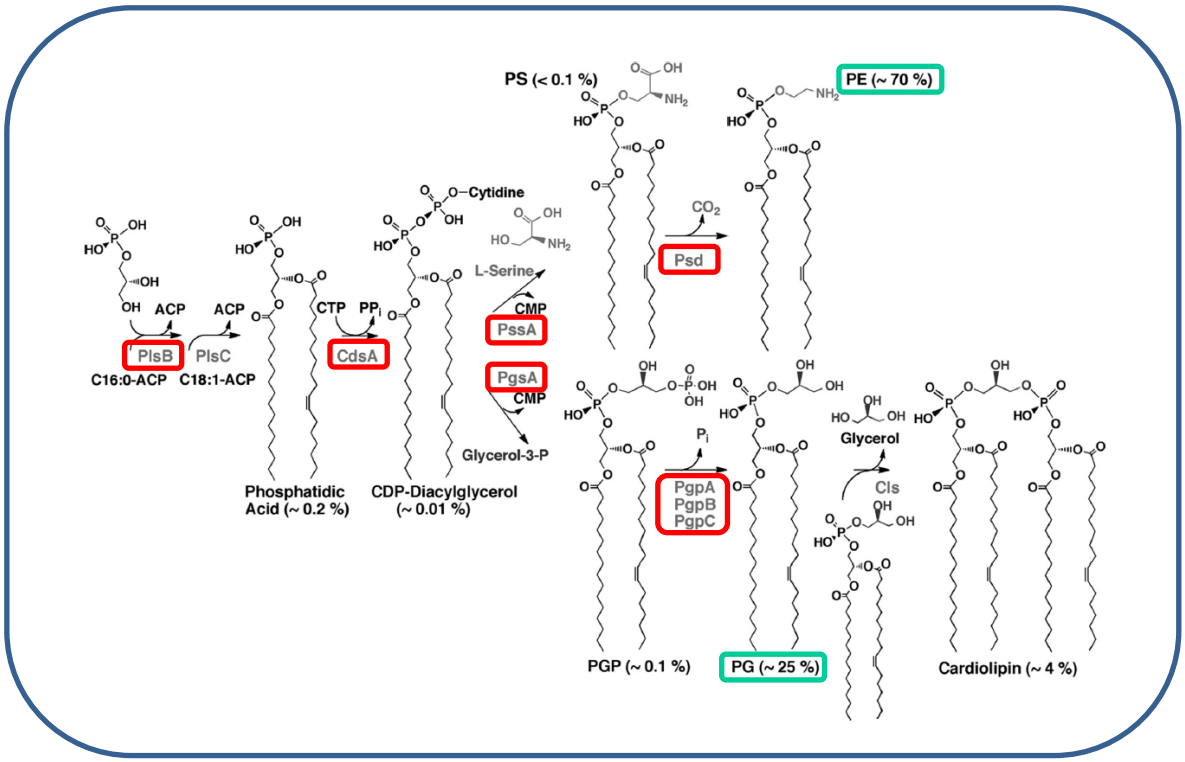

Figure 5.1. Kennedy pathway for the biosynthesis of *E. coli* phospholipids (Lu *et al*., 2011).

6.2 SC-CO_2 induces depolarization, permeabilization and biovolume reduction in *E. coli*

As previously reported (Tamburini *et al*., 2013), the double staining with SYBR-I and PI in FCM analysis allowed to distinguish different bacterial subpopulations: (i) intact cells, emitting green fluorescence; (ii) partially-permeabilized cells, emitting both green and red fluorescence and (iii) permeabilized cells, emitting red fluorescence. Figure 5.2 shows the distribution of *E. coli* subpopulations as a function of treatment time. After 15 min of SC-CO_2 treatment, a significant effect on the membrane was observed, as 18% of cells were permeabilized and 81% were partially-permeabilized. Cell depolarization also became effective after 15 min. For longer treatment times, the partially-permeabilized cells became permeabilized and the proportion of depolarized cells decreased. These results indicate that partial permeabilization leads to depolarization of the membrane. When the cells become fully-permeabilized, $DIBAC_4(3)$ dye likely diffuses out of the cells.

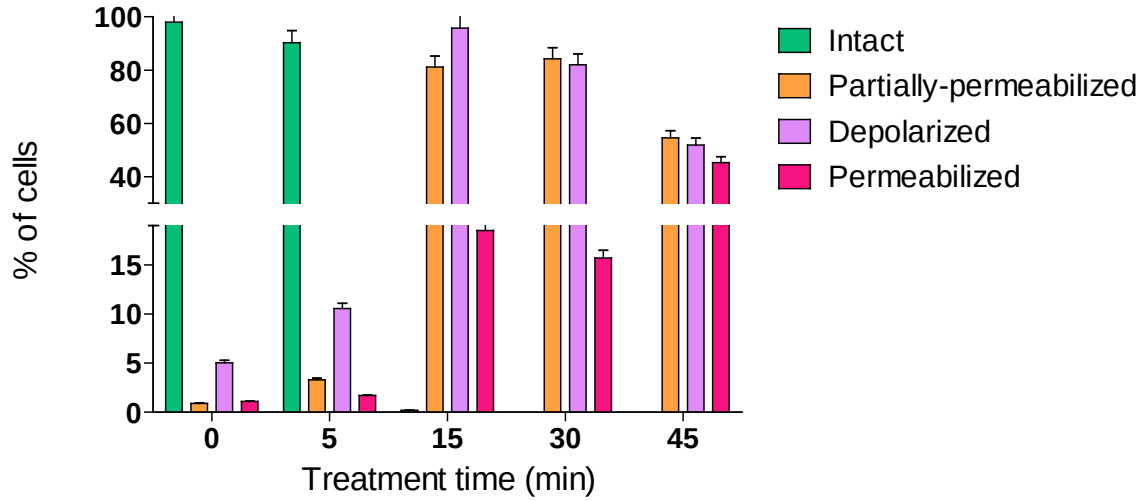

Figure 5.2. Proportions of intact, partially-permeabilized, permeabilized and depolarized *E. coli* cells during SC-CO_2 treatment assessed by FCM.

The comparison between untreated and SC-CO_2-treated samples did not show significant differences of LALS signals, indicating that the treatment has no detectable effect on cell density or granularity (data not shown). Conversely, FALS signals, which provide information on cellular biovolume, changed significantly after 15 min of treatment (Figure 5.3a). Referring to an arbitrary scale divided in 256 channels, the FALS peak of untreated cells and treated cells was at mean channel 126 and 98, respectively. The biovolume ratio was 1.3, indicating that the cellular biovolume decreased of about 20% after 15 min; longer treatment times did not induce further biovolume reduction (Figure 5.3b).

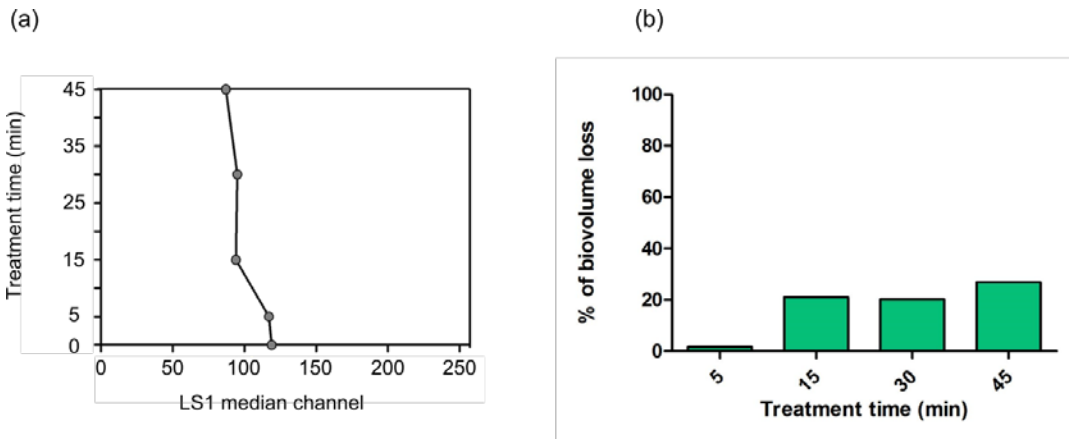

Figure 5.3. Reduction of cellular biovolume and phospholipids during SC-CO_2 treatment. (a) Median channels of FALS signals and (b) associated percentages of biovolume reduction.

6.3 Phospholipids profile of *Escherichia coli* K12 MG1665 by NMR

A preliminary NMR analysis was carried out in order to establish the phospholipid profile of *E. coli* inner membranes. The ^{1}H-NMR spectrum of a raw lipids extract (Figure 5.4a) clearly indicated the dominance of Phosphatidylethanolamine (PE) lipids species by the characteristic resonances of the ethanolamine head group (δ_H 3.16 and 4.03 for the methylene protons linked to α-carbon atoms at amino- and phosphate group, respectively) besides the expected proton-resonances attributable to the presence of two acyl chains on the glycerol backbone (multiplets at δ_H 5.23 and 4.44/4.18 for protons linked carbon atoms at sn-1 and sn-2 position of glycerol, respectively) and the presence of unsaturations on the same chains (triplet at δ_H 5.35). Other minor but characteristic signals in the $4.00 < \delta_H < 3.60$ chemical shifts range were initially guessed and after firmly confirmed to belong to Phosphatidylglycerol (PG) lipid species by comparison with ^{1}H-NMR spectra of pure PG 16:0/18:1. Another striking feature that could be obtained by analysis of the^{1}H-NMR spectrum through the ratio of the signal area at δ_H 5.35 (2H for every unsaturation) to that of the area at δ_H4.44 (2H for every PL species) was the averaged unsaturation index (UI) of the acyl chains in all the PE and PG species (UI = 0.82) pointing out that PE and PG are acylated mainly by saturated (or eventually monounsaturated) fatty chains. Finally the evaluated PG/PE % molar ratio (16%) must be considered just a rough estimation due both to the low signal/noise ratio of the spectrum and partial overlap of the PE/PG signals considered in the corresponding area integrations.

Further structural information was gained by ^{31}P-NMR spectrum (Figure 5.4b) carried out in CD_3OD; not only it confirmed the presence of only PE (δ_P 0.18) and PG (δ_P 0.73) lipid species but allowed to establish their correct molar fractions (% x_{PE} = 82 ;% x_{PG} = 18) by the relative area integrations. The same analysis carried out on a sample obtained by extraction of SC-CO_2 treated cells (60 min) gave us the first suggestion that the PG/PE ratio undergoes severe control by SC-CO_2 treatment. In fact, after overnight acquisition of the corresponding ^{31}P-NMR spectrum the signal of PG was found significantly decreased with respect to that of PE as much to hinder a reliable integration of the PG signal itself.

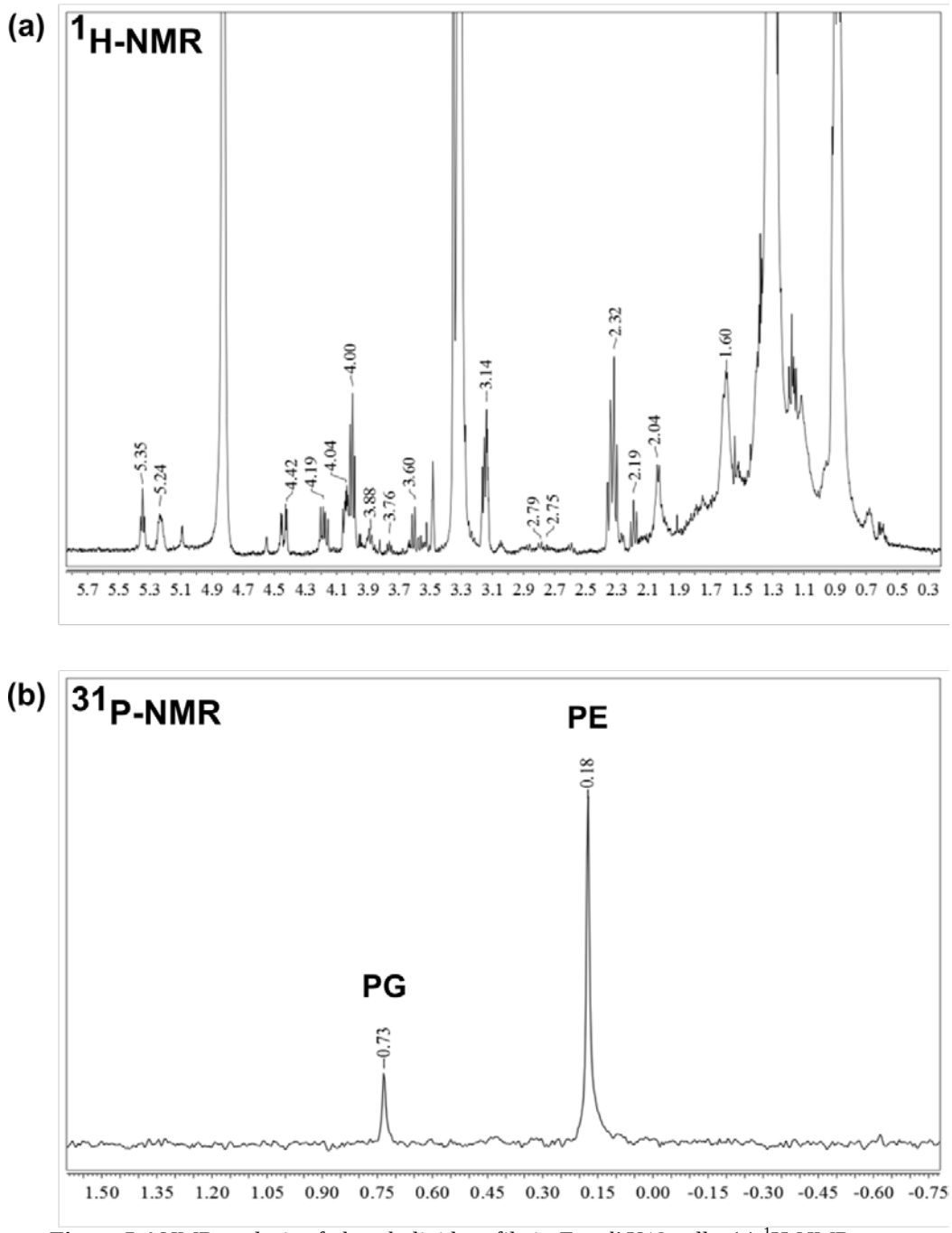

Figure 5.4 NMR analysis of phospholipid profile in *E. coli* K12 cells. (a) ^{1}H-NMR spectrum of a raw lipids extract to indentify PE and PG species; (b) ^{31}P- NMR spectrum carried out in CD_3OD to establish the correct molar fractions between PG and PE by the relative area integrations.

6.4 The phospholipids profile of *E. coli* K12 MG1665 by LC-MS

With the insight gained by preliminary NMR measurements *E. coli* lipid profile was performed by mass spectrometric techniques, in particular through high

performance liquid chromatography/electrospray ionization mass spectrometry (HPLC/ESI-MS).

A complete qualitative analysis was carried out on *E. coli* cells containing even a small amount of PC 12:0/12:0 added for the evaluation of extraction recovery. This analysis confirmed the previous NMR findings that more than 98% of our sample contained only PE and PG lipids with almost undetectable amount of lyso-PC (lyso PC 16:0, lyso PC 18:0 and lyso PC 18:1). However, a wide chemical diversity of the acyl chains was found both in PE (25 species) and PG (22 species) with chains length ranging from 14 to 19 carbon atoms and carbon-carbon double bonds from 0 to 3. A relevant source of chemodiversity was found to derive from the presence in significant amount of i) odd carbon atoms acyl chains (in particular 15:0 and 17:1), ii) structural isomers (such as PE 16:0/18:2 and PE 16:1/18:1) and iii) regiochemical isomers (such as PE 16:0/18:1 and PE 18:1/16:0). The complete lipid profile of the *E. coli* cells is reported in Figure 5.5. Among all Phospholipids (PL) species, PE 32:1, 34:1,34:2, 34:2 isomer, and 36:2 were found to dominate but even PE 30:0, 30:1, 32:1, 32:2, 33:1 and 36:3 were present in in relative amount higher than 2%; PG species were found in much lower amount than PE but essentially they shared the same acyl chains of PE species. The average molar fraction of all the PEs in *E. coli* cells was evaluated to be $x_{PE} = (80 \pm 3)\%$, whilst $x_{PG} = (20 \pm 2)\%$ according to ^{31}P-NMR measurements and Morein *et al.* (1996) and Lu *et al.* (2011).

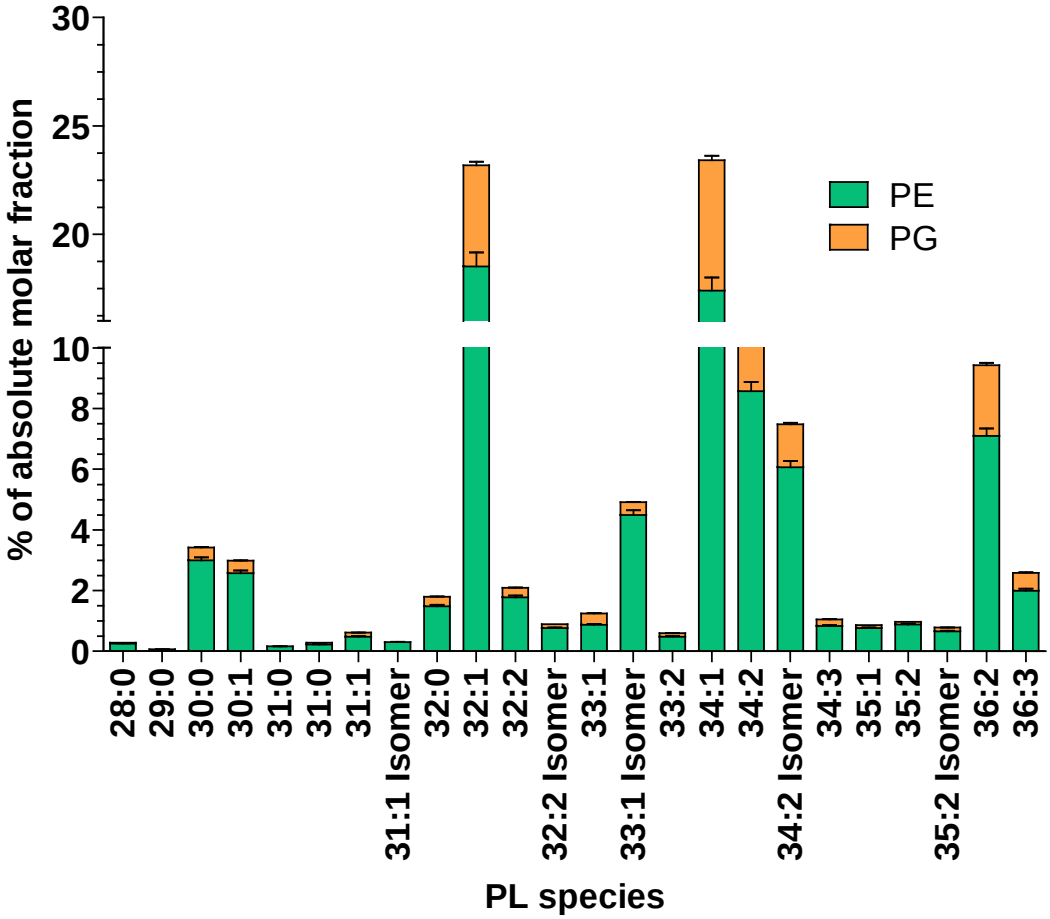

Figure 5.5. Phospholipid profile of *E. coli* K12 MG1665. The percentage of absolute molar fraction of each PE or PG species were indicated. Error bars represent the relative error.

6.5 SC-CO_2 has a more marked effect on PGs relative to PEs

A full quantitative analyses were performed through high performance liquid chromatography/electrospray ionization mass spectrometry (HPLC/ESI-MS) to compare *E. coli* lipids profile between untreated and

SC-CO_2 treated samples. The *E. coli* cells were treated at 120 bar, 35 °C up to 30 min. The integration of the extracted ion currents of all the PL species allowed to establish, through external calibration (working curve) and normalization of the recovery efficiency of every extraction (by added PC 12:0/12:0) the complete quantitative profile of the samples. The comparison of PE (Figure 5.6a) and PG (Figure 5.6b) quantitative profile of untreated and treated samples not only confirmed the first NMR results, but also allowed to gain much more structural details. The PG/PE molar ratio decreased significantly. The absolute amount of total phospholipids showed only

marginal change although the absolute amount of the PG species underwent a strong reduction (52% after 30 min, Figure 5.6b); The PGs decrease resulted somehow compensated by small random changes in the amount of the PE species. In particular, the % absolute molar fraction (%amf) of PE species, defined as %amf (PE)=[$\Sigma_i$mol(PE)$_i$/total mol (PL)]x100, changed from 80% (untreated) to 90.0% (after 30 min of treatment), whilst the corresponding %amf of PG species (%amf (PG)=[$\Sigma_i$mol(PG)$_i$/total mol(PL)]x100)) changed from 20 % (untreated) to 10% (after 30 min of treatment); a significant part of this reduction was obtained in the first 5 min of treatment where the PG species were found to reduce their total amount till 30% (60% of the overall observed reduction).

The % relative molar fraction (%rmf) of a single PL class (for PE class defined as %rmf (PE) = [$\Sigma_i$mol(PE)$_i$/total mol (PE)]x100) did not shown statically significant changes in the relative molar fraction both for PE and PG species after treatment, indicating that SC-CO_2 acted with the same effects on all PE or PG species. One exception was observed for the isomeric PG 34:2 species (PG 16:1/18:1) that unchanged after the treatment (Figure 5.7).

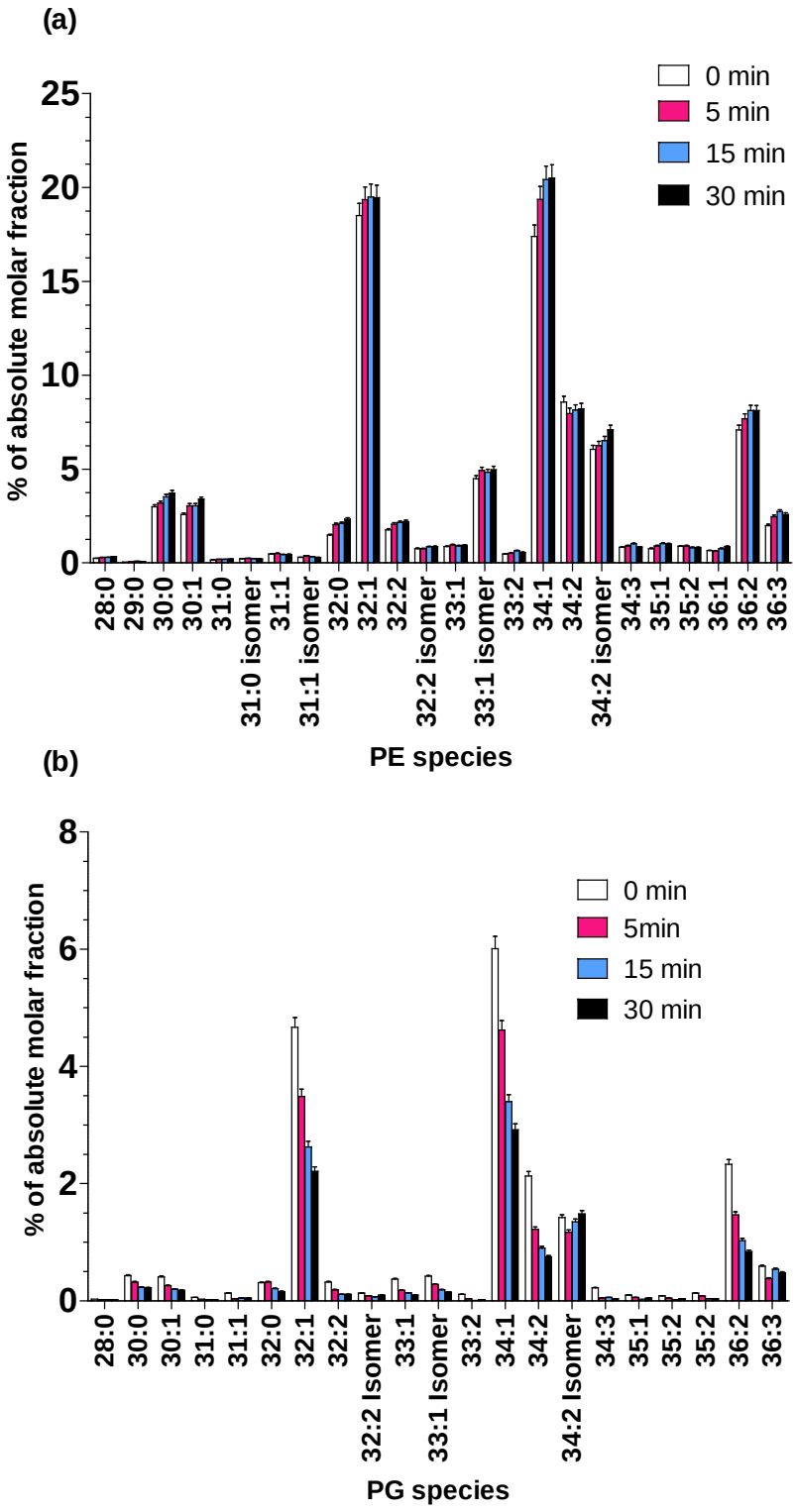

Figure 5.6. Quantitative lipids profile of untreated and SC-CO_2 treated *E. coli* cells: (a) PE species and (b) PG species

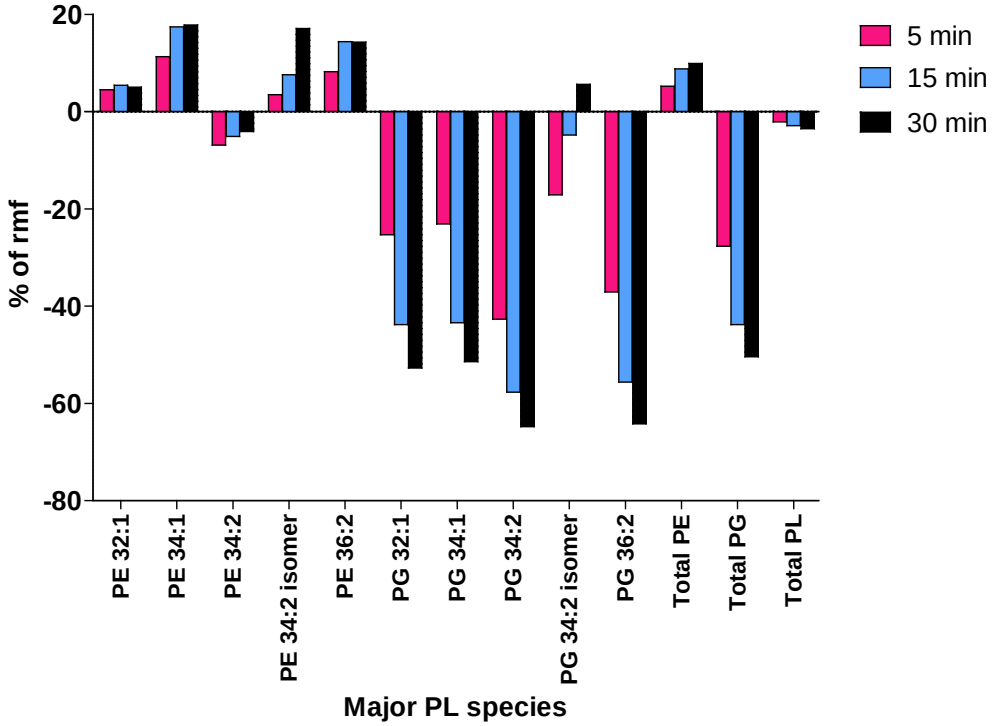

Figure 5.7. Percentages of relative molar fraction of the major PL species detected in *E. coli* K12 after SC-CO_2 treatment.

6.6 SC-CO_2 does not affect the acyl chains

The HPLC/ESI-MS permitted to determine whether SC-CO_2 treatment induced changes in the unsaturation and length of lipid fatty acids. The unsaturation index (UI) was defined as UI = Σ_i $(UN)_i$ x $(amf)_{i,}$ where *UN* represent the number of double bonds and *amf* the absolute molar fraction of a given species *i* and the sum is extended on all the PE and PG species. The data clearly indicated that UI (1.30 ±0.02) didn't show any change during the treatment. The same behavior was followed also by the averaged acyl chains lengths (defined by Σ_i $(TCL)_i$ x $(amf)_{i,}$, where TCL_i is the total carbon atoms of the acyl chains on the glycerol backbone of a given species) which was found (33.30 ± 0.03) absolutely constant during the time course of the treatment.

6.7 *E. coli* cells responds to treatment increasing PL synthesis

In an initial attempt to identify a bacterial response to loss of membrane PL by SC-CO_2 treatment the genes involved in biosynthesis of membrane phospholipids were selected (Figure 5.1). The *E. coli* cells in exponential growth phase were treated

with SC-CO_2 at 120 bar, 35°C up to 30 min. The expression level of selected genes was performed by RT-qPCR and was quantified using the delta delta Ct method (Figure 5.6) The p-values to identify the significant fold changed differences were calculated by Pearson correlation and are shown in Figure 5.8. Only *PssA* gene seemed to be up-regulated after 5 min of SC-CO_2 treatment, whilst *CdsA* and *Psd* genes were down-regulated. CdsA gene product is involved in the both synthesis of phospholipids, PEs and PGs, whilst *PssA* and *Psd*, up and down regulated, respectively only in the PE synthesis (see Figure 5.1).

.

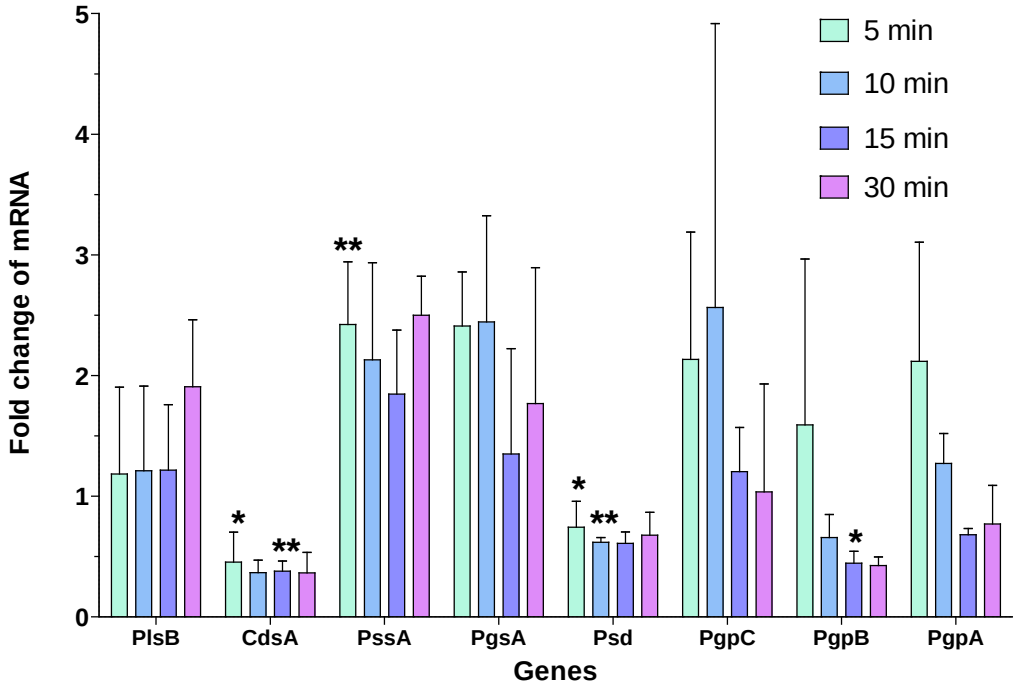

Figure 5.8. Expression analysis of genes involved in the Kennedy pathway of phospholipids biosynthesis in *E. coli*. Error bars indicate the standard deviation of five independent biological replicates.*p<0.05; **p<0.01.

6.8 Discussion

In this study, the changes of lipid profiles of *E. coli* K12 during SC-CO_2 treatment were compared with cellular features to get insights on the action mechanism of SC-CO_2 on bacterial cells. After 15 min of SC-CO_2 treatment most of bacterial cells lost their membrane potential (95%) and membrane integrity (81% of permeabilized and 18% of partially-permeabilized cells). Bacterial permeabilization was associated to a

20% decrease of cellular biovolume and to a strong decrease (more than 50%) reduction of PG membrane lipids.

PEs are zwitterionic lipids participating in a multitude of cellular task, such as fusion, vesiculation, curvature bilayers, influence permeation and cell division (Zhao *et al*., 2008). Conversely, PGs are anionic carrying a unit negative charge, playing an important role in the overall homeostatic equilibrium of cell membranes and in membrane-peptide interactions (Tari *et al*., 1989). Due to ammonium group in PE and hydroxyl groups in PG, both lipids are able to form hydrogen bonds. PE-PE hydrogen bonds have been observed both experimentally (Boggs, 1987) and in molecular simulations (Pink *et al*., 1998; Leekumjorn *et al*., 2006), whereas there is no experimental evidence of PG-PG hydrogen bonds. Zhao *et al*. (2008) suggested that PGs increase the bacterial membrane stability, because PGs reduce the PEs motion along bilayer, therefore promoting the formation of inter-lipid hydrogen bonds. Bacteria are able to adjust the relative concentrations of PEs and PGs when exposed to toxic organic solvents such ethanol increasing the PG/PE molar ratio (Weber *et al*., 1996). The lipid profiles of *E. coli* treated cells showed that i) SC-CO_2 treatment decreased by 50% the amount of total PGs whilst PEs remained almost unchanged, ii) the grade of this decrease is almost uniformly distributed among all the PG species and iii) the destabilizing effect induced by the PG decrease is most significant in the first minutes of the treatment.

Besides changing the headgroup of the phospholipids species, bacteria generally respond to environmental stress by increasing the number of unsaturated fatty acids and the length of acyl chains (Weber *et al*., 1996; Zhang and Rock, 2008). The data showed that both the factors did not play any role during SC-CO_2 treatment; in fact both the average unsaturation index (1.30 ±0.02) and the average acyl chain on the glycerol backbone (33.30 ±0.03) were found absolutely constant.

In addition, only *PssA* gene, involved in PE biosynthesis, was up-regulated after 5 min of SC-CO_2 treatment, whilst *Psd* gene was down-regulated. *CdsA* gene involved in the synthesis of both phospholipids was also down-regulated. All enzymes involved in phospholipid head-group synthesis are localized in the inner membrane, whith the exception of PssA, which is located in the cytoplasm (Zhang and Rock, 2008). PGs are constitutively produced by the action of PgsA and PgpP, whilst PEs synthesis depends on mole fraction of PGs and Cardiolipin in the membrane, which control the PssA

association to the membrane and their activity (Linde *et al*., 2004; Zhang and Rock, 2008). The mechanisms that regulate the amounts and the ratio among different PL classes seemed likely to be interrelated and to regulate by product feedback inhibition rather than an overall expression of the enzymes involved in the PL synthesis in *E. coli.* Even the competitive routes of PL synthesis which, starting from CDP-diacylglycerol, lead to PE and PG branches are unaffected by overexpression of *E. coli PssA* or *PgsA* (Jackson *et al*., 1986).

On the other hand, the intracellular pH in *Listeria monocytogenes* cells treated with SC-CO_2 decreased until <5 (Spilimbergo *et al*., 2010b). The pH change likely have detrimental effects on several biochemical processes, such as protein denaturation, loss of enzymatic activity and even in the structural architecture of cells membranes. Also the PE/PG cell membranes would be strongly affected by pH change, given that at pH=7 PGs are negatively charged and PEs are zwitterionic, while at pH=2.8, the phosphodiester group of PGs (pKa = 2.9) is mainly protonated (60%) (Garidel *et al.*, 1997). This biophysical effect could explain the reason why SC-CO_2 treatment result in a strong perturbation of membranes architecture in *E. coli*, where PG and in particular PE have been ever found as the dominant phospholipid species. Such alterations are likely associated with its strong inactivation effect. Why specifically PG species have been found to strongly decrease during treatment remains an open question. Further studies, including phospholipid biosynthesis mutant analysis, will help to determine *E. coli* response to the treatment.

Chapter 7: **Conclusion**

Supercritical carbon dioxide (SC-CO_2) has been widely investigated as an innovative technology for the preservation of food products. It is a promising alternative to the traditional processes used to inactivate pathogens (Gunes *et al*., 2006; Choi *et al*., 2009) and spoilage microorganisms (Gunes *et al*., 2005; Ferrentino *et al*., 2013), without negatively affecting the sensorial properties of products and decreasing their overall quality (Damar and Balaban, 2006; Chen *et al*., 2009).

The results showed that SC-CO_2 treatment was more efficient when applied on bacterial cells spiked on synthetic solid substrate and on food products rather than on cell suspensions. Batch tests showed that bacterial inactivation in liquid substrate proceeds in two phases: the early one is characterized by a slow rate of reduction of the number microbes, which then sharply decrease at a later stage, confirming previously published results (Dillow *et al*., 1999). Conversely, on solid substrate the first stage of inactivation proceeds at a fast rate of bacterial inactivation and the second one at a slower rate. The action of SC-CO_2 on solid substrate was more efficient, presumably because the supercritical fluid acted directly on bacterial cells without the need to dissolve in the liquid phase, although some studies reported that bacterial inactivation depends on water content of the medium and on water content inside the bacterial cells (Hong and Pyung, 1999; Spilimbergo and Bertucco, 2003).

The comparison of results obtained by plate counts, FCM and PMA-qPCR showed that a fraction of intact bacterial cells escaped detection by plate counts. This would suggest that these cells entered in a VBNC state, confirming that plate counts do not detect a significant proportion of cells that may re-grow after treatment.

The exact role of the VBNC state in bacteria and the mechanisms to reach this state is unknown and it could differ from bacterium to bacterium. In VBNC state pathogens can survive in environmental matrices over one year, maintaining the capability to develop diseases in their host (Oliver 2010). Flow cytometry coupled with cells-sorting could be applied to recover the putative VBNC cells and to study their capability to re-growth and determine whether the cells maintain their metabolic activity and pathogenic potential.

The adaptation of microorganisms to the stresses induced by food processing and food preservation technologies constitute a potential safety hazard. Co-evolution of commensal microorganisms and cooperative metabolic interaction among bacterial

species could be a survival strategy to stress (Hibbing *et al*., 2010; Freilich *et al*., 2011). Further studies to simulate the efficiency of treatment on real food matrices should be developed. The exposure to SC-CO_2 of commensal bacterial communities spiked on food product could be a good start point to study the evolution of bacterial communities associated to RTE products in response to SC-CO_2 treatment. In addition, bacteria live in multi-species communities both in planktonic form and associated in biofilm. The most common lifestyle of bacteria is surface-attached within a biofilm, because the extracellular polymeric substances (EPS) that encase them offer a protection from physical, chemical and biological stress (Mitchel et al., 2008). Bacteria associated in biofilm are indeed known to be more resistant to treatment than their planktonic form (Watnick *et al*., 2000). For instance *Bacillus mojavensis* biofilms have been shown to be more resistant to SC-CO_2 treatment than suspended cells (Mitchell *et al*., 2008).

E. coli and *L. monocytogenes* have yet shown an increase in the resistance of SC-CO_2 treatment after seven cycles of exposition (Garcia-Gonzalez *et al*., 2010b). To understand the action mechanism of SC-CO_2 on bacterial cells, it is necessary to depict the bacterial adaptation strategy. The data showed that SC-CO_2 permeabilized the bacterial cells and SC-CO_2 action on membrane permeabilization level depends on the bacterial species. In *E. coli*, the partial permeabilization, induced by SC-CO_2 was correlated to a decrease of cellular biovolume, depletion of potential membrane, loss of PG species, without altering their acyl chains, from the bacterial membrane, and to down-regulation of some genes involved in PL biosynthesis. The theoretical affinity between SC-CO_2 and the plasma membrane was measured revealing the possible accumulation of CO_2 into plasma membrane (Isenchmid *et al*., 1995; Spilimbergo and Bertucco, 2003). The accumulation may compromise the construction of membrane domains and increase its permeability. In *Listeria monocytogenes* cells after SC-CO_2 treatment the cytosolic pH decreased until <5 (Spilimbergo *et al*., 2010b) and the membrane was permeabilized (Tamburini *et al*., 2013). Lactic acid bacteria of coconut shown a minor inactivation rate compared with mesophilic bacteria of coconut (Ferrentino *et al*., 2012a). Lactic acid bacteria posse systems to regulate intracellular pH by using cytoplasmic buffering, proton symport system, production of bases and proton pumps (Hutkins and Nannen, 1993; Slonczewsky *et al*., 2009).

Further studies are necessary to understand both the action mechanism of SC-CO_2 on bacterial cells and the bacterial response to the treatment. Of particular interest

are the identification of the first target of SC-CO_2. This could be performed by constructing *E. coli* phospholipid biosynthesis mutants containing different amounts of PEs and PGs in their membranes. In addition, to understand the role of cytoplasm acidification associated to membrane permeabilization during SC-CO_2 treatment, it could be also of interest to evaluate the behavior of acid-resistant mutants respect to treatment.

Chapter 8: **References**

Anon (2002) Risk profile on the microbiological contamination of fruits and vegetables eaten raw. Scientific Committee on Food. SCF/C

ANZFA. (2001) Recall guidelines for packaged ready-to-eat foods found to contain *Listeria monocytogenes* at point of sale. Arkansas: Faculty Impact Statements.

Bae, Y.Y., Choi, Y.M., Kim, M.J., Kim, K.H., Kim, B.C. and Rhee, M.S. (2011). Application of supercritical carbon dioxide for microorganism reduction in fresh pork. *Journal of Food Safety* 31, 511–517

Ballestra, P., Abreu Da Silva, A., Cuq, J.L., (1996) Inactivation of *Escherichia coli* by carbon dioxide under pressure. *Journal of Food Science* 61, 829 -836

Barbesti, S., Citterio, S., Labra, M., Baroni, M.D., Neri, M.G., and Sgorbati, S. (2000) Two and Three-Color Fluorescence Flow CytometricAnalysis of Immunoidentified Viable Bacteria. *Cytometry Part A* 40, 214–218

Berche, B., Henkel, M., Kenna, R. (2009) Critical phenomena 150 years since cagniard de la Tour. *Journal of Physical Studie*s 13(3), 3001-3014

Berney, M., Weilenmann H.U., and Egli T. (2006) Flow-cytometric study of vital cellular functions in *Escherichia coli* during solar disinfection (SODIS). *Microbiology* 152, 1719-1729

Berney, M., Hammes, F., Bosshard, F., Weilenmann H.U., and Egli, T. (2007) Assessment and Interpretation of Bacterial Viability by Using the LIVE/DEAD BacLight Kit in Combination with Flow Cytometry. *Applied Environmental Microbiology* 73, 3283–3290

Belasco, J. (1993) mRNA degradation in Prokaryotic Cells: an overview. *Control of Messenger RNA stability:* Chapter 1, 3-12

Beuchat, L.R., Ward, T.E., and Pettigrew, C.A. (2001) Comparison of chlorine and a prototype produce wash product for effectiveness in killing *Salmonella* and *Escherichia coli* O157:H7 on alfalfa seeds. *Journal of Food Protection* 64, 152–158

Bogosian, G., and Bourneuf, E. (2001) A matter of bacterial life and death. *EMBO Reports* 2(9), 770-774

Boggs, J.M. (1987) Lipid intermolecular hydrogen bonding: influence on structural organization and membrane function. *Biochimica et Biophysica* Acta 906, 353-404

Breeuwer, P., and Abee, T. (2000) Assessment of viability of microorganisms employing fluorescence techniques. *International Journal of Food Microbiol*ogy 55, 193–200

Brunner, G. (2005) Supercritical fluids: technology and application to food processing. 67(1-2), 21-33

Centers for Disease Control and Prevention (CDC). (2003) Disease information (Listeriosis) http://www.cdc.gov/listeria/outbreaks/cantaloupes-jensen-farms/index.html

CFSAN/FSIS. (2003) Quantitative assessment of relative risk to public health from food-borne *Listeria monocytogenes* among selected categories of ready-to-eat foods. Silver Spring: Food and Drug Administration

Chen, J., Zhang, J., Feng, Z., Song, L., Wu, J., Hu, X. (2009) Influence of thermal and dense-phase carbon dioxide pasteurization on physicochemical properties and flavor compounds in hami melon juice. *J of Agric. and Food Chem.* 57, 5805 – 5808

Choi, Y.M., Bae, Y.Y., Kim, K.H., Kim, B.C., Rhee, M.S. (2009) Effects of supercritical carbon dioxide treatment against generic *Escherichia coli*, *Listeria monocytogenes*, *Salmonella typhimurium*, and *E. coli* O157:H7 in marinades and marinated pork. *Meat Science* 82, 419 – 424

Czajka J., and Batt, C.A. (1994) Verification of causal relationships between *Listeria monocytogenes* isolates implicated in food-borne outbreaks of listeriosis by randomly amplified polymorphic DNA patterns. *Journal of Clinical Microbiology* 32 (5), 1280-128

Damar, S., and Balaban, O. (2006) Review of Dense Phase CO_2 Technology: Microbial and Enzyme Inactivation, and Effects on Food Quality. *Journal of Food Science* 71(1), R1-R11

Davey, H.M. (2011) Life, Death and In-Between: Meaning and Methods in Microbiology. *Applied and Environmental Microbiology* 77(6), 5571-5576

Dillow, A.K., Dehghani, F., Hrkach, J.S., Foster, N.R., Langer, R. (1999) Bacterial inactivation by using near- and supercritical carbon dioxide. Proceedings of the National Academy of Sciences of the United States of America 96, 10344–10348

Edberg, S.C., Rice, E.W., Karlin, R.J., and Allen, M.J. (2000) *Escherichia coli*: the best biological drinking water indicator for public health protection. *Journal of Applied Microbiology* 88, 106S–116S

EFSA (European Food Safety Authority) (2013) Scientific Opinion on the risk posed by pathogens in food of non-animal origin. Part 1(outbreak data analysis and risk ranking of food/pathogen combinations. *EFSA Journal* 11(1), 3025

Enomoto, A., Nakamura, K., Nagai, K., Hashimoto, T., Hakoda, M. (1997) Inactivation of food microorganisms by high-pressure carbon dioxide treatment with or without explosive decompression. Bioscience, *Biotechnology and Biochemistry* 61, 1133–1137

Erkmen, O. (2000) Antimicrobial effects of pressurised carbon dioxide on *Brochothrix thermosphacta* in broth and foods. *Journal of the Science of Food and Agriculture* 80, 1365-1370

European Commission (2005) Regulation (EC) No. 2073/2005 of 15 November 2005 on microbiological criteria for foodstuffs. *Official Journal of the European Union*, L338, 1-26

Ferrentino, G., and Spilimbergo, S. (2011) High pressure carbon dioxide pasteurization of solid foods: Current knowledge and future outlooks. *Trends in Food Science and Technology* 22, 427-441

Ferrentino, G., Balzan, S., Dorigato, A., Pegoretti, A., Spilimbergo, S. (2012a) Effect of supercritical carbon dioxide pasteurization on natural microbiota, texture and microstructure of fresh cut coconut. *Journal of Food Science* 77, E137–E143.

Ferrentino, G., Balzan, S., Spilimbergo, S. (2012b) Supercritical carbon dioxide processing of dry cured ham spiked with *Listeria monocytogenes*: inactivation kinetics, color and sensory evaluations. *Food and Bioprocess Technology* 6, 1164-1174

Ferrentino, G., Belscak-Cvitanovic, A., Komes, D., and Spilimbergo, S. (2013) Quality Attributes of Fresh-Cut Coconut after Supercritical Carbon Dioxide Pasteurization. *Journal of Chemistry*, 1-9

Foladori, A., Quaranta, A., and Ziglio, G. (2008) Use of silica microspheres having refractive index similar to bacteria for conversion of flow cytometric forward light scatter into biovolume. *Water Research* 42, 3757-3766

Folkes (2004) Pasteurization of Beer by a Continuous Dense-phase CO_2 System. PhD thesis, University of Florida, USA

Foladori, P., Bruni, L., Tamburini, S., and Ziglio, G. (2010) Direct quantification of bacterial biomass in influent, effluent and activated sludge of wastewater treatment plants by using flow cytometry. *Water Research* 44(13), 3807-18

Freilich, S., Zarecki, R., Eilam, O., Segal, E.S., Henry, C.S. Kupiec, M., Gophna, U., Sharan, R., and Ruppin, E. (2011) Competitive and cooperative metabolic interactions in bacterial communities. *Nature Communications* 2, 589

Gandhi, M., and Chikindas, L. (2007) *Listeria*: A foodborne pathogen that knows how to survive. *International Journal of Food Microbiology* 113, 1–15

Gangola, P., Rosen, B.P. (1987) Maintenance of intracellular calcium in *Escherichia coli*. *Journal of Biological Chemistry* 262, 12570–12574

Garcia-Gonzalez, L., Geeraerd, A.H., Spilimbergo, S., Elst, K., Van Ginneken, L., Debevere, J., Van Impe, J.F., and Devlieghere, F. (2007) High pressure carbon dioxide inactivation of microorganisms in foods: The past, the present and the future. *International Journal of Food Microbiology* 117, 1–28

Garcia-Gonzalez, L., Geeraerd, A.H., Mast, J., Briers, Y., Elst, K., Van Ginneken, L., Van Impe J.F., and Devlieghere, F. (2010a) Membrane permeabilization and cellular death of *Escherichia coli*, *Listeria monocytogenes* and *Saccharomyces cerevisiae* as induced by high pressure carbon dioxide treatment. *Food Microbiology* 27, 541-549

Garcia-Gonzalez, L., Rajkovic, A., Geeraerd, A.H., Elst K., Van Ginneken L.,Van Impe J.F., Devlieghere F. (2010b) The development of *Escherichia coli* and *Listeria monocytogenes* variants resistant to high-pressure carbon dioxide inactivation. *Letters in Applied Microbiology* 50, 653-656

Garidel, P. Johann, C., Mennicke, L., Blume, A. (1997) The mixing behavior of pseudobinary phosphatidylcholine-phosphatidylglycerol mixtures as a function of pH and chain length**.** *European Biophysics Journal* 26, 447-459

Garidel, P., Blume, A. (2000) Miscibility of phosphatidylethanolamine-phosphatidylglycerol mixtures as a function of pH and acyl chain length. *European Biophysics Journal* 28, 629-638

Gunes, G., Blum, L.K., Hotchkiss, J.H. (2005) Inactivation of yeasts in grape juice using a continuous dense phase carbon dioxide processing system. *Journal of the Science of Food and Agriculture* 85, 2362 –2368

Gunes, G., Blum, L.K., Hotchkiss, J.H. (2006) Inactivation of *Escherichia coli* (ATCC 4157) in diluted apple cider by dense-phase carbon dioxide. *Journal of Food Protection* 69, 12 – 16

Haas, G.J., Prescott, H.E., Dudley, E., Dik, R., Hintlian, C., Keane, L. (1989) Inactivation of microorganisms by carbon dioxide under pressure. *Journal of Food Safety* 9(4), 253–265

Hibbing, M.E., Fuqua, C., Parsek, M.R., and Peterson, S.B: (2010) Bacterial competition: surviving and thriving in the microbial jungle. *Nature Review Microbiology*; 8(1): 15–25.

Hiraoka, Y., and Kimbara, K. (2002) Rapid assessment of the physiological status of the polychlorinated biphenyl degrader *Comamonas testosteroni* TK102 by flow cytometry. *Applied Environmental Microbiology* 68: 2031–2035

Hong, S.I., Park, W.S., Pyun, Y.R. (1999) Non-thermal inactivation of *Lactobacillus plantarum* as influenced by pressure and temperature of pressurized carbon dioxide. *International Journal of Food Science and Technology* 34, 125-130

Hong, S.I., and Pyun, Y.R. (1999) Inactivation kinetics of *Lactobacillus plantarum* by high pressure carbon dioxide. *Journal of Food Science* 64, 728–733

Hong S.I., and Pyun, Y.R. (2001) Membrane damage and enzyme inactivation of *Lactobacillus plantarum* by high pressure CO_2 treatment. I*nternational Journal of Food Microbiology*, 19–28

Ingram, L.O (1976) Adaptation of Membrane Lipids to Alcohols. *Journal of Bacteriology* 125(2)1976, 670-678

Isenschmid, A., Marison, I.W., von Stockar, U. (1995) The influence of pressure and temperature of compressed CO_2 on the survival of yeast cells. *Journal of Biotechnology* 39, 229–237

Jackson, B.J., Gennity, J.M., and Kennedy E.P. (1986) Regulation of the Balanced Synthesis of Membrane Phospholipids. Experimental test of models for regulation in *Escherichia coli*

Jamil, S., Keer, J.T., Lucas, S.B., Dockrell, H.M., Chiang, T.J., Hussain, R., Stoker, N.G. (1993) Use of polymerase chain reaction to assess efficacy of leprosy chemotherapy. *Lancet* 342, 264– 268

Jones, R.P., and Greenfield, P.F. (1982) Effect of carbon dioxide on yeast growth and fermentation. *Enzyme and Microbial Technology* 4, 210–223

Josephson, K.L., Gerba, C.P., Pepper, I.L. (1993) Polymerase chain reaction detection of nonviable bacterial pathogens. *Applied and Environmental Microbiology* 59, 3513–3515

Jung, W.Y., Choi, Y.M., and Rhee, M.S. (2009) Potential use of supercritical carbon dioxide to decontaminate *Escherichia coli* O157:H7, *Listeria monocytogenes*, and *Salmonella typhimurium* in alfalfa sprouted seeds. *International Journal of Food Microbiology* 136, 66-70

Kastbjerg, V.G., Nielsen, D.S., Arneborg, N., and Gram, L. (2009) Response of *Listeria monocytogenes* to Disinfection Stress at the Single-Cell and Population Levels as Monitored by Intracellular pH Measurements and Viable-Cell Counts. *Applied and Environmental Microbiology*, 4550-4556

Keer, J.T., and Birch, L. (2003) Molecular methods for the assessment of bacterial viability. *Journal of Microbiological Methods* 53,175-183

Kim, S.R., Rhee, M.S., Kim, B.C., Lee, H., Kim, K.H. (2007) Modeling of the inactivation of *Salmonella typhimurium* by supercritical carbon dioxide in physiological saline and phosphate-buffered saline. *Journal of Microbiological Methods* 70(1), 132-141

Kim, S.R., Park, H.J., Yim, D.S., Kim, H.T., Choi, I-G., Kim, K.H. (2008) Analysis of survival rates and cellular fatty acid profiles of *Listeria monocytogenes* treated with supercritical carbon dioxide under the influence of cosolvents. *Journal of Microbiological Methods* 75, 47–54

Kim, H.T., Choi, H.J., and Kim, K.H. (2009a) Flow cytometric analysis of *Salmonella enterica* serotype Typhimurium inactivated with supercritical carbon dioxide. *Journal of Microbiological Methods* 78, 155–160

Kim, S.R, Kim H.T., Park, H.J., Kim, S., Choi, H.J., Hwang, G.S., Yi, J.H., Ryu, D.H., and Kim, K.H. (2009b) Fatty acid profiling and proteomic analysis of *Salmonella enterica* serotype Typhimurium inactivated with supercritical carbon dioxide. *International Journal of Food Microbiology* 134, 190-195

Kuhne, K., and Knorr, D. (1990) Effects of high pressure carbon dioxide on the reduction of microorganisms in fresh celery. *Internationale Zeitschrift für Lebensmittel-Technik, Marketing, Verpackung und Analytik*, 41, 55-57

Leekumjorn, S., Sum, A.K. (2006) Molecular investigation of the interactions of trehalose with lipid bilayers of DPPC, DPPE and their mixture. *Molecular Simulation*, 32, 219-230.

Liao, H., Zhang, F., Liao, X., Hu, X., Chen, Y., and Deng, L. (2010) Analysis of *Escherichia coli* cell damage induced by HPCD using microscopies and fluorescent staining. *International Journal of Food Microbiology* 144, 169–176

Liao, H., Zhang, F., Hu, X., and Liao, X. (2011) Effects of high-pressure carbon dioxide on proteins and DNA in *Escherichia coli*. *Microbiology* 157, 709–720

Lin, H.M., Yang, Z.Y., Chen, L.F. (1993) Inactivation of *Leuconostoc dextranicum* with carbon dioxide under pressure. *Chemical Engineering Journal and the Biochemical Engineering Journal* 52, B29–B34

Lin, H.M., Cao, N.J., Chen, L.F. (1994) Antimicrobial effect of pressurized carbon dioxide on *Listeria monocytogenes*. *Journal of Food Science* 59, 657–659

Linde, K., Grobner, G., and Rilfors, L. (2004) Lipid dependence and activity control of phosphatidylserine synthase from *Escherichia coli*. *FEBS Letters* 575, 77–80

Liu, X.F., Zhang, B.Q., Li, T.J. (2005) Effects of CO_2 compression and decompression rates on the physiology of microorganisms. *Chinese Journal of Chemical Engineering* 13, 140–143

Lu, Y.H, Guan, Z., Zhao, J., and Raetz C.R.H. (2011) Three Phosphatidylglycerol-phosphate Phosphatases in the Inner Membrane of *Escherichia coli. The Journal of Biological Chemistry* 286, 5506-5518.

Lucien, F.P., and Foster, N.R. (1999) Phase behavior and solubility. In: Jessop, P.G., Leitner, W. (Eds.), Chemical Synthesis Using Supercritical Fluids. Wiley- VCH, Weinheim, 37–53

Mantoan, D., and Spilimbergo, S. (2011) Mathematical Modeling of Yeast Inactivation of Freshly Squeezed Apple Juice under High-Pressure Carbon Dioxide. *Critical Reviews in Food Science and Nutrition* 51, 91–97.

Masters, C.I., Shallcross, J.A., Mackey, B.M. (1994) Effect of stress treatments on the detection of *Listeria monocytogenes* and enterotoxigenic *Escherichia coli* by the polymerase chain reaction. *Journal of Applied Bacteriology* 77, 73–79

Mazzoni, A.M., Sharma, R.R., Demerci, A., and Ziegler, G.R. (2001) Supercritical carbon dioxide treatment to inactivate aerobic microorganisms on alfalfa seeds. *Journal of Food Safety* 21, 215-223

Mead, P.S., Slutsker, L., Dietz, V., McCaig, L.F., Bresee, J.S., Shapiro, C., Griffin, P.M., Tauxe, R.V. (1999) Food-related illness and death in the United States. *Emergency Infective Diseases* 5, 607–625

Meujo, D.A.F., Kevin, D.A., Peng, J., Bowling, J.J., Liu, J., and Hamann, M.T. (2010) Reducing oyster-associated bacteria levels using supercritical fluid CO_2 as an agent of warm pasteurization. International *Journal of Food Microbiology*, 138, 63-70

Meurehg, T.C.A. (2006). Control of *Escherichia coli* O157:H7, generic *Escherichia coli*, and *Salmonella* spp. on beef trimmings prior to grinding using a controlled phase carbon dioxide ($cpCO_2$) system. PhD Thesis, Manhattan, Kansas: Kansas State University.

Meyer-Rosberg, K., Scott, D.R., Rex, D., Melchers, K., Sachs, G. (1996) The effect of environmental pH on the proton motive force of *Helicobacter pylori*. *Gastroenterology* 111(4), 886-900

Mitchell, A.C., Phillips, A.J., Hamilton, M.A., Gerlach, R., Hollis, W.K., Kaszuba, J.P., Cunningham, A.B. (2008) Resilience of planktonic and biofilm cultures to supercritical CO2. *The Journal of Supercritical Fluids* 47, 318-325

Montville, T.J., and Matthews, K.R. (2008) *Food Microbology: an introduction*, 2nd edn. ASM Press, Washington, USA, ISBN 9781555813963

Morein, S., Andersson, A.S., Rilfors, L., and Lindblom G. (1996) Wild-type *Escherichia coli* Cells Regulate the Membrane Lipid Composition in a "Window" between Gel and Non-lamellar Structures. *The Journal of Biological Chemistry* 271(12), 6801-6809

Møretrø, T., and Langsrud, S. (2004) *Listeria monocytogenes*: biofilm formation and persistence in food-processing environments. *Biofilms* 1(2), 107-121

Müller, S., and Nebe-von-Caron, G. (2010) Functional single-cell analyses: flow cytometry and cell sorting of microbial populations and communities. *FEMS Microbiology Review* 34(4), 554-587

Mulvey, M.A, Schilling, J.D., and Hultgren, S.J. (2001) Establishment of a persistent *Escherichia coli* reservoir during the acute phase of a bladder infection. *Infection Immunology* 69: 4572–4579

Navarro Llorens, J.M., Torm, A., and Martnez-Garc, E. (2010) Stationary phase in gram-negative bacteria. *FEMS Microbiology Reviews* 34, 476–495

Nebe-von-Caron, G., Stephens, P.J., Hewitt, C.J., Powell, J.R., Badley, R.A. (2000) Analysis of bacterial function by multicolour fluorescence flow cytometry and single cell sorting. *Journal of Microbiological Methods* 42, 97-114

Newell, D.G., Koopmans, M., Verhoef, L., Duizer, E., Aidara-Kane, A., Sprong, H., Opsteegh, M., Langelaar, M., Threfall, J., Scheutz, F., van der Giessen, J. Kruse, H. (2010) Food-borne diseases — The challenges of 20 years ago still persist while new ones continue to emerge. *International Journal of Food Microbiology* 139, S3–S15

Nocker, A., Sossa-Fernandez, P., Burr, M.D., and Camper, A.K. (2007a) Use of Propidium Monoazide for Live/Dead Distinction in Microbial Ecology. *Applied Environmental Microbiology* 73 (16), 5111-5117

Nocker, A., Sossa, K.E., and Camper, A.K. (2007b) Molecular of disinfection efficacy using propidium Monoazide in combination with quantitative PCR. *Journal of Microbiological Methods* 70, 252–260

Nocker, A., Fernández, P.S., Montijn, R., Schuren, F. (2012) Effect of air drying on bacterial viability: A multiparameter viability assessment. *Journal of Microbiological Methods* 90, 86–95

Oliver, J.D. (2005) The Viable but Nonculturable State in Bacteria. *Journal of Microbiology* 43(S), 93-100

Oliver, J.D. (2010) Recent findings on the viable but nonculturable state in pathogenic bacteria. *FEMS Microbiology Reviews* 34 (4), 415-425

Pink, D.A., McNeil, S., Quinn, B., Zuckermann, M.J. (1998) A model of hydrogen bond formation in phosphatidylethanolamine bilayers. *Biochimica et Biophysica Acta* 1368, 289-305

Raj, H. and Liston, J. (1960) Detection and Enumeration of Fecal Indicator Organisms in Frozen Sea Foods. *Applied Environmental Microbiology* 9(2), 171–174

Sahena, F., Zaidul, I.S.M, Jinap S., Karim, A.A., K.A. Abbas, K.A., Norulaini, N.A.N., Omar, A.K.M. (2009) Application of supercritical CO_2 in lipid extraction – A review. *Journal of Food Engineering* 95, 240–253

Seok-In, H., Wan-Soo, P., and Yu-Ryang, P. (1999) Non-thermal inactivation of *Lactobacillus plantarum* as influenced by pressure and temperature of pressurized carbon dioxide. *International Journal of Food Science and Technology* 34(2),125-130

Simon, P.W, Roger E. Freeman, R.E., Vieira, J.V., Boiteux, L.S., Briard, M., Nothnagel, T., Michalik, B., Kwon Y.S. (2008) Carrots. Vegetables II Handbook of Plant Breeding Vol (2), 327-357.

Slonczewski, J.L., Fujisawa, M., Dopson, M., and Krulwich, T.A. (2009) Cytoplasmic pH Measurement and Homeostasis in Bacteria and Archaea. *Advances in microbial physiology* 55, ISBN 978-0-12-374790-7

Spilimbergo, S. (2002) A study about the effect of dense CO_2 on microorganisms. PhD thesis, University of Padova, Italy

Spilimbergo, S., and Bertucco, A (2003) Non-Thermal Bacteria Inactivation With Dense CO_2. *Biotechnology and Bioengineering* 84(6), 627-638.

Spilimbergo, S., Bertucco, A., Basso, G., Bertoloni, G. (2005) Determination of extracellular and intracellular pH of *Bacillus subtilis* suspension under CO_2 treatment. *Biotechnology and Bioengineering* 92, 447–451.

Spilimbergo, S., Mantoan, D., A. Quaranta., A., Della Mea, G. (2009). Real-time monitoring of cell membrane modification during supercritical CO_2 pasteurization. *Journal of Supercritical Fluids* 48, 93-97

Spilimbergo, S., Foladori, P., D. Mantoan, D., Ziglio, G., Della Mea, G. (2010a) High-pressure CO_2 inactivation and induced damage on *Saccharomyces cerevisiae* evaluated by flow cytometry. *Process Biochemistry* 45(5), 647-654

Spilimbergo, S., Quaranta, A., Garcia-Gonzalez, L., Contrini, C., Cinquemani, C., Van Ginneken, L. (2010b) Intracellular pH measurement during high-pressure CO_2 pasteurization evaluated by cell fluorescent staining. *The Journal of Supercritical Fluids* 53 (1–3), 185–191

Spilimbergo, S., Matthews, M.A, and Cinquemani, C. (2011) Chapter 4. Supercritical Fluid Pasteurization and Food Safety. *Book cover: Alternatives to Conventional Food Processing*, ISBN: 978-1-84973-037-2

Spilimbergo, S., Komes, D., Vojvodic, A., Levaj, B.,Ferrentino, G. (2012) High pressure carbon dioxide pasteurization of fresh-cut carrot. *Journal of Supercritical Fluids* 79, (92– 100)

Strawn, L.K., Schneider, K.R., Danyluk, M.D. (2011) Microbial safety of tropical fruits. *Critical Reviews in Food Science and Nutrition* 51, 142–55

Sun, F., Chen, J., Zhong, L., Zhang, X.H., Wang, R, Guo, Q. and Dong, Y. (2008) Characterization and virulence retention of viable but nonculturable *Vibrio harveyi*. *FEMS Microbiological Ecology* 64, 37–44

Suo, B., He, Y., Tu, S.I., and Shi, X. (2010). A multiplex real-time polymerase chain reaction for simultaneous detection of *Salmonella* spp., *Escherichia coli* O157, and *Listeria monocytogenes*in meat products. *Food-borne Pathogens Disease* 7(6), 619-28.

Tahiri, I., Makhlouf, J., Paquin, P., Fliss, I. (2006) Inactivation of food spoilage bacteria and *Escherichia coli* O157:H7 in phosphate buffer and orange juice using dynamic high pressure. *Food Research International* 39, 98–105.

Tamburini, S., Ballarini, A., Ferrentino, G., Moro, A., Foladori, P., Spilimbergo, S., Jousson, O. (2013) Comparison of quantitative PCR and flow cytometry as cellular viability methods to study bacterial membrane permeabilization following supercritical CO_2 treatment. *Microbiology* 159, 1056–1066.

Tari, A. and Huang, L. (1989) Structure and function relationship of phosphatidylglycerol in the of phosphatidylethanolamine bilayer. *Biochemistry* 28, 7708-7712

Toldrá, F. (2004) Dry-cured Ham Meat Products. Wiley-Blackwell, New York

Tsuji, M., Sato, Y., Komiyama, Y. (2005) Inactivation of microorganisms and enzymes in juices by supercritical carbon dioxide method with continuous flow system. *Nippon Shokuhin Kagaku Kogaku Kaishi* 52, 528–531

Tournas, V. H., Heeres, J., and Burgess, L. (2006) Moulds and yeasts in fruit salads and fruit juice. *Food Microbiology*, 23, 684-688

Valverde, M.T., Marin-Iniesta, F., and Calvo, L. (2010). Inactivation of *Saccharomyces cerevisiae* in conference pear with high pressure carbon dioxide and effects on pear quality. *Journal of Food Engineering*, 98, 421-428

Velusamy, V., Arshak, K.,Korostynska, O., Oliwa, K., and Adley, C. (2010) An overview of foodborne pathogen detection: In the perspective of biosensors. *Biotechnology Advanced* **28**, 232–254

Vugia, D., Cronquist, A., Hadler, J., Tobin-D'Angelo, M., Blythe, D., Smith, K., Thornton, K., Morse, D., Cieslak, P., **and other authors** (**2006)** PreliminaryFoodNet data on the incidence of infection with pathogens transmitted commonly through food — 10 states, United States, 2005 (Reprinted from MMWR 55, 392–395,). *The Journal of the American Medical Association* 295, 2241–2243

Wang, Y, Hammes, F., De Roy, K., Willy Verstraete, W., and Boon, N. (2010) Past, present and future applications of flow cytometry in aquatic microbiology. *Trends in Biotechnology* 28, 416–424

Watnick, P., and Kolter, R. (2000) Biofilm, City of Microbes. *Journal of Bacteriology*, 182(10), 2675

Weber, F.J., de Bont, J.A.M. (1996) Adaptation mechanisms of microorganisms to the toxic effects of organic solvents on membranes**.** *Biochimica et Biophysica Acta* 1286, 225-245

Winthrop, K.L., Palumbo, M.S., Farrar, J.A., Mohle-Boetani, J.C., Abbott, S., Beatty, M.E., Inami, G., and Werner, S.B. (2003) Alfalfa sprouts and Salmonella Kottbus infection: a multistate outbreak following inadequate seed disinfection with heat and chlorine. *Journal of Food Protection* 66, 1–13

Wouters, P.C., Bos, A.P., and Ueckert, J. (2001) Membrane Permeabilization in Relation to Inactivation Kinetics of *Lactobacillus* Species due to Pulsed Electric Fields. *Applied Environmental Microbiology* 67(7), 3092–3101

Xu, H.S., Roberts, N., Singleton, F.L., Attwell, R.W., Grimes, D.J., and Colwell, R.R. (1982) Survival and viability of nonculturable *Escherichia coli* and *Vibrio cholerae* in the estuarine and marine environment. *Microbial Ecology* 8,313–323

Yuk, H.G., Geveke, D.J., Zhang, H.Q. (2010) Efficacy of supercritical carbon dioxide for nonthermal inactivation of *Escherichia coli* K12 in apple cider. *International Journal of Food Microbiology* 138, 91–99

Zhang, Y.M., and Rock, C.O. (2008) Membrane lipid homeostasis in bacteria. *Nature Reviews* 6, 222-233.

Zhao, W., Ròg, T., Andrey A. Gurtovenko, A.A, Vattulainen, I., Karttunen, M. (2008) Role of phosphatidylglycerols in the stability of bacterial membranes. *Biochimie* 90, 930-938.

Zhong, Q., Black, D. G., Davidson, P. M., and Golden, D. A. (2008). Nonthermal inactivation of *Escherichia coli* K-12 on spinach leaves, using dense phase carbon dioxide. *Journal of Food Protection*, 71, 1015-1017

Ziglio, G., Andreottola, G., Barbesti, S., Boschetti, G., Bruni, L., Foladori, P., and Villa, R. (2002) Assessment of activated sludge viability with flow cytometry. *Water Research* 36, 460-468.

Chapter 9: **Appendix**

9.1 Publications and Contributions

9.1.1 Publications on the topic of the doctoral thesis:

My PhD project was focused on the development and application of new cellular viability assays, including propidium monoazide quantitative PCR (PMA-qPCR) and flow cytometry (FCM) to monitor the efficiency of SC-CO_2 treatment on relevant food-borne pathogens (*E. coli, S. enterica, L. monocytogenes*). The experiments were performed on bacteria grown in liquid cultures, on a synthetic solid substrate, and directly on food products. First, the data showed that FCM allows accurate monitoring of bacterial cellular status during treatment. The method could be applied, with some adjustments, to any field where determining microbial viability status is of importance, including food, environment or in the clinic. I published these results as first and corresponding author in *Microbiology*.

After optimization and validation, the FCM approach was subsequently applied to assess the evolution of viability and cultivability of *E. coli* cells spiked on fresh cut carrots during SC-CO_2 treatment. A large fraction of the non-cultivable cells that maintained the integrity of their membrane, likely entering in a Viable But Not Cultivable (VNBC) state, and potentially leading to a regrowth phenomenon, which has important practical implications on food processing. I submitted these results as first and corresponding author to *International Journal of Food Microbiology* (article under review).

To get insights into the mechanism of bacterial inactivation mediated by SC-CO_2, detailed structural (LC-MS), cellular (FCM) and gene expression (qPCR) experiments were performed. Specifically, NMR and HPLC/ESI-MS analysis were performed in collaboration with Professor Graziano Guella (Bioorganic Chemistry Laboratory, Physics Department, University of Trento). The data indicated that SC-CO_2 affected all Phosphatidylglycerol (PG) species inducing depolarization and partialy-permeabilization of all most of *E. coli* cells. These results would be published soon, the manuscript is in preparation and I will submitted these data as first author to *Journal of Biological Chemistry.*

Papers:

Tamburini, S., Andrea Anesi, A., Ferrentino, G., Spilimbergo, S., Guella G. Jousson, O. Supercritical CO_2 induces marked changes in membrane phospholipids composition in *Escherichia coli* K12. In preparation.

Tamburini, S., Foladori, P., Ferrentino, G., Spilimbergo S., Jousson O. Flow cytometry as an accurate tool to monitor *E. coli* subpopulations on solid food products after SC-CO_2 treatment. *International Journal of Food Microbiology*, under review. (Publication B)

Tamburini, S., Ballarini, A., Ferrentino, G., Moro, A., Foladori, P., Spilimbergo, S., Jousson, O. (2013). Comparison of quantitative PCR and flow cytometry as cellular viability methods to study bacterial membrane permeabilization following supercritical CO_2 treatment. *Microbiology* 159, 1056–1066. (Publication A)

Abstracts:

Tamburini S., Anesi, A., Ferrentino, G., Spilimbergo, S., Guella, G., Jousson, O. SC-CO_2 affects membrane phospholipids profile in *Escherichia coli* K12. Proceeding of FEMS2013. July 21-25, 2013. Leipzig, Germany.

Ferrentino, G., **Tamburini, S**., Foladori., Jousson, O. Spilimbergo, S. Evaluation of Supercritical Carbon Dioxide Inactivation effect on Salmonella enterica spiked on Fresh Cut Coconut by using Plate Count, Flow Cytometry and Real time PCR techniques. Proceeding of 10th Conference of Supercritical Fluids and their Applications. April 29- May 6 2013. Napoli, Italy.

Tamburini, S., Ballarini, A., Ferrentino, G., Foladori, P., Spilimbergo, S., Jousson, O. Supercritical CO_2 treatment induces membrane permeabilization in food-borne bacterial pathogens. Proceeding of SIMGBM 29th National meeting. September 21-23 2011. Pisa, Italy.

Tamburini, S., Ballarini, A., Ferrentino, G., Foladori, P., Spilimbergo, S., Jousson, O. Evaluation of cellular viability of food-borne bacterial pathogens after supercritical CO_2 treatment. Proceeding of FEMS2011. June 26-30, 2011. Geneve, Switzerland.

9.1.2 Publications on other microbiology topics

During this period, I also had the occasion to provide a contribution to other projects, resulting in co-authorship of other articles, including:

a collaboration with Dr. Paola Foladori (Department of Civil, Environmental and Mechanical Engineering, University of Trento), in which I performed FCM analysis to quantify viable and dead cells in a wastewater treatment plant and to evaluate viability of bacteria living in activated sludge after some sludge reduction technologies (Foladori *et al*., 2010)

a collaboration with Dr. Hussnain A. Janjua (Microbial Genomics Laboratory, CIBIO, University of Trento) where I performed gene expression analysis of virulence factors in clinical *Pseudomonas aeruginosa* strains isolated from acute infections (Janjua *et al*., 2012).

Papers:

Janjua, H.A., Segata, N., Bernabò, P., **Tamburini**, S., Ellen, A., Jousson, O. (2012) Clinical populations of *Pseudomonas aeruginosa* isolated from acute infections show a high virulence range partially correlated with population structure and virulence gene expression. *Microbiology* 158, 2089-2098. (Publication C)

Foladori, P., **Tamburini, S**., Bruni, L. (2010) Bacterial permeabilisation and disruption caused by sludge reduction technologies evaluated by flow cytometry. *Water Research* 44 (17), 4888-99. (Publication D)

Abstracts:

Tamburini, S., Foladori, P., Bruni., L. Application of flow cytometry for the rapid quantification of viable bacteria and biomass in wastewater and activated sludge. Proceeding of Cytometry. October 26-28 2011. Paris, France.

Tamburini, S., Foladori, P., Bruni, L., Menapace, V. Effects of ozonation on permeabilisation and disruption of bacteria in activated sludge evaluated by flow cytometry. Proceeding of SIMGBM 29th National meeting. September 21-23 2011. Pisa, Italy.

Tamburini, S., Foladori, P., Bruni, L. Flow cytometry as a rapid tool to assess toxic effects on activated sludge in wastewater treatment plants. Proceeding of FEMS2011. June 26-30, 2011. Geneve, Switzerlan

9.2 Publication A:

Tamburini, S., Ballarini, A., Ferrentino, G., Moro, A., Foladori, P., Spilimbergo, S., Jousson, O. (2013). Comparison of quantitative PCR and flow cytometry as cellular viability methods to study bacterial membrane permeabilization following supercritical CO_2 treatment. *Microbiology* 159, 1056–1066

The proper formatting of Figure 7 was add after the paper

Microbiology (2013), **159**, 1056–1066 **DOI** 10.1099/mic.0.063321-0

Comparison of quantitative PCR and flow cytometry as cellular viability methods to study bacterial membrane permeabilization following supercritical CO_2 treatment

Sabrina Tamburini,[1] Annalisa Ballarini,[1] Giovanna Ferrentino,[2] Albertomaria Moro,[1] Paola Foladori,[3] Sara Spilimbergo[2] and Olivier Jousson[1]

Correspondence
Sabrina Tamburini
tamburini@science.unitn.it

[1]Centre for Integrative Biology, University of Trento, 38123 Trento, Italy

[2]Department of Materials Engineering and Industrial Technologies, University of Trento, 38123 Trento, Italy

[3]Department of Civil and Environmental Engineering, University of Trento, 38123 Trento, Italy

Foodborne illness due to bacterial pathogens is increasing worldwide as a consequence of the higher consumption of fresh and minimally processed food products, which are more easily cross-contaminated. The efficiency of food pasteurization methods is usually measured by c.f.u. plate counts, a method discriminating viable from dead cells on the basis of the ability of cells to replicate and form colonies on standard growth media, thus ignoring viable but not cultivable cells. Supercritical CO_2 (SC-CO_2) has recently emerged as one of the most promising fresh food pasteurization techniques, as an alternative to traditional, heat-based methods. In the present work, using three SC-CO_2-treated foodborne bacteria (*Listeria monocytogenes*, *Salmonella enterica* and *Escherichia coli*) we tested and compared the performance of alternative viability test methods based on membrane permeability: propidium monoazide quantitative PCR (PMA-qPCR) and flow cytometry (FCM). Results were compared based on plate counts and fluorescent microscopy measurements, which showed that the former dramatically reduced the number of cultivable cells by more than 5 log units. Conversely, FCM provided a much more detailed picture of the process, as it directly quantifies the number of total cells and distinguishes among three categories, including intact, partially permeabilized and permeabilized cells. A comparison of both PMA-qPCR and FCM with plate count data indicated that only a fraction of intact cells maintained the ability to replicate *in vitro*. Following SC-CO_2 treatment, FCM analysis revealed a markedly higher level of bacterial membrane permeabilization of *L. monocytogenes* with respect to *E. coli* and *S. enterica*. Furthermore, an intermediate permeabilization state in which the cellular surface was altered and biovolume increased up to 1.5-fold was observed in *L. monocytogenes*, but not in *E. coli* or *S. enterica*. FCM thus compared favourably with other methods and should be considered as an accurate analytical tool for applications in which monitoring bacterial viability status is of importance, such as microbiological risk assessment in the food chain or in the environment.

Received 7 September 2012
Accepted 6 April 2013

INTRODUCTION

Foodborne illness is a public health challenge that, according to a World Health Organization report (WHO, 2007), caused almost 1.8 million human deaths in 2005 (Velusamy *et al.*, 2010). Such illness is mostly caused by eating food contaminated with pathogenic bacteria (e.g. *Escherichia coli* 0157 : H7, *Listeria monocytogenes*, *Salmonella enterica*), which enter the food supply through cross-contamination events or food handlers' poor hygiene. In particular, fresh or minimally processed fruit and vegetable products can easily become contaminated with pathogens along the food chain, from harvesting through transportation and processing, to handling. Food consumption patterns worldwide have now changed in favour of these

Abbreviations: FALS, forward angle light scatter; FCM, flow cytometry; FRET, fluorescence resonance energy transfer; gDNA, genomic DNA; LALS, large angle light scatter; PI, propidium iodide; PMA-qPCR, propidium monoazide quantitative PCR; SC-CO_2, supercritical CO_2; SYBR-I, SYBR Green I; VBNC, viable but not cultivable.

fresh (Anon, 2002) or minimally processed (Gandhi & Chikindas, 2007) ready-to-eat food products; as a consequence, the risk of foodborne illness is increasing.

Foodborne illnesses caused by fresh/minimally processed products can be prevented by applying pasteurization treatments aiming to reduce the number of viable pathogens without affecting food taste, appearance and quality. Thermal pasteurization procedures are highly effective, but they do not apply to fresh food products. Thus, non-thermal pasteurization methods have been developed, which inactivate microbes while not adversely compromising food integrity or nutritional quality, including high hydrostatic pressure and pulsed electrical fields (Devlieghere *et al.*, 2004), dense CO_2 or supercritical CO_2 (SC-CO_2) (Spilimbergo & Bertucco, 2003).

Among the latter methods, SC-CO_2 non-thermal pasteurization is one of the most promising for fresh food products. This method is based on the fluid state of CO_2 reached at or above its critical temperature and critical pressure. Compared with heat- and high hydrostatic pressure-based pasteurization, it has the advantage of working in a range of relatively low temperature (30–40 °C) and moderate pressure (80–120 bar), thus having a much lower impact on nutritional, organoleptic and physico-chemical properties of fresh/minimally processed food products (Garcia-Gonzalez *et al.*, 2007). The pasteurization efficiency of SC-CO_2 has been tested on several micro-organisms spiked into various substrates (Spilimbergo & Bertucco, 2003; Ferrentino & Spilimbergo, 2011). Specifically, treatments have led to a 3–4 log c.f.u. ml^{-1} reduction in physiological saline buffer (Ballestra *et al.*, 1996; Erkmen, 2000; Erkmen & Karaman, 2001) and to a 2–2.5 log c.f.u. cm^{-2} reduction on solid food products (Jung *et al.*, 2009; Bae *et al.*, 2011). The effect of SC-CO_2 on living cells has not been fully deciphered. Several hypotheses have been proposed based on experimental observations, including solubilization of pressurized CO_2 in the external liquid phase, cell membrane permeabilization, intracellular acidification, key enzyme inactivation/cellular metabolism inhibition due to pH lowering, direct (inhibitory) effect of molecular CO_2 and HCO_3^- on metabolism, disordering of the intracellular electrolyte balance, and removal of vital constituents from cells and cell membranes. Most of these steps may not occur consecutively, but rather take place simultaneously in a very complex and interrelated manner (Spilimbergo & Bertucco, 2003; Garcia-Gonzalez *et al.*, 2007).

To evaluate pasteurization efficiency, bacterial inactivation is typically deduced from c.f.u. plate counts, a viability test method measuring the bacterial ability to replicate and form colonies upon standard growth conditions. It is well known that, under environmental stress conditions (e.g. nutrient limitation, pressure, temperature), a number of pathogens enter into a so-called viable but not cultivable state (VBNC), becoming even more resistant to stress (Oliver, 2010). Thus, plate counts may overestimate pasteurization efficiency, by not detecting as viable reversibly damaged bacterial cells (Keer & Birch, 2003).

Additional viability test methods may be more suited for studying the efficiency of pasteurization treatment on bacterial cells, including propidium monoazide quantitative PCR (PMA-qPCR) (Nocker & Camper, 2006) and flow cytometry (FCM) (Müller & Nebe-von-Caron, 2010). Both methods employ cell-membrane permeability as the viability parameter. PMA-qPCR is a quantitative PCR amplification performed after PMA staining, an anologue of propidium iodide (PI) with a covalently linked azide group, used as a marker of bacterial cells with a permeabilized membrane. After photoactivation, PMA binds irreversibly to dsDNA, thus inhibiting DNA amplication during qPCR or causing DNA loss with cellular debris during DNA extraction. PMA was used to discriminate intact and permeabilized cells in an environmental matrix (Nocker *et al.*, 2007a) and was applied to monitor the effect of disinfection treatments altering membrane integrity (Nocker *et al.*, 2007b).

FCM is a multi-parametric and single-cell analysis technique for high-throughput and real-time quantification of multiple cellular parameters, such as cell size, surface granularity and physiological state. In FCM, two light-scattering signals can be collected simultaneously from each bacterial cell: the forward-angle light scatter (FALS), which is related to bacterial size (Foladori *et al.*, 2008), and the large-angle light scatter (LALS), measuring cell density or granularity (Müller & Nebe-von-Caron, 2010). In FCM studies, the fluorophore SYBR Green I (SYBR-I) is often used as a total cell marker, given its ability to cross the cell membrane and to bind to DNA (Barbesti *et al.*, 2000), whilst PI is used as a dead cell marker, as it penetrates only cells with a permeabilized membrane (Ziglio *et al.*, 2002). In permeabilized cells the simultaneous presence of SYBR-I and PI activates fluorescence resonance energy transfer (FRET), due to the total absorption of the fluorescent emission spectrum of SYBR-I by PI. In these conditions, it is therefore possible to distinguish intact cells emitting green fluorescence from permeabilized ones emitting red fluorescence. FCM coupled with fluorescent dyes (SYBR-I and PI or Syto9 and PI) was used to discriminate intact and permeabilized cells in a wastewater treatment plant (Foladori *et al.*, 2010) and to monitor the effect of various antibacterial treatments (Wouters *et al.*, 2001; Kim *et al.*, 2009).

In the present work, *L. monocytogenes*, *E. coli* and *S. enterica* were treated with SC-CO_2 to evaluate the performance of different cell viability assays. Data from FCM and PMA-qPCR were compared with plate counts and fluorescent microscopy, to evaluate which method is the most appropriate to correctly discriminate viable from dead cells after treatment.

METHODS

Bacterial strains and sample preparation. The three strains used in this study were purchased from the American Type Culture

Collection. *S. enterica* ATCC 14028 and *E. coli* ATCC 29522 were grown on solid Luria–Bertani (LB) agar medium (Sigma-Aldrich) at 37 °C for 16 h. *L. monocytogenes* ATCC 19111 was grown on solid brain heart infusion (BHI) medium (Becton Dickson) at 37 °C for 16 h. One colony was picked and inoculated into 200 ml of corresponding broth medium. Bacterial cultures were incubated at 37 °C with constant shaking (200 r.p.m.) to stationary phase (16 h). Cells were collected by centrifuging at 6000 r.p.m. for 10 min and were resuspended in an equal volume of PBS (Sigma-Aldrich).

SC-CO_2 treatment. The SC-CO_2 treatment was performed in a multi-batch apparatus as described by Mantoan & Spilimbergo (2011). Briefly, the system consisted of 10 identical 15 ml-capacity reactors operating in parallel. All reactors were submerged in the same temperature-controlled water bath to maintain the desired temperature constant throughout the process. Each reactor was connected to an on–off valve for independent depressurization and had an internal magnetic stirrer device to guarantee homogeneous dissolution in the cell suspension. Aliquots of 10 ml of each bacterial suspension, prepared as described above, were transferred to the reactors. The SC-CO_2 treatment was carried out at 120 bar and 35 °C, as these operative conditions were selected in preliminary plate counts experiments as the mildest ones that induced significant microbial inactivation. SC-CO_2 treatment was interrupted after 5, 15, 30, 45 or 60 min by slowly depressurizing the reactor over approximately 1 min.

Plate counts. Untreated and SC-CO_2-treated cells were serially diluted with 1× PBS (900 µl PBS and 100 µl sample) and were spread-plated on chromogenic coli/coliform agar (Liofilchem) for *E. coli*, on chromatic Salmonella agar (Liofilchem) for *S. enterica* and on O.A. Listeria agar (Liofilchem) for *L. monocytogenes*. The plates were incubated at 37 °C for 24 h. Three independent experiments were performed for each species.

Fluorescence microscopy. In total, 10^8 untreated or SC-CO_2-treated cells were stained with SYBR-I and PI, as described for FCM. After staining, cells were centrifuged at 10 000 r.p.m. for 10 min and the pelleted cells were resuspended in 1× PBS and 30 % Moviol. Fluorescence microscopy images were acquired in bright-field at 490 and 750 nm, with a ZeissAxio Observer Z.1 microscope with Zeiss ApoTome device using the AxioVision Rel. 4.8.1 software (Zeiss) according to the manufacturer's instructions.

Genomic DNA extraction and PMA staining. In total, 10^7–10^8 untreated or treated cells were stained with PMA (Biotium), at a final concentration of 50 µM, and incubated at room temperature in the dark for 5 min. Stained samples were then exposed to UV light for 5 min and centrifuged for 10 min at 12 000 r.p.m. Cell pellets were stored at −20 °C. Genomic DNA (gDNA) was extracted from unstained and PMA-stained samples using a Qiagen DNeasy Blood and Tissue kit, according to the manufacturer's instructions. A modified protocol was used for *L. monocytogenes*: cells were incubated at 37 °C for 1 h with the enzymic lysis buffer provided by the supplier. Cells were then incubated at 56 °C for 30 min and were treated with RNase A. After column purification, DNA was eluted with 100 µl 10 mM Tris/HCl, pH 8.0. DNA quality was assessed by 0.7 % agarose gel electrophoresis, run at 70 V for 30 min and followed by ethidium bromide staining. DNA concentration and purity were assessed by measuring the absorbance at 260 nm (A_{260}) and the ratio of the absorbance at 260 and 280 nm (A_{260}/A_{280}) with a NanoDrop ND-1000 spectrophotometer (Thermo Scientific).

Real-time qPCR. Primer and TaqMan probe set sequences targeting the *hlyA* and the *invA* genes were used for *L. monocytogenes* and *S. enterica* identification, respectively (Suo *et al.*, 2010). The best candidate primers and probe sets for *E. coli* identification were designed in-house on the *uidA* marker gene with AlleleID7.0 software (PREMIER Biosoft International). Primer sequences and their features are detailed in Table 1. The reaction mixture contained 1× iQ Multiplex Powermix (Bio-Rad Laboratories), 200 nM each primer, 200 nM probe and 2 µl template gDNA (or 2 µl distilled H_2O for the no-template control) in a total volume of 25 µl. Each TaqMan PCR assay was performed in triplicate using a CFX96 Real-time PCR Detection System (Bio-Rad Laboratories), with the following cycling programme: 3 min at 95 °C, 15 s at 95 °C and 1 min at 60 °C for 40 cycles. PCR results were analysed using CFX Manager 1.1 software (Bio-Rad Laboratories). The correlation between PCR *Ct* values and gene copy numbers was obtained by means of a standard curve. Cell number equivalents were then extrapolated by taking into account the mean bacterial genome size for each target bacterium available at NCBI (http://www.ncbi.nlm.nih.gov/genomes/MICROBES/microbial_taxtree.html), assuming each gene is present in a single copy per genome. The number of gDNA copies for experimental samples was determined by using the inverse formula of linear equation of each species (DNA copies$=10^{[(Ct-q)m-1]}$). The amplification efficiency for each primer/probe set was calculated as $E=10^{(-1/\text{slope})}-1$ (Klein, 2002). Assays were performed in parallel on cell suspensions before and after PMA staining to quantify total and intact cell number equivalents, respectively.

Flow cytometry. Untreated and SC-CO_2-treated cell suspensions were diluted to 10^7–10^8 cells ml^{-1}; then 1 ml was stained with 10 µl SYBR-I (Merck), 1 : 30 000 final concentration in DSMO, and 10 µl PI 1 mg ml^{-1} (Invitrogen). Peak excitation and emission wavelengths were at $\lambda_{ex}=495$ nm, $\lambda_{em}=525$ nm for SYBR-I and $\lambda_{ex}=536$ nm, $\lambda_{em}=617$ nm for PI. Samples were incubated at room temperature in the dark for 15 min. FCM analyses were performed with an Apogee-A40 flow cytometer (Apogee Flow Systems) equipped with an argon laser emitting at 488 nm. For each cell crossing the focus point of the laser, two light-scattering signals (FALS and LALS) and two fluorescence signals (red and green) were collected. LALS and FALS were collected on a 256-channel linear scale while fluorescence signals were collected with logarithmic amplifier gain. The conversion of FALS intensities to biovolumes was performed as proposed by Foladori *et al.* (2008). To exclude electronic noise, thresholds were set on green or red fluorescence histograms.

RESULTS

Cell viability evaluated by plate counts and fluorescence microscopy

The efficiency of SC-CO_2 treatment was evaluated by quantifying bacterial cells able to replicate using plate counts and observing PI uptake by fluorescence microscopy (Fig. 1). To compare the efficiency of treatment among the tested species, the bacterial inactivation was expressed as $\log_{10}(N_i/N_0)$, as a function of treatment time (Fig. 1a). After 5 min, only *S. enterica* cells showed more than 1 log reduction. After 30 min the process dramatically reduced the number of cultivable cells by more than 5 log in all three species. An increase of treatment time up to 60 min did not induce any additional significant inactivation.

Bacterial inactivation on the basis of PI uptake as a function of treatment time was evaluated by using fluorescent staining of SYBR-I and PI. Fluorescence microscopy images of untreated and treated bacterial cells (Fig. 1b) showed a significant shift from green fluorescence to yellow/red fluorescence after 30 min treatment: almost

Table 1. Gene targets, primers and probes used for qPCR

Dyes refer to the reporter and quenching fluorophores linked to the TaqMan probe sequences.

Oligo name	Gene target	Sequence (5′–3′)	T_m (°C)*	Dye (5′–3′)	Reference
EC-uidAF	*uidA*	CTCTGCCGTTTCCAAATC			This work
EC-uidAR		GAAGCAACGCGTAAACTC			
EC-uidAP		AATGTAATGTTCTGCGACGCTCAC			
SE-invAF	*invA*	GTTGAGGATGTTATTCGCAAAGG	70.1	HEX/BHQ1	Suo *et al.* (2010)
SE-invAR		GGAGGCTTCCGGGTCAAG			
SE-invAP		CCGTCAGACCTCTGGCAGTACCTTCCTC	69.0	FAM/BHQ1	
LM-hlyAF	*hlyA*	ACTGAAGCAAAGGATGCATCTG			Suo *et al.* (2010)
LM-hlyAR		TTTTCGATTGGCGTCTTAGGA			
LM-hlyAP		CACCACCAGCATCTCCGCCTGC	70.0	TR/BHQ2	

*T_m, Melting temperature.

all *L. monocytogenes* cells emitted yellow/red fluorescence whilst *E. coli* and *S. enterica* cells emitted green, yellow and red fluorescence.

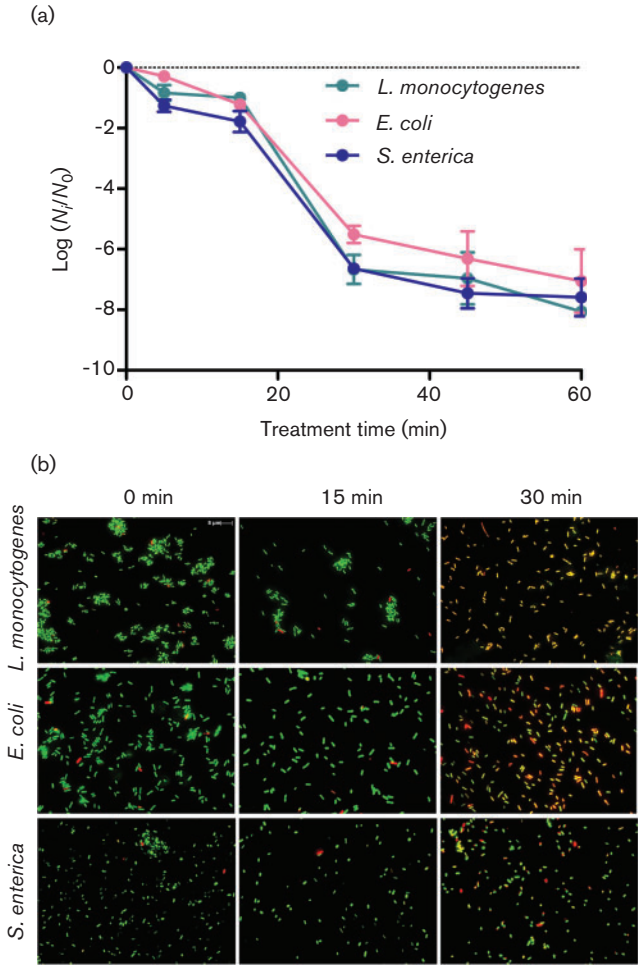

Fig. 1. Bacterial inactivation following SC-CO_2 treatment evaluated by (a) plate counts expressed as logN_i/N_0 and (b) fluorescence microscopy after staining by SYBR-I and PI.

Bacterial membrane permeabilization evaluated by PMA-qPCR

TaqMan qPCR analyses were performed on gDNA samples extracted from cell suspensions before and after PMA staining, to quantify both total and intact cell unit equivalents. qPCR data for each bacterial species revealed that the fraction of intact cells from all three species was reduced to less than 50 % cell equivalents. However, such reduction was reached after different treatment time periods: 30–45 min for *L. monocytogenes*, 15–30 min for *E. coli* and 5–15 min for *S. enterica* (Table 2). After 5 min, *L. monocytogenes* intact cells showed a 10 % reduction, whereas *E. coli* and *S. enterica* intact cells showed a 20 and 35 % reduction, respectively. After the longest treatment time (60 min), the proportion of permeabilized cells was 82.4 % for *L. monocytogenes*, 66.6 % for *E. coli* and 41.9 % for *S. enterica*.

Detection of intact and permeabilized cells by FCM

Upon staining of a mixed population of intact and permeabilized cells with SYBR-I and PI, FCM distinguishes among three cellular states: (i) intact cells, emitting only high FL1 intensity due to the absence of intracellular PI; (ii) partially permeabilized cells emitting high fluorescent intensity both in FL1 and in FL3 channels, due to incomplete FRET between SYBR-I and intracellular PI; and (iii) permeabilized cells emitting only high FL3 intensity, due to the simultaneous presence of SYBR-I and PI in the cells and complete FRET. Analyses were performed on cell suspensions stained with both SYBR-I and PI for quantification of total and permeabilized cells, respectively. The observed kinetics of cell membrane permeabilization was specific for each bacterial species (Table 3). With regard to *L. monocytogenes*, the percentage of intact cells was 99.5 % in the untreated suspension, but this decreased significantly with treatment time. After 5 min, a small fraction of cells (1.3 %) were partially permeabilized. After 30 min, the number of partially permeabilized cells reached its maximum, i.e. 17.2 % of total cells, whereas the percentage of

Table 2. Target gene copy numbers determined by qPCR following SC-CO_2 treatment

Mean (±SD) target-gene copy number were determined in triplicate for each species and each treatment time. The percentages of intact cells reduction were calculated as the ratio of treated PMA-stained cells relative to untreated. NA, Not applicable.

Species and fluorophores	Treatment time (min)	Target gene copy numbers		
		−PMA (total cell equivalents)	+PMA (intact cell equivalents)	% Intact cells reduction
L. monocytogenes				
hlyA (Texas Red)	0	$5.24 \times 10^7 \pm 0.86$	$7.28 \times 10^7 \pm 0.30$	NA
	5	$4.91 \times 10^7 \pm 0.67$	$6.81 \times 10^7 \pm 0.62$	6.43±6.41
	15	$4.89 \times 10^7 \pm 0.45$	$4.88 \times 10^7 \pm 0.10$	32.92±4.80
	30	$4.92 \times 10^7 \pm 0.89$	$4.91 \times 10^7 \pm 0.71$	32.55±7.60
	45	$9.46 \times 10^7 \pm 2.06$	$0.69 \times 10^7 \pm 0.57$	90.39±5.63
	60	$9.37 \times 10^7 \pm 1.02$	$1.27 \times 10^7 \pm 0.23$	82.44±6.06
E. coli				
uidA (HEX)	0	$1.89 \times 10^8 \pm 0.73$	$2.21 \times 10^8 \pm 0.19$	NA
	5	$1.45 \times 10^8 \pm 0.37$	$1.73 \times 10^8 \pm 0.25$	22.04±10.85
	15	$1.33 \times 10^8 \pm 0.52$	$1.78 \times 10^8 \pm 0.16$	19.57±12.00
	30	$0.80 \times 10^8 \pm 0.48$	$0.47 \times 10^8 \pm 0.17$	78.54±10.90
	45	$0.87 \times 10^8 \pm 0.09$	$0.80 \times 10^8 \pm 0.06$	63.55±13.10
	60	$0.90 \times 10^8 \pm 0.25$	$0.74 \times 10^8 \pm 0.20$	66.55±11.20
S. enterica				
invA (FAM)	0	$3.78 \times 10^8 \pm 0.18$	$5.62 \times 10^8 \pm 4.12$	NA
	5	$3.44 \times 10^8 \pm 1.20$	$3.47 \times 10^8 \pm 0.49$	34.57±10.51
	15	$2.57 \times 10^8 \pm 0.13$	$2.51 \times 10^8 \pm 0.00$	55.36±13.24
	30	$3.00 \times 10^8 \pm 0.12$	$3.11 \times 10^8 \pm 0.39$	44.66±11.45
	45	$3.77 \times 10^8 \pm 0.13$	$3.73 \times 10^8 \pm 0.58$	33.66±13.02
	60	$3.65 \times 10^8 \pm 1.10$	$3.27 \times 10^8 \pm 0.43$	41.85±14.07

intact cells decreased but remained high (71.2 %). After 45 min, the percentages of both intact and partially permeabilized cells decreased significantly and almost all cells (96.4 %) were fully permeabilized.

The untreated *E. coli* and *S. enterica* bacterial suspensions contained 99.8 and 98.6 % of intact cells, respectively. As for *L. monocytogenes*, after 5 min of treatment a small percentage of cells (3.0 and 4.8 %, respectively) became partially permeabilized, while a negligible amount of dead cells was detected. After 15 min, *E. coli* subpopulations maintained the same distribution, with 96.2 % of intact cells and 3.6 % of partially permeabilized cells. By contrast, almost all *S. enterica* cells were split between intact (59.9 %) and partially permeabilized (39.6 %). After 30 min, a similar behaviour was observed for *E. coli* and *S. enterica* populations: a large percentage of cells were partially permeabilized (95.3 and 93.7 %, respectively) but almost no totally permeabilized cells were detected. Longer SC-CO_2 treatment times did not lead to significant changes in population distribution, as the vast majority of cells (99.2 %) from both species remained in the partially permeabilized state.

Investigation of subpopulations of partially permeabilized cells by FCM

The kinetics of cell inactivation was further investigated by FCM, examining the variation over time in SYBR-I and PI uptake in SC-CO_2-treated samples. As shown in Fig. 2, *L. monocytogenes*, *E. coli* and *S. enterica* differed in their SYBR-I uptake kinetics, as shown by the green fluorescence intensity (FL1 channel) at each treatment time point. For example, the intensity measured in the FL1 median channel for *L. monocytogenes* was constant for treatment-time extensions from 5 to 30 min (Fig. 2a). The graph of FL1 intensity showed limited variations in the FL1 median channel, which ranged from 402 to 412 units based on the arbitrary 1024-channel scale. This result indicates that the uptake of SYBR-I in *L. monocytogenes* is complete even in the untreated cells. For treatment times higher than 45 min, the FL1 median channel decreased to 202–220 units, due to the large percentage of permeabilized cells, in which FRET (i.e. quenching of FL1 fluorescence by PI) occurred.

Conversely, the FL1 intensity of intact cells in untreated samples of *E. coli* was weak and close to the threshold of FL1-positive signals (Fig. 2b) due to partial staining of cells by SYBR-I. By increasing SC-CO_2 treatment time, both *E. coli* and *S. enterica* populations showed a progressive and significant increase of FL1 intensity, corresponding to a shift of the FL1 histogram peak from left to right and to an increase in peak intensity far above the background threshold of the instrument (Fig. 2b,c). *E. coli* and *S. enterica* populations reached their maximum value of FL1 median channel after 45 and 15 min, respectively. This

Table 3. Membrane permeabilization determined by FCM following SC-CO_2 treatment

Bacterial species	Treatment time (min)	Intact cells* (%)	Partially permeabilized cells† (%)	Permeabilized cells‡ (%)
L. monocytogenes	0	99.5	0.2	0.2
	5	97.4	1.3	1.3
	15	96.2	1.7	2.0
	30	71.2	17.2	11.0
	45	0.5	3.1	96.4
	60	0.5	7.3	92.2
E. coli	0	99.8	0.2	0.1
	5	96.8	3.0	0.2
	15	96.2	3.6	0.2
	30	4.5	95.3	0.2
	45	7.5	92.1	0.2
	60	0.3	99.2	0.2
S. enterica	0	98.6	1.0	0.3
	5	94.9	4.8	0.2
	15	59.9	39.6	0.3
	30	5.9	93.7	0.3
	45	11.5	88.0	0.3
	60	0.3	99.2	0.5

*Intact cells emitting only high FL1 intensity.
†Partially permeabilized cells emitting high fluorescent intensity in both FL1 and FL3 channels.
‡Permeabilized cells emitting only high FL3 intensity.

progressive increase in FL1 emission in *E. coli* and *S. enterica* is probably due to the gradual permeabilization of cells during SC-CO_2 treatment, which facilitated the uptake of SYBR-I.

As shown in Fig. 3, for the *E. coli* population, the presence of a subpopulation with high FL1 intensity was negligible in untreated samples, whereas it was detectable (15.2 %) after 5 min of treatment and dominant (86 %) after 30 min. Among the 15.2 % of *E. coli* cells with higher FL1 intensity after 5 min, 12.0 % represented intact cells whilst 3.2 % were partially permeabilized cells. After 30 min, the progressive staining by PI resulted in 95.3 % of partially permeabilized cells, with a fraction of 86 % with high FL1 intensity.

With regard to the *S. enterica* population, the FL1 intensity increased significantly in a group of cells after 15 min of treatment. This subpopulation moved to the right on the FL1 graph, being characterized by a higher SYBR-I uptake (Fig. 4). Only cells with initial high FL1 intensity moved towards the region of partially permeabilized cells. These results suggest that the treatment led first to the progressive introduction of SYBR-I with the complete staining of cells and the emission of high FL1 intensity, and, later, when the membrane became more permeable, to the progressive and partial staining of cells by PI. The co-occurrence of green and red fluorescence is probably a consequence of incomplete FRET occurring between SYBR-I and PI, due to a lower PI uptake.

Interestingly, while the group of cells with low SYBR-I concentration exhibited a unimodal distribution, the group of cells with high SYBR-I concentration was characterized by a noticeable bimodal distribution (Fig. 4) corresponding to two subpopulations with different amounts of DNA. The ratio of the FL1 intensity (high DNA peak/low DNA peak ratio) was about 1.5. Additionally, the FALS ratio of the two subpopulations was 1.4, indicating a larger brighter fluorescent peak, therefore confirming that the subpopulation of bacteria with a larger amount of DNA also had a larger biovolume. FL1 intensity and FALS ratios indicated that these cells are dividing actively.

Morphological changes evaluated by LALS and FALS FCM signals

The light-scattering signals collected by the flow cytometer, i.e. FALS and LALS, are related to physical properties of the bacteria. In particular, FALS depends on bacterial size (and cellular biovolume) while LALS is related to the complexity of the cellular surface, cell density and granularity. The FALS and LALS signals of *E. coli* and *S. enterica* populations did not change significantly over treatment time (data not shown). Conversely, *L. monocytogenes* cells showed changes in both light-scattering signals at different treatment times. In particular, although the scattering signals of intact and permeabilized *Listeria* cells were similar, as demonstrated by the overlapping distributions in Fig. 5, the partially permeabilized cells were characterized by a higher FALS intensity (larger size) and slightly higher LALS intensity. With reference to an arbitrary scale of 1024 channels, the peaks of the FALS distribution of intact and permeabilized cells of *L. monocytogenes* were at channels 187 and 133, respectively, whereas the peak of partially permeabilized cells

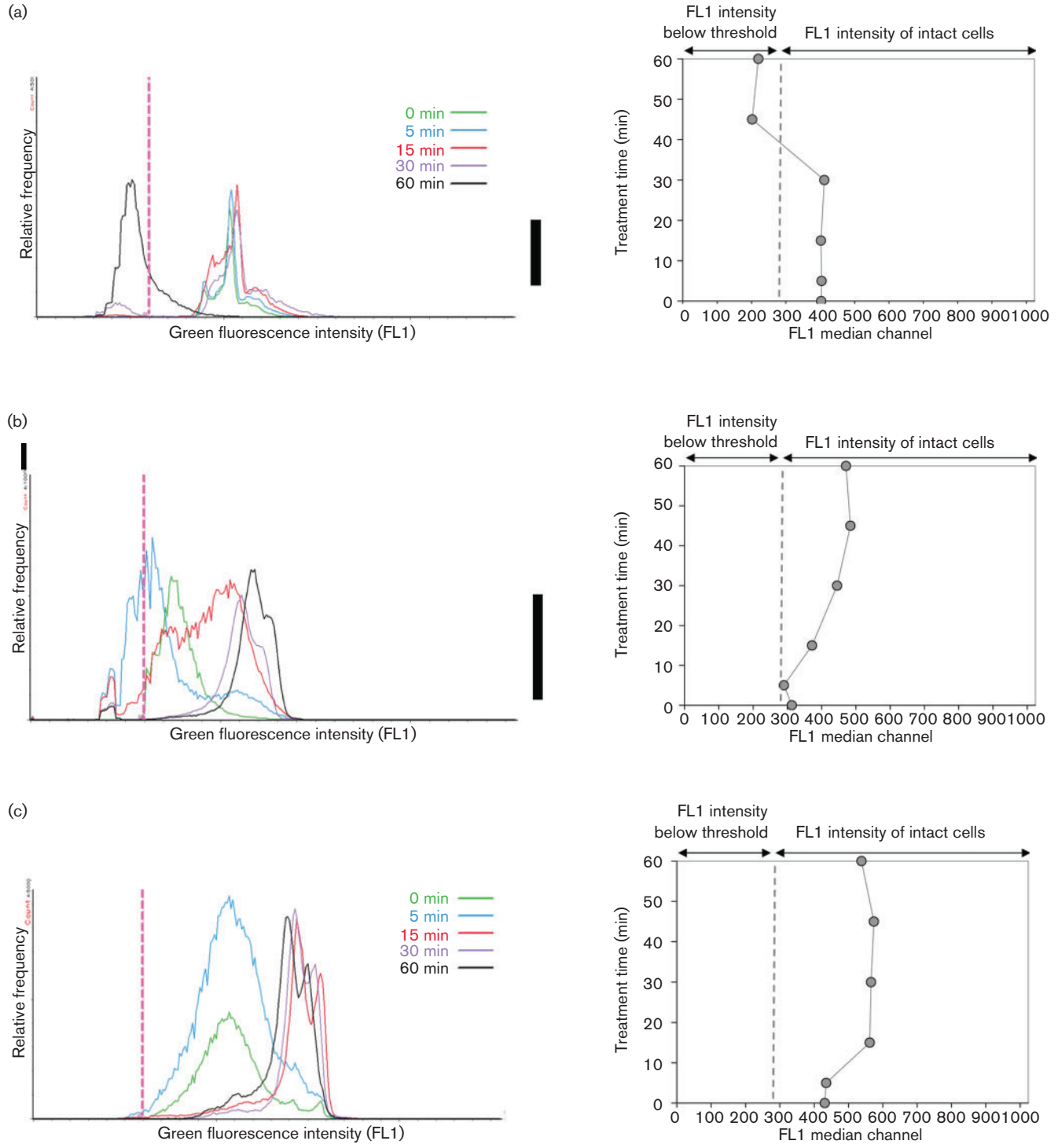

Fig. 2. FCM analysis showing SYBR-I uptake by *L. monocytogenes* (a), *E. coli* (b) and *S. enterica* (c) cells over treatment time. FL1 signal distribution for each treatment time (left) and corresponding FL1 median channels values (right) are shown.

was at channel 398. Conversion of FALS intensities produced a biovolume ratio of about 1.5 between partially permeabilized and intact cells. This ratio, together with the increase in LALS intensity, indicates that bacteria temporarily underwent a pronounced increase in biovolume.

Correlation between plate counts, qPCR and FCM methods in evaluating cell viability

We compared the concentration of viable cells obtained by plate counts with that of intact cells determined by PMA-qPCR and FCM during SC-CO_2 treatment. The three

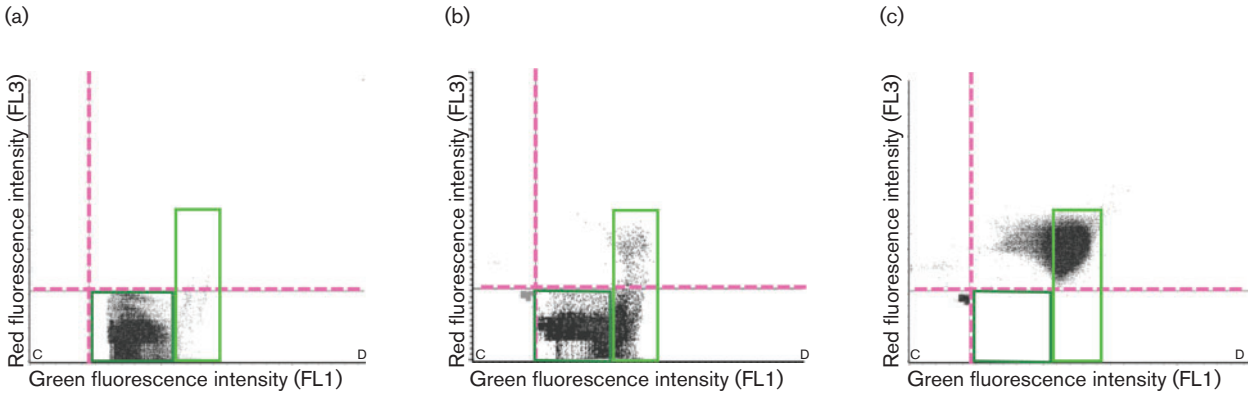

Fig. 3. High- and low-fluorescence subpopulations detected by FCM within *E. coli* populations after SC-CO_2 treatment. FL1–FL3 dot plots were obtained by measuring red versus green fluorescence in (a) untreated, (b) 5 min-treated and (c) 30 min-treated *E. coli* cell suspensions. Cell subpopulations characterized by low and high SYBR-I uptake are bordered by dark and light green boxes, respectively.

methods produced similar results during the initial phase (15 min) (Fig. 6). After 30 min, a dramatic decrease (>5 log) in the number of viable cells was observed with plate counts, whereas FCM and, in particular, qPCR showed a much more modest reduction of intact cells (about 0.9 and 0.5 log, respectively), indicating that only a small fraction of intact cells (as determined by FCM and qPCR) are effectively able to replicate *in vitro* (as determined by plate counts) after treatment.

To determine if the three methods produced consistent and comparable results, Pearson correlation coefficients (r) were calculated (Fig. 7). The highest correlation was between qPCR and FCM for *L. monocytogenes* and *E. coli* (r=0.91 and 0.92, respectively), and between qPCR and plate counts for *S. enterica* (r=0.92). The poorest correlations were between FCM and plate counts for both *E. coli* and *S. enterica* (r=0.60 and 0.62, respectively), and between qPCR and plate counts for *L. monocytogenes* (r=0.63).

DISCUSSION

In this study we compared different viability assays to monitor the efficiency of SC-CO_2 treatment on *L. monocytogenes*, *E. coli* and *S. enterica*. Plate counts showed that the treatment inactivated viable cells by >5 log.

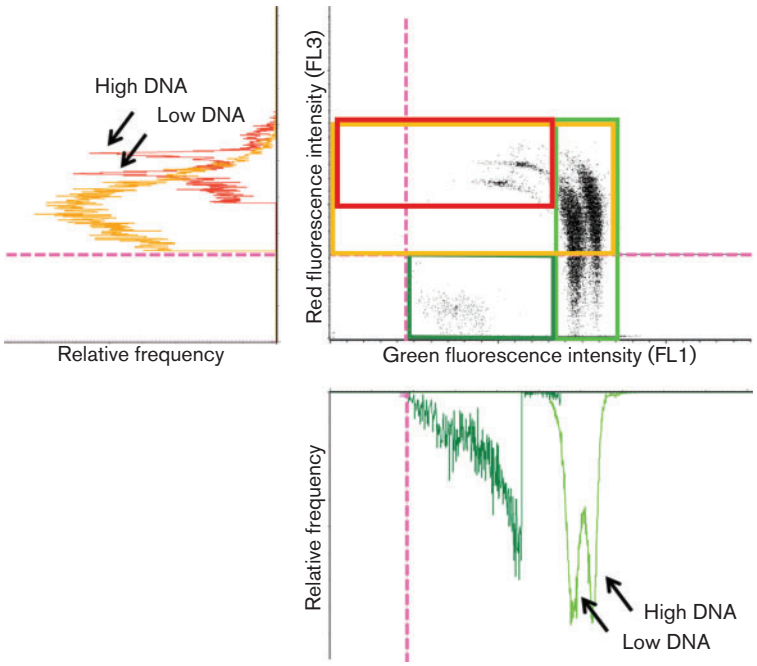

Fig. 4. Cell subpopulations identified by FCM in *S. enterica* cell suspensions after 15 min of SC-CO_2 treatment. Cells with low and high SYBR-I uptake are bordered by light and dark green boxes, respectively, whereas cells with low and high PI uptake are bordered by yellow and red boxes, respectively. The single channel distributions are shown next to their corresponding fluorescence channel. Arrows indicate cell subpopulations with low and high DNA content.

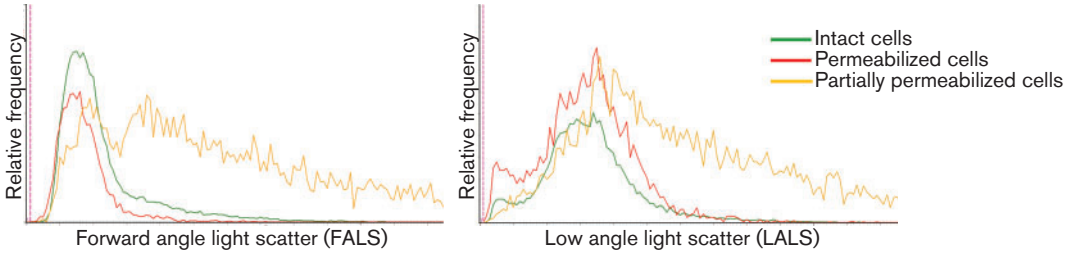

Fig. 5. FALS (left) and LALS (right) signal distributions evaluated by FCM analysis on *L. monocytogenes* cells treated for 30 min with SC-CO_2.

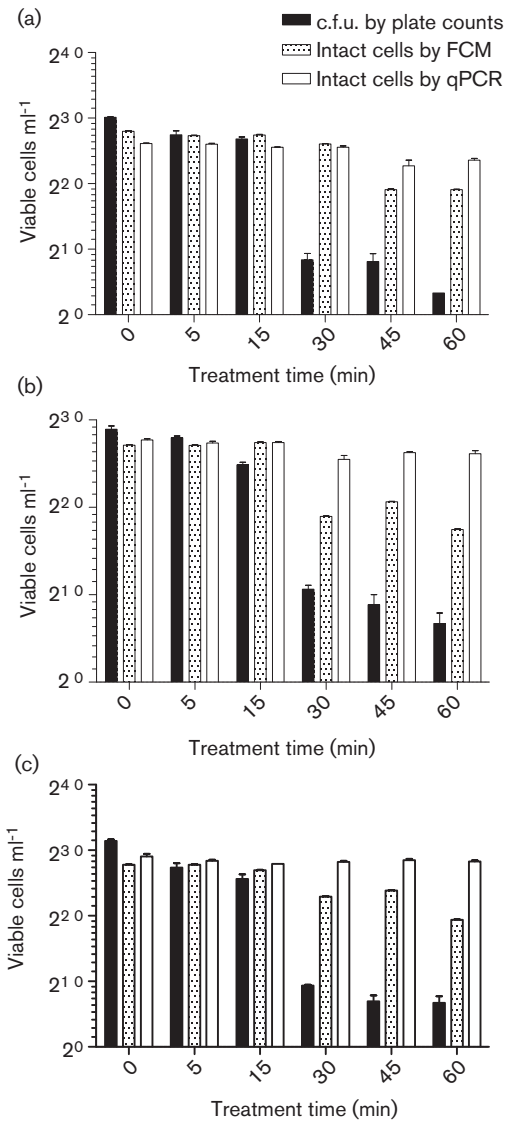

Fig. 6. Number of viable or intact cells monitored during SC-CO_2 treatment and inferred from plate counts, qPCR and FCM for *L. monocytogenes* (a), *E. coli* (b) and *S. enterica* (c). Error bars represent standard deviations from three independent replicates.

Fluorescence microscopy globally corroborated plate count data, with a marked bacterial permeabilization process revealed by PI uptake after 30 min treatment. Under environmental stress, many bacteria are known to enter in a so-called VBNC state, becoming even more resistant to stress (Oliver, 2010). Plate counts therefore probably overestimate bacterial inactivation, as VNBC cells escape detection by cultural methods. We applied two viability methods based on membrane integrity (PMA-qPCR and FCM) to overcome the limits of plate counts and to identify the proportion of VNBC cells in the populations. We showed that qPCR and FCM produced strongly correlated results for two out of three bacterial species tested, which was expected as both methods quantify cellular subpopulations on the basis of membrane permeability. Our results also confirmed that plate counts drastically underestimate the number of intact cells, being unable to detect those in a VBNC state.

According to Nocker *et al.* (2007b), PMA-qPCR is an adequate tool to monitor the effect of a given treatment affecting bacterial membrane integrity. PMA-qPCR produced inconsistent data to evaluate the efficiency of the treatment on *S. enterica*, while it correctly detected the effect of SC-CO_2 on *L. monocytogenes* and *E. coli*, supporting previously published data (Garcia-Gonzalez *et al.*, 2010). qPCR is a highly sensitive method able to detect fewer than 10 genome equivalents per reaction and is therefore the technique of choice for quantification of micro-organisms at low concentrations. A main disadvantage of PMA-qPCR applied to bacterial viability studies lies in the fact that variations in genomic DNA extraction and PMA-staining efficiency may cause biases in the determination of the number of intact cells.

Conversely, FCM coupled with SYBR-I and PI staining provided consistent and detailed information on the cell permeabilization process. This technique distinguished cells in three different states: intact, partially permeabilized and permeabilized. FCM analyses highlighted a diverse effect of the treatment on *L. monocytogenes* compared with *E. coli* and *S. enterica*. After 30 min treatment, 71.2 % of *L. monocytogenes* cells were intact, whereas 95.3 % of *E. coli* and 93.7 % of *S. enterica* cells were partially permeabilized.

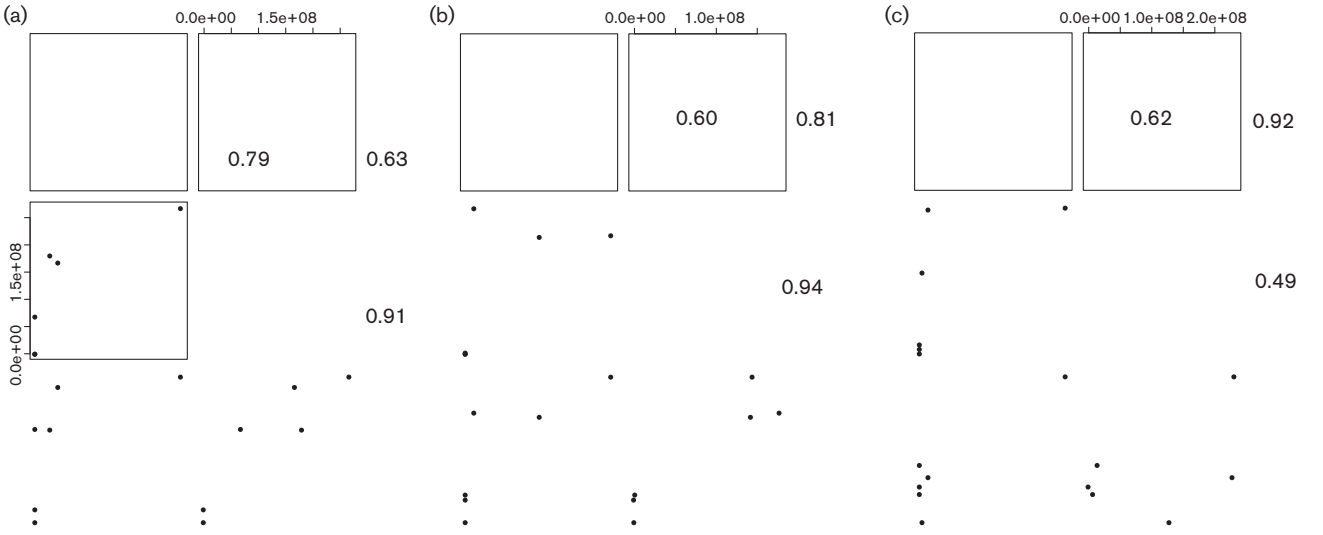

Fig. 7. Pairwise correlation analysis of plate counts, PMA-qPCR and FCM in estimating the number of viable or intact cells after SC-CO_2 treatment for *L. monocytogenes* (a), *E. coli* (b) and *S. enterica* (c).

By contrast, the fraction of cultivable cells was reduced by more than 5 log for all three species.

FCM estimated the variation of FL1 intensity during treatment in *E. coli* and *S. enterica*, indicating a gradual permeabilization of cells and facilitating the uptake of SYBR-I, as suggested by Liao *et al.* (2010). The emergence of subpopulations of cells with double the amount of DNA appeared only when SYBR-I completely entered the cells, in agreement with data reported by Berney *et al.* (2007) with SYTO-9. The double amount of DNA was detected both in partially permeabilized cells and in almost totally permeabilized cells, as shown by the overlapping green and red fluorescence peaks in the FL1 and FL3 channels, respectively. The ability of the fluorescent dyes to enter the cells depends on the level of outer membrane permeabilization for SYBR-I and on the level of both outer and cytoplasmic membrane permeabilization for PI. The double amount of DNA was not observed in the intact and permeabilized cells from the untreated sample, presumably due to limitations in the diffusion of SYBR-I across the membranes. In addition, a shift of both FALS and LALS signals in partially permeabilized *L. monocytogenes* cells suggested a temporary increase of biovolume and surface alteration during permeabilization, while in *E. coli* and *S. enterica* the process did not affect biovolume or cellular surface.

The FCM assay showed the best performance as a bacterial viability test method, evaluated here by monitoring membrane permeabilization following SC-CO_2 treatment. FCM allowed us not only to quantify the efficiency of treatment rapidly and with high sensitivity, but also to discriminate the subpopulations of partially permeabilized cells from totally permeabilized cells and identify variations in biovolume and alterations of the cellular surface. FCM compared favourably with other methods and should be considered as an accurate analytical tool for applications in which monitoring bacterial viability status is of importance, such as microbiological risk assessment in the food chain or in the environment.

ACKNOWLEDGEMENTS

S. T. and G. F. were supported by the European Community's Seventh Framework Program (FP7/2007–2013) under grant agreement no. 245280, acronym PRESERF: 'Processing Raw Materials into Excellent and Sustainable End products while Remaining Fresh'. We thank Nicola Segata for providing support with statistical analyses.

REFERENCES

Anon (2002). *Risk profile on the microbiological contamination of fruits and vegetables eaten raw: Report of the Scientific Committee on Food.* Brussels: SCF/CS/FMH/SURF.

Bae, Y. Y., Choi, Y. M., Kim, M. J., Kim, K. H., Kim, B. C. & Rhee, M. S. (2011). Application of supercritical carbon dioxide for microorganism reduction in fresh pork. *J Food Saf* **31**, 511–517.

Ballestra, P., Abreu da Silva, A. & Cuq, J. L. (1996). Inactivation of *Escherichia coli* by carbon dioxide under pressure. *J Food Sci* **61**, 829–831.

Barbesti, S., Citterio, S., Labra, M., Baroni, M. D., Neri, M. G. & Sgorbati, S. (2000). Two and three-color fluorescence flow cytometric analysis of immunoidentified viable bacteria. *Cytometry* **40**, 214–218.

Berney, M., Hammes, F., Bosshard, F., Weilenmann, H. U. & Egli, T. (2007). Assessment and interpretation of bacterial viability by using the LIVE/DEAD BacLight Kit in combination with flow cytometry. *Appl Environ Microbiol* **73**, 3283–3290.

Devlieghere, F., Vermeiren, L. & Debevere, J. (2004). New preservation technologies: possibilities and limitations. *Int Dairy J* **14**, 273–285.

Erkmen, O. (2000). Effect of carbon dioxide pressure on *Listeria monocytogenes* in physiological saline and foods. *Food Microbiol* **17**, 589–596.

Erkmen, O. & Karaman, H. (2001). Kinetic studies on the high pressure carbon dioxide inactivation of *Salmonella typhimurium*. *J Food Eng* **50**, 25–28.

Ferrentino, G. & Spilimbergo, S. (2011). High pressure carbon dioxide pasteurization of solid foods: current knowledge and future outlooks. *Trends Food Sci Technol* **22**, 427–441.

Foladori, P., Quaranta, A. & Ziglio, G. (2008). Use of silica microspheres having refractive index similar to bacteria for conversion of flow cytometric forward light scatter into biovolume. *Water Res* **42**, 3757–3766.

Foladori, P., Bruni, L., Tamburini, S. & Ziglio, G. (2010). Direct quantification of bacterial biomass in influent, effluent and activated sludge of wastewater treatment plants by using flow cytometry. *Water Res* **44**, 3807–3818.

Gandhi, M. & Chikindas, M. L. (2007). *Listeria*: a foodborne pathogen that knows how to survive. *Int J Food Microbiol* **113**, 1–15.

Garcia-Gonzalez, L., Geeraerd, A. H., Spilimbergo, S., Elst, K., Van Ginneken, L., Debevere, J., Van Impe, J. F. & Devlieghere, F. (2007). High pressure carbon dioxide inactivation of microorganisms in foods: the past, the present and the future. *Int J Food Microbiol* **117**, 1–28.

Garcia-Gonzalez, L., Geeraerd, A. H., Mast, J., Briers, Y., Elst, K., Van Ginneken, L., Van Impe, J. F. & Devlieghere, F. (2010). Membrane permeabilization and cellular death of *Escherichia coli*, *Listeria monocytogenes* and *Saccharomyces cerevisiae* as induced by high pressure carbon dioxide treatment. *Food Microbiol* **27**, 541–549.

Jung, W. Y., Choi, Y. M. & Rhee, M. S. (2009). Potential use of supercritical carbon dioxide to decontaminate *Escherichia coli* O157 : H7, *Listeria monocytogenes*, and *Salmonella typhimurium* in alfalfa sprouted seeds. *Int J Food Microbiol* **136**, 66–70.

Keer, J. T. & Birch, L. (2003). Molecular methods for the assessment of bacterial viability. *J Microbiol Methods* **53**, 175–183.

Kim, H. T., Choi, H. J. & Kim, K. H. (2009). Flow cytometric analysis of *Salmonella enterica* serotype Typhimurium inactivated with supercritical carbon dioxide. *J Microbiol Methods* **78**, 155–160.

Klein, D. (2002). Quantification using real-time PCR technology: applications and limitations. *Trends Mol Med* **8**, 257–260.

Liao, H., Zhang, F., Liao, X., Hu, X., Chen, Y. & Deng, L. (2010). Analysis of *Escherichia coli* cell damage induced by HPCD using microscopies and fluorescent staining. *Int J Food Microbiol* **144**, 169–176.

Mantoan, D. & Spilimbergo, S. (2011). Mathematical modeling of yeast inactivation of freshly squeezed apple juice under high-pressure carbon dioxide. *Crit Rev Food Sci Nutr* **51**, 91–97.

Müller, S. & Nebe-von-Caron, G. (2010). Functional single-cell analyses: flow cytometry and cell sorting of microbial populations and communities. *FEMS Microbiol Rev* **34**, 554–587.

Nocker, A. & Camper, A. K. (2006). Selective removal of DNA from dead cells of mixed bacterial communities by use of ethidium monoazide. *Appl Environ Microbiol* **72**, 1997–2004.

Nocker, A., Sossa-Fernandez, P., Burr, M. D. & Camper, A. K. (2007a). Use of propidium monoazide for live/dead distinction in microbial ecology. *Appl Environ Microbiol* **73**, 5111–5117.

Nocker, A., Sossa, K. E. & Camper, A. K. (2007b). Molecular monitoring of disinfection efficacy using propidium monoazide in combination with quantitative PCR. *J Microbiol Methods* **70**, 252–260.

Oliver, J. D. (2010). Recent findings on the viable but nonculturable state in pathogenic bacteria. *FEMS Microbiol Rev* **34**, 415–425.

Spilimbergo, S. & Bertucco, A. (2003). Non-thermal bacterial inactivation with dense CO_2. *Biotechnol Bioeng* **84**, 627–638.

Suo, B., He, Y., Tu, S. I. & Shi, X. (2010). A multiplex real-time polymerase chain reaction for simultaneous detection of *Salmonella* spp., *Escherichia coli* O157, and *Listeria monocytogenes* in meat products. *Foodborne Pathog Dis* **7**, 619–628.

Velusamy, V., Arshak, K., Korostynska, O., Oliwa, K. & Adley, C. (2010). An overview of foodborne pathogen detection: in the perspective of biosensors. *Biotechnol Adv* **28**, 232–254.

WHO (2007). *Global Public Health Security in the 21st Century*. Geneva: World Health Organization.

Wouters, P. C., Bos, A. P. & Ueckert, J. (2001). Membrane permeabilization in relation to inactivation kinetics of *Lactobacillus* species due to pulsed electric fields. *Appl Environ Microbiol* **67**, 3092–3101.

Ziglio, G., Andreottola, G., Barbesti, S., Boschetti, G., Bruni, L., Foladori, P. & Villa, R. (2002). Assessment of activated sludge viability with flow cytometry. *Water Res* **36**, 460–468.

Edited by: D. Mills

Fig. 7

A

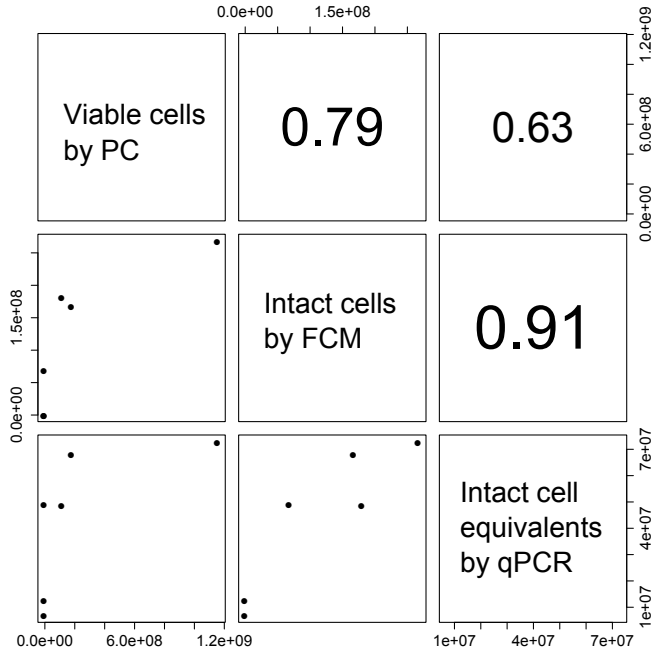
Viable cells by PC
0.79
0.63
Intact cells by FCM
0.91
Intact cell equivalents by qPCR
0.0e+00
1.5e+08
1.2e+09
6.0e+08
7e+07
4e+07
1e+07

B

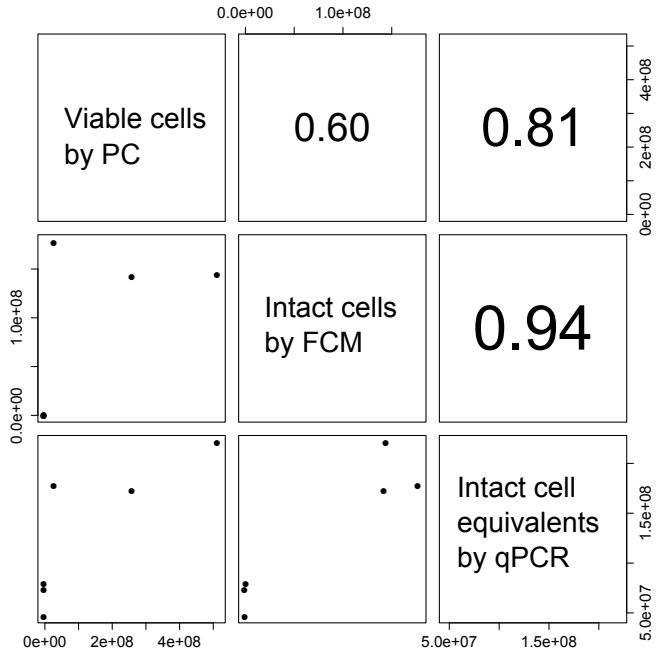
Viable cells by PC
0.60
0.81
Intact cells by FCM
0.94
Intact cell equivalents by qPCR
0.0e+00
1.0e+08
4e+08
2e+08
0e+00
5.0e+07
1.5e+08

C

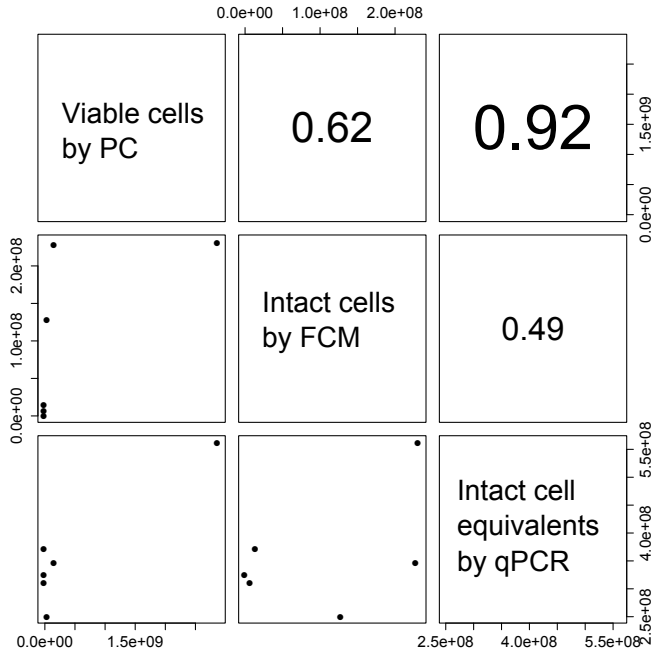
Viable cells by PC
0.62
0.92
Intact cells by FCM
0.49
Intact cell equivalents by qPCR
0.0e+00
1.0e+08
2.0e+08
1.5e+09
5.5e+08
4.0e+08
2.5e+08

9.3 Publication B:

Tamburini, S., Foladori, P., Ferrentino, G., Spilimbergo S., Jousson O. Flow cytometry as an accurate tool to monitor *E. coli* subpopulations on solid food products after SC-CO_2 treatment. *International Journal of Food Microbiology*, under review

Elsevier Editorial System(tm) for International Journal of Food Microbiology
Manuscript Draft

Manuscript Number:

Title: Flow cytometry as an accurate tool to monitor E. coli subpopulations on solid food products after SC-CO2 treatment

Article Type: Full Length Article

Keywords: SC-CO2 treatment; flow cytometry; Escherichia coli; fresh cut carrots; VBNC; food safety

Corresponding Author: Mrs Sabrina Tamburini,

Corresponding Author's Institution: University of Trento

First Author: Sabrina Tamburini

Order of Authors: Sabrina Tamburini; Paola Foladori; Giovanna Ferrentino; Sara Spilimbergo; Olivier Jousson

Abstract: Supercritical CO2 (SC-CO2) is one of the most promising non-thermal "mild processing" technique to pasteurize fresh food products. The effect of SC-CO2 treatment on microorganisms present on food products has been mainly evaluated by conventional cultivation-based methods, which may lead to large underestimation because under stress conditions, a number of pathogens enter in a so-called Viable But Not Cultivable (VBNC) state, thus escaping detection by cultivation methods. Flow cytometry (FCM) coupled with SYBR-Green I and Propidium Iodide allowed distinguishing E. coli cells from fresh carrots debris, to evaluate the reduction of E. coli total cells and to quantify viable and dead bacteria based on their membrane integrity after SC-CO2 treatment. FCM results were compared with conventional cultivation methods. SC-CO2 treatments performed at 120 bar and 22°C or 35°C disrupted 43% and 53% of bacterial cells, respectively, and produced a large percentage of permeabilized and partially-permeabilized cells. While treatments of 10 min at 22°C and 7 min at 35°C were enough to inhibit the capability of all E. coli cells to replicate with an inactivation of 8 Log, FCM analysis showed that the inactivation of intact cells was only 2-2.5 Log, indicating that the cells maintained the membrane integrity and entered in a VBNC state. The results confirmed the accuracy of FCM in monitoring the efficiency of SC-CO2 treatment on food products. Further, this powerful method could significantly assist to improve management of food-associated health risks increasing the knowledge about bacterial cells in a VBNC state.

Suggested Reviewers: Murat Balaban
Professor, Department of Chemical and Materials Engineering, University of Auckland
m.balaban@auckland.ac.nz
an expert in SC-CO2

Hongmei Liao
China Agricultural University
liaoxjun@hotmail.com

Hee Taek Kim
School of life Sciece and Biotechnology, Korea University
khekim@korea.ac.kr

He studies SC-CO2 and uses flow cytometry

Jim Oliver
Professor, Department of Biology, University of North Caroline at Charlotte
jdoliver@uncc.edu
an expert in Microbiology and VBNC status of bacterial cells

Dear Editor,

Please find enclosed the manuscript entitled “Flow cytometry as an accurate tool to monitor *E. coli* subpopulations on solid food products after SC-CO_2 treatment” to be considered for publication in International Journal of Food Microbiology. We report the application of flow cytometry (FCM) coupled with Sybr-Green I and Propidium Iodide to evaluated the efficiency of Supercritical Carbone Dioxide (SC-CO_2) one of the most promising non-thermal “mild processing” technique to pasteurize fresh food products, directly on fresh cut carrots. We monitor the treatment with FCM and plate counts to quantify the number of cells that was disrupted by the treatment and to distinguish the remaining *E. coli* cells on the basis of their physiological status, including permeabilized (dead) cells, viable but non culturable (VBNC) cells and culturable cells. The application of FCM could overcome the limitations of cultivation methods that may lead to underestimation of the number of viable cells after treatment, since bacterial cells under stress enter in VBNC state failing to grow, but could maintain the capability to develop human diseases.

Sincerely,

Sabrina Tamburini

Highlights

- SC-CO_2 treatment applied to inactivate *E. coli* cells spiked on fresh cut carrots.
- Flow cytometry (FCM), as safety tool, identifies VBNC *E. coli* cells not detectable by cultivation
- FCM profiling permitted to distinguish *E. coli* cells from natural flora of carrots.
- 5 min of SC-CO_2 at 120 bar 22°C and 35°C disrupted the total bacteri by 43% and 53%
- At the end of the treatment 10^5 cells per gram of *E. coli* enter in the VBNC status.

Flow cytometry as an accurate tool to monitor *E. coli* subpopulations on solid food products after SC-CO_2 treatment

Sabrina Tamburini[1*], Paola Foladori[3],Giovanna Ferrentino[2], Sara Spilimbergo[2], Olivier Jousson[1]

[1]: Centre for Integrative Biology, University of Trento, Italy

[2]: Department of Materials Engineering and Industrial Technologies, University of Trento, Italy

[3]: Department of Civil, Environmental and Mechanical Engineering, University of Trento, Italy.

[*] Corresponding author: Centre for Integrative Biology (CIBIO), University of Trento, Via delle Regole 101, 38123 Trento, Italy. E-mail: tamburini@science.unitn.it; Phone: +39 0461283665; Fax: +39 0461283091

Abstract:

Supercritical CO_2 (SC-CO_2) is one of the most promising non-thermal "mild processing" technique to pasteurize fresh food products. The effect of SC-CO_2 treatment on microorganisms present on food products has been mainly evaluated by conventional cultivation-based methods, which may lead to large underestimation because under stress conditions, a number of pathogens enter in a so-called Viable But Not Cultivable (VBNC) state, thus escaping detection by cultivation methods. Flow cytometry (FCM) coupled with SYBR-Green I and Propidium Iodide allowed distinguishing *E. coli* cells from fresh carrots debris, to evaluate the reduction of *E. coli* total cells and to quantify viable and dead bacteria based on their membrane integrity after SC-CO_2 treatment. FCM results were compared with conventional cultivation methods. SC-CO_2 treatments performed at 120 bar and 22°C or 35°C disrupted 43% and 53% of bacterial cells, respectively, and produced a large percentage of permeabilized and partially-permeabilized cells. While treatments of 10 min at 22°C and 7 min at 35°C were enough to inhibit the capability of all *E. coli* cells to replicate with an inactivation of 8 Log, FCM analysis showed that the inactivation of intact cells was only 2-2.5 Log, indicating that the cells maintained the membrane integrity and entered in a VBNC state. The results confirmed the accuracy of FCM in monitoring the efficiency of SC-CO_2 treatment on food products. Further, this powerful method could significantly assist to improve management of food-associated health risks increasing the knowledge about bacterial cells in a VBNC state.

Keywords: SC-CO_2 treatment, flow cytometry, *Escherichia coli*, fresh cut carrots, VBNC, food safety

1 Introduction

Carrot (*Daucus carota L.*) is among the top-ten most economically important vegetable crops in the world, since is a good source of natural antioxidants such as carotenoids and phenolic compounds and is consumed all year around (Simon *et al*., 2008) as fresh but also as ready-to-eat (RTE) product. During the last two decades, consumers demand for RTE fruits and vegetables has increased considerably, providing a constant and diverse supply of fresh products, which is not always possible, especially when off-season products have to be dealt. Preservation and safety of RTE products has become one of the main issue for the food industry since fresh vegetables and fruits are vehicle for international outbreak of foodborne diseases (EFSA, 2013), considering that traditional techniques -as thermal pasteurization, addition of preservatives or ionizing radiations, etc.- present some drawbacks in their exploitations in food applications. As a consequence, the interest in innovative "minimal processing" techniques has increased considerably in the last years. One of the most promising non-thermal preservation method is based on the use of Supercritical Carbon Dioxide (SC-CO_2), that works at relatively low temperature (30-40°C) and moderate pressure (80-120 bar), thus having a much lower impact on nutritional, organoleptic and physico-chemical properties of food products than heat-based methods (Garcia-Gonzalez *et al*., 2007). Recently published data demonstrated that this technology can effectively inactivate microorganisms both in culture media (Hong and Pyun, 1999; Erkmen, 2000) and liquid foods (Ferrentino *et al*., 2009; Liao *et al*., 2010; Spilimbergo and Ciola, 2010) but also in fresh cut fruits (Valverde *et al*., 2010; Ferrentino *et al*., 2012) and vegetables (Zhong *et al*., 2008, Spilimbergo *et al*., 2012). The effect of SC-CO_2 treatment on microorganisms spiked on food products has been mainly evaluated by standard conventional cultivation-based methods (Jung *et al*., 2009; Bae *et al*., 2011). Although cultivation methods are applied routinely, they may lead to strong underestimations of the actual concentration of microorganisms in the analyzed samples (Keer and

74 Birch, 2003; Oliver, 2005). Some bacterial species, when undergone to environmental stress
75 conditions (e.g. nutrient limitation, pressure, temperature), may become no more cultivable
76 although remaining alive, becoming even more resistant to stress (Bogosian & Bourneuf, 2001;
77 Oliver, 2010), therefore cultivation methods may lead to an overestimation of the pasteurization
78 efficiency after food treatments.
79 According to the viability concept proposed by Nebe-von-Caron *et al*. (2000) microbial cells can be
80 classified based on their physiological status: (i) culturable cells; (ii) viable-but-non-culturable cells
81 (VBNC); (iii) dead cells. Many viability indicators using fluorescent molecules have been applied
82 (Breeuwer and Abee, 2000) to identify and quantify viable bacterial cells (considered as the sum of
83 culturable and VBNC cells) on the basis of metabolic activity or membrane integrity (Nebe-von-
84 Caron *et al*., 2000; Nocker *et al*., 2012). Since membrane integrity is the minor restrictive
85 physiological parameter to define a viable cells compared with either capability to grow or
86 metabolic cellular activity, we called viable bacterial cells those with intact membrane, whilst the
87 dead cells have a permeabilized membrane.
88 Flow cytometry (FCM) is a multi-parametric and single-cell analysis method for high-throughput
89 and real time quantification of multiple cellular parameters, such as physiological status, cell size or
90 surface granularity. FCM, coupled with fluorescent dyes, has been used to follow the microbial
91 inactivation during new pasteurization treatments such as pulsed electric fields applied to
92 *Lactobacillus* strains (Wouters *et al*., 2001), high-intensity ultrasound treatment on *E. coli* and
93 *Lactobacillus rhamnosus (*Ananta *et al.*, 2005), and SC-CO_2 treatment on *Salmonella enterica*, *E.*
94 *coli* and *Listeria monocytogenes* (Kim *et al*., 2009; Tamburini *et al*., 2013, Ferrentino *et al*, 2013).
95 In FCM, two light scattering signals and some fluorescent signals can be collected simultaneously
96 from each bacterial cell. The Forward Angle Light Scatter (FALS) is related to bacterial size
97 (Foladori *et al*., 2008), whilst the Large Angle Light Scatter (LALS) measures cell density or
98 granularity (Müller and Nebe-von-Caron, 2010). SYBR Green I (SYBR-I) and Propidium Iodide

(PI) are two fluorescent dyes used in FCM analysis to distinguish viable cells from dead ones. SYBR-I is used as total cell marker, due to its ability to cross the cell membrane and to bind to DNA, whilst PI is used as dead cell marker, since it penetrates only cells with permeabilized membrane (Ziglio *et al*., 2002). In permeabilized cells, the simultaneous presence of SYBR-I and PI activates Fluorescence Resonance Energy Transfer, due to the total absorption of the fluorescent emission spectrum of SYBR-I by PI.

In this study, FCM was applied for the first time to evaluate the efficiency of SC-CO_2 treatment on *E. coli* cells spiked on fresh cut carrots. Agricultural irrigation with polluted surface water can be one of the sources of enteropathogenic contamination of vegetables and fruits, such as the Gram-negative *E. coli* and *Salmonella* (Velusamy *et al*., 2006). *E. coli* is commonly used as an indicator of fecal contamination in water samples and in food products (Raj and Liston, 1960; Edberg *et al*., 2000; Montville and Matthews, 2008). The FCM quantification of the bacterial cells before and after treatment permitted to evaluate the number of cells that was disrupted by the treatment and to distinguish the remaining *E. coli* cells on the basis of their physiological status, including permeabilized (dead) cells, VBNC cells and culturable cells, by combining cultivation methods (plate counts) and FCM analysis. The aim of the present work was to evaluate the efficacy of the minimal processing SC-CO_2 technique in the reduction of *E. coli* contamination, overcoming the limitations of cultivation methods that may lead to underestimation of microbiological risk assessment.

2 Materials and methods

2.1 *Bacterial strain and growth conditions*

Escherichia coli ATCC 29522 was grown on solid Luria-Bertani (LB) agar medium (Sigma-Aldrich Co., Milan, Italy) at 37°C for 16 h. One colony was picked and inoculated into 10 mL of LB

medium. Bacterial culture was incubated at 37°C with constant shaking (200 rpm) to stationary phase (16 hours). Cells were collected by centrifugation at 6000 rpm for 10 min and re-suspended in 5 mL of phosphate buffered saline solution (PBS, Sigma-Aldrich Co., Milan, Italy).

2.2 *Fresh carrots contamination*

Carrots (*Daucus carota*) were purchased from a local market. The food was washed with water, cut into 2 grams pieces and spiked with 50 µL of *E. coli* ATCC 25922 with a concentration of 10^8 CFU/mL. The samples were left 1 h in a sterile chamber at room temperature to let the microbial suspension absorb on the carrot and then were loaded in a SC-CO_2 multi – batch apparatus.

2.3 *SC-CO_2 treatment*

SC-CO_2 treatment was performed in a multi-batch apparatus as described by Mantoan and Spilimbergo (2011). Briefly, the system consisted of 10 identical 15 mL-capacity reactors operating in parallel. All reactors were immersed in the same temperature-controlled water bath to maintain the desired temperature constant throughout the process and were connected to an on-off valve for independent depressurization at different treatment times. The solid samples spiked with *E. coli* were loaded into the reactors and pressurized with CO_2. The operating parameters (temperature and pressure) were continuously recorded by a real time acquisition data system (NATIONAL INSTRUMENTS, field point FP-1000 RS 232/RS 485) and monitored by a specific software (LabVIEW ^{TM} 5.0). The process conditions tested were: 80-120 bar, 22-35°C and 5-30 min, followed by a slow depressurization of the reactors over approximately 1 min. The conditions were chosen based on previous data (Spilimbergo *et al*., 2012).

2.4 Sample homogenization

Untreated and treated solid samples were collected and suspended in 4 mL of PBS in a sterile plastic bag (Reinforced Round Bag- 400, International P.B.I., Milan, Italy) and homogenized in a Stomacher 400 (International P.B.I., Milan, Italy) at 230 rpm for 2 min. The resulting homogenate was taken from the sterile bag and used for plate counts and FCM analyses.

2.4 *Plate counts*

Untreated and treated homogenized samples were diluted 1:10 with PBS and spread-plated on chromogenic coli/coliform agar for *E. coli* detection (Liofilchem, Teramo, Italy). The plates were incubated at 37°C for 24 h. Three independent experiments were performed for each SC-CO_2 treatment. Bacterial inactivation was calculated as Log_{10} (N/N_0), where N were CFUs/g present in the treated sample and N_0 were CFUs/g in the untreated sample. The detection limit for plate count analysis was 30 CFUs/g.

2.5 *Flow cytometry*

Untreated and treated homogenized samples were diluted in PBS to 10^7-10^8 cells/mL. Then 1 mL was stained with 10 µL SYBR-I (1:30000 final concentration in DMSO; Merck, Darmstadt, Germany), and 10 µL PI (1 mg/mL; Invitrogen, Carlsbad, CA, USA). Peak excitation and emission wavelengths were λ_{ex}=495 nm and λ_{em}=525 nm for SYBR-I and λ_{ex}=536 nm and λ_{em}=617 nm for PI. Samples were incubated at room temperature in the dark for 15 min. FCM analyses were performed with an Apogee-A40 flow cytometer (Apogee Flow Systems, Hertfordshire, UK) equipped with an Argon laser emitting at 488 nm. For each cell crossing the focus point of the laser, two light scattering signals (FALS and LALS) and two fluorescence signals (green, FL1 and red, FL3) were collected. LALS and FALS were collected on a 256-channel linear scale while fluorescence signals were collected with logarithmic amplifier gain. The estimation of cellular biovolume from FALS intensities was performed as proposed by Foladori *et al.* (2008). To exclude

electronic noise thresholds were set on green or red fluorescence histograms. Fluorescent polystyrene spheres were used to verify steady-state optical properties of the instrument during operation. In this work, the detection limit in the FCM analysis was approximately 1 cell/μL.

3 Results and Discussion

3.1 SC-CO_2 inhibit the capability of E. coli cells to grow

The inactivation by SC-CO_2 treatment of culturable *E. coli* cells spiked on fresh cut carrots was evaluated quantifying bacterial cells able to replicate by plate count method. A set of experiments at 22°C (Fig. 1A) and at 35°C (Fig. 1B) and at different pressures were performed to evaluate the best conditions for bacterial inactivation expressed as $Log_{10}(N/N_0)$ as a function of the treatment time. At 22°C, inactivation to undetectable levels (about 8 Log reduction) was obtained in 30 min at 60-80 bar or in 10 min increasing the pressure to 100-120 bar. At 35°C, 8 Log reduction was reached in 10 min at 100-120 bar, 15 min at 80 bar and 20 min at 60 bar. On the basis of the results obtained from plate counts, a treatment time of 10 min at 120 bar appeared sufficient to inactivate all *E. coli* cells spiked on fresh cut carrots both at 22°C and 35°C. Spilimbergo *et al*. (2012) demonstrated that these SC-CO_2 conditions were sufficient to inactivate more than 2.5 Log of either mesophilic microorganisms or acid lactic bacteria and also 5 Log of yeast, molds and total coliforms that live on carrots. Bacterial inactivation on solid samples is known to require a shorter treatment time respect to liquid samples (Valverede et al., 2010)

3.2 FCM profiling permits to distinguish E. coli cells from natural flora of carrots

196 Homogenized suspensions of un-spiked and *E. coli*-spiked fresh cut carrots were stained with
197 SYBR-I and PI and analyzed with FCM to detect the profiling of natural microbial flora and *E. coli*
198 cells on the fresh carrots (Figure 2). The FCM profiling of natural microbial flora was used as a
199 control to investigate in details the FCM profiles obtained for samples of carrots with spiked *E. coli*.
200 The following scattering and fluorescent signals obtained from FCM were analyzed: (i) FALS
201 signal related to bacterial size and cellular biovolume; (ii) LALS signal related to the complexity of
202 cells; (iii) green fluorescence signals related to intact cells and (iv) red fluorescence related to
203 permeabilized cells. Referring to an arbitrary scale divided in 256 channels, the FALS histogram of
204 natural flora of carrots was divided in two parts: the first one representing 90% of bacterial cells
205 with small size with a mean channel at 24; the second one representing 10% of cells with large size
206 at mean channel 102 (orange line). The weighted mean channel of the two natural microbial
207 population was 32. *E. coli* cells showed a clear unimodal histogram at mean channel 56 (violet line)
208 (Figure 2A) and the biovolume ratio between *E. coli* cells and natural microbial cells was 1.7,
209 indicating that *E. coli* cells are longer than the cells belonging to natural flora, as expected. The
210 LALS signals of natural flora of carrots and *E. coli* did not shown a significant difference in the
211 cellular complexity. Due to the significant difference in FALS signals the cytogram FALS vs.
212 LALS obtained from un-spiked and *E. coli* spiked fresh carrots permitted to distinguish the
213 population of natural microflora from the population of *E. coli* cells (Figure 2B). Fluorescent
214 signals acquired for each bacterial cell were plotted in a two-dimensional dot plot (cytogram),
215 where the horizontal axis corresponding to the green fluorescence intensity (FL1) emitted by
216 SYBR-I, and the vertical axis indicating the red fluorescence intensity (FL3) emitted by PI. Upon
217 staining of a mix population of intact and permeabilized cells with these two fluorophores, up to
218 four regions could be distinguished in the two-dimensional dot plot. The two regions on the right
219 included a region of intact cells, emitting only high FL1 intensity due to the absence of intracellular
220 PI, and a region of partially-permeabilized cells emitting high fluorescent intensity both in FL1 and

221 FL3 channels, due to incomplete FRET between SYBR-I and intracellular PI. The two regions on
222 the left included one with permeabilized cells emitting only high FL3 intensity, due to the
223 simultaneous presence of SYBR-I and PI in the cells and complete FRET, and one due to noise
224 caused by non-biotic particles emitting FL1 and FL3 signals below the instrument background
225 threshold. Furthermore, the cytogram FL1 vs. FL3 signals permitted to distinguish debris of carrots
226 from intact and permeabilized microbial cells in natural flora and in *E. coli* cells spiked on carrots.
227 In particular, the green and red fluorescent population on the bisector line of the cytogram represent
228 the debris in the sample, which resulted auto-fluorescent. The natural microbial flora was made up
229 of cells in different physiological states (orange populations in Figure 2C): 33% of cells were
230 permeabilized whilst 66% of cells were intact, whereas most of the *E. coli* cells spiked on carrots
231 (99.2%) were intact. The intact natural flora cells quantified by FCM were $1.9 \cdot 10^7$ cells/g, whilst the
232 intact *E. coli* cells spiked on carrots were $2 \cdot 10^8$ cells/g. Due to the low concentration of natural
233 microbial flora compared to *E. coli* concentration and to the ability of FCM analysis to exclude a
234 selected population such as natural flora, the following results about SC-CO_2 treatment were
235 referred only to the *E. coli* population.

236

237 *3.3 SC-CO_2 induces membrane permeabilization of E. coli*

238 FCM analyses of untreated and treated *E. coli* ce lls produced different cytograms as shown in
239 Figure 3, highlighting the process of membrane permeabilization induced by SC-CO_2 treatment at
240 22°C and 35°C. The percentage of intact, partially and permeabilized cells were calculated respect
241 to the total number of cells per µL detected by the instrument. The percentage of intact cells was
242 99.2% in the untreated sample, while it decreased significantly with the treatment time. After even
243 few minutes of SC-CO_2 treatment, a large part of *E. coli* cells emitted red fluorescence indicating
244 the uptake of PI and the partial or total permeabilization of cells. Increasing the treatment time, the

temperature of 35°C appeared to be slightly more effective in cell permeabilization than 22°C. After 15 min of treatment at 35°C, 99.4% of *E. coli* cells moved to the region of partially-permeabilized or permeabilized cells, while at 22°C this percentage was lower (98.5%).

Figure 4 shows the scattering signals obtained by FCM for the *E. coli* in the untreated sample and SC-CO_2-treated sample at 35°C 120 bar and 15 min. The FALS signal (Fig. 4A) of treated *E. coli* cells was characterized by a shift of the peak respect to untreated cells. Referring to an arbitrary scale divided in 256 channels, the FALS peak of untreated cells was at mean channel 137 whilst the peak of treated cells at 94. The biovolume ratio of about 1.45 indicates that *E. coli* cells decreased their biovolume after treatment. LALS signals of untreated and treated *E. coli* cells did not show a significant difference (vertical axis in Figure 4B), indicating a negligible influence of the treatment on the complexity and internal structure of cells.

3.4 SC-CO_2 treatment induces disruption of a fraction of E. coli cells

The concentration of total *E. coli* cells obtained by FCM in the treated samples for each treatment time, at 22°C and 35°C, was compared with the concentration of total *E. coli* cells quantified in the untreated sample. After 5 min of SC-CO_2 treatment, the total cell concentration strongly decreased by 43% and 53% at 22°C and 35°C, respectively. The fraction of disrupted cells was compared to the intact, partially-permeabilized and permeabilized cell populations for each treatment time. The respective percentages are plotted in Figure 5. SC-CO_2 at 35°C (Fig. 5B) resulted more aggressive against *E. coli* cells than the treatment at 22°C (Fig. 5A). A large disruption of bacterial cells occurred even in the first 5 min of treatment, whilst the increase of the exposure to the treatment carried out a further reduction of the percentage of intact cells.

3.5 A fraction of E. coli cells enters in a VBNC state after SC-CO_2 treatment

The culturable *E. coli* cells spiked on carrots were compared to the total and intact cells (considered as viable) obtained by FCM (Fig. 6). Culturable cells obtained by plate counts were expressed as CFUs per gram. About $2 \cdot 10^8$ *E. coli* cells per gram were inoculated on fresh cut carrots and most of them were intact (99.2%) and culturable (85.5%). After 5 min of treatment at 22°C, 120 bar (Fig. 6A) only $4.6 \cdot 10^3$ of *E. coli* cells were culturable, but a higher concentration $4 \cdot 10^6$ cells remained intact, demonstrating that a fraction of *E. coli* cells, in the magnitude of 10^3 cells/g entered in VBNC state. After 7 min at 35°C and 120 bar of treatment all *E. coli* cells were no more culturable (Fig. 6B). At the end of treatment, both at 22°C and 35°C, a fraction of *E. coli* cells (10^5 cells/g) maintained membrane integrity. We observed a typical VBNC cellular response mediated by SC-CO_2 treatment and leading to total inhibition of *E. coli* growth. FCM analyses indicated that the number of total cells decreased by less than a half and that 10^5 *E. coli* cells per gram remained viable, as attested by the membrane integrity. Spilimbergo *et al*. (2012) demonstrated that natural microflora of vegetables, including mesophilic microorganisms and acid lactic bacteria, showed marked regrowth ability following a 1-2 weeks storage period upon SC-CO_2 treatment.

4. Conclusions

A number of antibacterial treatments, including milk heat treatments (Gunasekera *et al.*, 2002) and wastewater chlorination (Oliver *et al*., 2005), have been validated directly on food or environmental samples and immediately upon treatment by using plate count as a reference method. Such approach do not consider eventual regrowth phenomena of natural microflora or pathogens. The VBNC state is often interpreted as a bacterial survival strategy to resist to an adverse environment. The low metabolic activity characterizes the bacteria in the VBNC state and it could be a putative

294 mechanisms of pathogens to resist against some antibiotics, since many antibiotics act on growing
295 bacterial cells (Mar Lleo *et al*., 2007). The exact role of VBNC state in bacteria and the mechanisms
296 to reach this state is unknown and it could differ from bacterium to bacterium. In VBNC state
297 pathogens could be survive in environmental matrices over one year and to maintain the capability
298 to develop diseases in the host (Oliver 2010). Improving health risk assessment associated with the
299 increasing consumption of minimally processed fresh food products is a crucial need. To reach this
300 objective, the development and standardization of fast and accurate cultivation-independent assays
301 providing cellular and molecular information on microorganisms associated with food products are
302 required.
303

304 **AUTHORS' CONTRIBUTIONS**

305 ST and PF designed FCM methods, carried out the laboratory experiments, analyzed the data,
306 interpreted the results and wrote the paper. ST and GF designed SC-CO_2 experiments and GF
307 performed the SC-CO_2 treatments. OJ and SS discussed results and revised the manuscript. All
308 authors have contributed to, seen and approved the manuscript.

309 **ACKNOWLEDGMENTS**

310 This work was supported by the European Community's Seventh Framework Program (FP7/2007–
311 2013) under grant agreement nr. 245280, acronym PRESERF "Processing Raw Materials into
312 Excellent and Sustainable End products while Remaining Fresh.
313

314 **REFERENCES**

315 Ananta, E., Voight, D., Zenker, M., Heinz, V., Knorr, D., 2005. Cellular injuries upon exposure of
316 Escherichia coli and Lactobacillus rhamnosus to high-intensity ultrasound. Journal of
317 Applied Microbiology 99(2), 271-278.
318 Bae, Y.Y., Choi, Y.M., Kim, M.J., Kim, K.H., Kim, B.C. Rhee, M.S., 2011. Application of
319 supercritical carbon dioxide for microorganism reductions in fresh pork. Journal of Food
320 Safety 31, 511–517.
321 Bogosian, G., and Bourneuf, E.V., 2001. A matter of bacterial life and death. EMBO Reports 2(9),
322 770–774.
323 Breeuwer, P., and Abee, T., 2000. Assessment of viability of microorganisms employing
324 fluorescence techniques. Intern. Journal of Food Microbiology 55, 193-200.
325 Dehghani, F., Annabi, N., Titus, M., Valtchev, P., Tumilar, A., 2008.Sterilization of Ginseng using
326 a high pressure CO_2 at moderate temperatures. Biotechnology and Bioengineering, 102, 569-
327 576.
328 Edberg, S.C., Rice, E.W., Karlin, R.J., Allen, M.J., 2000. Escherichia coli: the best biological
329 drinking water indicator for public health protection. Journal of Applied Microbiology 88,
330 106S–116S.
331 EFSA (European Food Safety Authority) 2013. Scientific Opinion on the risk posed by pathogens
332 in food of non-animal origin. Part 1(outbreak data analysis and risk ranking of food/pathogen
333 combinations. EFSA Journal 11(1), 3025
334 Erkmen, O. (2000). Effect of carbon dioxide pressure on Listeria monocytogenes in physiological
335 saline and foods. Food Microbiol 17, 589-596.

336 Ferrentino, G., Bruno, M., Ferrari, G., Poletto, M., Balaban, M.O., 2009. Microbial inactivation
337 and shelf life of apple juice treated with high pressure carbon dioxide. Journal of Biological
338 Engineering 3(3),1-9.
339 Ferrentino G., Balzan S., Dorigato A., Pegoretti A., Spilimbergo S., 2012. Effect of supercritical
340 carbon dioxide pasteurization on natural microbiota, texture, and microstructure of fresh-cut
341 coconut. Journal of Food Science 77(5), 137-43.
342 Foladori, A., Quaranta, A., Ziglio, G., 2008. Use of silica microspheres having refractive index
343 similar to bacteria for conversion of flow cytometric forward light scatter into biovolume.
344 Water Research 42, 3757-3766.
345 Garcia-Gonzalez, L., Geeraerd, A.H., Spilimbergo, S., Elst, K., Van Ginneken, L., Debevere, J.,
346 Van Impe, J.F., Devlieghere, F., 2007. High pressure carbon dioxide inactivation of
347 microorganisms in foods: The past, the present and the future. International Journal of Food
348 Microbiology 117, 1–28.
349 Gunasekera, T.S., Sørensen, A., Attfield, P.V, Sørensen, S.J., Veal, D.A., 2002. Inducible gene
350 expression by nonculturable bacteria in milk after pasteurization. Applied Environmental
351 Microbiology 68, 1988-1993.
352 Hong, S. I., Park, W. S., Pyun, Y. R., 1999. Non-thermal inactivation of Lactobacillus plantarum
353 as influenced by pressure and temperature of pressurized carbon dioxide. International Journal
354 of Food Science and Technology 34, 125–130
355 Jung, W. Y., Choi, Y. M., Rhee, M. S., 2009. Potential use of supercritical carbon dioxide to
356 decontaminate Escherichia coli O157:H7, Listeria monocytogenes, and Salmonella
357 typhimurium in alfalfa sprouted seeds. International Journal of Food Microbiology 136, 66-
358 70.
359 Keer, J.T., and Birch, L., 2003. Molecular methods for the assessment of bacterial viability. Journal
360 of Microbiological Methods 53,175-183.

361 Kim, H.T., Choi, H.J., Kim, K.H., 2009. Flow cytometric analysis of Salmonella enterica serotype
362 Typhimurium inactivated with supercritical carbon dioxide. Journal of Microbiological
363 Methods 78, 155–160.
364 Liao, H., Zhang, L., Hu, X., Liao, X., 2010. Effect of high pressure CO_2 and mild heat processing
365 on natural microorganisms in apple juice. International Journal of Food Microbiology 137(1),
366 81-7.
367 Mantoan, D., and Spilimbergo, S., 2011. Mathematical Modeling of Yeast Inactivation of Freshly
368 Squeezed Apple Juice under High-Pressure Carbon Dioxide. Critical Reviews in Food
369 Science and Nutrition 51, 91–97.
370 Lleò MM., Benedetti, D., Tafi MC, Signoretto, C., Canepari, P., 2007. Inhibition of the
371 resuscitation from the viable but non-culturable state in Enterococcus faecalis. Environmental
372 Microbiology 9(9), 2313–2320.
373 Montville, T.J., and Matthews, K.R., 2008. Food Microbology: an introduction, Second edition.
374 ASM Press, Washington, USA, ISBN 9781555813963.
375 Müller, S., and Nebe-von-Caron, G., 2010. Functional single-cell analyses: flow cytometry and cell
376 sorting of microbial populations and communities. FEMS Microbiology Reviews 34 (4), 554-
377 587.
378 Nebe-von-Caron, G., Stephens, P.J., Hewitt, C.J., Powell, J.R. Badley, R.A., 2000. Analysis of
379 bacterial function by multi-colour fluorescence flow cytometry and single cell sorting. Journal
380 of Microbiological Methods 42, 97-114.
381 Nocker A, Fernández, P.S., Montijn, R., Schuren, F., 2012. Effect of air drying on bacterial
382 viability: A multiparameter viability assessment. Journal of Microbiological Methods 90, 86-
383 95.

384 Oliver, J.D., 2000. The public health significance of viable but nonculturable bacteria.
385 Nonculturable Microorganisms in the Environment (Colwell RR &Grimes DJ, eds), pp. 277-
386 299. ASM Press, Washington, DC.
387 Oliver, J.D., 2005. The Viable but Nonculturable State in Bacteria. Journal of Microbialogy 43(S),
388 93-100.
389 Oliver, J.D., 2010. Recent findings on the viable but nonculturable state in pathogenic bacteria.
390 FEMS Microbiology Reviews 34 (4), 415-425.
391 Oliver, J.D., Dagher M., Linden, K., 2005. Induction of Escherichia coli and Salmonella
392 typhimurium into the viable but nonculturable state following chlorination of wastewater.
393 Journal of. Water and Health 3(3), 249-257.
394 Raj, H., and Liston, J., 1960. Detection and Enumeration of Fecal Indicator Organisms in Frozen
395 Sea Foods. Applied Microbiology 9(2), 171–174.
396 Simon, P.W, Roger E. Freeman, R.E., V. Vieira, J.V., Boiteux, L.S., Briard, M., Nothnagel, T.,
397 Michalik, B., Kwon Y.S., 2008. Carrots. Vegetables II Handbook of Plant Breeding Vol (2),
398 327-357.
399 Spilimbergo, S., and Ciola, L., 2010. Supercritical CO_2 and N_2O pasteurisation of peach and kiwi
400 juice. International Journal of Food Science & Technology 45 (5),1619-1625.
401 Spilimbergo, S., Komes, D., Vojvodic, A., Levaj, B., Ferrentino, G., 2013. High pressure carbon
402 dioxide pasteurization of fresh cut carrot. The Journal of Supercritical Fluids 79, 92-100.
403 Tamburini, S., Ballarini, A., Ferrentino, G., Moro, A., Foladori, P., Spilimbergo, S., Jousson, O.,
404 2013. Comparison of quantitative PCR and flow cytometry as cellular viability methods to
405 study bacterial membrane permeabilization following supercritical CO_2 treatment.
406 Microbiology 159, 1056–1066.

Valverde, M.T., Marın-Iniesta, F., Calvo, L., 2010. Inactivation of Saccharomyces cerevisiae in conference pear with high pressure carbon dioxide and effects on pear quality. Journal of Food Engineering 98, 421-428.

Velusamy, V., Arshak, K., Korostynska, O., Oliwa, K., Adley, C., 2010. An overview of foodborne pathogen detection: In the perspective of biosensors. Biotechnology Advances 28, 232–254.

Wouters, P.C., Bos, A.P., Ueckert, J., 2001. Membrane permeabilization in relation to inactivation kinetics of Lactobacillus species due to pulsed electricelds. Applied Environmental Microbiology 67, 3092–3101.

Zhong, Q., Black, D. G., Davidson, P. M., Golden, D. A., 2008. Nonthermal inactivation of Escherichia coli K-12 on spinach leaves, using dense phase carbon dioxide. Journal of Food Protection 71, 1015-1017.

Ziglio, G., Andreottola, G., Barbesti, S., Boschetti, G., Bruni, L., Foladori, P., Villa, R., 2002. Assessment of activated sludge viability with flow cytometry. Water Research 36, 460-468.

Figure legends

Fig 1. Inactivation of culturable *E. coli* cells spiked on fresh cut carrots expressed as $Log_{10}(N_i/N_0)$ as a function of treatment time. SC-CO_2 treatment was performed at (A) 22°C and (B) 35°C.

Fig 2. FCM profiling of untreated natural flora (orange line) and *E. coli* cells (violet line) spiked on fresh cut carrots after SYBR-I and PI staining. (A) Overlapping of FALS histograms of natural flora and *E. coli* cells: the fraction percentage of small and large cells of natural flora and *E. coli* were indicated; (B) Cytogram of FALS vs. LALS signals of natural flora and *E. coli* cells; the cytogram of the green and red fluorescence signals of both populations are shown.

Fig 3. Progressive cell membrane permeabilization observed by FCM assays after SC-CO_2 treatment of *E. coli* cells spiked on fresh cut carrots. The treatments were performed at 120 bars, 22°C and 35°C, and up to 15 min. The percentages of intact, partially- and permeabilized cells are shown within each cytogram quadrant.

Fig 4. *E. coli* cells in untreated and SC-CO_2-treated (15 min, 35°C, 120 bar) samples: (A) FALS signals (B) and cytogram of LALS vs. FALS signal.

Fig 5. Percentages of *E. coli* cells subpopulations before and after SC-CO_2 treatment at (A) 22°C and (B) 35°C.

Fig 6. Comparison of total, viable and culturable *E. coli* cells per gram before and after SC-CO_2 treatment at 120 bar and at (A) 22°C and (B) 35°C.

454

455

456

457

458

459

460

Figure1

Fig 1

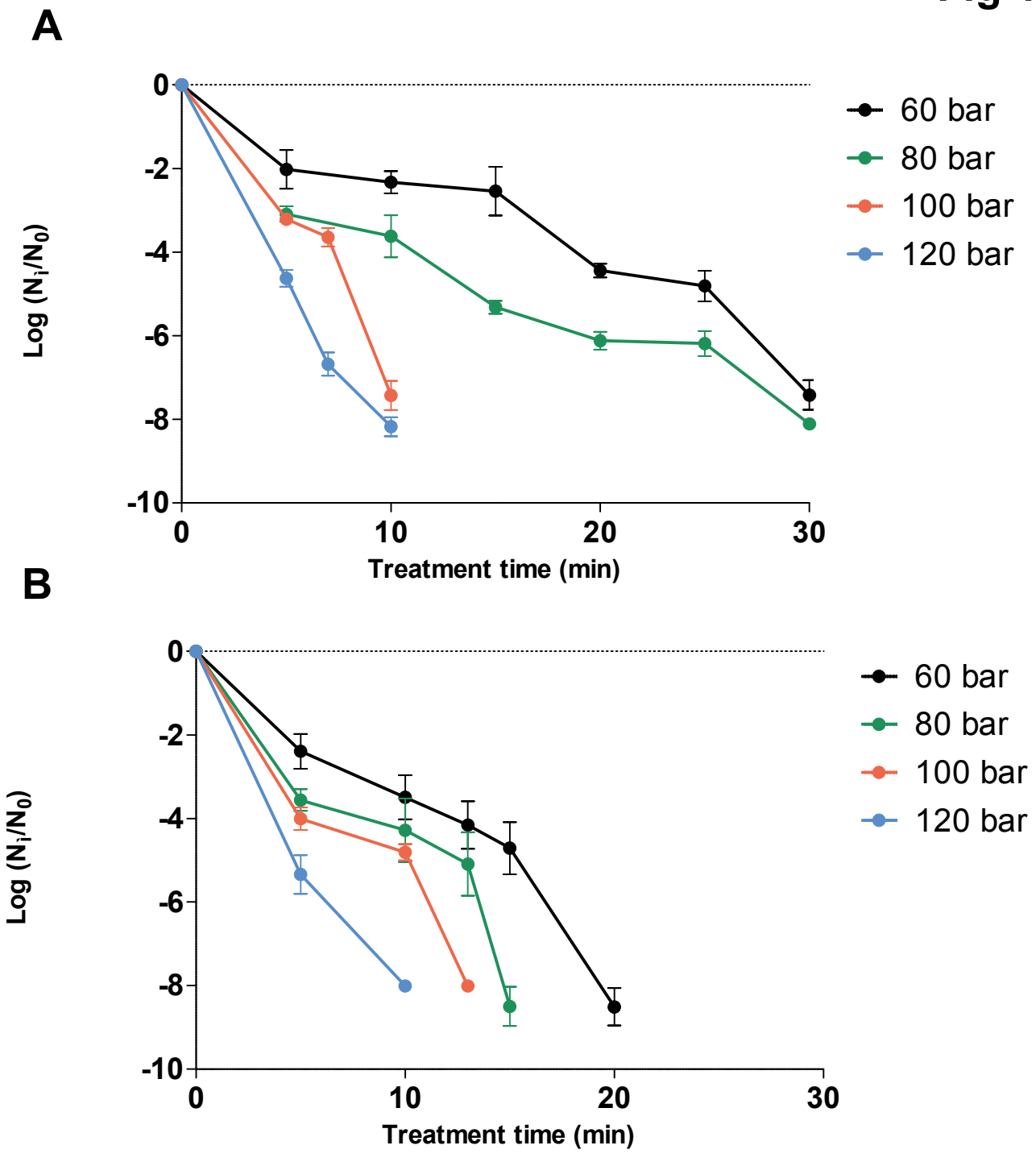

Figure2

Figure 2

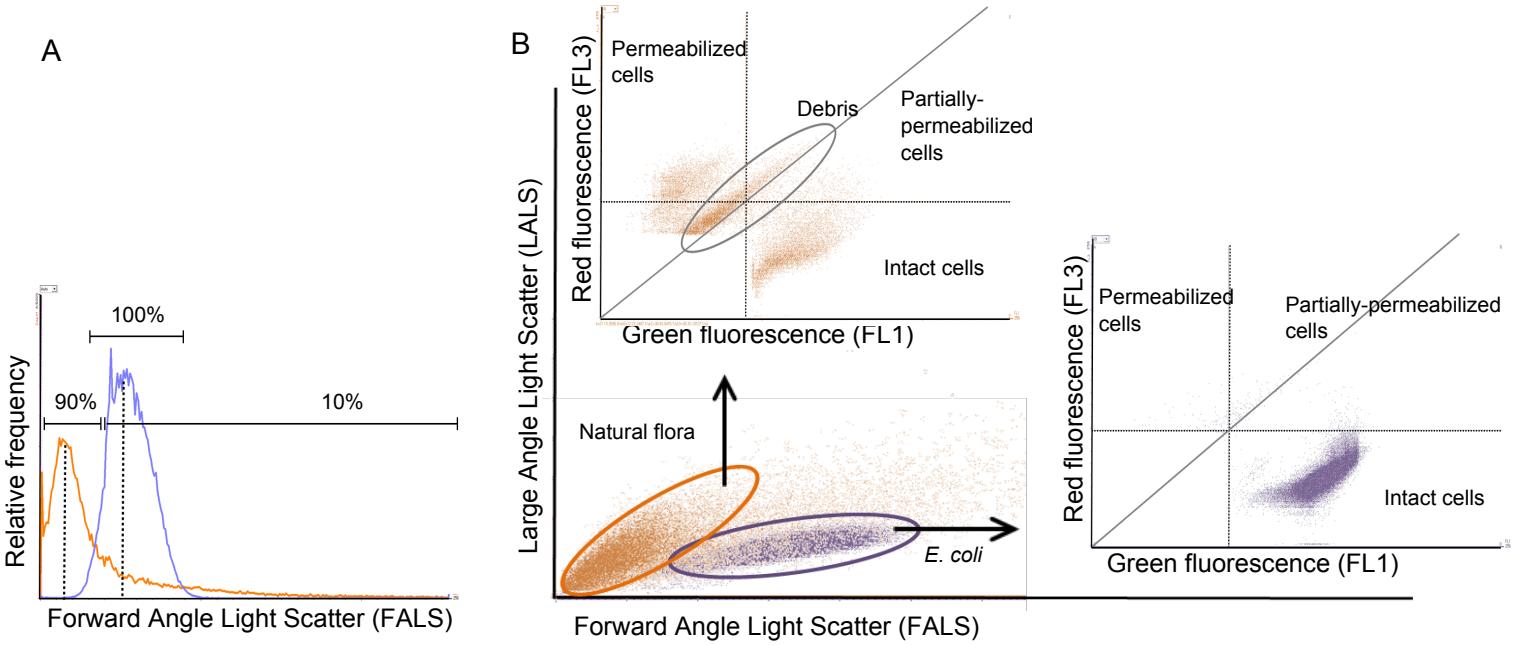

Figure3

Fig 3

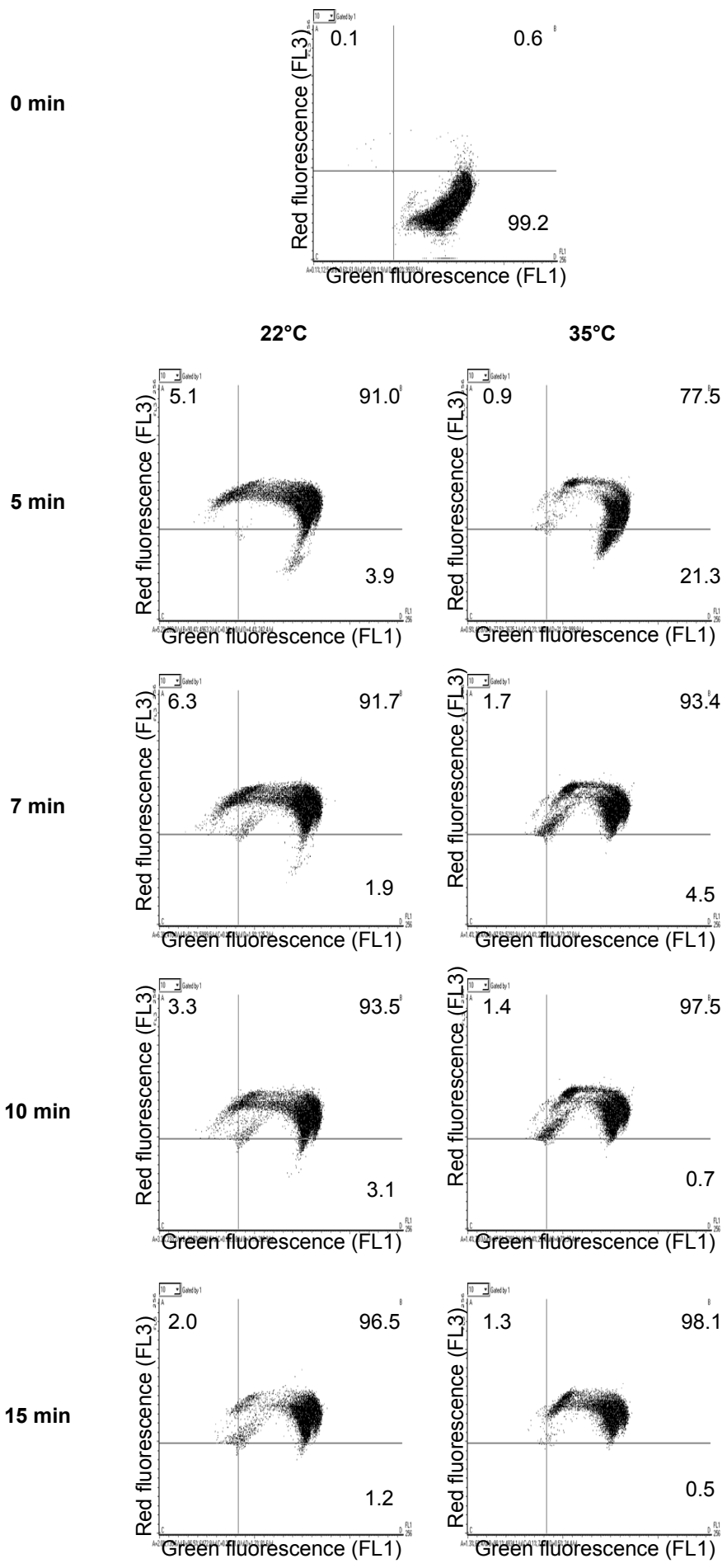

Figure4

Fig 4

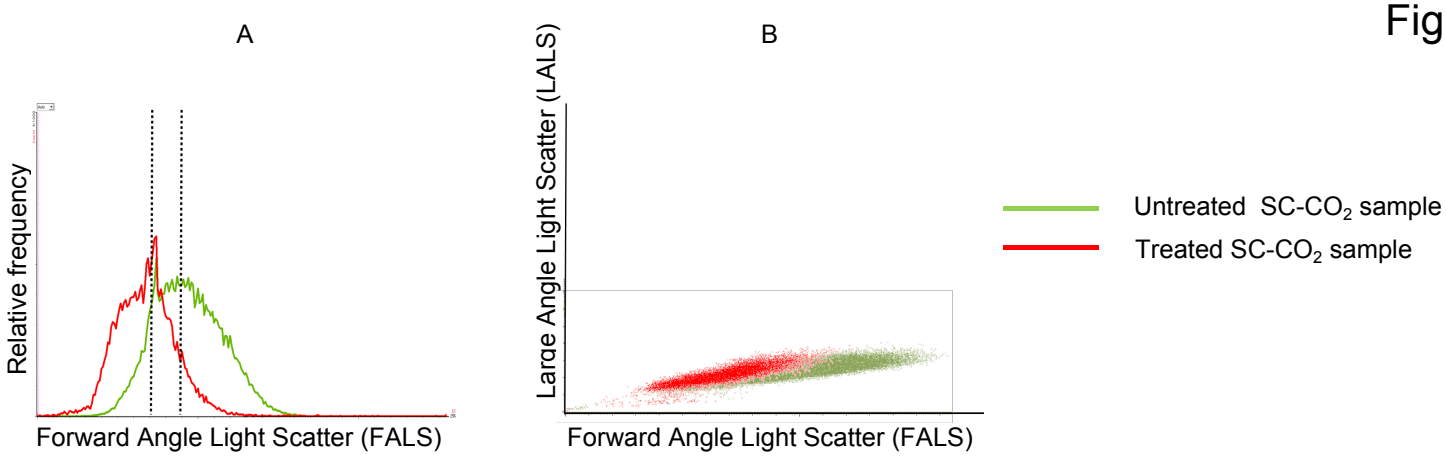

Figure5

Fig 5

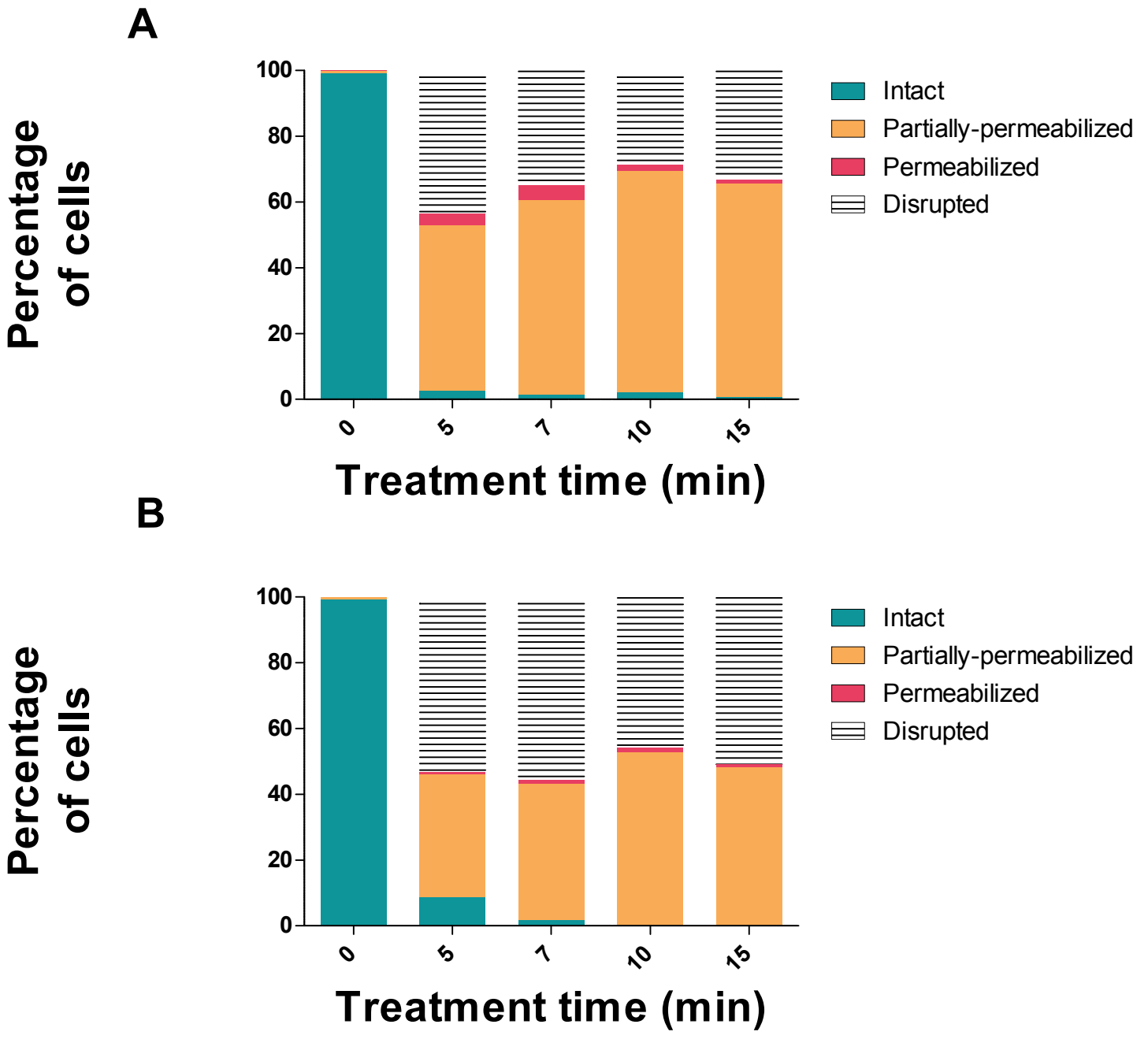

Figure6

Fig 6

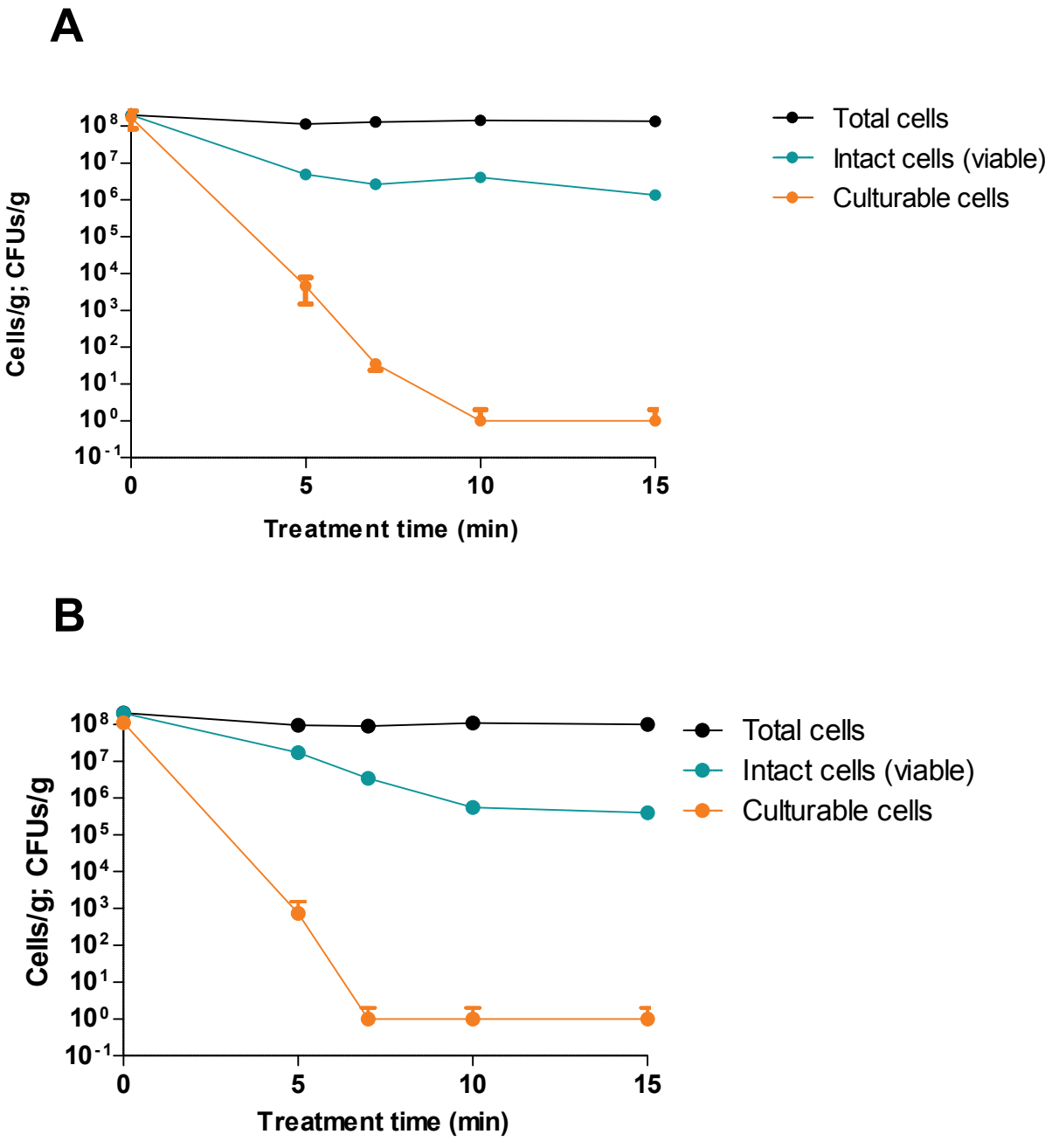

9.4 Publication C:

Janjua, H.A., Segata, N., Bernabò, P., **Tamburini**, S., Ellen, A., Jousson, O. (2012) Clinical populations of *Pseudomonas aeruginosa* isolated from acute infections show a high virulence range partially correlated with population structure and virulence gene expression. *Microbiology* 158, 2089-2098.

Microbiology (2012), **158**, 2089–2098 DOI 10.1099/mic.0.056689-0

Clinical populations of *Pseudomonas aeruginosa* isolated from acute infections show a wide virulence range partially correlated with population structure and virulence gene expression

Hussnain A. Janjua,[1] Nicola Segata,[2] Paola Bernabò,[1] Sabrina Tamburini,[1] Albert Ellen[1] and Olivier Jousson[1]

Correspondence
Olivier Jousson
jousson@science.unitn.it

[1]Centre for Integrative Biology (CIBIO), University of Trento, 38123 Trento, Italy

[2]Biostatistics Department, School of Public Health, Harvard University, Boston, MA 02115, USA

Pseudomonas aeruginosa is a ubiquitous environmental bacterium responsible for a variety of infections in humans, as well as in animal hosts. While the evolution of virulence in *P. aeruginosa* strains isolated from chronic lung infection in cystic fibrosis (CF) patients has been extensively studied, the virulence phenotype of *P. aeruginosa* isolated from other infection types or from the environment is currently not well characterized. Here we report an extensive analysis of the virulence of *P. aeruginosa* strains isolated from acute infections compared with population structure. Virulence profiles of individual strains were also compared with the expression levels of the *rhlR* gene, the transcriptional regulator of the rhl quorum-sensing system, and the gene encoding Crc, a global regulator controlling catabolite repression and carbon metabolism. Additionally, the presence/absence of the two mutually exclusive genes, *exoU* and *exoS*, encoding effectors of the type III secretion system, was assessed. In order to capture the widest range of genetic variability, a collection of 120 clinical strains was initially characterized by repetitive element-based PCR genotyping, and a selection of 27 strains belonging to different clonal lineages was subsequently tested using three different virulence assays, including two *Dictyostelium discoideum* assays on different growth media, and a *Caenorhabditis elegans* fast-killing assay. We show that the parallel application of virulence assays can be used to quantitatively assess this complex, multifactorial phenotypic trait. We observed a wide spectrum of virulence phenotypes ranging from weakly to highly aggressive, indicating that clinical strains isolated from acute infections can present a reduced or altered virulence phenotype. Genotypic associations only partially correlated with virulence profiles and virulence gene expression, whereas the presence of either *exoU* or *exoS* was not significantly correlated with virulence. Interestingly, the expression of *rhlR* showed a significant and positive correlation with the virulence profiles obtained with the three assays, while the expression of *crc* was either negatively or not correlated with virulence, depending on the assay.

Received 30 November 2011
Revised 28 April 2012
Accepted 2 May 2012

INTRODUCTION

Pseudomonas aeruginosa is a Gram-negative opportunistic pathogen and one of the main causes of nosocomial infections, including pneumonia, urinary tract infections, surgical wound infections and bloodstream infections. It is frequently isolated from immunocompromised individuals and intubated patients, and causes chronic lung infections in cystic fibrosis (CF) patients, as well as in adults with bronchiectasis and chronic obstructive pulmonary disease (Valderrey *et al.*, 2010).

Understanding bacterial virulence and, more generally, the host–pathogen relationship at the cellular and molecular level is essential to identify new targets and develop new strategies to fight infection. Molecular analysis of host–pathogen interactions benefits from the use of model systems, allowing a systematic study of the factors involved. In this regard the social amoeba *Dictyostelium discoideum* has been extensively used in recent virulence studies of various pathogenic bacteria, among which are *Salmonella typhimurium* (Sillo *et al.*, 2011), *Streptococcus suis* (Bonifait

Abbreviations: CF, cystic fibrosis; rep-PCR, repetitive element-based PCR.

et al., 2011), *Vibrio cholerae* (Miyata *et al.*, 2011), *Burkholderia pseudomallei* (Hasselbring *et al.*, 2011), *Legionella pneumophila* (Shevchuk & Steinert, 2009), *Klebsiella pneumoniae* (Pan *et al.*, 2011) and *P. aeruginosa* (Alibaud *et al.*, 2008). *Dictyostelium* cells are typically used as a screening system to determine the role of individual genes in virulence, by comparing the virulence phenotype of wild-type and mutant bacterial strains. In *P. aeruginosa*, such an approach has led to the identification of a number of virulence genes involved in various processes, among which are quorum-sensing (Pukatzki *et al.*, 2002; Cosson *et al.*, 2002), induction of the type III secretion system (Alibaud *et al.*, 2008) and global metabolic regulation (Linares *et al.*, 2010).

The microevolution of *P. aeruginosa* during the course of infection in CF patients has been extensively studied and typically leads to the selection of diversely virulent variants, based on mutations or expression changes in many virulence genes, including type III secretion, quorum sensing and iron acquisition (Hogardt & Heesemann, 2010; Lelong *et al.*, 2011; Kesarwani *et al.*, 2011). While early infection CF isolates are more virulent and more likely to cause acute infections than late isolates, the latter have been shown to maintain their ability to cause chronic infection and inflammation (Bragonzi *et al.*, 2009). Late CF isolates therefore exhibit an altered virulence pattern with respect to acute infection isolates, as recently confirmed by the comparison of transcriptomes of isogenic early acute infection versus chronic infection isolates (Naughton *et al.*, 2011). In contrast to CF isolates, very little is known about the virulence phenotype of *P. aeruginosa* isolated from other infection types or from the environment; a recent study (Bradbury *et al.*, 2011) showed that CF strains are globally less virulent against *D. discoideum* than those isolated from other sources. However, the experimental settings used by Bradbury and co-workers allowed the study of the virulence range of CF strains only, since only one non-CF strain supported growth of *D. discoideum*.

In the present study, we performed an extensive analysis of the virulence range of *P. aeruginosa* strains isolated from acute infections and compared it with the genotypic population structure. Additionally, we measured in a selection of strains the expression level of the *rhlR* gene, the transcriptional regulator of the rhl quorum-sensing system, and of the gene encoding Crc, a global regulator controlling catabolite repression and carbon metabolism in *P. aeruginosa*. Both genes have been shown to play a role in the virulence phenotype of *P. aeruginosa*, in particular against *D. discoideum* (Cosson *et al.*, 2002; Linares *et al.*, 2010). Furthermore, the presence/absence of the two mutually exclusive genes *exoU* and *exoS* (Wareham & Curtis, 2007), encoding effectors of the type III secretion system, was also assessed. In order to capture the widest range of genetic variability, a collection of 120 clinical strains was initially characterized by repetitive element-based PCR (rep-PCR) genotyping (Syrmis *et al.*, 2004), and a selection of 27 strains belonging to different clonal lineages was subsequently characterized using three different virulence assays, including two *D. discoideum* assays on SM and HL5 growth media (Froquet *et al.*, 2009), and a *Caenorhabditis elegans* fast-killing assay (Tan *et al.*, 1999). In a previous study (Fumanelli *et al.*, 2011), we showed the importance of determining the correct experimental parameters for the application of *Dictyostelium* virulence assays to bacterial species or strains of unknown aggressiveness. In order to quantitatively estimate the level of virulence associated with each strain and to make results directly comparable, a virulence score was defined for each assay. A surprisingly high range of virulence phenotypes was observed. Correlations between clonal lineages and virulence profiles of individual strains were examined by mapping virulence scores, virulence gene expression levels, and *exoU/exoS* genotype on a phylogenetic tree derived from rep-PCR genotyping data.

METHODS

Strains and growth media. A total of 120 strains of *P. aeruginosa* were isolated from patients at Santa Chiara Hospital (Trento, Italy) affected by lung infections, urinary tract infections or skin ulcers. These strains were initially grown on MacConkey agar and stored at −80 °C in 20 % (v/v) glycerol. *D. discoideum* NC4 strain (DBS0304666) was obtained from the Dicty Stock Center (Northwestern University, IL, USA). *C. elegans* strain N2 was obtained from the Caenorhabditis Genetic Center (University of Minnesota). *D. discoideum* NC4 was grown on SM broth using *Klebsiella aerogenes* as a food source, whereas *C. elegans* N2 was grown on NGM (nematode growth medium) agar plates with *E. coli* OP50 as a carbon source.

Rep-PCR-based genotyping assays. ERIC-PCR and BOX-PCR assays were performed as previously described (Syrmis *et al.*, 2004) on the whole *P. aeruginosa* collection, consisting of 120 clinical strains isolated from acute infections, and on reference strains PA14, PAO1, PA2192 and LESB58. The reaction mixture contained 6 mM $MgCl_2$, 1 × PCR buffer, 200 μM each dNTP, 1 μM each ERIC primer and 1.2 μM BOX primer, 2.5 U *Taq*, 0.2 % (v/v) glycerol and 100 ng genomic DNA. The final reaction volume was adjusted to 50 μl with PCR grade water. PCR amplification cycling was an initial denaturation step at 94 °C for 7 min, followed by 30 cycles with a denaturation step of 1 min at 94 °C, an annealing step of 1 min at 53 °C for BOX and 55 °C for ERIC primers, and an extension step of 2 min at 72 °C, followed by a final extension step of 10 min at 72 °C. Ten microlitres of each amplicon was loaded on a 2 % agarose gel made in 1 × Tris-acetate-EDTA (TAE) buffer and stained with ethidium bromide. The gels were visualized under UV light using a BioDoc-It gel documentation system (UVP). ERIC and BOX electrophoretic profiles were analysed and transformed into binary matrices using Cross Checker software, available at http://www.plantbreeding.wur.nl/UK/software_crosschecker.html.

Phylogenetic analyses. Phylogenetic analyses were initially performed on the whole collection of clinical strains (120) by merging BOX and ERIC band patterns in a single binary matrix. Cluster analyses were generated using the unweighted pair group method using arithmetic averages (UPGMA) and the Dice similarity coefficient was calculated using TREECON software (Van de Peer & De Wachter, 1994). The criterion for defining clonal lineages was taken as profiles with 85 % or more similar bands. At least one clinical strain per clonal lineage was selected for further virulence assays and correlation analyses. The resulting tree was represented as a radial cladogram using

an in-house tool (Segata *et al.*, 2011), and virulence profiles, virulence gene expression and *exoU*/*exoS* genotype of each taxon were mapped on the tree.

Virulence assays using *D. discoideum* NC4. Two *D. discoideum* virulence assays were applied, the standard SM agar assay (Cosson *et al.*, 2002) and the HL5 diluted medium assay (Froquet *et al.*, 2009). Both assays offer the opportunity to distinguish among different degrees of virulence of pathogenic bacteria. The HL5 assay proved to be more suitable to quantify virulence in bacterial strains with extreme virulence phenotypes, such as 'super-virulent' or 'non-virulent' strains (Froquet *et al.*, 2009). For the SM agar assay, *P. aeruginosa* cells were harvested during exponential phase and resuspended into SM broth at a final OD_{600} of 1, diluted into 5 ml SM broth and spread on SM agar plates to make a homogeneous bacterial lawn. *D. discoideum* NC4 was grown in SM broth with *K. aerogenes* as a food source. The cells were harvested after 2–3 days of incubation at 20 °C, and resuspended into HL5 medium and 1× Sorensen phosphate buffer. Cell concentration was determined using a Countess Automated Cell Counter (Invitrogen). Nine 5 µl droplets consisting of serial dilutions of *D. discoideum* cells were spotted on the bacterial lawn. The dilution factor was threefold, and the approximate number of cells in each droplet was 20 000, 6600, 2200, 750, 250, 90, 30, 10 and 3, respectively. Each assay was run in triplicate. A control plate was obtained using non-pathogenic *E. coli* DH5α instead of *P. aeruginosa* strains. The plates were incubated for 6 days at 19 °C before examining the growth pattern of *D. discoideum*.

For the diluted HL5 medium assay, *P. aeruginosa* strains were harvested during the exponential phase and diluted into 2.5 ml SM broth. A suspension of 500 µl of bacterial cells at a final OD_{600} of 1 was deposited into 12-well Corning Costar cell culture plates (Sigma-Aldrich) containing serially diluted (twofold) HL5 agar at the following concentrations: 100, 50, 25, 12.5, 6.25, 3.1, 1.5, 0.75, 0.37, 0.18, 0.09, 0.04 and 0.02 %. The plates with the bacterial lawn were initially dried at room temperature for 1 h before adding to *D. discoideum* cells. *D. discoideum* NC4 was grown in SM broth with *K. aerogenes* at 20 °C as a food source and resuspended into SM broth diluted 1 : 1 with 1× Sorensen buffer. Two microlitres of *D. discoideum* containing approximately 7000 cells was spotted on a *P. aeruginosa* lawn plated on HL5 medium at different concentrations. The plates were incubated at 19 °C for 6 days before examining the growth pattern of *D. discoideum*. Each assay was run in triplicate. As in the assay above, a plate incubated with *E. coli* DH5α was used as a control.

Fast-killing virulence assays using *C. elegans* N2. The *C. elegans* N2 strain was grown on NGM (nematode growth medium) agar plates with *E. coli* OP50 as a food source. The *C. elegans* fast-killing assay was performed as described elsewhere (Tan *et al.*, 1999). *P. aeruginosa* cells were grown in peptone glucose (PG) medium, harvested during exponential phase and resuspended into PG broth at a final OD_{600} of 1, and 200 µl was spread on PG agar plates. The plates were incubated at room temperature for 18 h. On average, 60–70 *C. elegans* individuals were picked and placed on PG plates, and incubated at 22 °C for 4 h. The viability/mortality of the worms was observed under a microscope using a ×10 lens and monitored with a CCD camera. The percentage killing of *C. elegans* was calculated by determining the number of dead worms out of the total worms deposited on each plate. Each assay was run in triplicate. As in the assays above, *E. coli* DH5α was used as a control.

Gene expression analyses. Two replicates of each *P. aeruginosa* strain were harvested during exponential phase at OD_{600} 0.6 and pelleted by centrifugation (6000 ***g*** for 5 min at 4 °C). Total RNA was isolated from bacterial pellets by using the TRIzol Max Bacterial Isolation kit (Life Technologies) as described by the manufacturer. Approximately 10 µg of the total RNA preparation was treated twice with the RNase-free DNase set (Qiagen) to remove genomic DNA contamination and was subsequently cleaned up with the RNeasy Mini kit (Qiagen) following the manufacturer's instructions. RNA concentration and purity were determined by UV absorption (260 : 280 nm) using a NanoDrop ND-1000 spectrophotometer (NanoDrop Technologies) and 0.8 % agarose gels stained with ethidium bromide. One microgram of DNase-treated RNA was reverse-transcribed into cDNA using a First Strand cDNA Synthesis kit (Fermentas). cDNAs were amplified by real-time PCR using Kapa Sybr Fast qPCR Mastermix (KapaBiosystems) and a CFX96 Real-Time PCR Detection System (Bio-Rad Laboratories). PCR conditions were as follows: 95 °C for 3 min, 40 cycles of 3 s at 95 °C and 30 s at 60 °C, with a final melting curve analysis from 72 to 95 °C, with increments of 1 °C every 5 s. Real-time PCR amplifications were performed with two experimental replicates for each sample.

Primers for the *rhlR*, *crc*, *exoU* and *exoS* genes were designed using Primer3 software (Rozen & Skaletsky, 2000) to produce amplicons ranging from 80 to 220 bp. Primers sequences are reported in Table 1. Each primer pair was controlled for dimer formation by melting curve analysis, and PCR efficiency was calculated over a sixfold 2× dilution series. The *rpoD* and *rplS* genes were used as housekeeping genes (Savli *et al.*, 2003; Llanes *et al.*, 2004), and gene expression values were further normalized to those obtained with PSUR28, the strain displaying the lowest score in virulence assays. Amplification profiles were analysed using Bio-Rad Manager Software and cycle threshold (C_t) values for each target gene were normalized to the geometric mean of the C_t of *rpoD* and *rplS* amplified from the corresponding sample. The fold change of target genes for each strain with respect to the PSUR28 control strain was calculated using the $\Delta\Delta C_t$ method.

Virulence scores and correlation analyses. In order to quantitatively estimate the level of virulence associated with each strain and to make them directly comparable, a virulence score was defined for each assay. For the SM agar assay using *D. discoideum*, the scores were attributed according to the most concentrated droplet for which no growth was observed, as follows: virulence score of 9 for inhibition of *D. discoideum* growth with 20 000 cells; score of 8 for inhibition with 6600 cells, and so on, down to a score of 0 for absence of growth inhibition, even at the lowest number of cells spotted (Table 2). For the diluted HL5 assay the same principle was applied: a virulence score of 9 was attributed to strains inhibiting *D. discoideum* growth at 0.02 % HL5 medium concentration; a score of 8 for growth inhibition at 0.04 % concentration, and so on, down to a score of 0 for absence of growth inhibition, even for the most concentrated HL5 medium used (Table 2). For the *C. elegans* assay, the scores were attributed as follows: a virulence score of 9 for $\geqslant$90 % killing; a score of 8 for killing percentages in the range 80–90 %, and so on, down to a score of 0 for killing percentages lower than 10 % (Table 2).

Pearson correlation analysis (producing correlation coefficients and *P* values) was applied on the virulence scores after averaging the replicates to check the consistency of the three virulence assays. The same approach was also employed to test the interdependency between the virulence profiles and the expression profiles of *rhlR* and *crc* genes, and to study the relationship between their expression patterns. For testing the hypothetical dependence of the virulence profiles with respect to the mutually exclusive presence of the *exoU* and *exoS* genes, we adopted the Wilcoxon test.

We investigated the correlation between genotype and virulence profiles by estimating the genetic versus virulence pairwise distances among strains and by comparing them using Pearson correlation. For the genotype profiles, the distance matrix was generated by computing the all-versus-all minimum branch length distance among leaf nodes in the phylogenetic tree. For the virulence profiles based on

Table 1. Sequences of primers (5′–3′) used in this study

Primers were designed for gene expression analysis of *rhlR* and *crc* using *rpoD* and *rplS* as housekeeping genes, and for determining *exoU/exoS* genotype.

Gene	Forward primer	Reverse primer
Target genes		
rhlR	TCCTCGGAAATGGTGGTCTG	CGCTCGAAGCTGGAGATGTT
crc	TCCTTCCAACTGGACGGCTA	AGCAGGGTGGCGATACTCAC
exoU	GGAGTATCTGCCAGCGCATC	GAACCCGGAGATCACAGACG
exoS	CTTCGGCGTCACTGTGGATG	AGGTCAGCAGAGTATCGGC
Housekeeping genes		
rpoD	GCTGCTGTCGTCGCTTTCTT	AGCATCCTGGCCGACTACAA
rplS	ACCCGCGTATACACCACCAC	CACACCCGGAAGGTCCTTTA

the three assays described above, the standard Euclidean distance was employed.

RESULTS AND DISCUSSION

Rep-PCR-based genotyping assays and phylogenetic analyses

A total of 31 and 26 different electrophoretic bands were generated by BOX and ERIC PCR amplifications, respectively, and binary data extracted from both genotyping techniques were merged for subsequent phylogenetic reconstruction. The 120 clinical strains analysed were clustered in a total of 27 different clonal lineages with a Dice coefficient of >15 %. Each clonal lineage included up to seven strains. In order to comprehensively represent the genetic diversity of the clinical strain collection, one strain from each clonal lineage was selected for further phylogenetic analyses and virulence assays. In order to determine the intra-clonal variability of virulence profiles, up to three strains from each clonal lineage were tested with the SM agar assay. Hierarchically clustering the genotyping profiles, a phylogenetic tree depicting the relationships between 31 strains (27 clinical strains and four reference strains) was reconstructed (Fig. 1), as described in Methods. Several pairs of strains showed very similar genotyping patterns and were thus tightly clustered in the tree. The three pairs with highest similarity were Hpu43/Hpu45 (eight synapomorphic characters), PSUR28/VRSP32 (seven) and LESB58/Hpu106 (seven). On the other hand, several pairs of strains had no synapomorphic characters (13 % of pairs) or a single one (41 %).

Virulence assays using *D. discoideum* NC4

In the first assay on SM agar plates, 5 µl droplets of *D. discoideum* culture were applied on a lawn of *P. aeruginosa*, with each droplet containing a number of *Dictyostelium*

Table 2. Parameters used for defining virulence scores for the three assays

Virulence score	Model organism		
	D. discoideum		*C. elegans*
	SM agar assay*	HL5 medium assay†	Fast-killing assay‡
0	3	12.5	<10 %
1	10	6.25	10–20 %
2	30	3.1	20–30 %
3	90	1.5	30–40 %
4	250	0.75	40–50 %
5	750	0.37	50–60 %
6	2200	0.18	60–70 %
7	6600	0.09	70–80 %
8	20 000	0.04	80–90 %
9	>20 000	0.02	>90 %

*Lowest number of *D. discoideum* cells spotted for which growth was inhibited.
†Concentration of HL5 medium (%) for which *D. discoideum* growth was inhibited.
‡Percentage of *C. elegans* individuals killed.

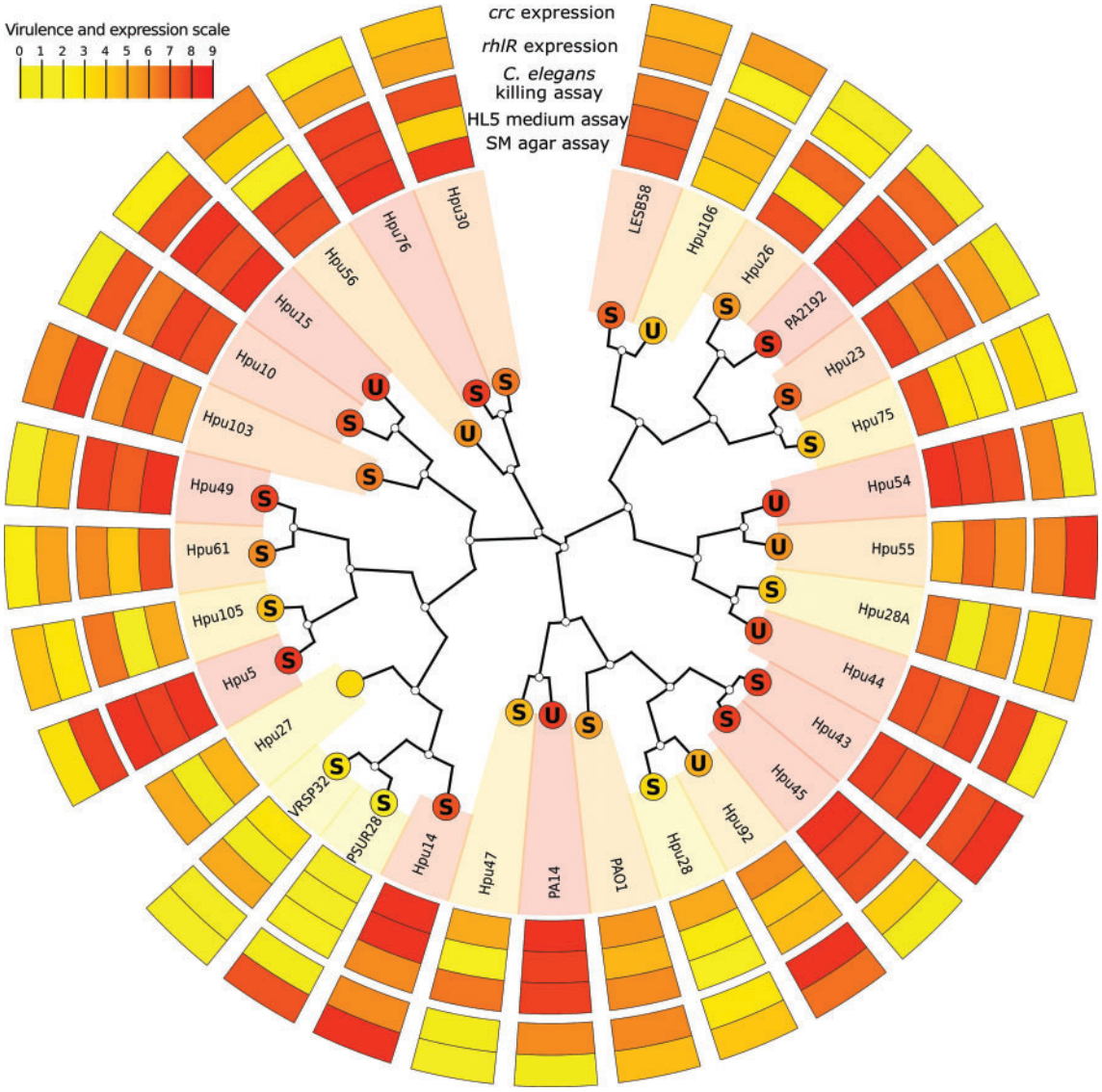

Fig. 1. Population structure of *P. aeruginosa* clinical strains according to rep-PCR genotyping, virulence phenotypes, virulence gene expression and *exoU*/*exoS* genotype. Names of strains are indicated on terminal branches. The inner cladogram represents the phylogenetic relationships between the 31 strains characterized genotypically. The first three inner coloured rings report the three virulence scores (from 0 to 9) for SM agar, HL5 medium and *C. elegans* killing assay, while the two external rings report the expression levels of *rhlR* and *crc* genes relative to the less virulent strain PSUR28. Log-ratio gene expression levels were normalized on a 0–9 scale, winsorizing the highest and the lowest values. The *exoU*$^{+}$/*exoS*$^{-}$ or *exoU*$^{-}$/*exoS*$^{+}$ genotype found on individual strains is indicated on leaf spots by 'U' or 'S', respectively. The colour of spots and of the radial background represents the mean of the three virulence scores.

cells ranging from 3 to 20 000 (Fig. 2). Under these conditions, even 20 000 *Dictyostelium* cells failed to create a phagocytic plaque in a lawn of the most virulent *P. aeruginosa* clinical strains (Table 3). Plaques instead appeared around *D. discoideum* cells spotted on moderately or weakly virulent strains. The most permissive *P. aeruginosa* strains, such as PSUR28 and VRPS32, allowed *D. discoideum* growth and radial expansion, even starting from a very limited number of cells (<250) (Table 3). Moderately virulent strains allowed *D. discoideum* growth when at least several hundred cells were deposited on the bacterial lawn. The mean virulence scores obtained with this assay on 43 *P. aeruginosa* strains ranged from 2.0 to 9.0, with a mean value of 7.14.

In the second virulence assay on diluted HL5 medium, the number of *D. discoideum* cells spotted on the bacterial lawn was constant (about 6000 cells in 2 µl). The serial dilution of HL5 medium is aimed at reducing the growth capacity of the strains, presumably rendering them less aggressive,

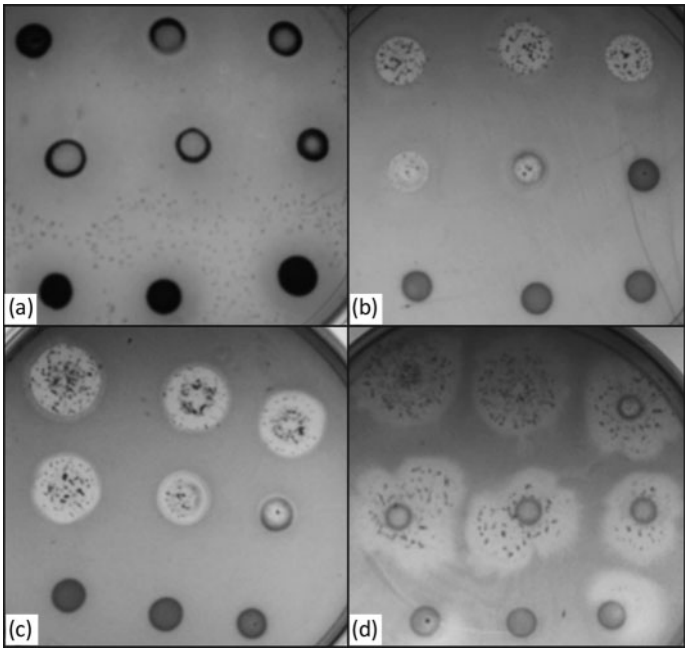

Fig. 2. Quantitative assessment of *D. discoideum* growth using SM agar assays in the presence of *P. aeruginosa*. For each bacterial strain, the most concentrated *Dictyostelium* spot is at the top left; concentration decreases serially to the bottom-left spot. (a) Highly virulent strain PA14 (mean virulence score 9.0); (b, c) moderately virulent strains Hpu105 and Hpu106 (mean virulence scores 5.7 and 4.3, respectively); (d) weakly virulent strain PSUR28 (mean virulence score 2.0).

and consequently diminishing their ability to resist phagocytosis by *D. discoideum*. Preliminary experiments showed that the majority of *P. aeruginosa* strains, including most of the weakly virulent ones, inhibited *D. discoideum* growth on HL5 dilutions ranging from 100 to 25 % (data not shown). We therefore started the dilution range at 12.5 % and decreased it serially (twofold dilutions) to 0.02 %. The minimal HL5 medium concentration at which a given bacterial strain allowed *D. discoideum* growth was used to define the virulence score of individual strains, as described in Methods. The HL5 medium virulence scores were globally consistent with those obtained with the assays on SM agar (in more than half of the cases the difference was smaller than 1 unit of virulence score values) and with a significant correlation (P value 9.7×10^{-5}), although in four cases a difference of more than 4 virulence score units was observed. The HL5 assay was more discriminating and showed less saturation than the SM agar assay for highly virulent strains, since only a few of the strains with a mean virulence score of 9 in the SM agar assay (nine strains) also displayed this value for the HL5 assay (two strains) (Table 3). The virulence scores obtained with this assay on 31 *P. aeruginosa* strains ranged from 0.3 to 9.0, with a mean value of 5.9.

Fast-killing virulence assays using *C. elegans* N2

We used an additional virulence and pathogenesis assay that consists of measuring killing percentages of the soil nematode *C. elegans* by *P. aeruginosa*. Previous studies using *C. elegans* as a virulence model have shown that, depending on the growth medium, *P. aeruginosa* causes different outcomes: slow or fast killing, lethal paralysis and red death (Tan *et al.*, 1999). We tested all *P. aeruginosa* clinical strains selected in the present study for their ability to kill *C. elegans* using the fast-killing assay, as described in Methods. As for the *D. discoideum* assays, a wide range of virulence phenotypes was observed (Table 3). Ten out of 31 *P. aeruginosa* strains were found to be highly aggressive, killing more than 80 % of the worms in 4 h (virulence score >8). The lowest percentage of killing was observed with strains Hpu28, Hpu56 and PSUR28 (20–30 % killing, mean virulence score of 2.3). The virulence scores obtained with this assay on 31 *P. aeruginosa* strains ranged from 2.3 to 9.0, with a mean value of 6.8.

Virulence gene expression and assessment of *exoU/exoS* genotype

The expression of *rhlR* and *crc* genes in 26 clinical strains and four reference strains of *P. aeruginosa* was analysed and is reported in Fig. 1 and Table 3. A single strain (Hpu27) was not analysed for gene expression as good quality RNA could not be obtained. The PSUR28 strain, which on average presented the lowest score for the three virulence assays (Table 3), was selected as a reference to evaluate the fold change in the other strains. For *rhlR*, all tested strains (n=30) showed a much higher level of expression compared with strain PSUR28. The fold change values (expressed as $\log_{10}$ values) obtained for this gene ranged from 3.04 in strain Hpu47 to 4.55 in strain Hpu103 (Table 3). In contrast, most of the tested strains presented a lower expression level (negative fold change value) of the *crc* gene with respect to PSUR28. The fold change values for this gene ranged from −0.43 (in Hpu45) to 0.21 (in Hpu55) (Table 3).

In addition, the presence in individual strains of genes encoding the type III secretion system effectors ExoU and

Table 3. Virulence assay scores using *D. discoideum* or *C. elegans* expressed as the mean of three replicates, *rhlR* and *crc* gene expression values (mean ± SD, values expressed as $\log_{10}$) relative to PSUR28 strain values, and *exoU*$^+$/*exoS*$^-$ (U) or *exoU*$^-$/*exoS*$^+$ (S) genotype

Data were obtained from 27 clinical *P. aeruginosa* strains belonging to different clonal lineages and from reference strains PAO1, PA14, LESB58 and PA2192. Non-pathogenic *E. coli* DH5α was used as a control strain for virulence assays. ND, Not determined.

Bacterial strain	*D. discoideum* SM agar	*D. discoideum* HL5 medium	*C. elegans* fast-killing	*rhlR* expression	*crc* expression	*exoU/exoS* genotype
Hpu5	9.0	8.7	9.0	4.35 ± 0.08	−0.20 ± 0.07	S
Hpu10	8.3	8.7	7.3	4.27 ± 0.03	−0.32 ± 0.02	S
Hpu14	9.0	9.0	6.7	4.05 ± 0.12	0.17 ± 0.03	S
Hpu15	9.0	8.3	9.0	4.30 ± 0.02	−0.23 ± 0.02	U
Hpu23	8.7	6.7	7.7	3.98 ± 0.03	−0.34 ± 0.00	S
Hpu26	8.3	3.0	7.7	3.45 ± 0.05	−0.31 ± 0.08	S
Hpu27	5.3	0.3	5.7	ND	ND	ND
Hpu28A	7.3	0.3	6.0	3.62 ± 0.10	−0.11 ± 0.07	S
Hpu28	5.7	3.0	2.3	3.52 ± 0.01	−0.15 ± 0.05	S
Hpu30	9.0	4.3	8.3	3.93 ± 0.01	−0.14 ± 0.03	S
Hpu43	8.7	8.3	9.0	4.29 ± 0.03	0.03 ± 0.09	S
Hpu44	8.3	8.0	8.7	4.33 ± 0.02	−0.24 ± 0.04	U
Hpu45	9.0	8.7	8.3	3.71 ± 0.06	−0.43 ± 0.04	S
Hpu47	5.7	2.3	7.3	3.04 ± 0.01	−0.28 ± 0.12	S
Hpu49	9.0	8.0	8.7	3.83 ± 0.03	−0.27 ± 0.01	S
Hpu54	9.0	8.7	8.3	4.06 ± 0.07	−0.32 ± 0.02	U
Hpu55	5.3	7.7	6.3	4.08 ± 0.06	0.21 ± 0.14	U
Hpu56	8.3	8.7	2.3	3.64 ± 0.04	−0.05 ± 0.02	U
Hpu61	8.3	4.7	6.7	3.93 ± 0.04	−0.23 ± 0.12	S
Hpu75	8.3	3.3	2.7	3.63 ± 0.00	−0.23 ± 0.00	S
Hpu76	9.0	8.7	8.7	3.89 ± 0.10	−0.22 ± 0.11	S
Hpu92	6.7	4.7	5.0	4.40 ± 0.02	−0.03 ± 0.00	U
Hpu103	6.3	8.3	6.7	4.55 ± 0.05	−0.06 ± 0.07	S
Hpu105	5.7	1.7	7.3	3.50 ± 0.19	−0.15 ± 0.12	S
Hpu106	4.3	5.0	5.3	3.41 ± 0.01	−0.09 ± 0.11	U
VRSP32	3.3	0.3	5.7	3.15 ± 0.02	−0.28 ± 0.07	S
PSUR28	2.0	1.7	2.3	0.00 ± 0.00	0.00 ± 0.00	S
PA2192	9.0	9.0	8.3	4.21 ± 0.02	−0.27 ± 0.02	S
PAO1	6.3	5.3	6.7	4.06 ± 0.08	−0.13 ± 0.04	S
PA14	9.0	8.7	8.7	4.05 ± 0.05	−0.33 ± 0.06	U
LESB58	8.3	8.0	7.0	3.98 ± 0.04	−0.12 ± 0.05	S
E. coli DH5α	0.0	0.0	0.0	–	–	–

ExoS was evaluated by PCR amplification. Our results confirm that both genes are mutually exclusive. The *exoU*$^+$/*exoS*$^-$ genotype was less prevalent (found in 26.7 % of the strains) than the *exoU*$^-$/*exoS*$^+$ genotype (73.3 %), as reported earlier (Feltman *et al.*, 2001; Wareham & Curtis, 2007) (Fig. 1, Table 3).

Virulence score consistency and virulence range

All three virulence profiling approaches were statistically significantly correlated. In particular, the two *D. discoideum* NC4 assays were strongly correlated (r=0.66, P value=3.9×10^{-5}), and both showed a slightly lower correlation with the *C. elegans* N2 assay (r=0.58 and P value=0.0005 for the SM agar assay, and r=0.48, P value=0.006 for the HL5 medium assay). Both assays using *D. discoideum* as a model organism showed saturation for highly virulent strains. These strains completely inhibited *D. discoideum* growth, even at high concentrations (20 000 cells per droplet) in the SM agar assay, whereas some of them also prevented *D. discoideum* growth at the lowest HL5 dilution (0.02 %). We noted that it was not possible to perform the HL5 assay by further decreasing the concentration of the medium below 0.02 %, as in these conditions the availability of nutrients was apparently insufficient to support bacterial growth, and consequently the formation of the lawn did not occur. Likewise, most of the strains also killed 90–100 % of the population using the *C. elegans* fast-killing assay. This implies that the assays cannot accurately quantify eventual differences between highly and 'extremely virulent' strains. Conversely, the virulence assays worked remarkably well in determining and quantifying the virulence phenotype of

weakly and moderately virulent bacterial strains. Globally, a surprisingly high virulence range was noted for the clinical strains, indicating that *P. aeruginosa* strains showing reduced or altered virulence are not exclusively a characteristic of chronic infections.

Correlation between virulence profiles and rep-PCR genotyping

By comparing genotyping with virulence profiling (Fig. 1), it can be noted that two pairs of genotipically more similar strains, Hpu43/Hpu45 and PSUR28/VRSP32, showed almost identical virulence patterns: the former is highly virulent (values higher or equal to 8.3 for all six mean scores), whereas the latter has much lower virulence values (means of the three scores of 2.0 and 3.1, respectively). Several other patterns of convergence between virulence and genotyping profiling were observed for the pairs Hpu92/Hpu28 and Hpu10/Hu15. In other cases, however, virulence was clearly uncoupled from genetic similarity, with the most striking examples being the pairs Hpu28A/Hpu44, Hpu47/PA14, HPu5/Hpu105 and LESB58/Hpu106.

Intra-clonal virulence variation was investigated for eight distinct lineages, testing multiple strains for each lineage with the SM agar assay. The three lineages represented by LESB58, VRSP32 and Hpu75 showed a marked virulence consistency, with a maximum variation lower than 1 virulence score unit (ranges 8.3–9.0, 2.7–3.3 and 8.0–9.0, respectively). In the other cases with three clonal strains tested, one clone with reduced virulence was detected; specifically, these cases were Hpu40 with score 2.0 in the Hpu44 lineage (score 8.3), Hpu105 with a smaller score (5.7) than its clonal counterparts Hpu6 and Hpu9, and Hpu39 (score 3.0), which was much less virulent than Hpu35 (8.7) and Hpu45 (9.0). Markedly different virulence phenotypes also characterized the two tested lineages with two clonal variants, as Hpu33 (score 2.3) and Hpu106 (score 4.3) were less virulent than their clonal counterparts Hpu43 and Hpu101, respectively (both 8.7). These data indicate that even closely related strains can present marked differences in their virulence profiles. Although more clonal strains should be investigated to test this hypothesis, it seems that variation of the virulence phenotype is due to the loss of virulence in a fraction of strains belonging to a given clonal lineage.

The global correlation between virulence profiles and genotyping distance was not statistically significant, but this appeared to be mainly due to genotypically distant strains. Given that few or no informative genotypic characters are shared by the most distantly related strains, precise long-range branching relations cannot be reliably estimated. For these reasons, we compared short-range genotyping distance (Euclidean distance below 1.0) with virulence distance. Under these conditions, a clear correlation ($r=0.68$, P value 6.5×10^{-5}) between virulence profiles and genotyping distance was found. The observation that some pairs of strains presented quite different virulence patterns despite their genetic closeness can have multiple explanations. Firstly, divergent genotypes are not necessarily also divergent in the virulence phenotype, as multiple virulence determinants may have evolved independently or have been transmitted horizontally. Additionally, rep-PCR genotyping targets specific repeated regions in the core genome and does not take into consideration either the variability in the accessory genome or mutations in virulence genes from the core genomes that could affect the virulence phenotype. The marked ability of *P. aeruginosa* to acquire or discard genes and genomic segments is considered to be the main factor explaining its capacity to colonize and survive in different host environments. While most known virulence factors located in the core genome of *P. aeruginosa* show a high degree of conservation (Wolfgang *et al.*, 2003), this bacterium possesses a large accessory genome consisting of blocks of genes distributed in several dozen regions of genomic plasticity (Mathee *et al.*, 2008). As a consequence, one may hypothesize that the genotypically closely related strains analysed in the present study that showed very different virulence patterns likely either differ in the composition of their accessory genome, as a consequence of the acquisition or deletion of virulence determinants, or have accumulated mutations in virulence genes located in the core genome.

Correlation between virulence profiles and virulence gene expression

We observed that the expression of the *rhlR* gene strongly and significantly correlated with all three virulence assays (correlations of 0.60, 0.73 and 0.50 for SM agar, HL5 medium and *C. elegans* assays, respectively; P values of 4.1×10^{-3}, 5.3×10^{-6} and 4.8×10^{-3}), confirming that quorum sensing, and in particular the rhl system, plays an important role in *P. aeruginosa* virulence (Cosson *et al.*, 2002). Such a strong correlation indicates that as an alternative to virulence assays, *rhlR* gene expression experiments can provide a reliable estimation of the aggressiveness of individual strains of *P. aeruginosa.*

In contrast, only a weak and negative correlation between *crc* expression and virulence was observable (correlations of 0.39, 0.68 and 0.42 for SM agar, HL5 medium and *C. elegans* assays, respectively; all P values >0.01). Accordingly, no significant patterns of co-expression could be detected for the *rhlR* and *crc* genes. The *C. elegans* assay seems to capture a partially distinct virulence phenotype, as it is more strongly correlated with *rhlR* expression than *D. discoideum* assays and is completely uncoupled from *crc* expression. It has been reported that a *P. aeruginosa* strain lacking the Crc regulator shows defects in type III secretion, motility and expression of quorum sensing-regulated virulence factors, and is less virulent against *D. discoideum* (Linares *et al.*, 2010). Crc is a global metabolic regulator controlling different cellular pathways, and its deletion apparently globally weakens physiological performance. Our results indicate that *crc* expression is either not correlated or negatively correlated with virulence,

and therefore do not support the hypothesis of a direct role of Crc in the aggressiveness of *P. aeruginosa*.

While the relative prevalence of *exoU* and *exoS* genes encoding type III secretion effectors has been shown to be associated with infection type (chronic infections in CF patients versus blood infections) (Wareham & Curtis, 2007) or even with specific hospital departments (Bradbury *et al.*, 2010), we showed here that the presence of either *exoU* or *exoS* was not associated with specific virulence patterns, which is not surprising. While almost no strain encodes or secretes all four known type III secretion effectors, the commonly found combinations of ExoU/ExoT or ExoS/ExoT provide redundant and failsafe mechanisms to cause mucosal barrier injury, and inhibit many arms of the innate immune response (Engel & Balachandran, 2009). Although ExoU has been shown to have a slightly greater impact on virulence than ExoS in the mouse lung (Shaver & Hauser, 2004), it is generally accepted that the secretion of different combinations of type III effectors does not translate into a synergistically significant enhancement of disease severity (Shaver & Hauser, 2006).

In the present study, we have shown that the parallel application of virulence assays can be used to quantitatively assess this complex, multifactorial phenotypic trait. A wide range of virulence phenotypes was observed, from weakly to highly aggressive, indicating that clinical strains isolated from acute infections can present a reduced or altered virulence phenotype, as known for chronic *P. aeruginosa* infections in CF patients (Bragonzi *et al.*, 2009; Lelong *et al.*, 2011). However, the time required by the host to exert selection pressure for mutations and reduced expression in CF patients is not applicable to *P. aeruginosa* isolates from acute infections. The low virulence of some of the strains analysed here may be due instead to their intrinsic reduced aggressiveness. Alternatively, they may have been previously involved in chronic infections. Further studies of *P. aeruginosa* clinical populations at the genomic, transcriptomic and proteomic levels are needed to better understand the molecular determinants and mechanisms underlying the wide virulence range of *P. aeruginosa* in acute infections.

ACKNOWLEDGEMENTS

H. A. J. and this work were supported by a grant from the Autonomous Province of Trento 'PAT-postdoc'. We thank Paolo Lanzafame for kindly providing clinical isolates and access to the operative unit of Microbiology and Virology at Santa Chiara Hospital, Trento, Italy.

REFERENCES

Alibaud, L., Köhler, T., Coudray, A., Prigent-Combaret, C., Bergeret, E., Perrin, J., Benghezal, M., Reimmann, C., Gauthier, Y. & other authors (2008). *Pseudomonas aeruginosa* virulence genes identified in a *Dictyostelium* host model. *Cell Microbiol* **10**, 729–740.

Bonifait, L., Charette, S. J., Filion, G., Gottschalk, M. & Grenier, D. (2011). Amoeba host model for evaluation of *Streptococcus suis* virulence. *Appl Environ Microbiol* **77**, 6271–6273.

Bradbury, R. S., Roddam, L. F., Merritt, A., Reid, D. W. & Champion, A. C. (2010). Virulence gene distribution in clinical, nosocomial and environmental isolates of *Pseudomonas aeruginosa*. *J Med Microbiol* **59**, 881–890.

Bradbury, R. S., Reid, D. W., Inglis, T. J. & Champion, A. C. (2011). Decreased virulence of cystic fibrosis *Pseudomonas aeruginosa* in *Dictyostelium discoideum*. *Microbiol Immunol* **55**, 224–230.

Bragonzi, A., Paroni, M., Nonis, A., Cramer, N., Montanari, S., Rejman, J., Di Serio, C., Döring, G. & Tümmler, B. (2009). *Pseudomonas aeruginosa* microevolution during cystic fibrosis lung infection establishes clones with adapted virulence. *Am J Respir Crit Care Med* **180**, 138–145.

Cosson, P., Zulianello, L., Join-Lambert, O., Faurisson, F., Gebbie, L., Benghezal, M., Van Delden, C., Curty, L. K. & Köhler, T. (2002). *Pseudomonas aeruginosa* virulence analyzed in a *Dictyostelium discoideum* host system. *J Bacteriol* **184**, 3027–3033.

Engel, J. & Balachandran, P. (2009). Role of *Pseudomonas aeruginosa* type III effectors in disease. *Curr Opin Microbiol* **12**, 61–66.

Feltman, H., Schulert, G., Khan, S., Jain, M., Peterson, L. & Hauser, A. R. (2001). Prevalence of type III secretion genes in clinical and environmental isolates of *Pseudomonas aeruginosa*. *Microbiology* **147**, 2659–2669.

Froquet, R., Lelong, E., Marchetti, A. & Cosson, P. (2009). *Dictyostelium discoideum*: a model host to measure bacterial virulence. *Nat Protoc* **4**, 25–30.

Fumanelli, L., Iannelli, M., Janjua, H. A. & Jousson, O. (2011). Mathematical modeling of bacterial virulence and host–pathogen interactions in the *Dictyostelium*/*Pseudomonas* system. *J Theor Biol* **270**, 19–24.

Hasselbring, B. M., Patel, M. K. & Schell, M. A. (2011). *Dictyostelium discoideum* as a model system for identification of *Burkholderia pseudomallei* virulence factors. *Infect Immun* **79**, 2079–2088.

Hogardt, M. & Heesemann, J. (2010). Adaptation of *Pseudomonas aeruginosa* during persistence in the cystic fibrosis lung. *Int J Med Microbiol* **300**, 557–562.

Kesarwani, M., Hazan, R., He, J., Que, Y. A., Apidianakis, Y., Lesic, B., Xiao, G., Dekimpe, V., Milot, S. & other authors (2011). A quorum sensing regulated small volatile molecule reduces acute virulence and promotes chronic infection phenotypes. *PLoS Pathog* **7**, e1002192.

Lelong, E., Marchetti, A., Simon, M., Burns, J. L., van Delden, C., Köhler, T. & Cosson, P. (2011). Evolution of *Pseudomonas aeruginosa* virulence in infected patients revealed in a *Dictyostelium discoideum* host model. *Clin Microbiol Infect* **17**, 1415–1420.

Linares, J. F., Moreno, R., Fajardo, A., Martínez-Solano, L., Escalante, R., Rojo, F. & Martínez, J. L. (2010). The global regulator Crc modulates metabolism, susceptibility to antibiotics and virulence in *Pseudomonas aeruginosa*. *Environ Microbiol* **12**, 3196–3212.

Llanes, C., Hocquet, D., Vogne, C., Benali-Baitich, D., Neuwirth, C. & Plésiat, P. (2004). Clinical strains of *Pseudomonas aeruginosa* overproducing MexAB-OprM and MexXY efflux pumps simultaneously. *Antimicrob Agents Chemother* **48**, 1797–1802.

Mathee, K., Narasimhan, G., Valdes, C., Qiu, X., Matewish, J. M., Koehrsen, M., Rokas, A., Yandava, C. N., Engels, R. & other authors (2008). Dynamics of *Pseudomonas aeruginosa* genome evolution. *Proc Natl Acad Sci U S A* **105**, 3100–3105.

Miyata, S. T., Kitaoka, M., Brooks, T. M., McAuley, S. B. & Pukatzki, S. (2011). *Vibrio cholerae* requires the type VI secretion system virulence factor VasX to kill *Dictyostelium discoideum*. *Infect Immun* **79**, 2941–2949.

Naughton, S., Parker, D., Seemann, T., Thomas, T., Turnbull, L., Rose, B., Bye, P., Cordwell, S., Whitchurch, C. & Manos, J. (2011). *Pseudomonas aeruginosa* AES-1 exhibits increased virulence gene expression during chronic infection of cystic fibrosis lung. *PLoS ONE* **6**, e24526.

Pan, Y. J., Lin, T. L., Hsu, C. R. & Wang, J. T. (2011). Use of a *Dictyostelium* model for isolation of genetic loci associated with phagocytosis and virulence in *Klebsiella pneumoniae*. *Infect Immun* **79**, 997–1006.

Pukatzki, S., Kessin, R. H. & Mekalanos, J. J. (2002). The human pathogen *Pseudomonas aeruginosa* utilizes conserved virulence pathways to infect the social amoeba *Dictyostelium discoideum*. *Proc Natl Acad Sci U S A* **99**, 3159–3164.

Rozen, S. & Skaletsky, H. J. (2000). Primer3 on the WWW for general users and for biologist programmers. In *Bioinformatics Methods and Protocols: Methods in Molecular Biology*, pp. 365–386. Edited by S. Krawetz & S. Misener. Totowa, NJ: Humana Press.

Savli, H., Karadenizli, A., Kolayli, F., Gundes, S., Ozbek, U. & Vahaboglu, H. (2003). Expression stability of six housekeeping genes: a proposal for resistance gene quantification studies of *Pseudomonas aeruginosa* by real-time quantitative RT-PCR. *J Med Microbiol* **52**, 403–408.

Segata, N., Izard, J., Waldron, L., Gevers, D., Miropolsky, L., Garrett, W. S. & Huttenhower, C. (2011). Metagenomic biomarker discovery and explanation. *Genome Biol* **12**, R60.

Shaver, C. M. & Hauser, A. R. (2004). Relative contributions of *Pseudomonas aeruginosa* ExoU, ExoS, and ExoT to virulence in the lung. *Infect Immun* **72**, 6969–6977.

Shaver, C. M. & Hauser, A. R. (2006). Interactions between effector proteins of the *Pseudomonas aeruginosa* type III secretion system do not significantly affect several measures of disease severity in mammals. *Microbiology* **152**, 143–152.

Shevchuk, O. & Steinert, M. (2009). Screening of virulence traits in *Legionella pneumophila* and analysis of the host susceptibility to infection by using the *Dictyostelium* host model system. *Methods Mol Biol* **470**, 47–56.

Sillo, A., Matthias, J., Konertz, R., Bozzaro, S. & Eichinger, L. (2011). *Salmonella typhimurium* is pathogenic for *Dictyostelium* cells and subverts the starvation response. *Cell Microbiol* **13**, 1793–1811.

Stewart, R. M., Wiehlmann, L., Ashelford, K. E., Preston, S. J., Frimmersdorf, E., Campbell, B. J., Neal, T. J., Hall, N., Tuft, S. & other authors (2011). Genetic characterization indicates that a specific subpopulation of *Pseudomonas aeruginosa* is associated with keratitis infections. *J Clin Microbiol* **49**, 993–1003.

Syrmis, M. W., O'Carroll, M. R., Sloots, T. P., Coulter, C., Wainwright, C. E., Bell, S. C. & Nissen, M. D. (2004). Rapid genotyping of *Pseudomonas aeruginosa* isolates harboured by adult and paediatric patients with cystic fibrosis using repetitive-element-based PCR assays. *J Med Microbiol* **53**, 1089–1096.

Tan, M. W., Rahme, L. G., Sternberg, J. A., Tompkins, R. G. & Ausubel, F. M. (1999). *Pseudomonas aeruginosa* killing of *Caenorhabditis elegans* used to identify *P. aeruginosa* virulence factors. *Proc Natl Acad Sci U S A* **96**, 2408–2413.

Valderrey, A. D., Pozuelo, M. J., Jiménez, P. A., Maciá, M. D., Oliver, A. & Rotger, R. (2010). Chronic colonization by *Pseudomonas aeruginosa* of patients with obstructive lung diseases: cystic fibrosis, bronchiectasis, and chronic obstructive pulmonary disease. *Diagn Microbiol Infect Dis* **68**, 20–27.

Van de Peer, Y. & De Wachter, R. (1994). TREECON for Windows: a software package for the construction and drawing of evolutionary trees for the Microsoft Windows environment. *Comput Appl Biosci* **10**, 569–570.

Wareham, D. W. & Curtis, M. A. (2007). A genotypic and phenotypic comparison of type III secretion profiles of *Pseudomonas aeruginosa* cystic fibrosis and bacteremia isolates. *Int J Med Microbiol* **297**, 227–234.

Wolfgang, M. C., Kulasekara, B. R., Liang, X., Boyd, D., Wu, K., Yang, Q., Miyada, C. G. & Lory, S. (2003). Conservation of genome content and virulence determinants among clinical and environmental isolates of *Pseudomonas aeruginosa*. *Proc Natl Acad Sci U S A* **100**, 8484–8489.

Edited by: H. Hilbi

9.5 Publication D:

Foladori, P., **Tamburini, S**., Bruni, L. (2010) Bacterial permeabilisation and disruption caused by sludge reduction technologies evaluated by flow cytometry. *Water Research* 44 (17), 4888-99

WATER RESEARCH 44 (2010) 4888–4899

Available at www.sciencedirect.com

ScienceDirect

journal homepage: www.elsevier.com/locate/watres

Bacteria permeabilisation and disruption caused by sludge reduction technologies evaluated by flow cytometry

P. Foladori [a,*], S. Tamburini [a], L. Bruni [b]

[a] Department of Civil and Environmental Engineering, University of Trento, via Mesiano, 77, 38050 Trento, Italy

[b] Laura Bruni, Chemical and Biological Laboratories, ADEP, Agenzia per la depurazione (Wastewater Treatment Agency), Autonomous Province of Trento, via Lung'Adige Braille, Trento, Italy

ARTICLE INFO

Article history:
Received 2 April 2010
Received in revised form
1 July 2010
Accepted 9 July 2010
Available online 16 July 2010

Keywords:
Activated sludge
Sludge reduction
Ozonation
Sonication
Thermal treatment
High pressure homogenisation
Flow cytometry
Bacterial integrity
Bacterial permeabilisation

ABSTRACT

Technologies proposed in the last decades for the reduction of the sludge production in wastewater treatment plants and based on the mechanism of cell lysis-cryptic growth (physical, mechanical, thermal, chemical, oxidative treatments) have been widely investigated at lab-, pilot- and, in some cases, at full-scale but the effects on cellular lysis have not always been demonstrated in depth. The research presented in this paper aims to investigate how these sludge reduction technologies affect the integrity and permeabilisation of bacterial cells in sludge using flow cytometry (FCM), which permits the rapid and statistically accurate quantification of intact, permeabilised or disrupted bacteria in the sludge using a double fluorescent DNA-staining instead of using conventional methods like plate counts and microscope.

Physical/mechanical treatments (ultrasonication and high pressure homogenisation) caused moderate effects on cell integrity and caused significant cell disruption only at high specific energy levels. Conversely, thermal treatment caused significant damage of bacterial membranes even at moderate temperatures (45–55 °C). Ozonation significantly affected cell integrity, even at low ozone dosages, below 10 $mgO_3/gTSS$, causing an increase of permeabilised and disrupted cells. At higher ozone dosages the compounds solubilised after cell lysis act as scavengers in the competition between soluble compounds and (particulate) bacterial cells. An original aspect of this paper, not yet reported in the literature, is the comparison of the effects of these sludge reduction technologies on bacterial cell integrity and permeabilisation by converting pressure, temperature and ozone dosage to an equivalent value of specific energy. Among these technologies, comparison of the applied specific energy demonstrates that achieving the complete disruption of bacterial cells is not always economically advantageous because excessive energy levels may be required.

1. Introduction

In the future, excess sludge quantities produced in wastewater treatment plants (WWTPs) can be expected to increase and further restrictions on disposal options will probably increase the cost of disposal, which is currently in the range of 200–650 €/t of dry weight. Since the mid '90s, various technologies have been developed and proposed on the market for the reduction of sludge production (expressed as dry mass and not only in volume) directly on-site, very diverse and based on

* Corresponding author.
E-mail addresses: paola.foladori@ing.unitn.it (P. Foladori), laura.bruni@provincia.tn.it (L. Bruni).
0043-1354/$ – see front matter © 2010 Elsevier Ltd. All rights reserved.
doi:10.1016/j.watres.2010.07.030

physical, mechanical, chemical, thermal or biological treatments (*inter alia* Foladori et al., 2010).

Most sludge reduction (SR) technologies are aimed at solids solubilisation, the disintegration of the biological floc structure and the disruption of bacterial cells. In this way the cells undergo lysis and the intracellular compounds are released and further degraded in biological reactors, through the mechanisms of cell lysis-cryptic growth (*inter alia* Gaudy et al., 1971).

To investigate the efficiency of an SR technology to damage or lysate bacterial cells, conventional cultivation methods using selective media have been widely used, but it is well known that the culture-dependent analysis of microbial populations in activated sludge produces partial and heavily biased results (Wagner et al., 1993), because only a small proportion (about 5%) are able to grow in nutrient media. In fact, most bacteria in activated sludge are in a physiological state known as "*viable-but-not-culturable*" (Nebe-von-Caron et al., 2000). Microscopic observations of biological flocs have also been carried out frequently to investigate the efficiency of SR technologies with the aim of evaluating the disaggregation or dispersion of flocs, as frequently shown in photos in the literature, rather than observing single cells embedded in the highly aggregated structure of activated sludge, which interferes with the microscopic images.

Often, the fact that SR technologies cause bacteria damage and lysis is assumed as an obvious statement or a reliable expected result, which is not always fully confirmed by experimental results. Only a few, recent contributions have investigated in depth the effect of SR technologies on bacteria integrity, activity, permeabilisation or death (Prorot et al., 2008; Yan et al., 2009) by using direct advanced approaches, which allow us to obtain a more realistic view of bacteria populations in activated sludge and the assessment of their physiological status.

The research presented in this paper aims to investigate how some SR technologies, exploiting the mechanism of cell lysis-cryptic growth, affect integrity and permeabilisation of bacterial cells in sludge using flow cytometry (FCM), which allows us to quantify bacteria using fluorescent DNA-staining. The advantages of FCM for the rapid quantification of intact or permeabilised cells in bacterial population in various environments have been highlighted many times in the environmental field (*inter alia* Porter et al., 1997; Steen, 2000; Vives-Rego et al., 2000). FCM, capable of counting more than 1000 cells per second, is a powerful multi-parametric and single-cell analysis, which is faster and able to give a more precise quantification of free cells in a suspension compared to conventional observation of bacteria suspensions under the microscope.

Four SR technologies which cause cell lysis-cryptic growth, of certain growing interest were selected (Fig. 1) and applied at lab-scale: (1) physical treatment: ultrasonication at specific energy up to 53,000 kJ $kgTSS^{-1}$, (2) mechanical treatment: high pressure homogenisation, at pressure up to 1500 bar, (3) oxidation treatment: ozonation at low ozone dosages up to 0.028 gO_3 $gTSS^{-1}$, (4) thermal treatment at moderate temperatures up to 90 °C. As a consequence of these SR treatments a reduction of intact cells is expected, as is an increase in permeabilised cells or a net loss when disrupted. Biological processes based on a side-stream anaerobic reactor such as the Oxic-Settling-Anaerobic (OSA) process or the Cannibal® process were not investigated in this paper. Various, intriguing explanations have been given in the literature to describe the basic mechanism of these last processes: uncoupled metabolism, cell lysis-cryptic growth, release of organic matter associated with iron (Saby et al., 2003; Chen et al., 2003; Novak et al., 2007; Sun et al., 2010), but some uncertainties remain.

An original aspect of this paper is the comparison of the effects of the SR technologies on bacterial cell integrity and permeabilisation using the effective applied energy level, to help to answer the following question, which has not yet been fully investigated: "What is the energy level required to destroy the bacterial cell structure, release intracellular compounds and favour cell lysis-cryptic growth in biological processes such as activated sludge?" This paper contributes in this direction, demonstrating that not all the SR technologies are able to disrupt bacteria at operational conditions which favour energy savings and sustainable application, but the damage to bacterial cells often requires an energy level which may exceed economical feasibility.

2. Materials and methods

2.1. Activated sludge

Activated sludge samples were collected from the municipal wastewater treatment plant (WWTP) of Trento Nord (Italy), characterised by an oxidation-nitrification configuration, with a sludge age of about 12 d and an average organic load of 0.15 $kgBOD_5$ $kgTSS^{-1}$ d^{-1}. Grab samples of sludge used in the experimental tests were taken from the oxidation tank with a typical Total Suspended Solid (TSS) concentration around 4 kgTSS m^{-3}.

Soluble COD (SCOD) and TSS concentrations in sludge were measured according to Standard Methods (APHA, 1998).

2.2. Sludge reduction (SR) technologies

2.2.1. Ultrasonication

Ultrasonication was applied to 100-mL activated sludge by using a Branson 250 Digital Ultrasonifier operating at 20 kHz with a horn tip. The main parameters considered in ultrasonication were: (1) transferred power, P, expressed in W; (2) time, t, expressed in seconds; (3) treated volume, V; (4) and TSS concentration in sludge, expressed in gTSS L^{-1}. These parameters were used to calculate the specific energy (E_s) as reference parameter and expressed in kJ $kgTSS^{-1}$ ($E_s = P\ t\ V^{-1}\ TSS^{-1}$). The use of the transferred power instead of applied power is preferable for E_s calculation, to obtain results comparable with results from different instruments. Calorimetry was used to measure the transferred power input (Mason et al., 1992). In this research E_s up to 53,000 kJ $kgTSS^{-1}$ was used.

2.2.2. High pressure homogenisation

The high pressure homogeniser (HPH) at lab-scale consisted of a high pressure pump which compressed sludge up to

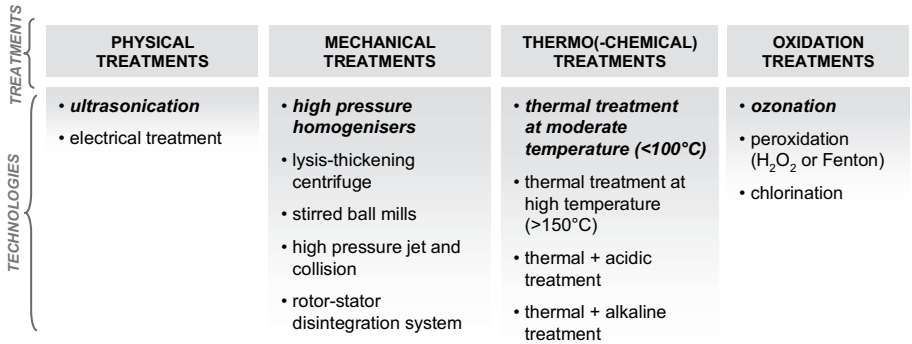

Fig. 1 – Sludge reduction technologies exploiting the mechanism of cell lysis-cryptic growth. SR technologies indicated in bold and italic were considered in this paper.

pressures of 1500 bar and an adjustable homogenisation valve where sludge decompression to atmospheric pressure took place. The main parameters in HPH are: (1) applied pressure, P, expressed in bar and (2) the number of passages through the homogenisation valve, considered as 1 in this research. For the calculation of the specific energy, E_s, a linear relationship between E_s and the applied pressure was considered (Engelhart et al., 2000). E_s was calculated considering a conversion factor of 23.8 kJ/L to increase the pressure by 100 bar (own data), multiplied by the pressure up to the desired value and divided by the TSS concentration of sludge.

2.2.3. *Thermal treatment*

The temperature range of 20–90 °C was investigated with a contact time of 30 min at the fixed temperature, while about 15–20 min were required to heat the sludge and reach the desired temperature. The heating energy expressed as E_s was calculated considering the specific heat capacity of water (4.18 kJ kg^{-1} °C^{-1}), divided by the TSS concentration of sludge and multiplied by the increase of temperature from 20 °C (environmental temperature) to the desired final temperature. The heat losses in the contact reactor during the treatment were not taken into account, due to the short contact time.

2.2.4. *Ozonation*

Ozone was generated by a generator fed with filtered and dehumidified air. The ozone gas was injected into a column (diameter 7 cm; height 2 m) using a loop equipped with a booster pump and an injector. The ozone dosage was up to 0.028 gO_3 $gTSS^{-1}_{treated}$. To calculate an equivalent amount of energy (E_s), a conversion factor of 20 kWh (corresponding to 72,000 kJ) for the production of 1 kg of ozone was assumed (Böhler and Siegrist, 2007; Goel et al., 2003).

2.3. *Bacterial cell fluorescent staining + FCM*

To distinguish intact and permeabilised bacteria, cells were stained with SYBR-Green I (SYBR-I, 1:30 dilution of commercial stock; from Invitrogen, USA; $\lambda_{ex} = 495$ nm, $\lambda_{em} = 525$ nm) diluted in dimethyl sulfoxide (DMSO, Merck, Germany) and Propidium Iodide (PI, stock solution concentration 1 mg mL^{-1}; Invitrogen, USA; $\lambda_{ex} = 536$ nm, $\lambda_{em} = 617$ nm). An amount of 10 μL of both fluorochromes was added to 1 mL of bacterial suspension containing about 10^6–10^7 cells/mL. Samples were incubated in the dark for 15 min at room temperature. SYBR-I is capable of staining all cells, whereas the polarity of PI allows it to penetrate only cells with permeabilised membranes, which can be considered as dead (Ziglio et al., 2002). In the permeabilised cells, the simultaneous staining with SYBR-I and PI activates energy transfer between the fluorochromes. As a consequence, intact bacteria emit green fluorescence, while permeabilised bacteria emit red fluorescence.

FCM analyses were performed with an Apogee-A40 flow cytometer (Apogee Flow Systems, UK) equipped with an Ar laser (488 nm). Collected signals were green and red fluorescence, acquired with logarithmic gain and Forward Angle Light Scatter (FALS), which is related to cell size (Foladori et al., 2008). Data acquisition gates were set on green and red fluorescence distribution to eliminate non-bacterial particles and debris. At least 10,000 cells were analysed for each sample in a few minutes, providing good statistical data. The accuracy of the staining method and the FCM analysis was previously evaluated with epifluorescence microscopy (Ziglio et al., 2002).

2.4. *Outline of the procedure for testing SR technologies*

Fig. 2 shows the whole procedure for the quantification of intact and permeabilised cells in activated sludge by FCM after the application of each of the four SR technologies. Without any previous pre-treatment, activated sludge underwent ultrasonication, HPH, thermal treatment or ozonation with variations in the operational parameters. After each treatment, 2 quantities of activated sludge were collected and underwent 2 different procedures (Fig. 2):

1) Quantification of free cells: these include the cells free in the suspension as single cells and not aggregated in flocs;
2) Quantification of total cells: these include cells both free in the suspension and aggregated in flocs. To quantify total cells, activated sludge underwent a disaggregation step performed by sonication (US) at volumetric specific energy of 80 kJ/L. This disaggregation step was previously defined as optimal, since it provides a very extensive, although incomplete, disaggregation of flocs and the release of the maximum possible number of free cells in the suspension, while avoiding cell damage or death (Foladori et al., 2007).

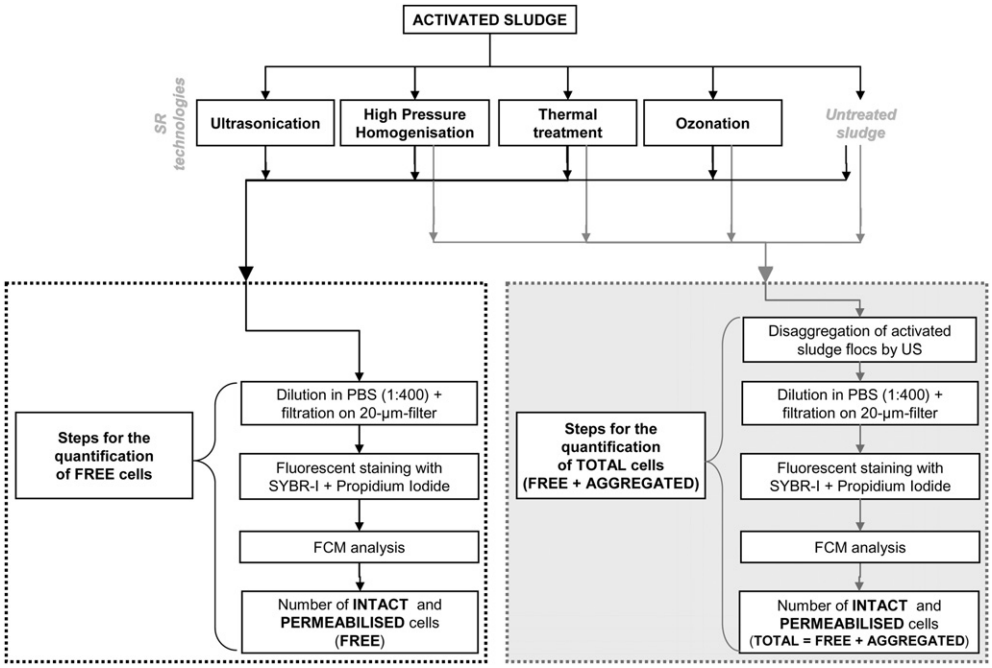

Fig. 2 – Outline of the procedure based on FCM for the quantification of free and total cells, distinguished as intact and permeabilised cells, after the application of the 4 SR technologies.

In fact, since FCM analysis is a single-cell analysis, activated sludge flocs must be previously disaggregated and dispersed to obtain free cell suspensions while maintaining bacterial integrity.

Then the cell suspensions were diluted with Phosphate-Buffered-Saline (PBS, 3 g K_2HPO_4, 1 g KH_2PO_4 and 8.5 g NaCl per Litre; pH = 7.2) to reach 10^6–10^7 cells/mL (optimal for FCM analysis) and filtered on 20-µm membranes (Celltrics, Partec) in order to eliminate coarse particles which may clog the nozzle of the flow cytometer. The coarse particles excluded from the FCM analysis were:

1) Most flocs during the quantification of free cells (aggregated cells are excluded);
2) Less than 3% of the initial flocs total (as estimated under epifluorescence microscope) during the quantification of total cells (aggregated cells are included).

The cells suspension obtained was lastly stained with fluorescent dyes SYBR-I + PI and underwent FCM analysis.

3. Results and discussion

3.1. COD solubilisation of sludge

SR technologies based on physical, mechanical, thermal or oxidation are expected to generate soluble organic matter by the disintegration of sludge solids and/or the oxidation of organic polymers. Production of soluble COD in the application of an SR technology is in fact generally correlated with TSS disintegration.

COD solubilisation (S_{COD}) is usually calculated with the following expression, as a percentage (*inter alia* Bougrier et al., 2005; Cui and Jahng, 2006; Benabdallah El-Hadj et al., 2007; Yan et al., 2009):

$$\text{COD solubilisation} = S_{COD}(\%) = \frac{SCOD_t - SCOD_0}{COD_0 - SCOD_0} \times 100$$

where: $SCOD_0$ = concentration of soluble COD in the untreated sludge; $SCOD_t$ = concentration of soluble COD in the sludge after the application of the SR technology; COD_0 = concentration of total COD in the untreated sludge. S_{COD} is the immediate result of the application of an SR treatment and depends strongly on the specific energy applied per mass of solids treated (E_s) as compared in Fig. 3. Data indicated in Fig. 3 allows an immediate comparison between the SR technologies. S_{COD} rose for increasing values of E_s in a linear way for thermal treatment and ozonation, while data from physical/mechanical treatments (ultrasonication, HPH) fit better with a sigmoid function, due to the need for a minimal energy input to initiate solubilisation and slower solubilisation at the highest energy level. S_{COD} refers to the release of soluble COD after the application of an SR technology, excluding the contribution of COD mineralisation and biodegradation in the subsequent biological stages.

From a theoretical point of view, S_{COD} is the result of the action of an SR technology against both non-biotic organic matter, and the disruption of bacterial cells. S_{COD} gives us no information about the damage or disruption of bacterial cells, although the sludge solubilisation is often approximately used to identify the occurrence of bacteria lysis. From the

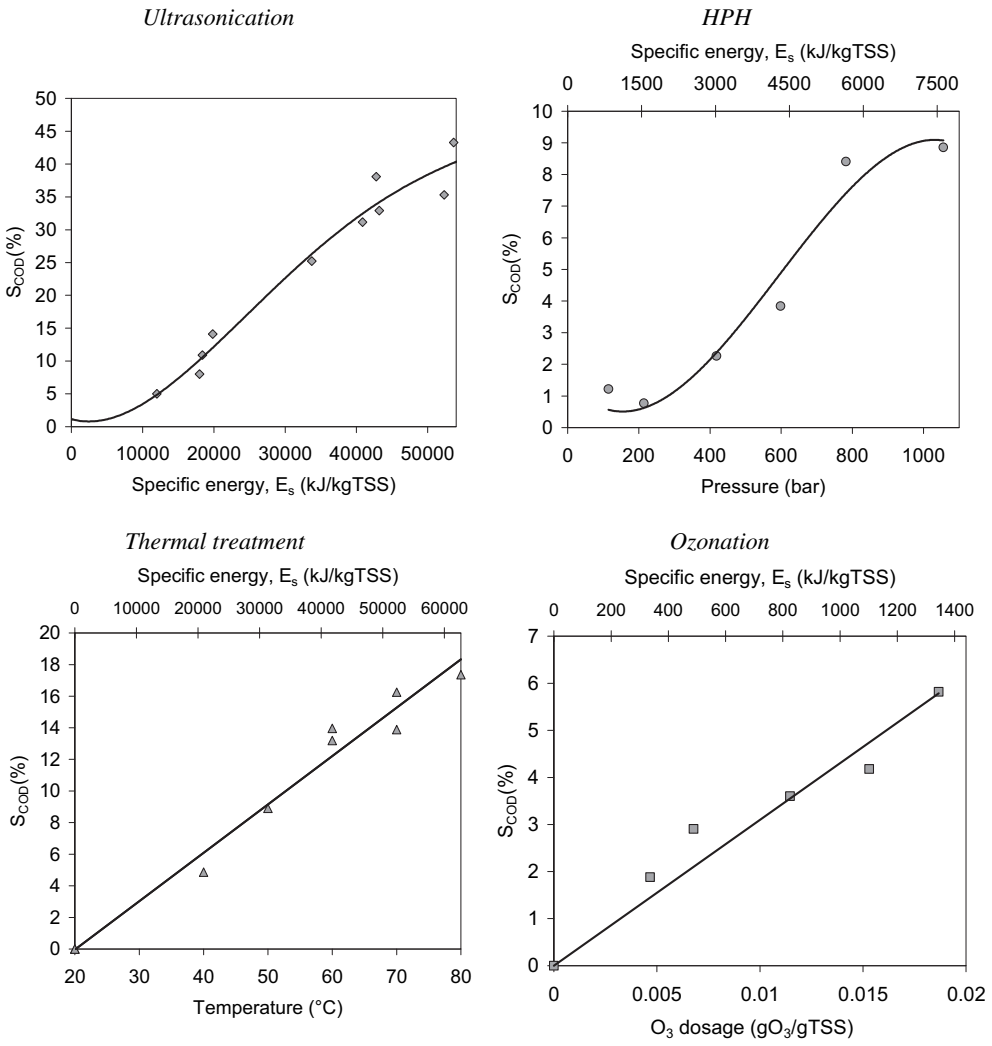

Fig. 3 – Profiles of COD solubilisation during the application of SR technologies as a function of operational conditions and for increasing E_s levels.

comparison in Fig. 3, very different solubilisation levels were obtained depending on the type of SR technology applied. But, what about the lysis of cells? Are there different results among the SR technologies, as per S_{COD}?

3.2. *Quantification of intact, permeabilised and disrupted bacteria by FCM*

Intact and permeabilised cells were identified simultaneously on the basis of their membrane integrity by applying the double fluorescent staining PI (a dye which can enter only damaged or permeabilised cells) and SYBR-I (which can enter all cells, intact or permeabilised) (Ziglio et al., 2002; Foladori et al., 2007). Membrane integrity demonstrates the protection of constituents in intact cells and the potential capability of metabolic activity/repair and potential reproductive growth. Cells without an intact membrane are considered permeabilised and can be classified as dead cells. As their structures are freely exposed to the environment they will eventually decompose (Nebe-von-Caron et al., 2000).

The use of the two dyes (SYBR-I + PI) and the setting of two thresholds on red and green fluorescences generate four regions in the FCM cytograms as shown in the example in Fig. 4. Depending on the intensity of the green and red fluorescences emitted, the following regions are distinguished: permeabilised cells (red), intact cells (green), small aggregates (both red and green) and instrument background or noise (red and green below thresholds). Activated sludge contains some small aggregates, formed by clusters of intact and permeabilised cells clumped together, appearing fluorescent both in red and green. In spite of the optimization of disaggregation, a moderate presence of small aggregates may remain.

Some significant FCM cytograms obtained for the most relevant operating conditions when applying the 4 SR technologies are summarised in Fig. 5 which shows an immediate comparison of the effects of the SR technologies on the total cells (free + aggregated), distinguished as intact and permeabilised cells. For a better comparison of effects, operating conditions such as pressure, temperature and ozone dosage were converted to an equivalent value of E_s.

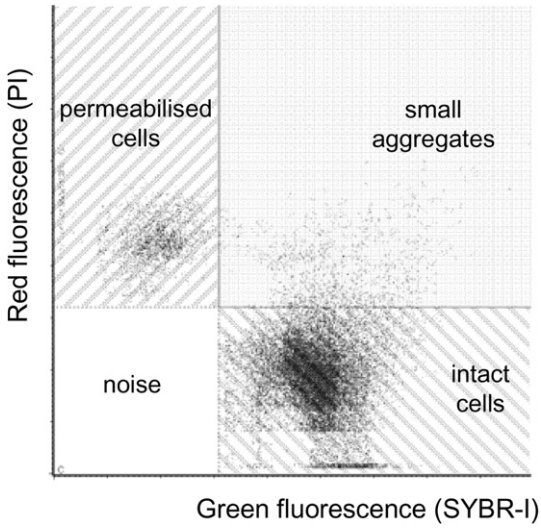

Fig. 4 – Example of an FCM cytogram of activated sludge with the indication of the four regions to distinguish intact cells and permeabilised cells.

Physical/mechanical treatments (ultrasonication and HPH) did not cause a significant shift from the region of intact cells to permeabilised ones, while thermal treatment differed significantly due to the significant damage to bacteria causing cell permeabilisation. The effects of ozonation are intermediate and a moderate increase of permeabilised cells was observed.

In the untreated sludge + disaggregation (first column in Fig. 5), the mean concentration of intact cells was 3.8 ± 0.16E + 12 cells/L (75.6 ± 4.3% of total cells), while the mean concentration of permeabilised cells was 1.01 ± 0.15E + 12 cells/L (20 ± 3.4% of total cells); small aggregates were 0.46 ± 0.06E+12 per Litre. Total cells in the untreated sludge + disaggregation (indicated as N_0) were considered as the sum of intact cells, permeabilised cells and small aggregates, which are considered to be approximately composed of two cells. After an SR treatment, damage to the membrane structure of bacteria may occur, leading to a progressive loss of membrane integrity, permeabilisation or cell disruption. With regard to disrupted cells, their concentration was calculated as the difference N_0–N_t, where N_t was the concentration of total cells after the application of an SR technology.

The variations of the concentrations of total, intact, permeabilised and disrupted cells in the sludge after the application of ultrasonication, HPH, ozonation and thermal treatment are discussed and compared in the following sections.

3.3. *Ultrasonication*

Ultrasonication is a "no touch and no moving mechanical parts" technique (Winter, 2002), based on ultrasonic cavitation. In Fig. 6 the percentages of intact, permeabilised and disrupted cells (calculated referring to N_0) are indicated for increasing E_s levels. Fitting curves in Fig. 6 are only indicated for easier observation of the data.

The application of E_s up to 30,000 kJ $kgTSS^{-1}$ produced a further disaggregation of small aggregates and an increase in the number of intact and permeabilised cells, without an appreciable loss of membrane integrity or increase in cell disruption. The ratio between permeabilised and intact cells was around 0.18, indicating that the increase of permeabilised cells is not caused by progressive cell damage, but is mainly due to the disaggregation of small clusters in which permeabilised cells are embedded. Thus the simple permeabilisation of intact cells is negligible.

Disruption of cells started only for E_s above 30,000 kJ/kgTSS, but the amount of destroyed bacteria remained moderate (−22.5% of intact cells and −6.5% of permeabilised cells at 53,000 kJ $kgTSS^{-1}$) and intact and permeabilised cells were destroyed with a similar trend.

The slight cell disruption during ultrasonication does not agree with the high COD solubilisation shown in Fig. 3. Similar findings by Salsabil et al. (2009) using FCM analysis indicated that organic matter solubilisation after ultrasonication was not due to cell membrane breakage but more probably to floc disintegration and especially to EPS destructuration promoting the solubilisation of extracellular proteins and polysaccharides and increasing soluble COD.

3.4. *High pressure homogenisation*

Passing through the homogenisation valve the sludge speed increases by up to fifty times (up to 300 m/s), due to the intense restriction, causing a rapid drop of pressure to below vapour pressure (cavitation). These conditions favour disaggregation of flocs and the damage of cells (Fig. 7) which depend on the applied pressure and the E_s level:

1) moderate pressures below 400 bar caused modification and physical destruction of the network of sludge, increasing the number of free cells in the bulk liquid as well appreciable in Fig. 7B, in which the very significant increase in the number of free intact cell and free permeabilised cells can be observed. These pressures did not induce a loss of cell integrity or significant cell damage or permeabilisation (Fig. 7A);
2) pressures in the range 400–1500 bar caused high shear stress, significant damage to cellular structures, leading to the immediate disruption of a portion of total cells: at 1500 bar intact cells decreased by −40.7% of N_0 and permeabilised cells decreased by −9.7% of N_0 (Fig. 7A). Consequently the number of disrupted cells increased linearly, up to 52% of N_0 at 1500 bar (Fig. 7A). The ratio between permeabilised and intact cells (free + aggregated) was around 0.18 and remained approximately constant for increasing E_s values, indicating that the mechanical action (shear forces) affects intact or permeabilised cells similarly, independent of their functional status.

Similar findings have already been reported and confirmed by other authors (Camacho et al., 2002; Strünkmann et al., 2006), who observed that the supplied energy is initially used to disrupt non-covalent forces between cells (embedded

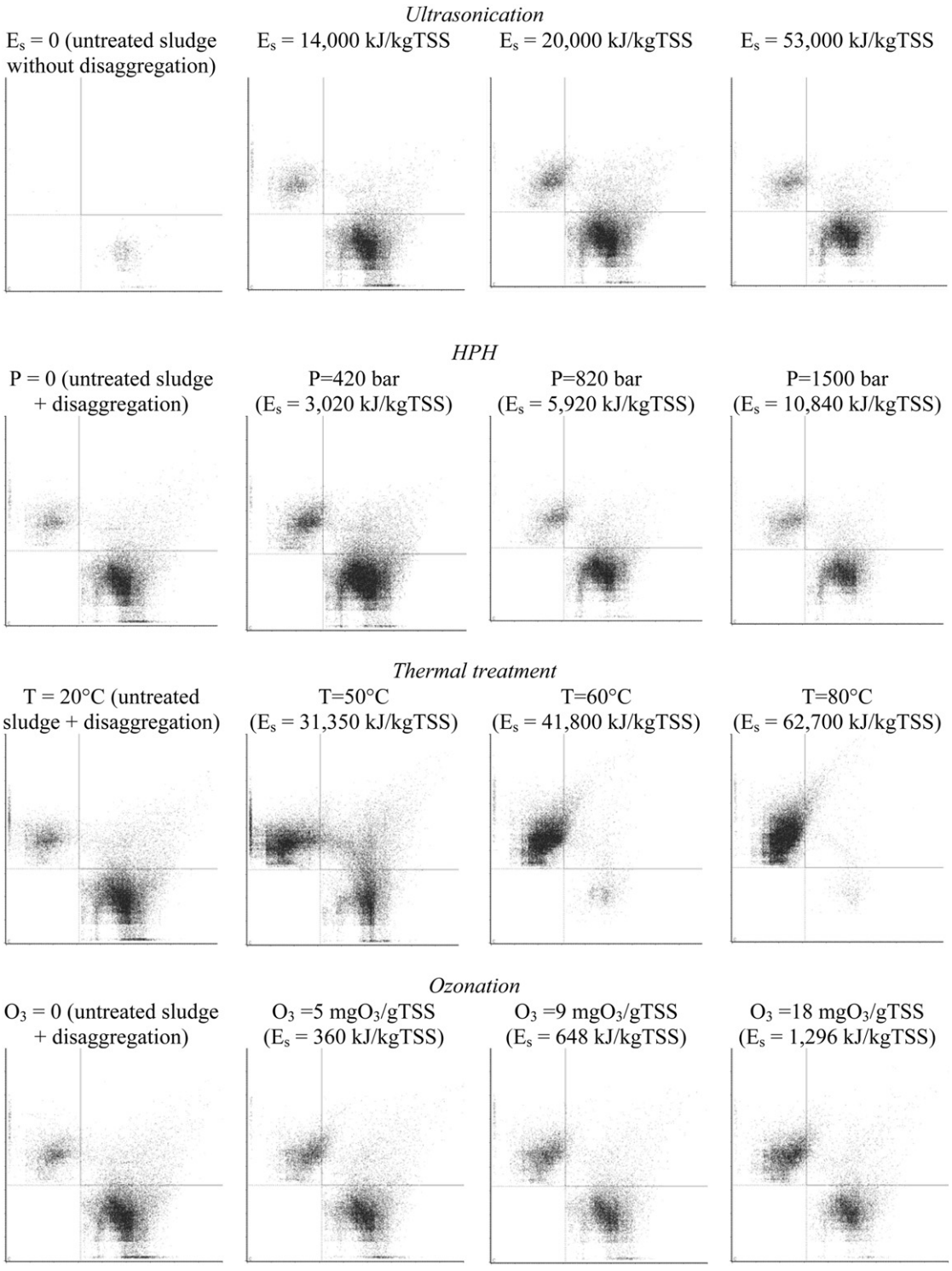

Fig. 5 – FCM cytograms of total cells (free + aggregated), distinguished in intact and permeabilised cells, after the application of the 4 SR technologies. Regions of the cytograms are indicated above in Fig. 4.

in flocs), and then to disrupt the cell walls (covalent and non-covalent bonds). However, in practice and in full-scale applications, excessively high pressures are uneconomic. Furthermore, we should consider that some bacteria populations are able to resist high pressures, even up to 1000 bar (Pagán and Mackey, 2000; Hayakawa et al., 1998).

3.5. *Thermal treatment*

Thermal treatment affected bacterial integrity especially after the application of temperatures in the range 45–60 °C for 30 min, which led immediately to a decrease in intact cells (free + aggregated, see Fig. 8A) from 77.9% of N_0 at 45 °C to

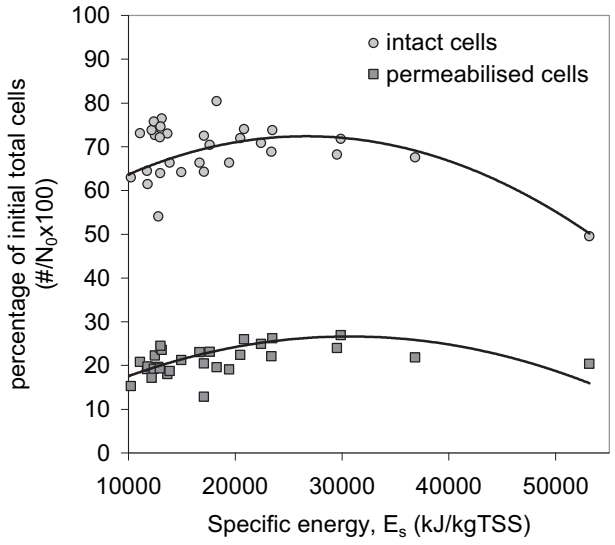

Fig. 6 – Percentages of intact and permeabilised cells calculated referring to N_0 during ultrasonication.

17.4% of N_0 at 60 °C and a consequent increase in permeabilised cells. The same behaviour was observed for free cells heated to 45–60 °C, applying the thermal treatment as an independent treatment without the disaggregation step (Fig. 8B). As shown in Fig. 8B, thermal treatment over 45 °C caused a decrease of the small number of free intact cells and a rapid and significant increase in free permeabilised cells. The reason is because thermal treatment causes cell permeabilisation and affects sludge properties, with the release of EPS and a partial deflocculation. The result is the release of permeabilised cells from the flocs to the bulk liquid, which are detected as free permeabilised cells by FCM.

These results are in agreement with other recent findings in the literature; it was demonstrated that after 1 h of thermal treatment at 60 °C nearly 98% of the mesophilic and psychrophilic microorganisms in sludge die and the proteins of the bacterial membrane undergo the defolding of their structure causing cell permeabilisation, leaving 2% of thermophilic microorganisms, which are able to secret proteases and grow (Yan et al., 2008).

An increase in the number of total cells (free + aggregated) was observed after heating in the range 45–55 °C compared to the value N_0 (Fig. 8A). In fact, the concentration of total cells increased from $N_0 = 4.9E + 12$ cells/L in the untreated sludge to $7.04E + 12$ cells/L (140% of N_0) after the application of 55 °C. It is not clear why the number of total cells increased when the temperature was raised. We hypothesized that the thermal treatment caused a denaturation of cell membranes with a consequent loss of bacterial integrity and the rupture of some cells in a few fragments of sizes which can be detected by FCM as single fluorescent particles. The reduction of particle size after thermal treatment was demonstrated using the Forward Angle Light Scatter (FALS) signal acquired by FCM (data not shown) using an innovative method to convert the FALS signal into particle sizes (Foladori et al., 2008).

The thermal treatment at temperatures over 45 °C and up to 90 °C for 30 min did not cause the complete disruption of cells and thus the profile of disrupted cells is not indicated in Fig. 8A. The thermal treatment causes bacteria permeabilisation but not complete disruption of the cells and further enzymatic hydrolysis of the permeabilised cells would be needed during real sludge digestion to obtain effective solubilisation. Appels et al. (2010) confirmed that a temperature of 70 °C seems to be too low for effective solubilisation.

It is well known that the enzymatic hydrolysis of solids may be the rate-limiting step in the digestion process. In practice, the sludge reduction expected during thermophilic digestion (which reaches 40–45% of VSS or 30% of TS), is similar to mesophilic digestion, but by changing from mesophilic to thermophilic digestion, the retention time can be reduced from 20 to 30 d to 10–12 d (Nielsen and Petersen, 2000) due to the acceleration of cell lysis and biochemical reactions by heat stable exoenzymes and the physical/chemical effect of the heat shock when the sludge enters a warm environment at 50–60 °C.

3.6. *Ozonation*

The ozone dosages used in the various studies in the literature cover a very wide range, from less than 0.01 gO_3 $gTSS^{-1}$ to much high dosages of 1 gO_3 $gTSS^{-1}$. Nowadays, the recommended ozone dosage in full-scale applications does not exceed 0.03–0.05 gO_3 $gTSS^{-1}$ to achieve a balance between

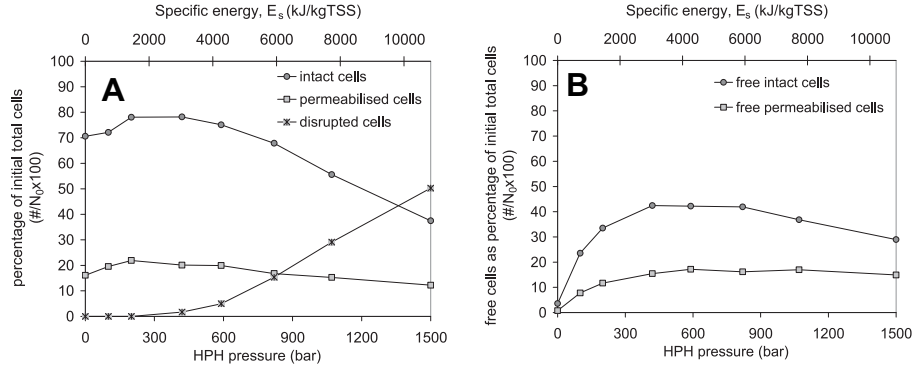

Fig. 7 – Profiles of percentages of intact, permeabilised and disrupted cells calculated referring to N_0 during HPH: (A) total cells (free + aggregated); (B) free cells (excluding aggregated).

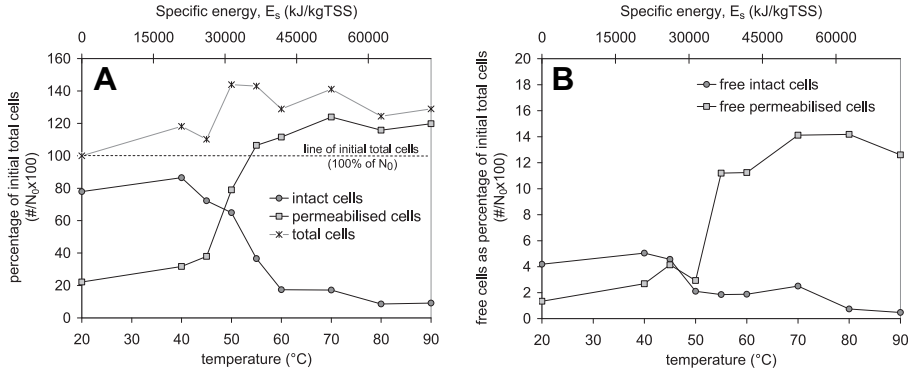

Fig. 8 – Profiles of percentages of intact, permeabilised and disrupted cells calculated referring to N_0 during thermal treatment: (A) total cells (free + aggregated); (B) free cells (excluding aggregated).

sludge reduction efficiency and costs (Foladori et al., 2010). The research is continuously oriented towards the optimisation of the ozonation process, both in the reactor configuration and in gas transfer systems, with the aim of minimising ozone dosages (*inter alia* Yan et al., 2009; Foladori et al., 2010). For this reason we investigated a range of very low ozone dosages, below 30 mgO_3 $gTSS^{-1}$ (Fig. 9).

As shown in Fig. 9A, intact cells decreased significantly at low ozone dosages up to 10 mgO_3 $gTSS^{-1}$ (from 78% to 40% of N_0) while for higher dosages the percentage of intact cells decreased more slowly. Below 10 mgO_3 $gTSS^{-1}$, intact cells underwent a progressive permeabilisation and significant disruption, while above 10 mgO_3 $gTSS^{-1}$ the disruption of cells levelled off (Fig. 9A).

This behaviour is due to the competition for ozone in reaction between soluble and particulate organic matter. The reaction between ozone and sludge occurs only near the gas–liquid interface, a liquid film with a thickness to the order of μm (El-Din and Smith, 2001). It is expected that the applied ozone will react first with soluble compounds and then attack the particulate solids (Cesbron et al., 2003). Even at low solubilisation levels, hydroxyl radicals produced by ozone react quickly with solubilised compounds which act as scavengers of particulate solids. On the basis of these assumptions, we can consider that ozone initially attacks bacterial cells in the flocs near the gas–liquid interface producing soluble compounds and small sized colloids (Paul and Debellefontaine, 2007). Subsequently, as the concentration of solubilised compounds gradually increases, they may have a screening effect on the further lysis of bacterial cells especially when aggregated in clusters or microcolonies and located in the inner part of flocs and thus protected against oxidation.

Ozonation did not cause a significant disaggregation of flocs, as can be observed from the data of free cells shown in Fig. 9B. A part an initial slight increase in the number of free intact cells, they decrease for ozone dosages higher than 5 mgO_3 $gTSS^{-1}$ (Fig. 9B). On contrary, free permeabilised cells increase continuously, indicating that ozonation causes both cell permeabilisation and the detachment of cells from the flocs. The hypothesis is that ozonation act against cell structure but also against Extracellular Polymeric Substances which have a role in bacteria aggregation.

3.7. *Comparison of SR technologies using E_s*

A qualitative comparison regarding the main effects on sludge structure and bacterial cells by the 4 SR technologies tested is indicated in Table 1 and is a synthesis of the observations made in the sections above.

A quantitative comparison among SR technologies should take into account energy consumption. S_{COD} is compared

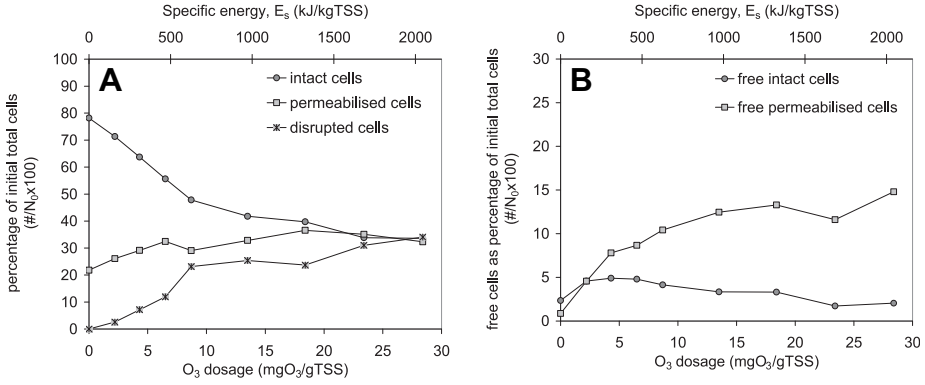

Fig. 9 – Profiles of percentages of intact, permeabilised and disrupted cells calculated referring to N_0 during ozonation: (A) total cells (free + aggregated); (B) free cells (excluding aggregated).

Table 1 – Synthesis of the main effects on sludge structure and bacterial cells by the SR technologies tested.

Effect caused by SR technology	SR technology			
	Ultrasonication	HPH	Thermal treatment	Ozonation
COD solubilisation	++	+	++	+
Sludge flocs disaggregation and release of free cells from flocs	++	++	+	+
Permeabilisation of intact cells	–	–	++	+
Disruption of intact cells	+	+	–	++
Disruption of permeabilised cells	+	+	–	++

in Fig. 10A, while the percentage of intact cells (free + aggregated) referred to the initial number of total cells (N_0) are shown in Fig. 10B as a function of the specific energy, E_s (a logarithmic scale was chosen due to the very wide range of E_s levels used with the SR technologies tested). To convert operational parameters for each SR treatment into an equivalent E_s value the assumptions described in the "Materials and Methods" section were used.

The conservation of intact cells (free + aggregated) after an SR treatment was also evaluated as the ratio $\log(I_E/I_0)$, where:

- I_E is the number of intact cells after the application of an SR technology at a certain E_S level;
- I_0 is the initial number of intact cells in untreated sludge.

This ratio $\log(I_E/I_0)$ is similar to that often used in the literature to describe the survival of viable cells. In a semi-logarithmic plot (Fig. 10C) linear survival curves were used as a good fit for the experimental data for the 4 SR treatments, with the slope indicated in the diagram. A slow inactivation rate was observed for ultrasonication, while ozonation showed a faster inactivation rate.

Among physical/mechanical treatments, ultrasonication produces the highest S_{COD} and the maximum loss of membrane integrity, but resulted in an excessive energy consumption similar to thermal treatment. In the thermal treatment, the need to heat the sludge leads to high operational costs when a thermal source is not available within the WWTP. However, thermal treatment may become more feasible when

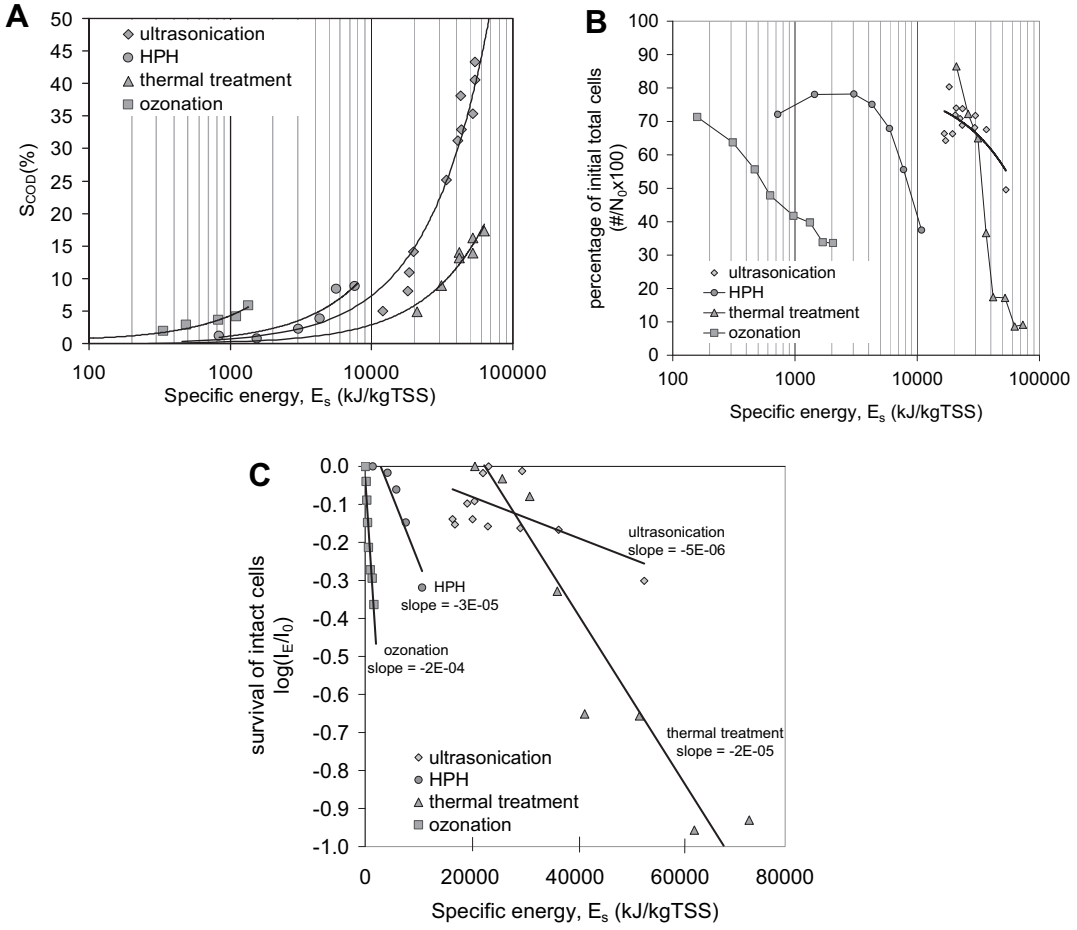

Fig. 10 – (A) Profiles of S_{COD}, (B) percentages of intact bacteria (calculated referring to N_0), (C) survival of intact cells. All parameters are as a function of the E_s level applied in the SR technologies tested.

solid content of sludge is increased by sludge thickening and the specific energy consumption per unit of TSS is thus reduced. In spite of the low S_{COD} released, ozonation caused a significant loss of membrane integrity, achievable in practice without excessive energy levels. Mechanical disintegration is not so energy-hungry to achieve significant damage to cells, but the equipment is often considered to have high investment costs and there is a technological limit in the application of very high pressures (risk of clogging, wear, etc.).

4. Conclusions

FCM was effectively used for the assessment of damage to bacterial membranes in activated sludge after the application of the 4 SR technologies selected for this research. In all cases the damage to cells increased for increasing levels of applied energy, but to a different extent:

- ultrasonication and HPH (belonging to physical/mechanical treatments): they act in a similar manner against both intact and permeabilised cells causing their disruption independently of the functional status. The HPH mechanism generates strong shear forces which causes cellular damage at lower E_S than ultrasonication which is based on ultrasonic waves;
- Thermal treatment, even when applied at moderate temperatures (up to 90 °C) causes significant cell permeabilisation, due to denaturation phenomena, which also produces a biased increase in the number of fluorescent particles at temperatures above 45–55 °C compared to 20 °C;
- Ozonation causes both permeabilisation and disruption of cells, but permeabilisation occurs to a lesser extent. At low ozone dosages, ozone firstly causes the lysis of bacteria free in suspension or in the external parts of flocs, while at higher dosages ozone reacts preferentially with the solubilised compounds released by cell lysis and floc disaggregation.

Among these SR technologies, the comparison of applied E_S demonstrated that it is often not so economic to reach the complete disruption of bacterial cells which usually requires very high energy levels. Therefore, to reduce sludge production it is probably more advantageous to cause sludge floc disintegration and only partial damage to bacterial cells, in order to promote better interaction between bacteria, enzymes and substrates to favour the biodegradation process.

Acknowledgements

The authors thank the anonymous reviewers for their stimulating, in depth suggestions.

REFERENCES

APHA, AWWA, WPCF, 1998. Standard Methods for the Examination of Water and Wastewater Washington DC, USA.

Appels, L., Degrève, J., Van der Bruggen, B., Van Impe, J., Dewil, R., 2010. Influence of low temperature thermal pre-treatment on sludge solubilisation, heavy metal release and anaerobic digestion. Bioresour. Technol. 101 (15), 5743–5748.

Benabdallah El-Hadj, T., Dosta, J., Márquez-Serrano, R., Mata-Álvarez, J., 2007. Effect of ultrasound pre-treatment in mesophilic and thermophilic anaerobic digestion with emphasis on naphthalene and pyrene removal. Water Res. 41, 87–94.

Böhler, M., Siegrist, H., 2007. Potential of activated sludge ozonation. Water Sci. Technol. 55 (12), 181–187.

Bougrier, C., Carrère, H., Delgenès, J.P., 2005. Solubilisation of waste-activated sludge by ultrasonic treatment. Chem. Eng. J. 106, 163–169.

Camacho, P., Déléris, S., Geaugey, V., Ginestet, P., Paul, E., 2002. A comparative study between mechanical, thermal and oxidative disintegration techniques of waste activated sludge. Water Sci. Technol. 46 (10), 79–87.

Cesbron, D., Déléris, S., Debellefontaine, H., Roustan, M., Paul, E., 2003. Study of competition for ozone between soluble and particulate matter during activated sludge ozonation. Trans IChemE 81 (Part A), 1165–1170.

Chen, G.H., An, K.J., Saby, S., Brois, E., Djafer, M., 2003. Possible cause of excess reduction in an oxic-settling-anaerobic activated sludge process (OSA process). Water Res. 37 (16), 3855–3866.

Cui, R., Jahng, D., 2006. Enhanced methane production from anaerobic digestion of disintegrated and deproteinized excess sludge. Biotechnol. Lett. 28, 531–538.

El-Din, M.G., Smith, D.W., 2001. Designing ozone bubble columns: a spreadsheet approach to Axial dispersion model. Ozone Sci. Eng. 23 (5), 369–384.

Engelhart, M., Krüger, M., Kopp, J., Dichtl, N., 2000. Effects of disintegration on anaerobic degradation of sewage excess sludge in downflow stationary fixed film digesters. Water Sci. Technol. 41 (3), 171–179.

Foladori, P., Bruni, L., Andreottola, G., Ziglio, G., 2007. Effects of sonication on bacteria viability in wastewater treatment plants evaluated by flow cytometry—fecal indicators, wastewater and activated sludge. Water Res. 41, 235–243.

Foladori, P., Quaranta, A., Ziglio, G., 2008. Use of silica microspheres having refractive index similar to bacteria for conversion of flow cytometric forward light scatter in biovolume. Water Res. 42 (14), 3757–3766.

Foladori, P., Andreottola, G., Ziglio, G., 2010. Sludge Reduction Technologies in Wastewater Treatment Plants. IWA Publishing, London, UK, ISBN 9781843392781.

Gaudy, A.F., Yang, P.Y., Obayashi, A.W., 1971. Studies on the total oxidation of activated sludge with and without hydrolytic pretreatment. J. Water Pollut. Control Fed. 43 (1), 40–54.

Goel, R., Tokutomi, T., Yasui, H., 2003. Anaerobic digestion of excess activated sludge with ozone pre-treatment. Water Sci. Technol. 47 (12), 207–214.

Hayakawa, K., Ueno, Y., Kawamura, S., Kato, T., Hayashi, R., 1998. Microorganisms inactivation using high-pressure generation in sealed vessels under sub-zero temperature. Appl. Microbiol. Biotechnol. 50, 415–418.

Mason, T.J., Lorimer, J.P., Bates, D.M., 1992. Quantifying sonochemistry: casting some light on a 'black art'. Ultrasonics 30 (1), 40–42.

Nebe-von-Caron, G., Stephens, P.J., Hewitt, C.J., Powell, J.R., Badley, R.A., 2000. Analysis of bacterial function by multi-colour fluorescence flow cytometry and single cell sorting. J. Microbiol. Methods 42, 97–114.

Nielsen, B., Petersen, G., 2000. Thermophilic anaerobic digestion and pasteurisation. Practical experience from danish wastewater treatment plants. Water Sci. Technol. 42 (9), 65–72.

Novak, J.T., Chon, D.H., Curtis, B.-A., Doyle, M., 2007. Biological solids reduction using the Cannibal process. Water Environ. Res. 79 (12), 2380–2386.

Pagán, R., Mackey, B., 2000. Relationship between membrane damage and cell death in pressure-treated *Escherichia coli* cells: differences

between exponential- and stationary-phase cells and variation among strains. Appl. Environ. Microbiol. 66 (7), 2829–2834.
Paul, E., Debellefontaine, H., 2007. Reduction of excess sludge produced by biological treatment processes: effect of ozonation on biomass and on sludge. Ozone Sci. Eng. 29 (6), 415–427.
Porter, J., Deere, D., Hardman, M., Edwards, C., Pickup, R., 1997. Go with the flow – use of flow cytometry in environmental microbiology. FEMS Microbiol. Ecol. 24, 93–101.
Prorot, A., Eskicioglu, C., Droste, R., Dagot, C., Leprat, P., 2008. Assessment of physiological state of microorganisms in activated sludge with flow cytometry: application for monitoring sludge production minimization. J. Ind. Microbiol. Biotechnol. 35, 1261–1268.
Saby, S., Djafer, M., Chen, G.H., 2003. Effect of low ORP in anoxic sludge zone on excess sludge production in oxic-settling-anoxic activated sludge process. Water Res. 37 (1), 11–20.
Salsabil, M.R., Prorot, A., Casellas, M., Dagot, C., 2009. Pre-treatment of activated sludge: effect of sonication on aerobic and anaerobic digestibility. Chem. Eng. J. 148 (2–3), 327–335.
Steen, H.B., 2000. Flow cytometry of bacteria: glimpses from the past with a view to the future. J. Microbiol. Methods 42, 65–74.
Strünkmann, G.W., Müller, J.A., Albert, F., Schwedes, J., 2006. Reduction of excess sludge production using mechanical disintegration devices. Water Sci. Technol. 54 (5), 69–76.
Sun, L., Randall, C.W., Novak, J.T., 2010. The Influence of sludge Interchange Timeson the Oxic–Settling–Anoxic process. Water Environ. Res. 82, 519–523.
Vives-Rego, J., Lebaron, P., Nebe-von-Caron, G., 2000. Current and future applications of flow cytometry in aquatic microbiology. FEMS Microbiol. Rev. 24, 429–448.
Wagner, M., Amann, R., Lemmer, H., Schleifer, K.H., 1993. Probing activated sludge with oligonucleotides specific for proteobacteria: inadequacy of culture-dependent methods for describing microbial community structure. Appl. Environ. Microbiol. 59 (5), 1520–1525.
Winter, A., 2002. Minimisation of costs by using disintegration at a full-scale anaerobic digestion plant. Water Sci. Technol. 46 (4–5), 405–412.
Yan, S., Miyanaga, K., Xing, X.-H., Tanji, Y., 2008. Succession of bacterial community and enzymatic activities of activated sludge by heat-treatment for reduction of excess sludge. Biochem. Eng. J. 39, 598–603.
Yan, S.-T., Chu, L.-B., Xing, X.-H., Yua, A.-F., Sunc, X.-L., Jurcik, B., 2009. Analysis of the mechanism of sludge ozonation by a combination of biological and chemical approaches. Water Res. 43, 195–203.
Ziglio, G., Andreottola, G., Barbesti, S., Boschetti, G., Bruni, L., Foladori, P., Villa, R., 2002. Assessment of activated sludge viability with flow cytometry. Water Res. 36 (2), 460–468.